HYDROGEOLOGICAL AND THREE-DIMENSIONAL NUMERICAL GROUNDWATER FLOW MODELLING OF THE LAKE SIBAYI CATCHMENT, NORTHERN KWAZULU-NATAL, SOUTH AFRICA

JAN CHRISTIAN WEITZ

Submitted in fulfilment of the academic requirements of
Doctor of Philosophy

In Hydrogeology
Geological Science
College of Agriculture, Engineering and Science
University of KwaZulu-Natal
Durban
South Africa

December 2016

As the candidate's supervisor I have/have not approved this thesis/dissertation for submission.

Signed: _____ Name: _____ Date: _____

ABSTRACT

Lake Sibayi, a topographically closed fresh water lake in northern KwaZulu-Natal, South Africa, and the coastal aquifers surrounding the lake, are important water resources for the local community and the surrounding ecosystem. A significant decline in lake levels has been experienced over the last decade, dropping from approximately 20 m above mean sea level (amsl) in early 2000 to below 16 m amsl at present. It is believed that this decrease could be attributed to an increase in water abstraction from the lake and surrounding groundwater, the rapidly increasing commercial plantations within the catchment and recent droughts. The effective management of this hydrological system needs a thorough understanding of the interaction of the lake with the surrounding aquifer. In recent years, hydrogeological and numerical groundwater flow modelling have become standard tools with which these interactions are studied.

This thesis describes the process of conceptual model design through to the development and calibration of steady-state and transient numerical groundwater flow model for the lake Sibayi system. Through a series of field campaigns, on site measurements of depth to groundwater with surface and groundwater sampling, for hydrochemical and environmental isotope analysis, were undertaken. Hydrochemical parameters and environmental isotopes for the various water sources within the Lake Sibayi hydrological system were determined following standard procedures to study the relationship between these resources. A slight distinction between shallow and deep aquifers appears to be present, where the shallow groundwaters are dominated mainly by a Na-Cl hydrochemical facies, while the deeper boreholes are dominated mainly by a Na-Ca-HCO_3-Cl hydrochemical facies. Shallow groundwater samples have relatively low EC values averaging 278 mS/m, while the deeper wells had average EC concentrations of 409 mS/m. Groundwater samples collected along the dune cordon, show a similar hydrochemical and environmental isotope composition as that of the lake. Multivariate statistical analyses including principal component factor analysis and hierarchical cluster analysis (HCA) were undertaken on the hydrochemical data. The HCA grouped the water samples into two clusters, which represented surface and groundwaters. Each of these two clusters were in turn divided into two sub-clusters, representing the shallow and deep aquifers, and stream and lake samples, respectively.

As part of the conceptual modelling, the long-term water balance of the lake has been quantified by defining the various inflow and outflow components of the lake. All hydrological information including precipitation, evaporation, surface water runoff, abstraction, as well as geological, hydraulic, hydrogeochemical and environmental isotope information were used to

conceptualise the hydrological system of the Lake Sibayi catchment. Local geologic, groundwater head distribution, lake level, hydrochemical and environmental isotope data were used to constrain the link between groundwater and the lake. In the western section of the catchment, groundwater flows to the lake where groundwater head is above lake stage, whereas along the eastern section, the presence of mixing between lake and groundwater hydrochemical and isotopic compositions indicate that the lake recharges the aquifer. Stable isotope signals further revealed the movement of lake water through and below the coastal dune cordon before eventually discharging into the Indian Ocean.

Groundwater recharge to the catchment was estimated using the chloride mass balance (CMB) method and the results compared with estimates based on published maps. The CMB recharge estimate resulted in 126 mm/a (12 % MAP) against 95 mm/a (10% MAP), estimated using published maps. The total evaporation and evapotranspiration from the lake and its catchment were estimated at 1 495 mm/a and 1 090 mm/a, respectively. Estimated surface water runoff from the catchment to the lake is about 1% of MAP. Calculated lake water outflow to the sea through the dune cordon opposite the lake, along a 12 km seepage face, is 2.3×10^7 m^3/a. The total amount of water abstracted from both surface and groundwater resources within the catchment is about 4.5×10^6 m^3/a. The water balance of Lake Sibayi shows that lake levels fluctuate in response to varying amounts of groundwater and surface water inflow into the lake, seepage loss through the coastal dune, abstraction, and evaporation from the lake.

Based on the conceptual hydrogeological model, a steady-state and transient numerical groundwater flow model, were developed for the Lake Sibayi system using two independent approaches, namely, the High-K method and Lake Package. Groundwater Modelling Systems (GMS), which runs on the modular finite difference code, MODFLOW 2005 with its several packages were used to characterise the three dimensional flow conditions around the lake. Two layer models were used to simulate the lake stage and aquifer conditions over a forty three year period from January 1970 to September 2014. The simulation period was broken down into 536 monthly stress periods with calibrated parameter values for each of the boundary conditions over the simulation period. The calibrated steady-state model simulation results for the two methods were comparable. While, transient model calibration results show that the Lake Package was more suitable in simulating lake level fluctuations with low calibration errors. The calibrated transient groundwater flow models were further used to evaluate the hydrological response of the lake and the groundwater system to various stress scenarios, including changes in evaporation, precipitation and land use. Once again, the High-K method was very sensitive to changes in model input, simulating rapid changes to the system, while Lake Package

simulations results were in line with known changes in the system. Therefore, the High-K technique is most suitable for simple applications, while complex lake-aquifer interactions are better simulated using the Lake Package.

Key words/Phrases: Conceptual modelling, High-K method, Lake Package, Lake Sibayi, MODFLOW, Numerical steady-state and transient groundwater flow modelling, Surface water - Groundwater interactions, South Africa

PREFACE

The research contained in this PhD thesis was carried out in the Discipline of Geological Science, School of Agricultural, Earth and Environmental Sciences, University of KwaZulu-Natal, Westville campus from January 2012 to December 2016, under the supervision of Dr Molla Demlie.

The study represents original work by the author and has not otherwise been submitted in any form for any degree or diploma to any tertiary institution. Where use has been made of the work of others it is duly acknowledged in the text.

DECLARATION 1: PLAGIARISM

I, Jan Christian Weitz, declare that:

i. The research reported in this dissertation, except where otherwise indicated or acknowledged, is my original work;

ii. This dissertation has not been submitted in full or in part for any degree or examination to any other university;

iii. This dissertation does not contain other persons' data, pictures, graphs or other information, unless specifically acknowledged as being sourced from other persons;

iv. This dissertation does not contain other persons' writing, unless specifically acknowledged as being sourced from other researchers. Where other written sources have been quoted, then:

   a. Their words have been re-written but the general information attributed to them has been referenced;
   b. Where their exact words have been used, their writing has been placed inside quotation marks, and referenced;

v. Where I have used material for which publications followed, I have indicated in detail my role in the work;

vi. This dissertation is primarily a collection of material, prepared by myself, published as journal articles or presented as a poster and oral presentations at conferences. In some cases, additional material has been included;

vii. This dissertation does not contain text, graphics or tables copied and pasted from the Internet, unless specifically acknowledged, and the source being detailed in the dissertation and in the References sections.

_____

Signed: Jan Christian Weitz

Date: December 2016

DECLARATION 2: PUBLICATIONS AND CONFERNECES

Publication 1 (Chapter 5): Published in the South African Journal of Geology

Weitz, J. and Demlie, M. 2015. Hydrogeological System Analyses of the Lake Sibayi catchment, north-eastern South Africa. South African Journal of Geology. Volume 118(1), Pages 91-106.

Contribution: As first author on the papers, I was responsible for sample collection (with the aid of my supervisor), undertaking of major anion and cation analyses, collection and interpretation of all data, writing, editing and preparation of all the manuscripts and figures, and all submissions, editorial, peer-review and revision processes resulting in the publication of the manuscripts. The second author is my supervisor, who provided guidance throughout the project as well as editing the manuscript.

Publication 2 (Chapter 6): Published in the Journal of African Earth Sciences

Weitz, J. and Demlie, M. 2014. Conceptual modelling of groundwater–surface water interactions in the Lake Sibayi Catchment, Eastern South Africa. Journal of African Earth Sciences. Volume 99, Part 2, November 2014, Pages 613–624. Special Volume of the 24th Colloquium of African Geology.

Contribution: As first author on the papers, I was responsible for sample collection (with the aid of my supervisor), undertaking of major anion and cation analyses, collection and interpretation of all data, writing, editing and preparation of all the manuscripts and figures, and all submissions, editorial, peer-review and revision processes resulting in the publication of the manuscripts. The second author is my supervisor, who provided guidance throughout the project as well as editing the manuscript.

Publication 3 (Chapter 7): To be submitted to the Journal of Hydrology

Weitz, J. and Demlie, M. 2016. Comparative analyses between the LAK3 package and the High Conductivity (High-K) techniques used for numerical simulation of lake-aquifer interaction in the Lake Sibayi catchment, north-eastern South Africa.

Contribution: As first author on the papers, I am responsible for conceptual and numerical model design, calibration and prediction for the two methods analysed. The second author is my supervisor, who provided guidance throughout the project as well as editing the manuscript.

Publication 4 (Chapter 7): To be submitted to the Journal of Hydrogeology

Weitz, J. and Demlie, M. 2016. Three-dimensional numerical modelling of lake-aquifer interaction in the Lake Sibayi catchment, north-eastern South Africa.

Contribution: As first author on the papers, I am responsible for conceptual and numerical model design, calibration and prediction for steady-state and transient models. The second author is my supervisor, who provided guidance throughout the project as well as editing the manuscript.

Conferences Attended

Weitz, J. and Demlie, M. 2013. Conceptual modeling of Groundwater – Surface water interactions in the Lake Sibayi Catchment, Eastern South Africa. **Oral presentation at the 24th Colloquium of African Geology (CAG24) in Addis Ababa, Ethiopia, 8th to 14th January 2012.**

Weitz, J. and Demlie, M. 2012. Hydrogeology of the Lake Sibayi Catchment, Eastern South Africa. **Poster presentation during UKZN's College of Agriculture, Engineering and Science Post-Graduate Research Day in Pietermaritzburg, 29 October 2012.**

Weitz, J. and Demlie, M. 2013. Hydrogeological conceptual modeling of the Lake Sibayi Catchment, Eastern South Africa. **Oral presentation at the 13th Biennial Groundwater Division Conference and Exhibition (GWD) in Durban, 17th to 19th September 2013.**

Weitz, J. and Demlie, M. 2015. Comparative analyses of the LAK3 package and the High Conductivity (High-K) technique used for numerical simulation of lake-aquifer interactions in the Lake Sibayi catchment, north-eastern South Africa. **Oral presentation at the 14th Biennial Groundwater Division Conference and Exhibition (GWD) in Muldersdrift, 21st to 23rd September 2015.**

_____

Signed: Jan Christian Weitz

Date: December 2016

TABLE OF CONTENTS

Page No.

ABSTRACT ii

PREFACE v

DECLARATION 1: PLAGIARISM vi

DECLARATION 2: PUBLICATIONS AND CONFERNECES vii

LIST OF FIGURES xiv

LIST OF TABLES xviii

ACKNOWLEDGEMENTS xx

LIST OF ABBREVIATIONS AND NOTATIONS xxi

CHAPTER ONE: INTRODUCTION 1

1.1. Background to the research 1

1.2. Research aims and objectives 3

1.3. Thesis structure 3

CHAPTER TWO: DESCRIPTION OF THE STUDY AREA 5

2.1. Location 5

2.2. Climate and Hydrometeorology 6

2.3. Physiography and Drainage 9

2.4. Vegetation and land cover 11

2.5. Population and water use 12

2.6. Lake Morphology and Bathymetry 13

2.7. Geological Setting 16

2.7.1. Lebombo Group 16

2.7.2. Zululand Group 17

2.7.3. Maputaland Group 17

2.7.4. Recent Lake Sediments 21

2.8. General Hydrogeological setting 21

CHAPTER THREE: LITERATURE REVIEW 22
3.1. Previous hydrogeological studies on the Coastal Plain 22
3.2. Groundwater Modelling 23
3.2.1. Types of models 23
3.2.2. Governing equations 24
3.3. Numerical Methods 24
3.4. Conceptual Hydrogeological Modelling 26
3.4.1. Defining Hydrostratigrapic Units 26
3.4.2. Water Budget 27
3.5. Defining the Flow System (s) 27
3.6. Code Selection 27
3.6.1. MODFLOW 28
3.6.2. MODLFOW Packages 28
3.7. Simulating Lake –Aquifer interaction using the High Conductivity Technique 33
3.8. Groundwater Modelling System (GMS) 33
3.9. Addition considerations for transient simulation 33
3.9.1. Storage Parameters 34
3.9.2. Initial conditions 34
3.9.3. Transient Boundary Conditions 34
3.9.4. Discretising Time 34
3.10. Calibration 35
3.10.1. Trail-and-Error Calibration 35
3.10.2. Automated Parameter Estimation 36
3.11. Catchment Water Budget 36
3.11.1. Precipitation 37
3.11.2. Surface Runoff 37
3.11.3. Groundwater Recharge Estimation 37
3.11.4. Evaporation and evapotranspiration 40

3.12. Environmental Isotope Analyses 41
3.12.1. Stable Isotopes 41
3.12.2. Radio isotopes 42
CHAPTER FOUR: RESEARCH METHODOLOGY AND APPROACH 43
4.1. Desktop review 43
4.2. Field measurement, analyses and sampling procedures 43
4.3. Laboratory analysis 44
4.4. Statistical Analyses of hydrochemical data 44
4.5. Water Balance 45
4.5.1. Precipitation 46
4.5.2. Runoff 46
4.5.3. Recharge 46
4.5.4. Evaporation and evapotranspiration 47
4.5.5. Surface and groundwater abstraction 49
4.5.6. Groundwater outflow 50
4.6. Numerical Modelling 50
4.6.1. Modelling Approach 50
4.6.2. Conceptual modelling 52
4.6.3. Definition of model domain 52
4.7. Data interpretation tools 54
CHAPTER FIVE: HYDROGEOLOGICAL, HYDROCHEMICAL AND ENVIRONMENTAL ISOTOPE CHARACTERISTICS OF THE LAKE SIBAYI SYSTEM 56
5.1. Hydrogeological units and their hydraulic characteristics 56
5.2. Recharge 57
5.3. Regional groundwater flow direction 60
5.4. Water balance of Lake Sibayi 61
5.5. Hydrochemical characteristics of the Lake Sibayi system 64
5.6. Statistical analyses of the hydrochemical results 68

5.6.1. Correlation Matrices 68
5.6.2. Factor analyses 70
5.6.3. Cluster Analyses 71
5.7. Environmental isotopes characteristics 74
5.8. General water quality of the study area 77
CHAPTER SIX: HYDROGEOLOGICAL CONCEPTUAL MODELLING OF THE LAKE SIBAYI SYSTEM, NOTHEASTERN SOUTH AFRICA 79
6.1. Groundwater flow around the Lake Sibayi catchment 79
6.2. Geological Conceptual Model for the Lake Sibayi System 80
6.3. Areal Groundwater Recharge for the Catchment 82
6.4. Water Balance components of the Lake Sibayi system 83
6.4.1. Precipitation 83
6.4.2. Surface Runoff 83
6.4.3. Evaporation and evapotranspiration 84
6.4.4. Abstraction 84
6.4.5. Groundwater outflow to the sea 85
6.5. Generalized conceptualization of the hydrological and hydrogeological characteristics of the Lake Sibayi system 85
CHAPTER SEVEN: NUMERICAL GROUNDWATER FLOW MODELLING OF THE LAKE SIBAYI SYSTEM, NORTH-EASTERN SOUTH AFRICA 87
7.1. Introduction 87
7.2. Model Design 87
7.2.1. Model layers 87
7.2.2. Model domain and model grid design 90
7.2.3. Model boundary conditions 90
7.2.4. Initial conditions 94
7.2.5. Solvers used 94
7.2.6. Representation of the lake 94
7.2.7. Sensitivity Analysis 94

7.2.8. Calibration techniques 95
7.3. Modelling the Lake Sibayi System using the High-K Method 98
7.3.1. Sensitivity analyses 99
7.3.2. Steady-state trial-and-error calibration 99
7.3.3. Steady-state automated calibration 100
7.3.4. Evaluation of steady-state calibration 100
7.3.5. Evaluation of transient model calibration for the High-K method 103
7.4. Modelling the Lake Sibayi system using the Lake Package 105
7.4.1. Sensitivity Analyses 106
7.4.2. Steady-state calibration 106
7.4.3. Steady-state calibration errors 107
7.4.4. Evaluation of steady-state calibration 107
7.4.5. Evaluation of transient calibration for the Lake Package model 109
7.5. Long-term (Transient/Time series) water balance analyses 111
7.6. Scenario analyses 114
7.6.1. Evaluation of the various scenario results 114
7.7. Model Limitations 119
7.8. Evaluation of the Lake Package and High-K method 119
7.9. Summary 120
CHAPTER EIGHT: CONCLUSIONS AND RECOMMENDATIONS 121
REFERENCES 124
APPENDICES 141

LIST OF FIGURES

Figure **Page No.**

Figure 2.1. Location map showing Lake Sibayi and other coastal lakes of the Maputaland coastal plain. 6

Figure 2.2. 15 year average meteorological variables from the Mbazwana Airfield Station (data sourced from SAWS, 2015). 8

Figure 2.3. Rainfall distribution over the Lake Sibayi catchment (mm/a) from 1990 to 2013 (SAWS, 2015). 9

Figure 2.4. Topographic surface of the area surrounding Lake Sibayi with significant regional features 10

Figure 2.5. Land use distribution within the Lake Sibayi catchment (Ezemvelo KZN Wildlife, 2011). 12

Figure 2.6. Population growth for the uMhlabuyalingana Local Municipality (1996 to 2011) showing percentage of population with access to piped water and those without any access to piped water (Statistics South Africa, 2012). 13

Figure 2.7. Bathymetric map of Lake Sibayi (interpolated based on data from Miller, 2001). .. 15

Figure 2.8. Depth – Area (a) and Depth – Volume (b) relationships for Lake Sibayi. 16

Figure 2.9. Geological map of the study area (Modified from Porat and Botha, 2008). 18

Figure 2.10. Schematic representation of the Maputaland Group lithostratigraphic units. Not to scale. LIG-Last Interglacial (adapted from Porat and Botha, 2008). 19

Figure 3.1. Finite difference and finite element representation of an aquifer region (Adapted from Wang and Anderson, 1995). 25

Figure 3.2. Conceptual model of vertical river transmission process (adapted from McDonald and Harbourgh, 1988). 29

Figure 3.3. Diagrammatic representation of the evaporation model (Adapted from Kelbe *et al*., 2001) 30

Figure 3.4. Diagrammatic representation of the Lake Package showing its volumetric water budget components (Adapted from Council, 1998). 32

Figure 3.5. Trial-and-error calibration procedure (modified from Peters, 1987). 36

Figure 4.1. Spatial distribution of sampling sites, with proposed surface water catchment boundary in the Lake Sibayi catchment. 43

Figure 4.2. Modelling approach for numerical modelling (Adapted from Anderson and Woessner (1992). 51

Figure 5.1. Spatial distribution of groundwater recharge within the Lake Sibayi catchment using the CMB method. 59

Figure 5.2. Regional groundwater flow distribution map showing local flow vectors (groundwater elevation (m amsl) presented at 10 m contour interval). 61

Figure 5.3. Long-term lake-level fluctuations along with monthly precipitation from 1980 to 2012 (DWA, 2013; SAWS, 2015). The 12-month moving average precipitation is shown in black. 63

Figure 5.4. Groundwater and surface samples within the Lake Sibayi Catchment plotted on. (a) Piper trilinear diagram, (b) Schoeller diagram (c) Durov diagram and (d) indicates the sample labels. 68

Figure 5.5. Principal component analyses plot of the variables in rotated space. 71

Figure 5.6. Dendrogram of the hierarchical cluster analysis of the water quality parameters of various water sources within the Lake Sibayi catchment using Ward method. 72

Figure 5.7. Groundwater and surface hydrochemical groups within the Lake Sibayi Catchment plotted on (a) Piper trilinear diagram, (b) Schoeller diagram and (c) Durov diagrams. 74

Figure 5.8. Relationship between $\delta^{18}O$ and Deuterium from various water resources within the study area in relation to the LMWL (IAEA, 2012) and GMWL (Craig, 1961). 76

Figure 6.1. Groundwater flow distribution map showing local flow vectors (groundwater elevation (m amsl) presented at 10 m contour interval). 80

Figure 6.2. Classification of the various geological formations into their respective hydrostratigraphic units (adapted from Porat and Botha, 2008). 81

Figure 6.3. Hydrogeological conceptual model of the Lake Sibayi Catchment. a) East-West section b) North-South section. 86

Figure 7.1. Digital elevation model of the topographic surface (USGS, 2015) incorporating the lake bathymetry as measured by Miller (2001). 88

Figure 7.2. Estimated upper surface of the Miocene Uloa Formation (Second model layer) 89

Figure 7.3. Estimated upper surface of the basement St Lucia Formation (Bottom impermeable model layer) 90

Figure 7.4. Model boundary conditions representing the various inflow and outflow components 91

Figure 7.5. Sediment type distribution in Lake Sibayi (Adapted after Miller, 2001). 93

Figure 7.6. Transient lake mass balance components for lake Sibayi with the resultant residual volume used to represent the recharge to lake cells in the High-K method 98

Figure 7.7. The relative sensitivities of the various model parameters for steady-state simulation (a) and transient simulation (b). 99

Figure 7.8. Scatter plot of computed vs. observed heads for the steady-state High-K simulation 101

Figure 7.9. Contour map of simulated groundwater head distribution with associated error bars for the High-K method 102

Figure 7.10. Transient scatter plot data of observed and simulated heads for the High-K method (1975 to 2014) 104

Figure 7.11. Time series plot of observed and High-K method simulated lake levels from January 1970 to September 2014. 105

Figure 7.12. The relative sensitivity of the various water balance components for the Lake Package simulation steady-state simulation (a) and the relative sensitivity of the storage parameters for the transient simulation (b). 106

Figure 7.13. Scatter plot of computed vs. observed heads for the Lake Package 107

Figure 7.14. Contour map of simulated groundwater head distribution with associated error bars for the Lake Package 108

Figure 7.15. Lake Package Transient scatter plot observed versus simulated lake stage for the period between 1975 and 2014. 110

Figure 7.16. Time series plot of observed and Lake Package simulated lake levels from January 1970 to September 2014. 110

Figure 7.17. Long-term (1970 -2014) model domain water balance components for the Lake Package showing the various inflows and outflows. 112

Figure 7.18. Long-term (1970 -2014) model domain water balance for the High-K method showing the various components of inflows and outflows. 113

Figure 7.19. Contour plot of Scenario 1 including the proposed forestry applications..... 115

Figure 7.20. Contour plot of Scenario 2 where precipitation has been decreased by 10% and evaporation increased by 5%. 116

Figure 7.21. Contour plot of Scenario 3 where precipitation has been increased by 10% and evaporation decreased by 5%. 117

Figure 7.22. Modelled groundwater and lake level map for Scenario 4 representing the worst case scenario. 117

LIST OF TABLES

Table **Page No.**

Table 2.1. Mean monthly meteorological data obtained from 1997 to 2014 at the Hlabisa Mbazwana, Mbazwana Airfield Meteorological Station and Makatini Research Centre (SAWS, 2015). 7

Table 2.2. Depth - area - volume relationships. 16

Table 4.1. WARMS Annual Abstraction from Lake Sibayi for local community water supply. 49

Table 4.2. The physical and hydrological framework requirements for conceptual model formulation and calibration. 52

Table 5.1. Hydraulic characteristics of the different aquifer units present in the study area (compiled from various sources). 57

Table 5.2. Groundwater recharge estimation from the saturated zone (MAP of 1012 mm/a). ... 58

Table 5.3. Recharge estimation using qualified guesses, after Bredenkamp *et al*., (1995) and Kirchner *et al*., (1991) 60

Table 5.4. Estimated long-term (1970 -2014) monthly major water balance components of Lake Sibayi (in 10^6 m^3). 62

Table 5.5. Long-term (1970 -2014) annual lake water balance of the Lake Sibayi catchment (10^6 m^3). 63

Table 5.6. Univariate statistical overview of the groundwater results. All values in mg/l unless otherwise stated 65

Table 5.7. On site and laboratory measured surface water and groundwater physical and chemical parameters generated during this research. All values in mg/l unless otherwise stated 66

Table 5.8. Surface water and groundwater physical and chemical parameters sourced from Jeffares and Green (2012, 2014a, 2014b) and Terratest (2009a, 2009b, 2011, 2014, 2015a, 2015b, 2016a, 2016b). All values in mg/l unless otherwise stated 67

Table 5.9. Pearson's correlation matrices for groundwater hydrochemical data 69

Table 5.10. Results of principal component factor analysis of the hydrochemical data with Varimax rotation. 71

Table 5.11. Univariate statistical analyses of the hydrochemical components with the greatest variation determined from factor analyses..... 73

Table 5.12. Environmental isotope data of the study area. 75

Table 6.1. Average hydraulic characteristics of the shallow and deep HSUs 82

Table 7.1. Groundwater monitoring boreholes with time series water level measurements. 98

Table 7.2. Calibrated parameter values for the High-K method 100

Table 7.3. High-K steady-state model calibration error criterion. 101

Table 7.4. Average steady-state water budget for the model domain using the High-K method 103

Table 7.5. Transient High-K model calibration errors for lake level and aquifer calibration ... 104

Table 7.6. Lake Package steady-state model calibration error 107

Table 7.7. Lake Package steady-state modelled water budget for the model domain..... 109

Table 7.8. Lake Package transient model calibration error 109

Table 7.9. Description of proposed scenarios for model simulation 114

Table 7.10. Simulated lake levels for the various scenarios obtained using the Lake Package and High-K method. 118

Table 7.11. Computed water balance components for the various model scenario. 118

ACKNOWLEDGEMENTS

I would first and foremost like to thank my supervisor, Dr Molla Demlie, for giving me the opportunity to undertake my PhD study and for his guidance. This project would not have been possible without his guidance and patience throughout the research.

I would also like to thank Mark Schapers (Jeffares and Green), Dr. Greg Botha (CGS) and the Department of Water Affairs for providing relevant reports for the study area and geological information. I would also like to thank Professor Simon Lorentz and Cobus Pretorius from School of Bioresources Engineering and Environmental Hydrology with Mike Butler from iThemba Labs and Dr. Marlina Elburg from UKZN for providing environmental isotope and trace metal analysis respectively. Special thanks are also expressed to Sheila Imrie and Shuaib Dustay (SRK) for providing me with invaluable assistance with the numerical modelling aspect of the project. I would also like to thank the South African Weather Services for all the meteorological data as well as Cameron Tylcoat and Natasha Mangaroo from DWA for abstraction and lake level data respectively.

Saving the best for last, I would like to thank all my friends and family who has become my pillar of support throughout my studies. To all my friends in the department, Lauren Pretorius, Talisha Pillay, Errol Wiles, Clarice Romer, Lauren Hoyer, Prof Andy Green, Carlos Loureiro, Shannon Dixon and former colleagues Alex Metz and Mbali Ndlovu, I would not have been able to do this without all your support and assistance.

The financial assistance in the form of scholarship provided by the National Research Foundation (NRF) during the duration of the study is acknowledged. Any opinions, findings, and conclusions are those of the author and the NRF does not accept any liability in regard thereto.

LIST OF ABBREVIATIONS AND NOTATIONS

amsl	Above mean sea level
ACRU	Agricultural Catchments Research Unit
bmsl	Below mean sea level
C	Runoff coefficient
Cl_p	Chloride concentration in precipitation (mmol/l)
Cl_{sw}	Chloride concentration in soil water (mmol/l)
CMB	Chloride Mass Balance
Dd	Dry deposition of chloride (mg/l)
DEM	Digital Elevation Model
DO	Dissolved Oxygen (ppm)
DWA	Department of Water Affairs
EC	Electrical conductivity (mS/m)
Eh	Reduction potential (mV)
e°(T)	Saturation vapour pressure at air temperature T (kPa)
e_s	Saturation vapour pressure for a given time period (kPa)
e_a	Actual vapour pressure (kPa)
e_s- e_a	Saturation vapour pressure deficit
ET_o	Reference crop evapotranspiration
ET_c	Crop evapotranspiration under standard conditions (mm day-1)
FAO	Food and Agriculture Organisation
G	Soil heat flux (MJ m-2 day-1)
GMS	Groundwater Modelling System
GMWL	Global Meteoric Water Line
GNIP	Global Network of Isotopes in Precipitation
GRIP	Groundwater Resource Information Project
GUI	Graphical User Interface
HP	Harvest Potential (m3/yr)
IAEA	International Atomic Energy Agency
I	Thermal index
IC	Ion-Chromatograph
ICP-MS	Inductively Coupled Plasma Mass Spectrometry
K_c	Crop Coefficient
LMWL	Local Meteoric Water Line
m^3/a	Cubic meter per annum

N	Maximum possible sunshine duration in a day, daylight hours (hour)
NGA	National Groundwater Archive
NGDB	National Groundwater Database
Nm	Latitude correction factor
n	Actual duration of sunshine in a day (hour)
ORP	Oxygen Reduction Potential (mV)
P	Precipitation (mm/month)
Q	Peak runoff rate (m^3/s)
Q	Yield (usually in L/s or m3/d)
q	Monthly runoff (mm)
R_a	Extraterrestrial radiation (MJ m-2 day-1)
R_n	Net radiation (MJ m-2 day-1)
R_{nl}	Net longwave radiation (MJ m-2 day-1)
R_{ns}	Net solar or shortwave radiation (MJ m-2 day-1)
R_s	Solar or shortwave radiation (MJ m-2 day-1)
R_{so}	Clear-sky solar or clear-sky shortwave radiation (MJ m-2 day-1)
r_a	Aerodynamic resistance (s m-1)
r_l	Bulk stomatal resistance of well-illuminated leaf (s m-1)
R_s/R_{so}	Relative solar or relative shortwave radiation
RH	Relative humidity (%)
S	Storativity or specific yield
SAWS	South African Weather Services
SRTM	Shuttle Radar Topography Mission
T	Transmissivity (m^2/d)
t	Time (usually in days)
T	Air temperature (°C)
TAL	Total alkalinity (mg/l)
TDS	Total dissolved solids (mg/l)
V-SMOW	Vienna Standard Mean Ocean Water
WMA	Water Management Area
u^2	Wind speed at 2 m above ground surface ($m\ s^{-1}$)
γ	Psychrometric constant ($kPa\ °C^{-1}$)
Δ	Slope of saturation vapour pressure curve ($kPa\ °C^{-1}$)
Δs	Change in soil water storage (mm/month)
$\delta^{18}O$	Oxygen-18 (‰)

δ^2H	Deuterium (‰)
^3H	Tritium (TU)
ρa	Mean air density (kg m^{-3})
σ	Stefan-Boltzmann constant (4.903 10^{-9} MJ K^{-4} m^{-2} day^{-1})
φ	latitude (rad)
ωs	Sunset hour angle (rad)

CHAPTER ONE: INTRODUCTION

1.1. Background to the research

South Africa is a semi-arid country, where water resources are limited. The utilization of this limited water resources in a sustainable and wise manner is, therefore, essential for the future of the country (Davies, Lynn and Partners, 1992). Water in South Africa is recognized as a fundamental element in the fight against poverty, the cornerstone of its prosperity, and its shortage can be a limiting factor to growth (Basson *et al*., 1997). Thus, development and management of surface and groundwater resources is essential, particularly with respect to rural water supply, helping the previously disadvantaged communities through enabling economic development and poverty alleviation (Mkhwanazi, 2010; Kelbe and Germishuyse, 2010).

The National Water Act (Act 36 of 1998) recognises that water resources cannot be managed in isolation and that development and use of all surface water, groundwater and unconventional water resources are undertaken in a way that is sensitive to the environment. A greater understanding of the water resources and the processes that sustain them, hydraulically and ecologically, is therefore necessary.

The country is currently grappling with a devastating drought. The iSimangaliso Wetland Park in particular located in in the Maputaland region in north-eastern South Africa is being severely affected by the worst drought in 65 years (iSimangaliso, 2015), placing even further stress on the already limited resources.

The Maputaland region is characterized by a number of ecologically important coastal lakes. These coastal lakes, such as Lake Sibayi, are important hydrological features which have great scientific and economic value. Lake Sibayi, the largest inland freshwater lake in South Africa, is exploited for urban and rural water supply. Lake Sibayi and its catchment are intrinsically linked to the primary aquifer and provide a vital source of fresh water, which the ecology and local community depend on. It is therefore vital that all input and output parameters pertaining to the lake and its catchment are understood to allow for effective planning, development and management of the water resources of the area.

Historically, the inflow and outflow components of the Lake Sibayi system have been in dynamic equilibrium. Surface runoff, groundwater recharge and precipitation on the lake have, on an annual basis, equated to evaporation from the lake and groundwater outflow to the sea, resulting in relatively constant lake levels. Recently, groundwater abstraction from within the lake catchment and abstraction from the lake itself for local community water supply have commenced. This artificial

abstraction from the lake and groundwater that used to recharge the lake, compounded by the effects of the current drought, could have a significant impact on the lake level.

The current fresh water nature of the lake is due to a sustained flow of freshwater from the lake through the neighbouring coastal dune cordon into the ocean (Meyer *et al.*, 2001). However, should lake levels drop to mean sea level or lower, the rate of the flow through the dune cordon might not be sufficient to prevent the intrusion of saline water. Once the aquifer, and eventually the lake, is affected by salt water; it would alter the water quality thereby destroying the freshwater ecosystem.

Consequently, in order to prevent loss of one of South Africa's largest primary aquifers and potential salinization of the lake, it is vital that all components pertaining to the water balance of the Lake Sibayi system be understood, quantified and the interaction of lake-groundwater understood.

In recent years, groundwater modelling has become common practice when dealing with groundwater and surface water interactions (Anderson and Woessner, 1992; Wang and Anderson, 1995). Several computer programmes have been developed to integrate groundwater with surface water in order to quantify the interaction between them. The USGS three-dimensional finite-difference modular ground-water flow model (MODFLOW) (Harbaugh *et al.*, 2000, Harbaugh, 2005) has become one of the more popular and industry standard modelling tools to simulate such interactions. MODFLOW has several separate subroutines, or packages, to handle the numerous types of hydrological conditions. These represent certain hydrological processes including rivers, drains, evapotranspiration, wells, and lakes among others. Effective utilization of such models requires development of accurate conceptual hydrogeological models, and the availability of high-resolution time series data.

In order to make accurate predictions of the lake-groundwater interactions within the Lake Sibayi catchment, it was found necessary to develop a detailed numerical groundwater flow model based on an improved understanding of the hydrogeology of the area. This is achieved by integrating the information on geology, groundwater flow, hydrochemistry, environmental isotopes and aquifer boundaries which would help to construct the robust conceptual hydrogeological model. This high resolution conceptual hydrogeological model will be used as an input to develop the envisaged three-dimensional numerical model of the lake-groundwater interaction within the catchment. This numerical model would allow for accurate prediction of the flow system and provide realistic view of the lake-aquifer setting. The model would contribute to a detailed understanding of the lake-aquifer system, allowing for better groundwater resource planning and management, including monitoring and assessment of the scarce resources. The numerical model is pivotal in understanding the various processes and interactions of the hydrological elements.

1.2. Research aims and objectives

The principal aim of the research project is to establish the flow dynamics of the hydrogeological systems of the Lake Sibayi catchment. This would entail collection of all pertinent information relating to the surface water and groundwater interactions. The specific objectives of the research are:

- Characterise groundwater occurrence, movement and hydrochemistry: hydrochemical evolution patterns and its implication on circulation, flow, transfer and quality of groundwater within the Lake Sibayi catchment.
- Quantify the present day water balance of Lake Sibayi and its catchment.
- Quantify the effect of anthropogenic water abstraction from the lake and groundwater in the catchment and the effect it would have on the groundwater hydraulic gradient around the lake.
- Development of a conceptual hydrogeological model of groundwater and surface water interaction within the Lake Sibayi catchment which would serve as an input to a numerical model.
- To develop a three-dimensional groundwater flow model simulating the lake-aquifer interactions around Lake Sibayi and its catchment.
- Development of monitoring and management recommendations for the lake and its catchment water resources.

1.3. Thesis structure

The thesis is divided into eight chapters. The content of each chapter is summarized as follows:

Chapter one introduces the study, outlining the background and rationale, and the aims and objectives of the current research.

Chapter two presents a description of the study area in terms of the location, climate, drainage, hydrometeorology, physiography, land use and vegetation, coastal evolution, geology and hydrogeology.

Chapter three provides a literature review, outlining the processes involved in analysing the geological, hydrological, hydrogeological, hydrochemical and environmental isotope data. The approaches and methodologies related to the water balance estimation are reviewed. This chapter also offers background to the processes involved in both conceptual and numerical modelling and modelling of surface water-groundwater interactions in a coastal setting

Chapter four outlines the research approaches, methodology and the material used in the study to collect, analyse, and present the various data. The processes involved in conceptual and numerical model construction, data reduction and model input preprocessing for conceptual and numerical modelling are discussed.

Chapter five deals with the hydrogeological, hydrochemical and environmental isotope characteristics of the Lake Sibayi system.

Chapter six deals with the conceptual modelling of groundwater–surface water interactions in the Lake Sibayi catchment. Results of surface and subsurface geological information, groundwater head, hydrochemical and environmental isotope data analysis and interpretation of the conceptual model of aquifer– lake interaction are reported as well as the recharge estimation techniques, as well as the various water balance components for the lake.

Chapter seven presents the results of the three-dimensional numerical groundwater modelling of the Lake Sibayi system. All aspects pertinent to the numerical groundwater flow model around the lake are discussed. It includes the results of various scenario analyses to determine the effects of land use and climate change on the catchment.

Chapter eight highlights the main conclusions drawn from the research and indicates some recommendations based on the research results.

CHAPTER TWO: DESCRIPTION OF THE STUDY AREA

2.1. Location

Lake Sibayi is a coastal freshwater lake situated on the seaward margin of the Maputaland Coastal Plain along the northern KwaZulu-Natal coastline (Figure 2.1). The lake is situated approximately 180 km north of Richards Bay and 60 km from the Mozambique border, occupying a position between 27°15′ S to 27°25′ S and 32°33′ E to 32°43′ E. The Lake Sibayi catchment falls within the uMhlabuyalingana Local Municipality in the Umkhanyakude District Municipality situated in the north-eastern part of the KwaZulu-Natal Province. The neighbouring rural towns of Mbazwana and Mseleni are located around the periphery of the lake. The lake has an average surface area of 73 km^2, with a maximum depth of 41 m making it the largest inland freshwater lake in South Africa (Meyer *et al.*, 2001). The surface of the lake is located at approximately 20 m above mean sea level (amsl), with the bottom of the lake located at approximately 23 m below mean sea level (bmsl).

Recent satellite imagery (Google Earth, 2014) indicates that the surface area of the lake has been significantly reduced in recent years and currently has an average surface area of 56 km^2 with an updated total catchment area of approximately 521 km^2 (465 km^2 excluding the lake). The lake and its catchment fall within the W70A quaternary catchment and W3E rain zone (Middleton and Bailey, 2009; Midgley *et al.*, 1994) and within the Usutu-Mhlathuze Water Management Area (WMA 6). Lake Sibayi forms part of the iSimangaliso Wetland Park which has been given UNESCO World Heritage Site status and it is classified as one of the RAMSAR Convention Wetlands of International Importance (RAMSAR Site #528) (Obura *et al.*, 2012). Furthermore, the lake and rivers feeding the lake are classified as one of the National Freshwater Ecosystem Priority Areas (NFEPA) of South Africa (Nel *et al.*, 2011). The lake is of great ecological importance to the local community and is home to a large variety of fauna and flora. The lake is therefore a vital source of fresh water for the ecology and local community, and is often the only source of water for certain animals during periods of drought.

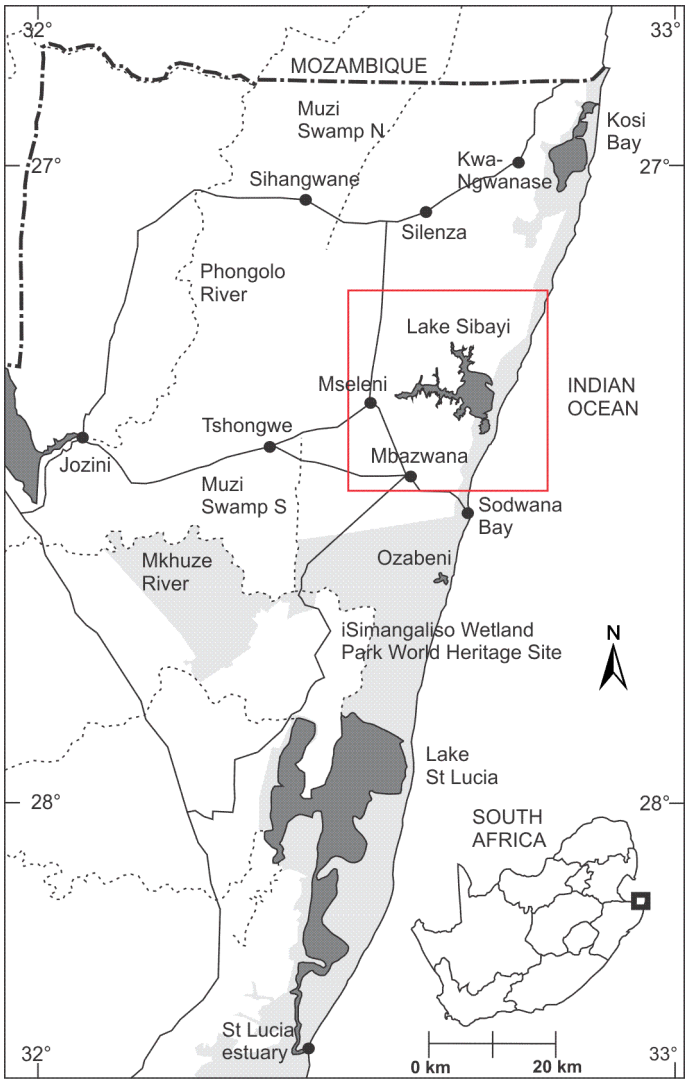

Figure 2.1. Location map showing Lake Sibayi and other coastal lakes of the Maputaland coastal plain.

2.2. Climate and Hydrometeorology

Climate has a strong influence on the water resources of a region. The surface and groundwater regime in the Maputaland coastal region is a direct response to local climatic conditions. The system is recharged through precipitation while evaporation causes depletion of surface and subsurface moisture. Hydrological processes such as surface runoff and the groundwater recharge rate are strongly influenced by the type of rainfall and its frequency. A thorough understanding of local weather conditions is therefore imperative for hydrological studies.

The region is characterised by a humid and wet subtropical climate with warm summer temperatures, dominated by the southern subtropical high-pressure belt (Boucher, 1975; Hunter, 1988; Money, 1988). Rainfall in the area is derived from both tropical and middle latitude weather systems (Garstang *et al.*, 1987). The tropical influence results in easterly waves which advect warm moist air

from the Indian Ocean in association with equatorial troughs and the Inter-Tropical Convergence Zone (ITCZ). Low-level convergence in the presence of unstable atmosphere produces frequent cumulus convective rainfall during the summer months (Kelbe *et al.*, 2001). Extreme rainfall events are brought about when occasional tropical cyclones over the Indian Ocean make landfall. Widespread frontal precipitation, producing heavy localised rainfall, result from westerly waves originating in the temperate middle latitude (Kelbe *et al.*, 2001). During the mid-1980s, the KwaZulu-Natal coast experienced two major flood events: Cyclone Domonia and Imboa, which made landfall during January and February 1984 respectively (Van Heerden and Swart, 1986, Kelbe *et al.*, 2001), and the September 1987 cut-off low pressure flood event (Wright, 1995). This resulted in increased lake levels over the corresponding time periods. Since the early 2000s, lake levels have started decreasing at a rapid rate.

A decade of regional drought was experienced from 2001 to 2012 resulting in below average rainfall recorded in the St Lucia area (Taylor, 2013). WRC (2016) compares the current 2015/2016 drought with the 1991-1992 drought which was regarded as the worst drought of the 20th century in southern Africa. The 1991-1992 droughts were brought about by a powerful El Niño event which was associated with below normal rainfall (WRC, 2016).

Due to a lack of comprehensive measurements from single stations, the use of multiple stations had to be employed to derive the required meteorological information for the study area. The Hlabisa Mbazwana Meteorological Station was used for precipitation readings; the Mbazwana Airfield Meteorological Station (established in 1997) was used for temperature, humidity and wind-speed data, while the Makatini Research Centre was used for sunshine duration (SAWS, 2015). All of these stations are located in the immediate vicinity of the research catchment with a summary of the data presented in Table 2.1 with a comprehensive set of measurements presented in Appendices A to D.

Table 2.1. Mean monthly meteorological data obtained from 1997 to 2014 at the Hlabisa Mbazwana, Mbazwana Airfield Meteorological Station and Makatini Research Centre (SAWS, 2015).

	Jan	Feb	Mar	Apr	May	Jun	Jul	Aug	Sep	Oct	Nov	Dec
Precipitation (mm)	139	150	97	73	34	41	25	26	62	80	126	94
Evaporation (mm)	179	154	148	111	85	60	68	96	121	142	158	177
Temperature (°C)	25.8	26.1	25.4	23.1	20.8	19.0	18.4	20.0	21.2	22.2	23.9	25.1
Humidity (%)	82.8	84.6	87.3	88.8	89.1	90.5	90.5	86.4	82.4	81.3	80.4	80.5
Sunshine (h/d)	6.4	7.0	7.1	7.0	7.3	6.7	7.2	7.7	6.6	5.5	5.7	5.9
Wind speed (m/s)	2.6	2.0	1.7	1.7	1.5	1.5	1.8	2.1	2.6	2.8	2.9	2.7

A strong season precipitation pattern is observed in the region (Figure 2.2) with most of rainfall occurring during the summer months (with over 40% falling in the 3-month period from January to March) with occasional cyclone activity. In general, the winter period experiences around 25% of the

summer rainfall. Potential evaporation rates for the Lake Sibayi area are high, peaking during the summer months. The rainfall distribution map (Figure 2.3), constructed based on data obtained from SAWS (2015), indicates an increase in precipitation in an easterly direction over the catchment. Precipitation in the region is generally found to increase from approximately 700 mm/a along the western margin of the catchment to approximately 1 000 mm/a along the coast. These latest rainfall data show a slight reduction in precipitation in the area when compared to those reported by Pitman and Hutchison (1975) which ranged from 700 mm/a in the southwest of the catchment to 1 200 mm/a in the east. These data are indicative of a gradual decrease in rainfall across the area. According to WR2005 (Middleton and Bailey, 2009), annual pan evaporation data ranged between 1 400 mm/a and 1 500 mm/a for the S class pans and between 1 800 mm/a and 2 000 mm/a for the A class pans. This is in agreement with the published evaporation maps of the region by Schulze *et al*. (1997). Temperatures also showed seasonal variation, however, more subdued than rainfall. Temperatures peaked in the summer months with the highest mean monthly temperature experienced in February (26.1°C), while the lowest temperatures were experienced in July (18.4°C).

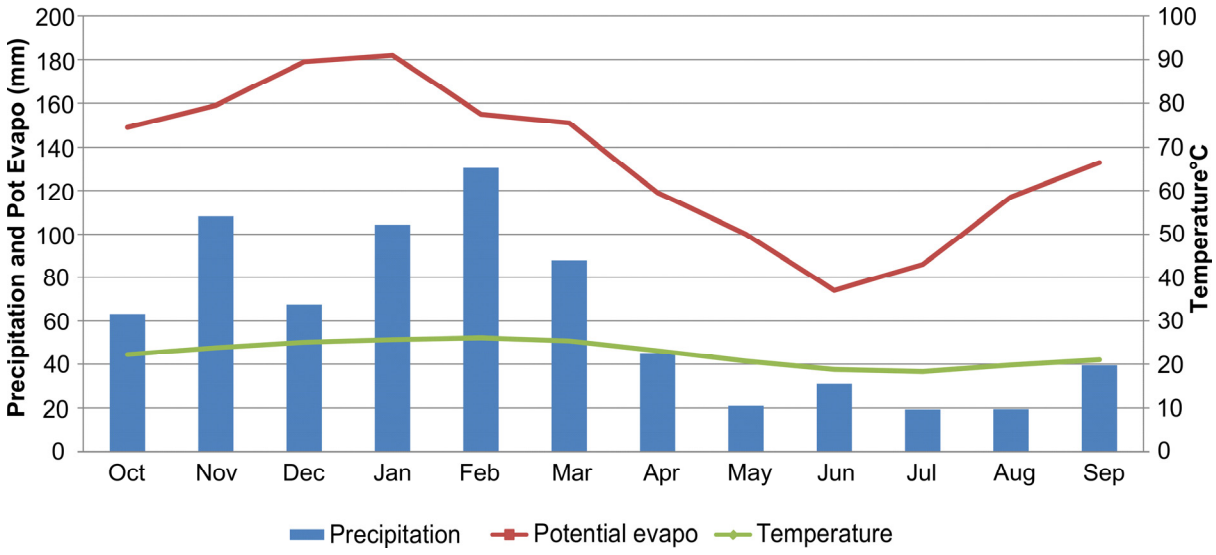

Figure 2.2. 15 year average meteorological variables from the Mbazwana Airfield Station (data sourced from SAWS, 2015).

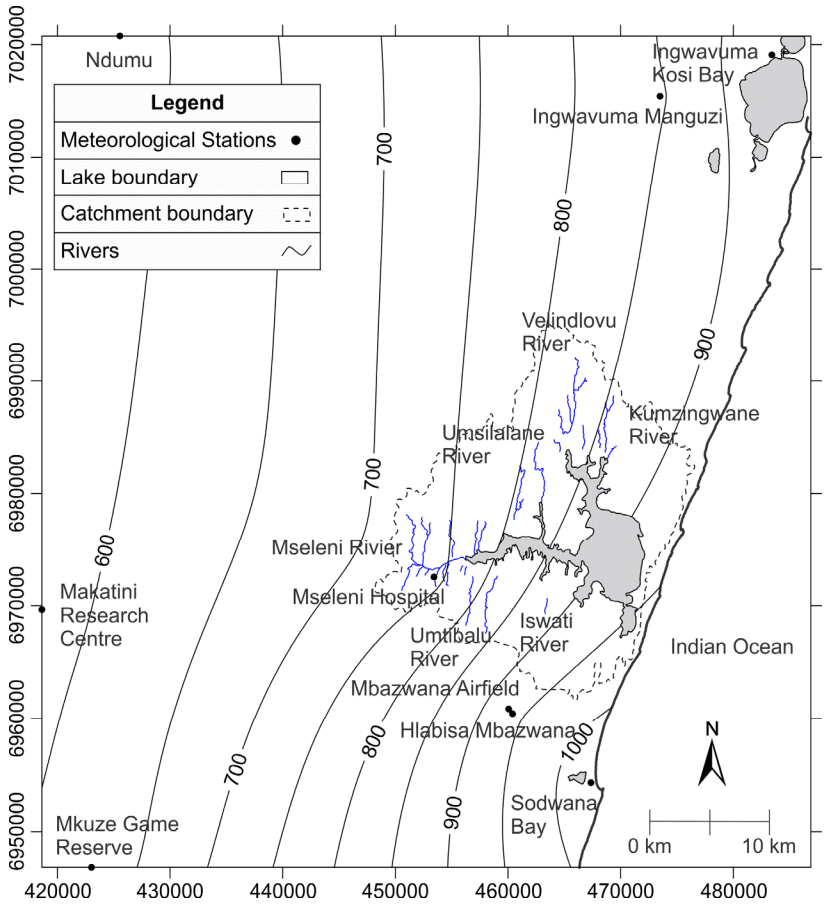

Figure 2.3. Rainfall distribution over the Lake Sibayi catchment (mm/a) from 1990 to 2013 (SAWS, 2015).

North to north-easterly winds prevail during the summer months while winter experiences both northerly and southerly winds (Wright, 1999). The southerly winds have greater velocities but tend to blow less frequently than the northerly winds (Wright and Mason, 1993). The mean wind speed measured at the station was 2.22 m s^{-1} while maximum gust speeds of up to 23.7 m s^{-1} were measured at the Mabibi School, adjacent to Lake Sibayi. Dominant wind directions are NE and SW (Diab and Sokolic, 1996).

2.3. Physiography and Drainage

The topography of the Maputaland coastal plain region made up of ancient to young sandy dunes which have relatively elevated topography and low-lying plains to the east and a series of rugged terraces deeply incised by river valleys in the central and western parts. Most of the region is covered by the recent, infertile, wind distributed (aeolian) sands. This resulted in the formation of a series of north-south trending dune ridges orientated parallel to the present coastline (Goodman, 1990) (Figure 2.4).

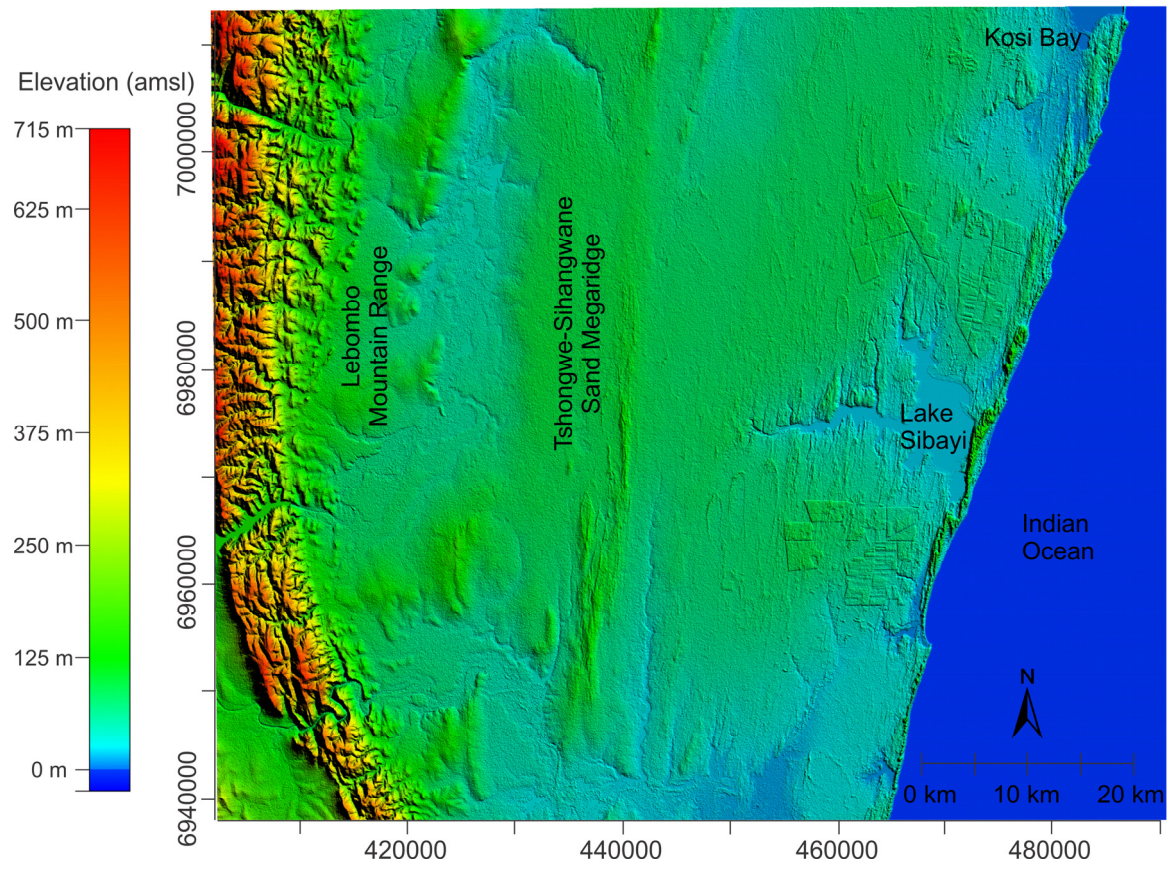

Figure 2.4. Topographic surface of the area surrounding Lake Sibayi with significant regional features

The sandy substrate of the catchment coupled with a relatively flat topography and shallow water table result in a close relationship between surface waters of the lake and the groundwater. This relationship is evident as the lake forms a surface expression of the groundwater (Meyer *et al.*, 2001). The lake is essentially underlain by unconsolidated to semi-consolidated fine sands that blanket most of the Maputaland coastal plain. These highly permeable sediments, which are mainly Cretaceous to Quaternary in age, abut landward against late Karoo volcanics of the Lebombo Mountain Range (Hobday, 1979) and promote rapid recharge to the shallow aquifer (Kelbe and Germishuyse, 2010). Relatively thin, discontinuous, shallow marine and beach deposits of Tertiary age unconformably overlie the Cretaceous sediments, while Quaternary age sediments of a variety of depositional environments form the cover sediments for most of the coastal plain (Hobday, 1979). These highly permeable sediments promote rapid recharge to the aquifers and strong interactions with wetlands in the region (Mkhwanazi, 2010).

The lake is cut off from the sea by a series of high north - south trending forested sand dunes, thereby having no connection to the sea. The dune ridge attains a maximum height of 172 m in the vicinity of Ntambama, opposite the lake. During its evolution, the Lake Sibayi system was separated from the sea by the dunes, allowing it to evolve from a saline lagoon to a freshwater system (Roberts *et al.*, 2006).

Lake Sibayi and its associated rivers and wetlands are predominantly groundwater driven as the sandy substrate within the plain limits the amount of surface runoff (Pitman and Hutchinson, 1975; Kelbe and Germishuyse, 2010). The water levels within Lake Sibayi constantly fluctuate in response to varying amounts of groundwater and surface water discharge into the lake, seepage loss through the coastal dunes, abstraction, and evaporation from the lake surface (Maud, 1980; Miller, 2001). Water levels in Lake Sibayi are highly sensitive to local weather conditions and show direct responses to local rainfall conditions and seasonal cycles (Pitman and Hutchinson, 1975).

The only significant surface drainage feature for the Lake Sibayi catchment is the Mseleni River feeding the western arm of the lake. The non-perennial KuMzingwane and Velindlovu streams feed into the northern arm of the lake, while the Umtibalu and Iswati streams and the Umsilalane stream feed the southern and northern portion of the western arm, respectively (Figure 2.3).

2.4. Vegetation and land cover

The catchment of Lake Sibayi falls into the Coastal Lake Zone proposed by Mountain (1990). This area is characterised by a chain of barrier lakes, lagoons and swamps, situated behind high vegetated dunes. The vegetation within the catchment consists predominantly of grassland (natural and degraded) flanked by forests along the coastal dune cordon, dense bush along the western extremes and exotic plantations to the north and south of the lake (Figure 2.5). Only a very small percentage, nearly 2%, of the catchment is occupied by rural urban or built-up areas (Ezemvelo KZN Wildlife, 2011). The lake and large portions of the eastern coast forms part of the iSimangaliso Wetland Park conservation area.

The area surrounding Lake Sibayi is covered extensively by plantations; the most prominent of these are the Mbazwana and Manzengwenya plantations situated on the southern and northern side of the catchment, respectively. A large scale cashew nut plantation is situated northwest of the lake while numerous small scale plantations are scattered throughout the catchment. These plantations occupy approximately 221 km^2 (Ezemvelo KZN Wildlife, 2011) with approximately 88 km^2 situated within the lake's catchment. The exotic plantations consist mainly of Eucalyptus grandis, Eucalyptus camaldulensis (51%) and Pinus elliottii (34%), while the remaining 15% of the plantation is clear-felled (Ezemvelo KZN Wildlife, 2011). Evapotranspiration rates by the plantations are higher than that of the natural vegetation (Albaugh et al., 2013) and therefore any expansion of the plantation would increase the loss of water from the catchment. Plantations utilise soil water, preventing aquifer recharge or by extracting water directly from below the root zone and capillary fringe, resulting in a lowered groundwater table (Kienzle and Schulze, 1992; Scott, 1993). The evapotranspiration rate for commercial forestry, usually pine and eucalyptus plantations, has been calculated by numerous

authors. The evapotranspiration rate was found to range from 1000 mm/a (Sunder, 1993) to over 2500 mm/a (Albaugh et al., 2013).

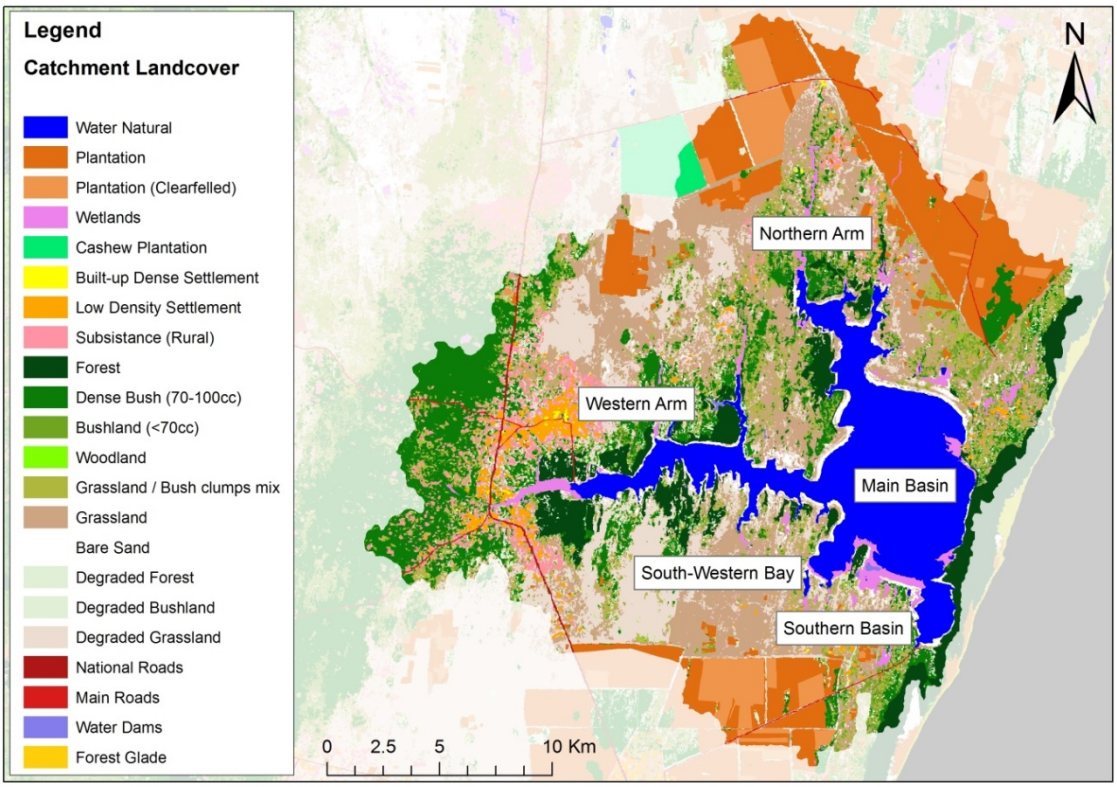

Figure 2.5. Land use distribution within the Lake Sibayi catchment (Ezemvelo KZN Wildlife, 2011).

2.5. Population and water use

The uMhlabuyalingana Local Municipality has seen population growth rates of approximately 11% over the period 1996 to 2001 (2.2 % pa) and approximately 10 % from 2001 to 2011 (1 % pa) (Statistics South Africa, 2012) (Figure 2.6).

The proportion of the population with access to piped water, either private or communal, has increased from 2 % to 12 % during the period 1996 to 2011, while the proportion of the population without access piped water has decreased from 13 % to 9% during the same period. The distribution of water sources in the municipality primarily originate from regional/local municipal water schemes (41%), followed by boreholes (30%), and rivers and streams (13%), while the remainder is made up of a combination of springs, rain water tanks, water tankers and others (Statistics South Africa, 2012).

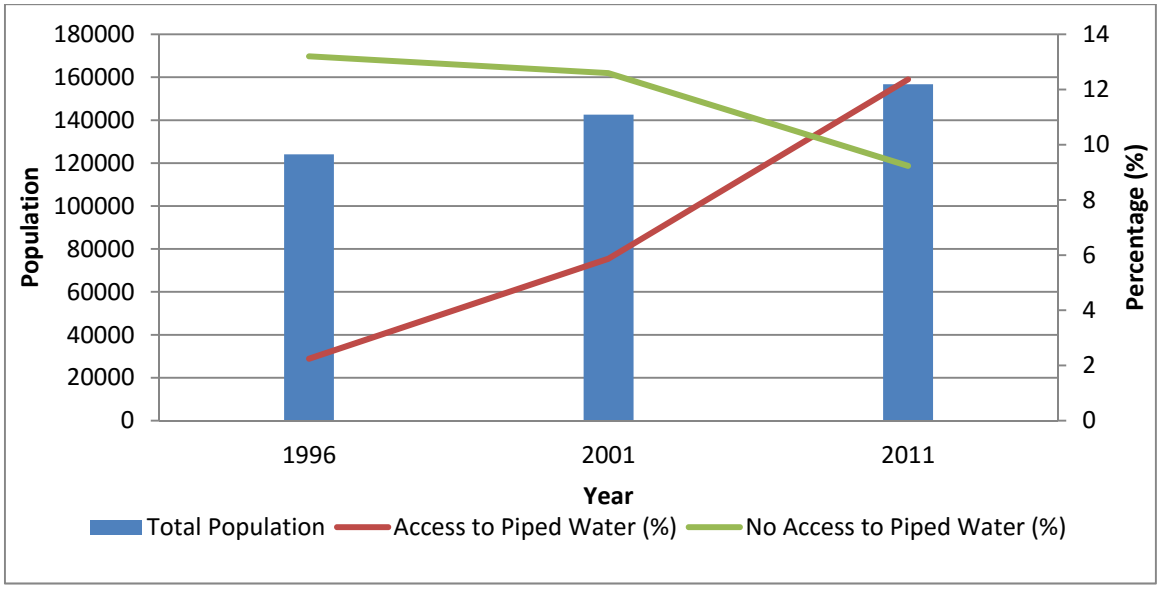

Figure 2.6. Population growth for the uMhlabuyalingana Local Municipality (1996 to 2011) showing percentage of population with access to piped water and those without any access to piped water (Statistics South Africa, 2012).

In recent years, significant development has occurred around the lake, which has been brought about primarily through human settlement and land use change (Bruton *et al.*, 1980; Combrink *et al.*, 2011). These new developments are located within the lake's catchment, which does not fall within the conservation area, making conservation and management of the lake challenging. Catchment activities include commercial forestry, subsistence agriculture, and rural development, particularly near the town of Mseleni. The increase in water demand has prompted the then Department of Water Affairs and Forestry to undertake a reserve determination of Lake Sibayi for additional lake abstraction (Meyer and Godfrey, 2003).

2.6. Lake Morphology and Bathymetry

Lake Sibayi can be divided into five morphological regions, the Main Basin, Northern Arm, Western Arm, South-Western Bay and Southern Basin (Figure 2.5). The Main basin is the largest of these, comprising almost 60% of the area of the lake and containing the deepest water. The roughly oval shaped Main Basin is characterized by straight or gently curving shorelines, punctuated by sand bodies or dune ridges (Miller, 2001). Two smaller regions in the south, the South-Western Bay and Southern Basin account for about 9% of the lake area. The Northern and Western Arms of the lake are extremely dendritic and make up about 12 to 20% of the lake area. These two regions have however several non-perennial streams of varying sizes draining into them (Hill, 1979; Miller, 2001). The Northern and Western Arm as well as the South-Western Bay seem to be continuous with the bathymetric profile running across the floor of the Main Basin. The Southern Basin however shows no continuation and is nearly isolated from the Main Basin (Hill, 1979).

The morphology of Lake Sibayi is a result of Neogene and Pleistocene low sea-level still stands that allowed for the development of incised channels into the underlying Cretaceous and Palaeocene sedimentary sequences (Wright *et al*., 2000). The dendritic nature of the Western and Northern Arms, combined with the fact that large portions of the lake is situated below sea-level, indicate that Lake Sibayi represents a series of drowned river valleys that were cut when sea level was significantly lower (Ramsay, 1991; Miller, 2001). Rapidly dropping sea levels experienced after the Last Interglacial high stand (125,000 BC) led to incision of fluvial channels down to 10 m below sea level, forming a broad shallow depression in the vicinity of Lake Sibayi. Stabilisation of sea levels led to the re-establishment of the coastal dune barrier and the development of lagoonal conditions behind it (Wright *et al*., 2000; Wright, 2002). Regressive marine conditions experienced during the period leading up to the Last Glacial Maximum (18,000 BP), when sea level was about 125 m lower than present (Green and Uken, 2005), caused increased hydraulic head between the lake and dropping sea level. This resulted in breaching of the coastal dune barrier and subsequent scour of a NW–SE orientated channel down to depth of more than 40 m bmsl. This scour is still reflected in the bathymetry of Lake Sibayi (Wright *et al*., 2000; Miller, 2001; Wright, 2002). Infilling by marine wash-over deposits during the Holocene transgression (7000–5000 BP) isolated the lake from the sea by the re-establishment of the coastal dune barrier, resulting in the impoundment of lake water. Following the re-establishment of the dune barrier, the lake has evolved into a completely freshwater system with lake levels having risen to 20 m amsl (Wright *et al*., 2000; Miller, 2001).

Bathymetric readings taken by Miller (2001) were obtained from the Council for Geoscience. The raw data was contoured and blanked using modern satellite images obtained from NASA (2006) to produce the updated bathymetric map (Figure 2.7). The relevant measurements were referenced against a height of 19.82 m amsl correlating to lake levels during May 1992 when the survey was conducted.

The lake has undergone little sedimentation since its formation, as the narrow steep-sided valleys are still preserved as can be seen in the bathymetric map of the lake (Figure 2.7). This could be as a result of the relatively low amount of surface inflow and the fact that its small catchment is sandy and flat. During high lake levels, erosional forces increase the supply of sand to the eastern shore. The current drought conditions and associated low lake levels have accentuated the two sand spits in the vicinity where the Southern Basin joins the Main Basin. As these spits continue to grow, segmentation of the lake becomes more prominent where the Southern Basin might eventually become completely isolated from the rest of the lake (iSimangaliso, 2015).

The storage capacity of Lake Sibayi was derived from the above-mentioned bathymetric survey data of Miller (2001). Based on the bathymetric surface compiled, the capacity of the lake, at the time of

the survey (lake level of 19.82 m amsl), was approximately 816 x 10^6 m^3 corresponding to an area of 73 km^2.

The depth-area and depth-volume relationships were constructed using the bathymetric data compiled by Miller (2001) and are presented in Figures 2.8 and Table 2.2. The results show that both area and volume decrease drastically down to depths of approximately 24 m; this can be attributed to the predominantly shallow nature of the lake. After depths of approximately 24 m, area and volume decrease at a much slower rate, due to limited areas of greater depth (Miller, 2001).

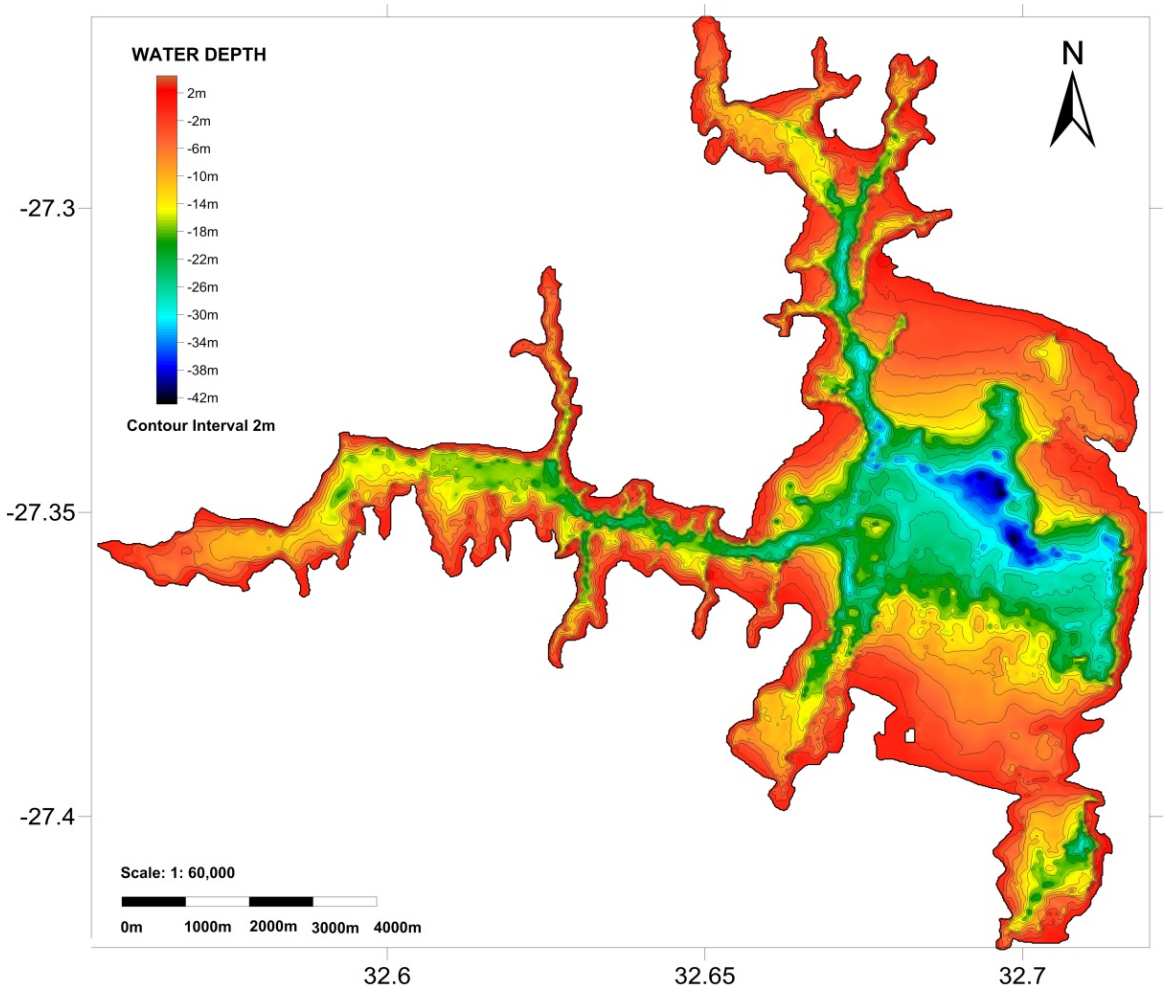

Figure 2.7. Bathymetric map of Lake Sibayi (interpolated based on data from Miller, 2001).

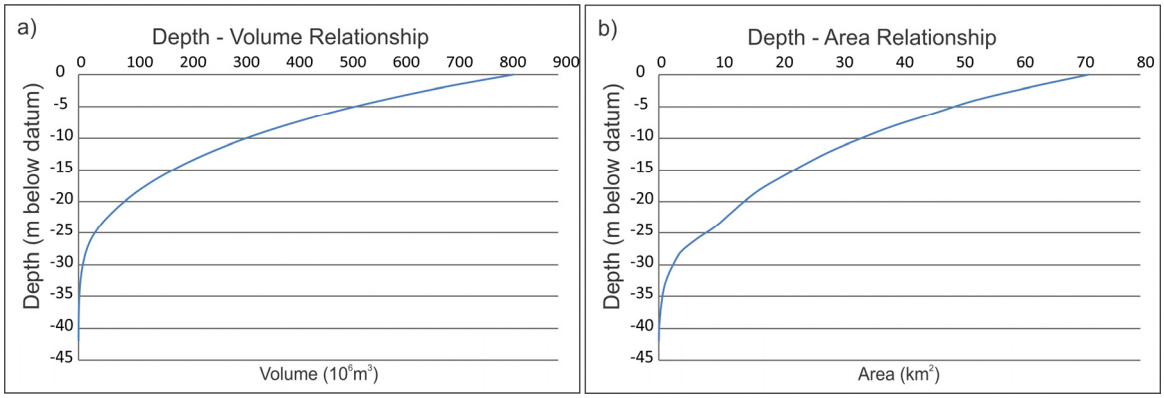

Figure 2.8. Depth – Area (a) and Depth – Volume (b) relationships for Lake Sibayi.

Table 2.2. Depth - area - volume relationships.

Depth (m)	Volume (10^6m^3)	Area (km^2)
0	816	73
-4	569	52
-8	386	39
-12	252	29
-16	155	21
-20	86	14
-24	39	9
-28	14	4
-32	4	1
-36	1	0
-40	0	0

2.7. Geological Setting

The nature of the geological strata governs the basic physical features of the aquifers of the Maputaland coastal plain, while the geological processes occurring during formation define the physical and chemical characteristic of the aquifer (Mkhwanazi, 2010).

Lake Sibayi lies on the Maputaland coastal plain which stretches from the Umlalazi River in the south, up the coast of Maputaland and northward through Mozambique. The entire Maputaland coastal plain (Figure 2.9) was formed in recent geological time (post Cretaceous) through erosion and deposition along the marine zone (Kelbe *et al.*, 2001; Mkhwanazi, 2010). The Lake Sibayi system is one of the few coastal water bodies along the South African coastline that has its palaeotopography partially preserved as a surface feature (Wright *et al.*, 2000).

2.7.1. Lebombo Group

Regionally, the oldest rock exposures in the Maputaland area are the mafic picritic/olivine-rich continental flood basalts of the Letaba Formation and the rhyodacites and rhyolites of the Jozini Formation (Watkeys *et al.*, 1993, Botha and Singh, 2012). These two units of the Jurassic age

Lebombo Group, outcrop to the west of the coastal plain as the Lebombo Mountain range. The Lebombo Group is the uppermost of the Karoo Supergroup (Wolmarans and Du Preez, 1986, Joubert and Johnson, 1998). The volcanic suite is draped over a major crustal fracture and dips eastward under the Cretaceous and Cenozoic sediments of the Maputaland coastal plain (Dingle *et al.*, 1983).

2.7.2. Zululand Group

The Cretaceous age Zululand Group, comprising thick successions of marine sediments deposited during the Mesozoic era, unconformably overlies the Lebombo Group volcanic rocks (Dingle *et al.*, 1983, Botha and Singh, 2012). The succession comprises the Makatini, Mzinene and St Lucia Formations which are exposed in the eastern Lebombo foothills (Kennedy and Klinger, 1975, Shone, 2006). The Makatini Formation comprises small-pebble conglomerates, sandstones, siltstones and limestones. The Mzinene Formation consists of glauconitic siltstones and cross-bedded sandstones containing fossils and shell fragments. The composition of the overlying St Lucia Formation is similar to the underlying Mzinene Formation but contains abundant plant and marine invertebrate fossils (Dingle *et al.*, 1983). Coastal upliftment and regressive conditions resulted in the erosion of the marine strata to create a gently seaward dipping surface of 1 to 3 degrees (Worthington, 1978).

Transgressive and regressive alluvial processes have left significant palaeo-channels in the St Lucia Formation. Investigations by Miller (2001) indicated the presence of a subsurface paleo-channel, acting as a preferential pathway of lake water to the sea, along the eastern shore of Lake Sibayi. The channel has subsequently been filled with Holocene age sediments. Geophysical investigations undertaken by Meyer *et al*. (2001) estimated that the paleo-channel has an average depth of 100 m bmsl.

2.7.3. Maputaland Group

The Cenozoic deposits along the northern KwaZulu-Natal coastline are the youngest in the study region and comprise the sediments of the Maputaland Group (Figure 2.10). These deposits unconformably overlie the upper Cretaceous sediments, forming a thin veneer of sediments overlying the coastal region (Botha, 1997; Maud and Botha, 2000). The deposits of this age include those of littoral marine, estuarine, lacustrine and aeolian origin. These were deposited in response to a long series of marine transgressions and regressions, induced by glacio-eustatic sea-level changes, and by uplift and seaward marginal tilting of the subcontinent during the Neogene and Quaternary (Maud and Botha, 2000).

The late Miocene Uloa Formation (Maud and Orr, 1975; Stapleton, 1977; Cooper and McCarthy, 1988; Watkeys *et al.*, 1993; Lui, 1995, Roberts *et al.*, 2006) comprises an intermittent sequence of calcified coquina, conglomerates, sandstone and siltstone. The coquina, known locally as the “Pecten

Bed", attains a thickness of approximately 5 m (Dingle *et al*., 1983; Lui, 1995; Roberts *et al*, 2006). The coquina is overlain by up to 20 m of aeolian cross-bedded calcarenites in places (Wright, *et al*, 2000) which was initially regarded as the Upper Uloa Formation (Frankel, 1966; Maud and Orr, 1975; Cooper and McCarthy, 1988; Lui, 1995). A marked lithological break exists between the calcarenites and the underlying coquina (Maud and Orr, 1975; Lui, 1995) it was therefore suggested by Botha (1997) that this unit be given a separate formation status, namely the Umkwelane Formation.

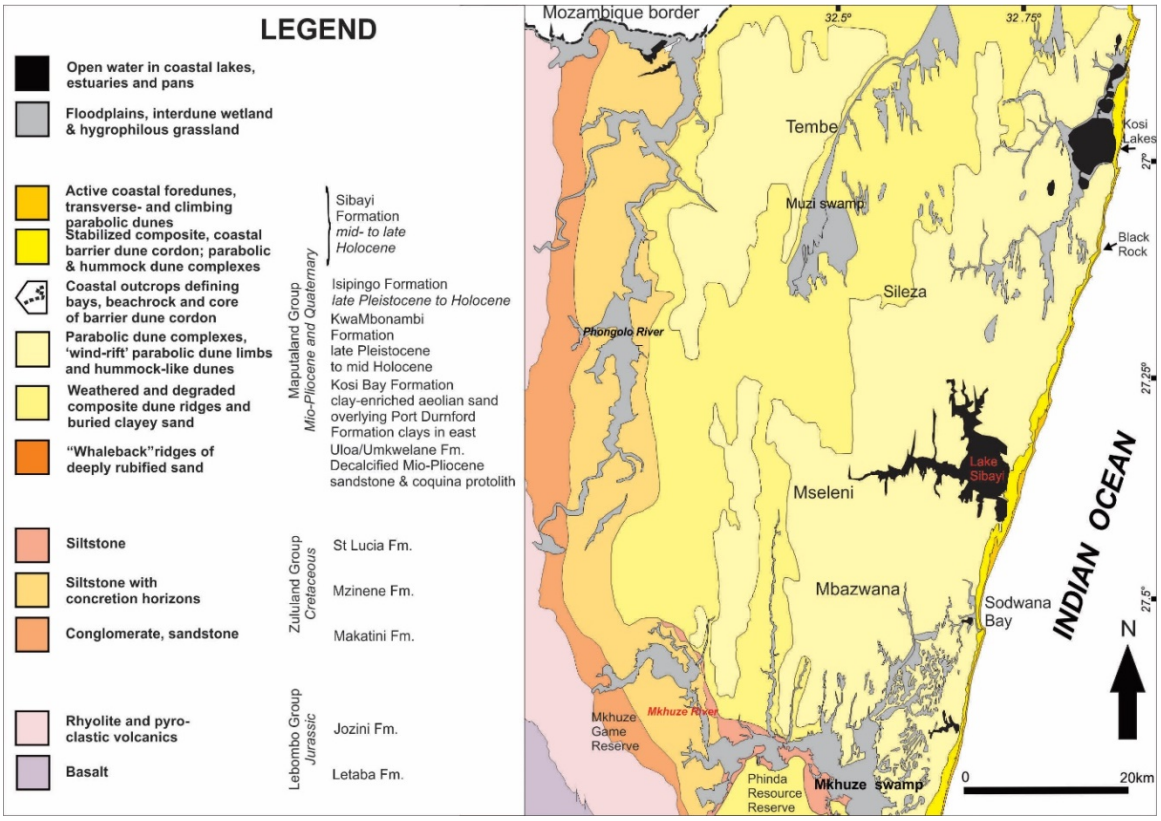

Figure 2.9. Geological map of the study area (Modified from Porat and Botha, 2008).

The early Pliocene Umkwelane Formation, comprises up to 25 m of cross-bedded aeolianites (Stapleton, 1977), which commonly overlies the stratified shallow-marine calcarenite (5-8 m thick) and interbedded gravel beds of the Uloa Formation (Maud and Orr, 1975; Lui, 1995, Roberts *et al.*, 2006). The argillaceous dune sands in the area, previously mapped as the Muzi Formation (Geological Survey, 1985 a, b), are now considered to be the weathering product of Umkwelane Formation (Botha *et al.*, 2003; Botha and Porat, 2007; Porat and Botha, 2008; Botha and Singh, 2012). The top of the Unkwelane Formation coincides with mean sea-level in the Richards Bay area with minor fluctuations between -10 m and +5 m amsl (Worthington, 1978).

Deposits of these intermittent layers generally coincide with higher regions of the Cretaceous siltstone, suggesting that they also underwent erosion during periods of transgression. The full extent of this formation is uncertain due to the limited number of boreholes in the area.

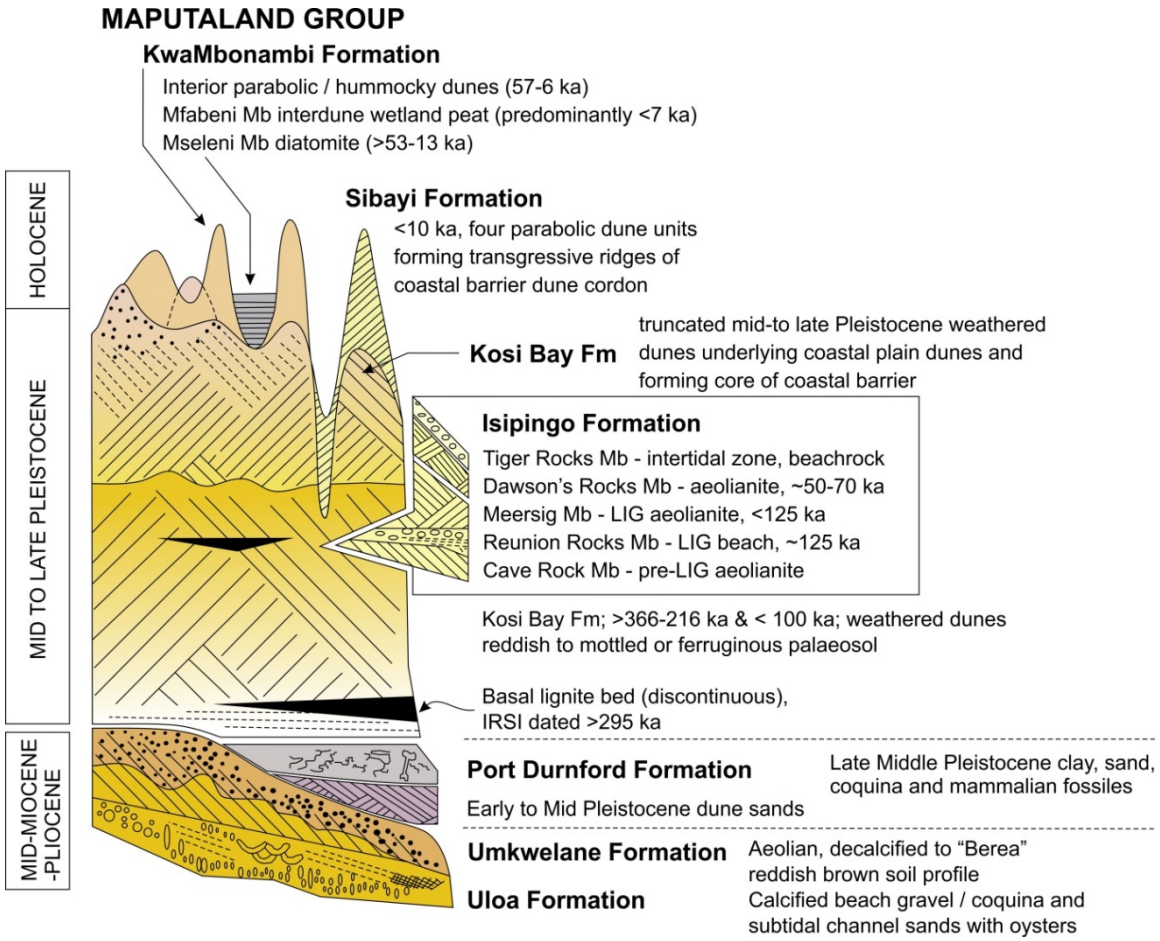

Figure 2.10. Schematic representation of the Maputaland Group lithostratigraphic units. Not to scale. LIG-Last Interglacial (adapted from Porat and Botha, 2008).

The Early to Late Pleistocene age sediments of the Port Durnford Formation ("Lower Argillaceous Member" described by Hobday and Orme, 1974 and SACS, 1980) rest unconformably on either Cretaceous sediments or the Uloa and Umkwelane Formations. The sediments of the Port Durnford Formation, resting unconformably on stratified sands in the type area, comprise a succession of carbonaceous muds and sands. A basal bioturbated, cross-bedded sandstone with ferruginous mottles is overlain by grey or black fossiliferous shallow marine sands and organic-rich lagoonal clays (Hobday and Orme, 1974; Maud, 1993, Roberts *et al.*, 2006). The unit is up to 10 m thick and is overlain by a distinctive 1 - 1.5 m thick lignite horizon (Hobday and Orme, 1974; Maud, 1993). Hobday and Orme (1974) consider the Lower Argillaceous Member to be a transgressive barrier-lagoon complex which is related to the last interglacial high stand ca. 120 000 BP. Fossiliferous beach rocks considered to be contemporaneous with the last interglacial high-stand are elevated ca. 3.5 m amsl on the Nibela Peninsula at Lake St. Lucia (Wright *et al.*, 2000).

The lignite bearing unit overlying fossiliferous strata of the Port Durnford Formation, as well as the overlying white and orange mottled clayey sand, which Hobday and Orme (1974) considered the "Upper Arenaceous Member", is now considered to be the Kosi Bay Formation (Roberts *et al.*, 2006).

With similar sand deposits underlying younger dune sand, they cover over much of the coastal plain. The predominantly non-calcareous, uncemented sediments of the Kosi Bay Formation, resting unconformably on the Uloa, Umkwelane and Port Durnford Formations, comprise composite, multi-phase dune-sand deposits. These deposits form the core of coastal dune cordon as well as the lower parts of the inland dune cordon exposed around the coastal lakes (Roberts *et al.*, 2006). Over large parts of the Maputaland area north of Lake St Lucia, the unit averages a thickness of about 45 m and underlie the younger cover sands (10-15 m thick) and dune systems which have been derived from reworking of this older, pedogenically weathered dune sands (Roberts *et al.*, 2006).

The KwaMbonambi Formation comprises extensively reworked sediments of the underlying Kosi Bay Formation during marine regression and dry periods spanning from Late Pleistocene to Holocene transition (Botha and Porat, 2007). The resulting sediments consist of decalcified dune sediments, redistributed sand, coastal wetland deposits and freshwater diatomite accumulations (Botha, 1997). Relic cordons of late Pleistocene dunes dominate the eastern margin of the coastal plain particularly in the Lake Sibayi region, creating a characteristic low undulating topography (Wright, 1995; Miller, 1998; Wright *et al.*, 2000). Freshwater diatomite deposits and calcareous clays, banked up against the late Pleistocene dunes on the western shores of Lake Sibayi near Mseleni and south of Mbazwana, attain a thickness of up to 4m and developed during the period 45 000 to 25 000 years BP (Maud 1993; Miller, 1996; Miller, 2001; Porat and Botha, 2008). The surface of the 143 m high Tshongwe-Sihangwane sand megaridge, located inland of the coastal lakes of Lake Sibayi and Kosi Bay (Figure 2.4), is formed of low KwaMbonambi Formation parabolic dunes (Botha and Singh, 2012).

The Late Pleistocene to Holocene Isipingo Formation comprises the intertidal rocky outcrops in the calcified dune deposits (aeolianite) and beachrock (Botha and Singh, 2012). These represent dune accretion and sea-level still-stand events spanning the past 200 000 years (Ramsay, 1995, 1996; Wright *et al.*, 2000, Ramsay and Cooper, 2002, Porat and Botha, 2008). The last major marine regression (~110 to 18 ka) allowed for the formation of dunes on the exposed continental shelf as sea-level dropped to -130 m (Green and Uken, 2005). These calcified dune deposits were subsequently submerged due to increasing sea-levels over the past 18 000 years forming significant structures on the continental shelf (Martin and Flemming, 1988).

The Holocene age Sibayi Formation represents the high coastal barrier dune stretching along the shoreline from St Lucia estuary to the Mozambique border. It is a composite aeolian deposit, comprising a core of Kosi Bay and Isipingo Formation dune sands overlain by at least four phases of parabolic dune accretion over the past 10 000 years (Porat and Botha, 2008). The Sibayi Formation attains a thickness of up to 150 m in certain areas (Maud and Botha, 2000; Porat and Botha, 2008).

2.7.4. Recent Lake Sediments

Due to its small catchment area and limited amount of runoff, the amount of fluvial sediment reaching Lake Sibayi is restricted; therefore Lake Sibayi has undergone very little sedimentation since its formation (Miller, 2001). The only new sediments introduced to the lake are wind-blown sediments and organic sediment that are added during high lake levels. During high water levels, large areas surrounding the lake are inundated by water, causing vegetation destruction and erosion of the surrounding dunes (Allanson, 1979). Decaying vegetation is transferred rapidly by wave action into deeper areas of the lake, where it contributes to the lake sediments in the form of a dark-brown to grey-black, organic rich, pulpy, anaerobic fresh-water sapropel termed gyttja (Wright and Mason, 1990; Miller, 1994, Wright 2002). Aeolian sediments, which are stripped from surrounding dunes during high lake levels, accumulate in shallow areas of the lake (Miller, 1998).

2.8. General Hydrogeological setting

The hydrogeological units which constitutes the primary aquifer in the Maputaland region comprises shallow marine, alluvial and Aeolian sediments overlying the Cretaceous sediments (Meyer *et al.*, 2001; Kelbe and Germishuyse, 2010).

The Cretaceous-age succession of mainly fine siltstones, conglomerates and sandstones collectively known as the Zululand Group underlie the Miocene to Holocene sediments of the Maputaland Group. Due to very low permeability, groundwater quality and quantity, the Zululand Group can be regarded as the impermeable basement to the overlying sediments (Meyer and Godfrey, 2003).

The Cretaceous rocks are overlain by the Mio-Pliocene Formation and decalcified and locally karst weathered Umkwelane/Uloa Formations which constitute the main aquifer in the region (Jeffares and Green, 2012; Kelbe *et al*., 2013; Worthington, 1978). Thicknesses of up to 35 m were encountered in the north and north-west of the Lake Sibayi catchment (Kruger and Meyer, 1988).

These units are overlain by a thick succession of low-yielding silty sands and silts of the Late Pleistocene Kosi Bay Formation (Porat and Botha, 2008). The elevation of the upper surface of this unit was found to increase from 50 m amsl in the southeast of the lake (Fockema, 1986; Kruger and Meyer, 1988; Davies, Lynn and Partners, 1992) to 60 m amsl towards the north-west of the lake (Meyer, 1994).

The Kosi Bay Formation is overlain by shallow unconfined sediments associated with the superficial dune sands of the Late Pleistocene KwaMbonambi Formation (Botha and Porat, 2007; Porat and Botha, 2008). The final sedimentary unit is the Holocene Sibayi Formation which constitutes the coastal barrier dune cordon (Botha and Porat, 2007). Thicknesses for these cover sands were found to exceed 70 m in places (Meyer and Godfrey, 2003).

CHAPTER THREE: LITERATURE REVIEW

3.1. Previous hydrogeological studies on the Coastal Plain

Over the years, numerous hydrogeological investigations, of various scales, have been conducted over various parts of the Maputaland coastal plain. The more prominent investigations were those conducted by Van Wyk (1963), Australian Groundwater Consultants (1975), Worthington (1978), Meyer *et al*. (1982), Kruger (1986), Kelbe and Rawlins (1992), and some more recent detailed investigations of well field developments east of Kwambonambi (Meyer *et al*., 2001). The studies conducted by Van Wyk (1963) and Kruger (1986), concentrated on the northern parts of the coastal plain, whereas those by the Australian Groundwater Consultants (1975) and Worthington (1978) focused on the area around Richards Bay, Lake Mzingazi and Lake Nhlabane.

Worthington (1978) adopted an integrated approach where geophysical and hydrogeological investigations were directed at a detailed evaluation of the hydrological conditions around Richards Bay and Lake Mzingazi. Through geoelectrical surveys and pumping tests, he was able to establish the distribution and hydraulic characteristics of the Miocene age compacted coquina and calcarenite. Isopleths of aquifer transmissivity has been used by Worthington (1975) in conjunction with the distribution of potentiometric levels to estimate the subsurface seepage into Lake Mzingazi. He further revealed that the coastal dunes, which reach an elevation of up to 130 m amsl, are virtually dry and do not contain any perched water tables.

Several hydrogeological investigations of the aquifer were commissioned by the Water Research Commission and conducted by the University of Zululand (Kelbe *et al*., 2001; Kelbe and Germishuyse 2010) and a joint venture between the CSIR and the University of the Free State (Meyer *et al*. (2001). In addition, several hydrological studies were conducted on the coastal lakes that frequent the plain. The predominant studies on the northern parts of the plain were conducted by Hutchinson and Pitman (1973) and Pitman and Hutchinson (1975) of the Hydrological Research Unit of the University of the Witwatersrand, focusing on Lake St Lucia and Lake Sibayi respectively.

Hydrogeological modelling of the Maputaland Coastal Plain Aquifer was undertaken by Meyer *et al*. (2001). All the ancillary hydrogeological information such as the geophysical results and hydrochemical analyses were incorporated into a conceptual hydrogeological model of the coastal plain. Based on the conceptual model, a regional mathematical simulation model was designed to simulate steady-state conditions and determine regional groundwater flow directions and velocities.

The geology and morphometry of Lake Sibayi has been studied in detail by Miller (2001), where the morphology, bathymetry, sediment distribution and stratigraphy were reported. A preliminary effort to map the surrounding aquifer has been presented by Meyer and Godfrey (1995). Due to the increase in water demand in the Lake Sibayi area, the then Department of Water Affairs and Forestry

commissioned Meyer and Godfrey (2003) to undertake a reserve determination of the lake to determine the sustainability of additional abstraction.

3.2. Groundwater Modelling

A model is a tool designed to represent a simplified version of reality (Anderson and Woessner, 1992). A model is any device which represents an approximation of a field situation. Physical models, such as laboratory sand tanks simulate groundwater flow directly, while mathematical models simulate groundwater flow indirectly by means of a governing equation to represent the physical processes that occur in the system. The latter would also require equations which describe the heads or flows along the boundary of the model (boundary conditions) as well as the initial head distribution (initial conditions) in time-dependent problems. When these simulations become too complex, a numerical model may be selected. The model is based on a set of commands used to solve a mathematical model which forms the computer program or code. The code is generic, while the model, with its user specified parameters, are based on site-specific conditions (Anderson and Woessner, 1992). Thus, groundwater models are representations of reality and, if properly constructed, can be a valuable predictive tool for management of groundwater resources. Numerical models pertaining to groundwater and surface water interactions help in the understanding of environmental systems, identify the important parameters affecting flow, and predict responses to resource development (Council, 1997).

3.2.1. Types of models

Several types of models exist to study groundwater flow systems. These can be divided into three broad categories (Prickett, 1975); sand tank models, analogue models (viscous fluid analogue and electric analogue models), and mathematical models (analytical and numerical models). A mathematical model consists of a set of differential equations that are known to govern the flow of groundwater (Wang and Anderson, 1995). The reliability of the model depends on how well the model approximates the field conditions. Simplifying assumptions are necessary as field conditions are often too complex to simulate. These assumptions are generally quite restrictive and require the model domain, for example, to be assumed as homogeneous and isotropic. To represent more realistic situations, it is usually necessary to solve the mathematical model using numerical techniques. With the introduction of high-speed computers since the 1960s, the use of numerical models has been favoured (Wang and Anderson, 1995).

3.2.2. Governing equations

The flow of groundwater can be described by differential equations derived from the basic principles of physics (Wang and Anderson, 1995). Before a governing equation for groundwater flow can be derived, a suitable conceptual model of the system needs to be established (Anderson and Woessner, 1992).

The general form of the governing equation of transient groundwater flow is described by the following equation (Harbaugh *et al.*, 2000).

$$\frac{\partial}{\partial x}\left(K_{xx}\frac{\partial h}{\partial x}\right)+\frac{\partial}{\partial y}\left(K_{yy}\frac{\partial h}{\partial y}\right)+\frac{\partial}{\partial z}\left(K_{zz}\frac{\partial h}{\partial z}\right)+W=S_s\frac{\partial h}{\partial t} \quad (1)$$

Where

h is hydraulic head, K_{xx}, K_{yy} and K_{zz} are the hydraulic conductivities in the x,y and z directions, S_s is the storage coefficient; W is the sink/source term which is used to represent recharge and if negative to represent withdrawal; t represents time.

3.3. Numerical Methods

The use of numerical solutions for groundwater modelling has become a standard tool in recent years. This is due to the fact that these models are much more versatile and easier to use than some of the more complex analytical solutions (Anderson and Woessner, 1992). There are various numerical approaches used in groundwater modelling, which include finite differences, finite elements, integrated finite differences, the boundary integral equation method, and analytic elements. Finite differences and finite elements are most commonly used to solve groundwater flow and contaminant transport problems (Anderson and Woessner, 1992).

In both cases, they consist of a system of nodal points superimposed over the problem domain (Wang and Anderson, 1995). The finite element models use irregular arrays of elemental units to describe the dynamics of the system using triangulation techniques. The triangular elements are defined by three nodes – one at each corner. The finite difference models use regular rectangular elemental units. Finite elements define the variation of head within an element using interpolation functions while the finite difference method defines heads at the nodal points themselves, which could be based on either a block-centred or mesh-centred grid (Anderson and Woessner, 1992).

Finite difference grids can be one of two types, either a block-centred grid or a mesh-centred grid (Figures 3.1). They are differentiated in the way in which they handle the flux boundaries. In a block-centred grid, the flux boundaries are always located at the edge of the block, whereas, in a mesh-centred grid, the boundary coincides with a node. Finite difference boundaries are best handled using

the block-centred approach and is therefore favoured in programs such as MODFLOW. Finite elements allow for greater variation when designing a grid. Two-dimensional elements are either triangles or quadrilaterals, while three-dimensional elements are tetrahedrons, hexahedrons, or prisms (Anderson and Woessner, 1992).

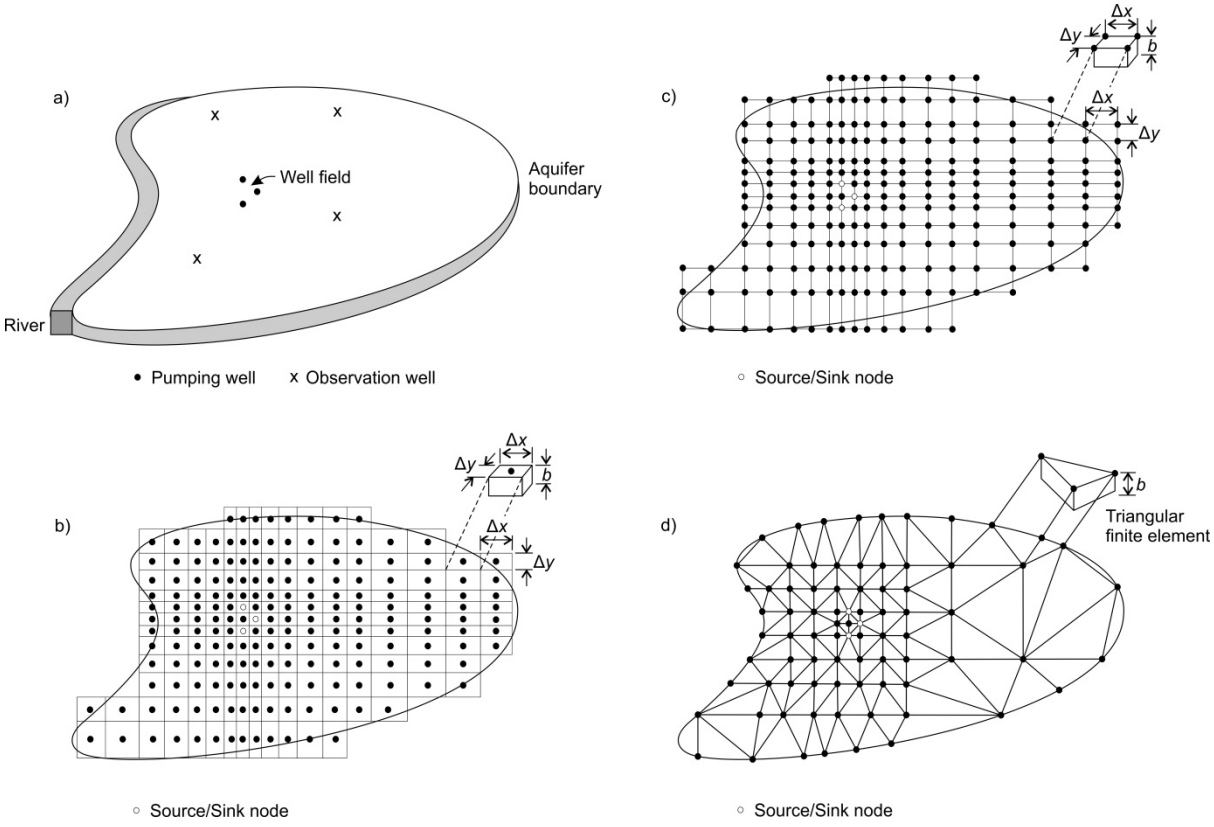

Figure 3.1. Finite difference and finite element representation of an aquifer region (Adapted from Wang and Anderson, 1995). Where a) Map view of aquifer showing well field, observation wells, and boundaries, b) Finite difference grid with block-centred nodes, where Δx is the spacing in the x direction, Δy is the spacing in the y direction, and b is the aquifer thickness.

The choice between finite difference and finite element models depend on the problem requiring solution and on the preference of the user. Finite differences are easier to understand and program, and generally require fewer input data to construct the grid. The advantage of finite elements over finite difference is better approximation of irregular shaped boundaries; easier adjustment of individual elements as well as the location of the boundaries; it's also better suited to handle internal boundaries such as fault zones and can simulate point sources and sinks, seepage faces, and moving water tables better than finite differences. The two methods differ fundamentally in their philosophy. Finite difference methods compute a value for the head at the node which is also the average head for the cell surrounding the node. There is no assumption made about head variation from one node to the next. Conversely, finite elements, precisely define the variation of head within an element by means

of interpolation (basis) functions. Heads are calculated at the nodes for convenience, but heads are defined everywhere by means of basis functions. The head in each finite difference cell is equal to the average of the heads in the four neighbouring cells (Anderson and Woessner, 1992).

3.4. Conceptual Hydrogeological Modelling

One of the most important steps in the groundwater flow modelling is the conceptual model design. According to Wang and Anderson (1995), a conceptual model is graphic representation of the groundwater flow system, usually represented in the form of a block diagram or cross-section. The conceptual model serves as a basis on which the numerical model and subsequent grid design will be based.

Successful quantification and qualification of surface water / groundwater interactions is based on a conceptual understanding or model of the system. The conceptual model will consider the main feature of the aquifer and the response in the receiving environment as well as delineation of the boundary conditions.

The purpose of the conceptual model is to simplify the field parameters and associated field data into a system that can be analysed more readily. The closer the model represents the field conditions, the more accurate the numerical model, however, complete reconstruction of field parameters would be too complex and unfeasible. The model is simplified as much as possible while still adequately reproducing the system's behaviour.

The initial step in constructing the conceptual model is to identify the area of interest, and define the boundary conditions which constrain it. The natural hydrogeologic boundaries should be used for the model whenever possible. For successful conceptual model construction, the following three steps need to be adhered to: (1) definition of stratigraphic units; (2) preparation of a water budget; (3) definition of the flow system (Anderson and Woessner, 1992).

3.4.1. Defining Hydrostratigrapic Units

The concept of Hydrostratigraphic Units (HSU) aims to classify geological units with similar hydrogeological properties (Maxey, 1964; Seaber, 1988). These take cognisance of all geological information including geologic maps, geological cross-sections, and well logs which are combined with information on hydrogeological properties (Anderson and Woessner, 1992). The hydrostratigraphic units defined within the conceptual model would determine the number of layers needed for the model.

3.4.2. Water Budget

All sources of water to the system, as well as expected flow directions and exit points, should be included in the conceptual model. Inflows may include groundwater recharge from precipitation, overland flow, or recharge from surface water bodies, while outflows may include spring discharge, baseflow to streams, evapotranspiration and pumping through shallow and deep wells for various purposes. Subsurface flow may occur as either inflow or outflow. All inflow and outflow parameters are to be quantified based on field data and later compared to values computed during model calibration (Anderson and Woessner, 1992). A complete description of the water budget is provided in the succeeding Section 3.12.

3.5. Defining the Flow System (s)

The hydrostratigraphy serves as the foundation of the conceptual model. Hydrological information related to precipitation, evaporation, surface water runoff, as well as hydraulic head data, and hydrogeochemical and environmental isotope information are used to conceptualise the movement of water through the hydrological system under consideration. Water level measurements allow for the determination of groundwater flow direction, location of recharge and discharge areas and the connection between aquifers and surface water systems (Anderson and Woessner, 1992). Hydrochemical and environmental isotope data supports the physical hydrological data in the conceptual model design. Water flow directions could be determined using hydrochemical data (Swenson, 1968; and Bredehoeft *et al*., 1983). It also helps in the identification of sources and amounts of recharge (Knott and Olimpio, 1986; Bredenkamp *et al*., 1995), to estimate groundwater flow rates (Krabbenhoft *et al*., 1990), and define local, intermediate, and regional flow systems (Lee and Strickland, 1988).

3.6. Code Selection

When selecting a modelling computer code, the user needs to ensure that the code has been verified, that it includes a water balance, and whether it has a proven track record. Codes for groundwater flow are verified by comparing the numerical results with one or more analytical solutions. MODFLOW has been one of the industry standard computer codes that produce numerically stable solutions. MODLFOW also contains a water balance calculation in its code. The water balance is important as it allows for computation of flows across boundaries, to and from sources and sinks and storage. Additionally, the water balance also provides information about discharge rates to surface water bodies or recharge rates across the water table. MODLFOW also has a proven track record as it is one of the most widely used flow models and has been applied to numerous field problems.

3.6.1.MODFLOW

MODFLOW is a modular computer program that simulates three-dimensional ground-water flow through a porous medium by using a finite-difference method (McDonald and Harbaugh, 1988). It is capable of simulating steady and transient flow in an irregularly shaped flow system in which aquifer layers can be confined, unconfined, or a combination thereof. The modular structure is based on a main program linked to a number of highly independent primary and secondary subroutines grouped into “packages”. These packages are capable of simulating specific features of the hydrologic system; these include flow to wells, areal recharge, evapotranspiration, flow to drains, and flow through river beds. A thorough understanding of the concepts associated with MODFLOW is imperative for the correct estimation of boundary conditions and in the simulation of surface water-groundwater interactions.

3.6.2.MODLFOW Packages

MODFLOW has several separate subroutines, or packages, to handle the numerous types of head-dependent conditions. These represent certain hydrological processes including recharge, rivers, drains, evapotranspiration, well, lake and boundary heads.

Recharge Package

The Recharge Package is designed to simulate aerially distributed recharge to the groundwater system. It refers to the volume of infiltrated water that crosses the water table and becomes part of the groundwater system (Anderson and Woessner, 1992). No universally accepted method for recharge estimation has thus far been devised. Groundwater recharge is generally represented in the form of a spatially uniform recharge rate across the water table as a percentage of precipitation that percolates to the groundwater system (McDonald and Harbaugh, 1988; Anderson and Woessner, 1992). Recharge is discussed further in the succeeding Section 3.11.

River Package

Rivers and streams contribute water to the groundwater system or drain water from it depending on the head gradient between the stream and groundwater regime. The River Package (RIV Package) is used to simulate the effects of flow between surface water reservoir such as a river and groundwater aquifer (McDonald and Harbaugh, 1988; Anderson and Woessner, 1992). The River Package allows water to flow from the aquifer to the source reservoir (discharge) when the surrounding groundwater elevation is above the surface water body. Water can also flow out of a stream and into the aquifer (recharge) when the water table is below the elevation of the river bed. This is shown diagrammatically in Figure 3.2.

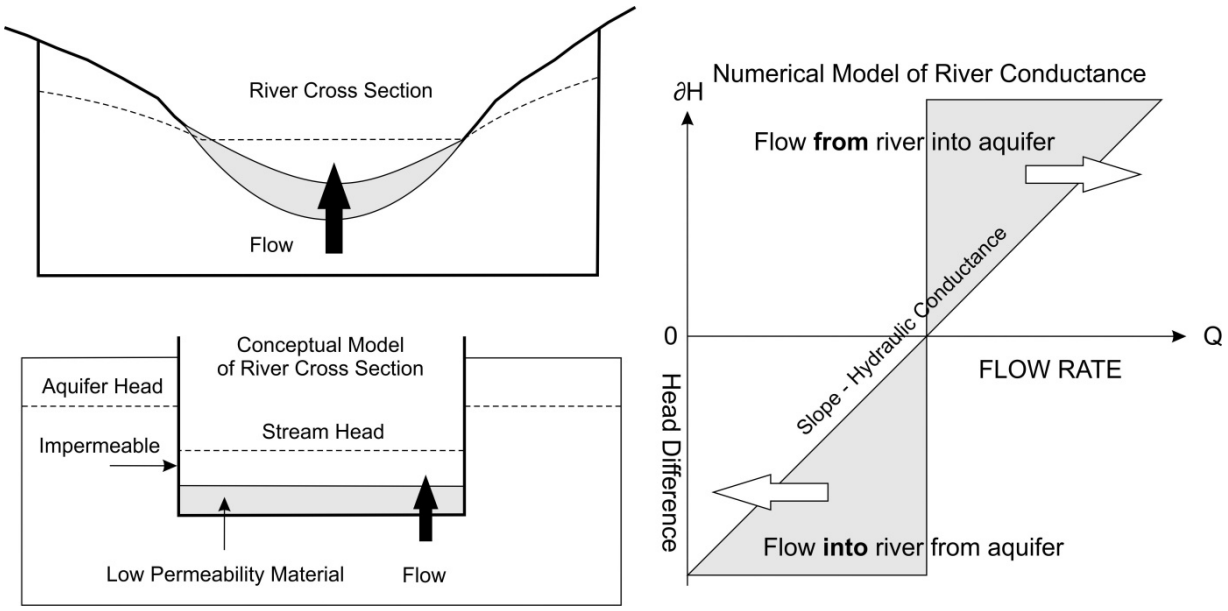

Figure 3.2. Conceptual model of vertical river transmission process (adapted from McDonald and Harbourgh, 1988).

The RIV package uses the streambed conductance (CRIV) to account for the length (L) and width (W) of the river channel in the cell, the thickness of the riverbed sediments (M) and their vertical hydraulic conductivity (K_r). The flow between the groundwater and river in each cell is described by

$$CRIV = \frac{K_r LW}{M} \qquad (2)$$

It is assumed that the cells remains fully saturated and that the water level does not drop below the bottom of the streambed layer. The package also assumes impermeable sides to the river channel so that only vertical flow is possible (McDonald and Harbaugh, 1988; Kelbe *et al*., 2001). Prudic (1989) developed an updated version of the river package, the Stream Routing Package (STR1), this added additional functionality, as it accounted for downstream water routing as well. This was subsequently replaced by a new Streamflow-Routing (SFR1) Package written by Prudic *et al*. (2004). The SFR1 Package was designed to simulate stream-aquifer interactions and to route flow and a single solute through a network of surface-water channels.

Drain Package

The Drain Package is designed to remove water from the aquifer at a rate proportional to the difference between the head in the aquifer and some fixed head or elevation (McDonald and Harbaugh, 1988; Kelbe *et al*., 2001). When the head in the aquifer is above the level of the drain, water is removed from the model. Discharge to the drain is zero when the heads in the cells adjacent to the drain are equal or less than the elevation of the drain. (Anderson and Woessner, 1992; Kelbe

and Germishuyse, 2010). Springs and seeps are generally simulated using the Drain Package (Anderson and Woessner, 1992).

Evapotranspiration Package

The Evapotranspiration (ET) Package simulates the effects of plant transpiration and direct evaporation removing water from the groundwater regime. Evapotranspiration of groundwater occurs when the water table is close to the land surface or when phreatophytes draw water from below the water table (McDonald and Harbaugh, 1988, Anderson and Woessner, 1992). The Evapotranspiration Package requires the user to assign a specified elevation for the water table "ET surface" at which evapotranspiration from the water table occurs at a maximum rate specified by the user (Figure 3.3). The water table elevation at which evapotranspiration is at its maximum generally corresponds to the land surface. No evapotranspiration occurs when the water table declines below an assigned "extinction" depth. In between these limits, evapotranspiration from the water table varies linearly with water table elevations (Anderson and Woessner, 1992; Kelbe and Germishuyse, 2010).

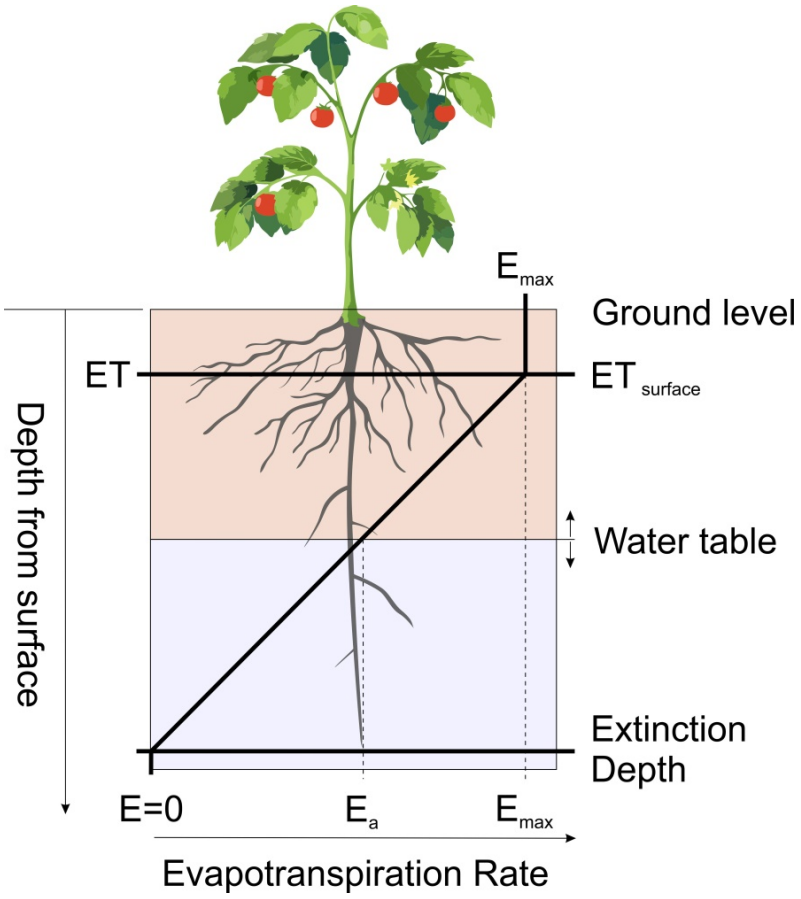

Figure 3.3. Diagrammatic representation of the evaporation model (Adapted from Kelbe *et al*., 2001)

Well Package

Water may enter or leave a model in one of two ways, either through boundaries as specified by the boundary conditions, or through internal sources and sinks. Injection and pumping wells are nodal point sources and sinks which add and withdraw water from the model respectively. The user specifies an injection or pumping rate (Q) in units of volume of water per time for each well node. Negative values for Q indicate a discharging well, while a positive value represents a recharging well. The point source or sink is represented by the entire cell. It is therefore advisable to have finer grid spacing in the vicinity of the wells.

Lake Package

Simulating the interaction between groundwater and surface water bodies, such as lakes, has a significant impact on water resource development in the Lake Sibayi catchment. Several attempts have been made to simulate these lake-aquifer interactions, the most recent being the Lake (LAK3) Package by Merritt and Konikow (2000). The LAK3 package was designed to compute water fluxes between lakes and neighbouring aquifer in MODFLOW (Harbaugh *et al*., 2000; Harbaugh, 2005) and represents the most advanced lake-aquifer interactions package to date.

The LAK3 package was built on the capabilities of its predecessor (LAK2 Package) by adding the ability to simulate solute transport, dealing with multiple lake basins and improved transient solver. According to Merritt and Konikow (2000), the LAK3 Package represents a lake as a volume of space within the model grid composed of inactive cells, while active model grid cells bordering this space represent the adjacent aquifer (Figure 3.4). The LAK package is therefore an advanced method to employ when modelling lake-aquifer interactions as it offers a practical tool to surface water and groundwater modelling (Council, 1998). It provides powerful post-simulation reporting features and allows for explicit inclusion of surface water flow to and from lakes (Hunt *et al*., 2003).

The exchange of water between the lake and adjacent aquifers is quantified by formulating the seepage through the material that separates them (Merritt and Konikow, 2000). The flow from the aquifer into the lake is a function of both the lake-bed leakance and the conductance of aquifer cells adjacent to the lake. The formulation is based on the comparison of heads in the aquifer with those of the lake. In transient simulations, a new lake water budget is performed at the end of each time step to account for the lake stage fluctuations. The lake stage is crucial in making the estimates of ground-water seepage to and from the lake that are used by MODFLOW. Lake budgets account for all atmospheric, surface water and subsurface fluxes into and out of each lake (Figure 3.4). The Stream Package (Prudic, 1989) has been incorporated into the Lake Package to identify stream connections to lakes for accurate inflow and outflow volume calculations. The LAK package computes the lake water budget by balancing the changing volume with multiple inflow and outflow processes. The

water budget procedure incorporated in the Lake Package is implied by the equation used to update the lake stage. The explicit form of this equation is given by (Merritt and Konikow, 2000):

$$h_l^n = h_l^{n-1} + \Delta t \frac{p - e + rnf - w - sp + Q_{si} - Q_{so}}{A_s} \quad (3)$$

Where, h_l^n and h_l^{n-1} are the lake stage (L) from the present and previous time steps; Δt is the time step length (T); p is the rate of precipitation (L^3/T) on the lake during the time step; e is the rate of evaporation (L^3/T) from the lake surface during the time step; rnf is the rate of surface runoff to the lake (L^3/T) during the time step; w is the rate of water withdrawal from the lake (L^3/T) during the time step (a negative value is used to specify a rate of augmentation); Q_{si} is the rate of inflow from streams (L^3/T) during the time step; Q_{so} is the rate of outflow to streams (L^3/T) during the time step; A_s is the surface area of the lake (L^2) at the beginning of the time step; and sp is the net rate of seepage between the lake and the aquifer (L^3/T) during the time step (a positive value indicates seepage from the lake into the aquifer).

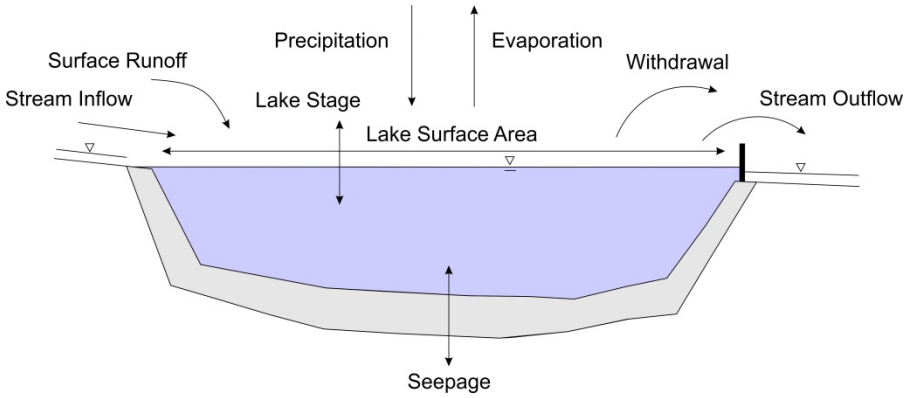

Figure 3.4. Diagrammatic representation of the Lake Package showing its volumetric water budget components (Adapted from Council, 1998).

Depending on the bathymetry of the lake, the reduction in lake stage would reduce the lake surface area and could result in the division of the lake into two or more water bodies (sublakes), each having a separate water budget. Subsequent increase in lake stage would result in coalescence of the separate lakes into a single water body with a single budget and stage (Merritt and Konikow, 2000).

Seepage between the lake and aquifer depend on the lake stage and the hydraulic head in the aquifer. Typical seepage scenarios could be from the aquifer into the lake; recharge from the lake to the aquifer; or a lake can represent a mixed or “flow-through” condition where, in some areas of the lakebed, seepage is into the lake and in other areas, seepage is out of the lake. Quantification of seepage between the lake and aquifer is therefore imperative. Seepage in the Lake Package is calculated by applying Darcy’s Law as presented below:

$$q = K\frac{h_l - h_a}{\Delta l} \quad (4)$$

Where, q is the specific discharge (seepage rate) (L/T); K is the hydraulic conductivity (L/T) of materials between the lake and a location within the aquifer below the water table; h_l is the stage of the lake (L); h_a is the aquifer head (L); Δl is the distance (L) between the points at which h_l and h_a are measured; and L and T denote length and time units.

3.7. Simulating Lake –Aquifer interaction using the High Conductivity Technique

An alternative approach to the simulation of lake-aquifer interaction, one that does not require any modular package, is to specify the lake cells with a high hydraulic conductivity. This technique, often referred to as the "High-K" technique (Lee, 1996; Hunt and Krohelski, 1996; Hunt *et al*., 2000), represents a hypothetical porous medium with a very high hydraulic conductivity; usually three orders of magnitude greater than that of the surrounding aquifer. A storage coefficient of 1.0 is usually specified for the surficial lake layer (Merritt and Konikow, 2000). Due to the high hydraulic conductivity, little or no spatial variation in head (stage) will be experienced across the lake grid cells. This technique was used successfully by Anderson *et al*. (2002) where similar results to the LAK3 Package were reported. The results also compared favourably to field measurements in both, steady-state and transient simulations. The advantage of using the High-K technique is that it is easy to use and is stable over a wide variety of conditions. The main disadvantage of the method is that it is limited to seepage lakes without any surface water inflow or outflow. The technique is therefore best suited to simple application problems.

3.8. Groundwater Modelling System (GMS)

Numerous three-dimensional finite difference graphical user interfaces (GUI) have been developed to run the MODFLOW code. For this study the GUI of Groundwater Modelling System (GMS) is applied. GMS, developed by Aquaveo, consist of a comprehensive package which allows it to perform both steady-state and transient analyses and has a wide variety of boundary conditions and input options. Additional tools provided by the program allow for site characterisation, model conceptualisation, mesh and grid generation, geostatistics, and post-processing. GMS supports MODFLOW as a pre- and post-processor.

3.9. Addition considerations for transient simulation

Transient simulations are used to solve time-dependent problems. When a transient problem is undertaken, it starts with steady-state initial conditions and ends when a new steady-state is reached. A set of heads is produced at every time step during the simulation and are therefore more complex

than steady-state simulations. According to Anderson and Woessner (1992), there are a number of additional reasons why transient problems are more complicated.

3.9.1. Storage Parameters

During transient simulations, water is released or taken into storage within the aquifer. This transfer of water results in a change in head with time. It is therefore necessary to specify the capacity of the aquifer to transfer water to and from storage. This is referred to as storativity and could be described by one of the following parameters: specific storage (S_s), storage coefficient (S), or specific yield (S_y). Specific storage (S_s), which is used in three-dimensional simulations, is equal to the volume of water released from storage within a unit volume of porous material per unit decline in head. Storage coefficient (S), used in two-dimensional areal simulations, is the volume of water released per unit area of aquifer per unit decline in head. When simulating unconfined aquifers, specific yield (S_y), which is a measure of volume of water per volume of porous material released due to gravity in response to a decline in water table, is employed.

3.9.2. Initial conditions

The initial conditions describe the hydraulic head distribution throughout the model domain at the start of the simulation (Anderson & Woessner, 1992). Good initial conditions are imperative for convergence and allows for confidence in model simulation results. The potentiometric surface is generally used to represent the initial conditions.

3.9.3. Transient Boundary Conditions

Transient simulations need to take cognisance of the way in which transient effects propagate to the boundaries. These could cause the heads and flows (e.g., moving groundwater divide) to change in areas of the model which are designated to be a boundary. This could be rectified by expanding the grid and moving the boundary conditions farther from the centre of the grid (Anderson and Woessner, 1992).

3.9.4. Discretising Time

The selection of time steps and grid construction are crucial parts of model design as they have a strong influence on the numerical results. For the model to best approximate field conditions, it is advisable to use small nodal spacing and small time steps. The use of extremely small time steps is impractical and therefore best practice would be to make several trail runs and selecting the largest time step that does not significantly change the solution.

The simulation period can be discretised into smaller blocks of time of variable length, known as stress periods. These allow for the option of changing some of the parameters or stresses while the simulation is in progress.

3.10. Calibration

A successfully calibrated flow model is able to demonstrate that the model is capable of producing field-measured heads and flows. This is accomplished by finding a set of parameters and boundary condition that match the field-measured values within a predetermined error range (Anderson and Woessner, 1992). Most calibrations are conducted under steady-state conditions before being implemented in the transient simulation. Groundwater models are most often used as predictive tools. If the model is calibrated to a set of historical conditions, it is likely that the model would be able to make accurate future predictions (Waterloo Hydrogeologic, 2015). Model calibration is commonly either through manual trail-and-error adjustment of the parameters or through automated parameter estimation.

3.10.1. Trail-and-Error Calibration

In this method, parameter values are adjusted in sequential model runs to simulate observed heads and flows. In hydrogeological modelling, it is often easier to measure the model output parameters (heads, fluxes, concentrations) than it is to measure the input parameters (hydraulic conductivity, storativity, porosity, etc.) Most modelling problems are therefore solved using a process called inverse problem, whereby, the system inputs are determined based on the system outputs (results) (Anderson and Woessner, 1992). A detailed sensitivity analyses should follow the calibration process. It is often good practice to assess model calibration manually; as it provides the user with a good understanding of model sensitivity/uncertainty.

The procedure for trail-and-error calibration is illustrated in Figure 3.5. The field system is converted to a numerical model and calibration targets are set. The model is executed and results are compared to the calibration targets. If the error in the simulated results is acceptable, the model is considered calibrated; if the level of error is unacceptable, parameter values are adjusted and the model is run again until acceptable results are achieved (Anderson and Woessner, 1992).

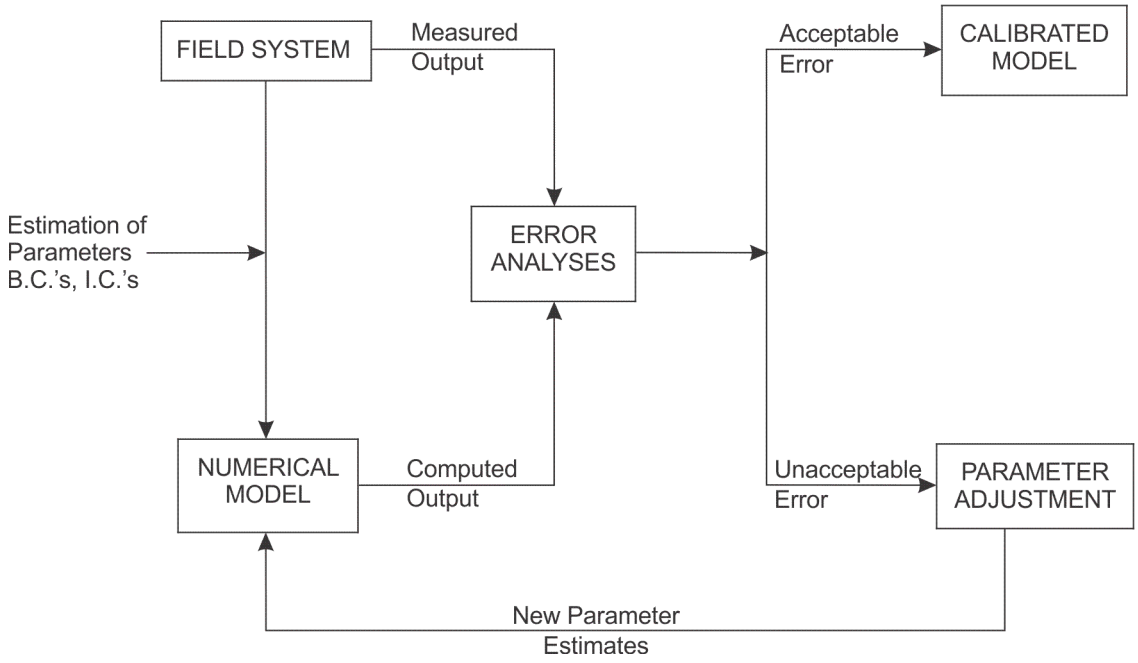

Figure 3.5. Trial-and-error calibration procedure (modified from Peters, 1987).

3.10.2. Automated Parameter Estimation

The most commonly used automated parameter estimation code to address these inversion problems is the non-linear inverse modelling parameter estimation code, PEST (Doherty, 2010). PEST is an open-source, public-domain software suite that allows model-independent parameter estimation and parameter/predictive-uncertainty analysis. PEST uses powerful mathematical techniques to estimate a new set of input parameters by comparing model results to a set of observations, and provides valuable insight into the conceptual model.

The advantage of automated calibration, such as PEST, is that the powerful numerical algorithms can consider more possibilities and give quantitative insight into the model. A major disadvantage is that there is no user intuition to guarantee that the results are reasonable. That's why it's important to understand the parameter ranges and set reasonable parameter bounds when selecting automated calibration.

3.11. Catchment Water Budget

All sources of water to the system, as well as expected flow directions and exit points, should be included in the previously described conceptual model. Inflows may include groundwater recharge from precipitation, overland flow, or recharge from surface water bodies, while outflows may include spring discharge, baseflow to streams, evapotranspiration and pumping through shallow and deep wells for various purposes. Subsurface flow may occur as either inflow or outflow. All inflow and

outflow parameters are to be quantified based on field data and later compared to values computed during model calibration (Anderson and Woessner, 1992).

The development of a successful groundwater–surface conceptual model requires thorough examination of the various components of the water resources and the main hydrological processes involved in their interaction. The various inflow components of the water balance for Lake Sibayi include precipitation, surface runoff and groundwater recharge, while the outflow component include evaporation, groundwater outflow and lake abstraction. Consequently, analysing these resources requires a thorough understanding of their interactions. The quantification of these water balance components would be used as input parameters to the numerical model.

3.11.1. Precipitation

Precipitation is defined as any form of water which falls on the earth's surface by the process of condensation. It constitutes the largest term in the water balance equation and varies both temporally and spatially (Zhang *et al*., 1999).

Rainfall is the predominant source inflow to the Lake Sibayi system as it forms the basis of recharge and has consequently been used as a direct index of recharge (Meyer and Godfrey, 1995; Worthington, 1978; Meyer and Kruger, 1987; Bredenkamp *et al*., 1995).

3.11.2. Surface Runoff

Surface runoff can be generated when the soil is saturated with water or when rainfall intensity exceeds infiltration capacity. Surface runoff is affected by the presence of vegetation through rainfall interception and evapotranspiration (Zhang *et al*., 1999). The runoff component of the water balance constitutes the portion of precipitation in excess of infiltration, flowing along the surface towards streams, lakes or the ocean. The amount of runoff achieved is based on factors associated with precipitation and watershed characteristics. Precipitation factors include the characteristics of the rainstorm, its intensity, duration and frequency while watershed characteristics are based on topography, geology and vegetation cover (Tripathi and Singh, 1998). Based on the hydraulic properties of the soil in the region, it is assumed that very little rainfall leads to direct runoff (Kelbe, 2009).

3.11.3. Groundwater Recharge Estimation

The concept of recharge is based on the process of rainfall which is intercepted by surface features, infiltrates the soil and then percolates to the groundwater (saturated zone). Recharge can be defined as the addition of water to the saturated zone, either naturally (by rainfall, precipitation, or runoff) or artificially (by spreading zones or injection) (Poehls and Smith, 2009). The amount of recharge to

groundwater is controlled by the amount of precipitation available after runoff; the vertical hydraulic conductivity; the transmissivity of the aquifer; and the vertical infiltration through vadose zone.

Several techniques to quantify recharge are available; selecting the most appropriate method is often difficult and is dependent on the goal of the recharge study (Scanlon *et al*., 2002). Considerations to be made when selecting a recharge technique are space/time scales, range, and reliability of recharge estimates based on different techniques; other factors may limit the application of particular techniques. Information relating to the potential controls on recharge, such as climate, hydrology, geomorphology, and geology are pertinent in the development of a conceptual model of recharge in the system. This conceptual model would describe the location, timing, and likely mechanisms of recharge and provides initial estimates of recharge rates (Scanlon *et al*., 2002).

Accurate estimation of groundwater recharge is an essential component in the assessment and management of groundwater resources (Bredenkamp, 2008). In spite of a variety of methods that have been tried, the reliability of the recharge estimates have been relatively low. Great progress has however been made in recent years in relation to recharge estimation in Southern African. Several investigations have been conducted to establish the most appropriate recharge estimation techniques. These methods have been reviewed by Bredenkamp *et al*. (1995), van Tonder and Xu (2001) and Beekman and Xu (2003) in the South African context.

Recharge to the shallow aquifer is primarily through rainfall, therefore a direct relationship between rainfall and groundwater response should be present. Studies by Kelbe and Germishuyse (2010) in the Richards Bay area along the coastal plain revealed a very rapid response from the groundwater/piezometric surface to rainfall fluctuations which could apply to the Lake Sibayi system as well, given the similar conditions.

Quantification of groundwater recharge is an essential task for water resource management. Several methods are used to estimate recharge rates and all have their limitations. Simmers (1988) and Bredenkamp *et al*. (1995) were unable to identify a single flawless recharge estimation technique and the use of multiple recharge estimation techniques was therefore employed (Bredenkamp *et al*., 1995). The techniques used in this study are the chloride mass balance and qualified guesses approaches.

The Chloride Mass Balance Method

Direct recharge to an aquifer is often difficult to measure; it is therefore more practical to develop a model for recharge based on rainfall. Bredenkamp *et al*. (1995) and Meyer and Godfrey (1995) successfully used chloride measurements of rainfall and groundwater to estimate recharge.

The environmental tracer, chloride (Cl^-) is commonly used to estimate recharge due to its conservative nature and relative abundance in precipitation. The popularity of the Chloride Mass Balance (CMB)

method, developed by Eriksson and Khunakasem (1969) is due to its ease of use and cost effectiveness (Allison *et al*., 1994). This method was applied by Bredenkamp *et al*. (1995) around the Lake St. Lucia area, where recharge estimates for the eastern shore compared favourably with those derived by Kelbe and Rawlins (1992) using a conceptual model. More recently, the method was used successfully by Meyer *et al*. (2001) to estimate recharge for the Maputaland Coastal Plain Aquifer.

The method is based on comparison of the chloride deposition rate at the soil surface with the concentration in the soil water or groundwater (Allison *et al*., 1984). Subsurface chloride concentrations increase relative to the concentration in the rainwater as a result of interception, soil evaporation and/or root water uptake by vegetation. The total (wet and dry) chloride deposition and the total precipitation depth determine the chloride concentration of the rainwater at the surface. Subsequent evapotranspiration can then be estimated from the increase in concentration, provided that no other major sources of chloride exist (Allison *et al*., 1984).

The assumptions necessary for successful application of the CMB Method are that:

- There are no sources of chloride in the soil water or groundwater other than from precipitation,
- Chloride is conservative in the system,
- Steady-state conditions are maintained with respect to long-term precipitation and chloride concentration in that precipitation,
- Precipitation is evaporated and/or recharged to groundwater with no surface runoff leaving the aquifer's catchment,
- No recycling of chloride occurs within the basin, and
- No evaporation of groundwater occurs upgradient of the groundwater sampling points (Bazuhair and Wood, 1996).

Meyer *et al*. (2001) stated that the Maputaland coastal plain conforms to all these conditions, resulting in reliable recharge estimates.

Groundwater recharge estimate based on published maps

Published Groundwater Recharge maps proposed by (Vegter, 1995), Agricultural Catchments Research Unit (ACRU) (Schulze, 1989), Groundwater Resources of RSA (WRC, 1995) and Groundwater Harvest Potential (Baron *et al*., 1996) were used to estimate groundwater recharge. These maps were used in conjunction with the physical properties of the catchment, in the form of soil, vegetation, slope and lithology, to estimate recharge for the area. The qualified guesses for recharge from the soil/vegetation and geology are from expert opinions and general equations proposed by Bredenkamp *et al*. (1995) and Kirchner *et al*. (1991).

3.11.4. Evaporation and evapotranspiration

Evaporation and transpiration are primary mechanisms for the loss of water from the system and can occur from all water resources in varying amounts and at different rates. In both cases, water vapour is lost to the atmosphere at a maximum rate determined by the atmospheric demand. This demand is determined by meteorological factors such as radiation, temperature, wind and atmospheric temperature and humidity (Jager and van Zyl, 1989; Shaw, 1994).

Evaporation

Evaporation is the primary process of water transfer in the hydrological cycle. The water is transformed into vapour and transported to the atmosphere. Evaporation is one of the most difficult components of the hydrological cycle to quantify, yet accounts for a large proportion of the water balance (Shaw, 1994). Evaporation can be defined as the direct transfer of water from an open water surface such as lakes, reservoirs and rivers to the atmosphere. The evaporation process depends on the availability of thermal energy and the vapour pressure deficit between the evaporating surface and the overlying air, which is in turn depend on meteorological factors such as temperature, relative humidity and wind speed (Gianniou and Antonopoulos, 2007).

The widely used Penman Formula (Combination Method), developed by Penman (1948) was employed to calculate open water evaporation during the course of this research. The formula is based on fundamental physical principles, with some empirical concepts incorporated, enabling standard meteorological observations to be employed. This semi-empirical equation is a combination of the mass transfer and energy budget methods. The mass transfer method calculates the upward flux of water vapour from the evaporating surface while the energy budget method considers the heat sources and sinks of the water body and air, isolating the energy required for the evaporating process (Shaw, 1994).

Evapotranspiration

Evapotranspiration is the combination of separate processes, evaporation from the soil surface and transpiration from vegetation (Allen *et al*., 1998). It therefore represents the total loss by both evaporation and transpiration from a land surface and its vegetation (Shaw, 1994). The rate of evapotranspiration is dependent on many factors; these include the rooting depth and density, the availability of water, the physiology of the plants and the length of the pathway from adsorption in the roots to evaporation in the leaves (Allen *et al*., 1998).

The Penman-Monteith combination method is recommended as the standard for reference evapotranspiration (Allen *et al*., 1998) and is therefore used for the current study. Evapotranspiration may be estimated from reference crop evapotranspiration (ET_o). According to Allen *et al*. (1998), the

reference evapotranspiration represents the evaporation rate of an extensive surface of green, well-watered grass of uniform height, actively growing and completely shading the ground. Evapotranspiration varies according to the type of vegetation, its ability to transpire and to the availability of water in the soil. Specific crop evapotranspiration (ET_c) is therefore markedly different from the reference evapotranspiration (ET_o) as the ground cover, canopy properties and aerodynamic resistance of the specific crop differs from grass. The effects of characteristics that distinguish field crops from grass are integrated into the crop coefficient (K_c) (Allen *et al*., 1998).

The extinction depth represents the elevation of the phreatic surface when it breaks hydraulic contact with the evaporating surface i.e. falls below the rooting zone. The rooting depth of plants varies, as the Eucalyptus plantations have much deeper rooting system with higher rates of evapotranspiration than the surrounding vegetation (Kelbe and Germishuyse, 2010).

3.12. Environmental Isotope Analyses

3.12.1. Stable Isotopes

Isotopes of a particular element have the same atomic number but different atomic weights due to varying numbers of neutrons in the nucleus (Fetter, 2001). Physical processes such as evaporation, condensation, melting, etc. produce isotopic differentiation where isotopes are separated into light and heavy fractions (Fetter, 2001). Variations in the isotopic composition, produced by chemical or physical processes, in compounds or phases, present in the same system, are called isotopic fractionation (Geyh, 2000). Water molecules containing isotopes of deuterium (^2H) and oxygen-18 (^{18}O) are heavier than a normal hydrogen (^1H) and oxygen-16 (^{16}O) water molecule. The water vapour forming precipitation would therefore be depleted in the heavier isotopes relative to ocean water. Condensation would reverse this process, as the heavier molecules condenses first, producing an isotopically enriched rain and subsequently depleted cloud moisture (IAEA, 2012). Evaporation of water from open water bodies, such as lakes, result in enrichment (i.e. increase) of both heavy isotope ratios of the water remaining in the reservoir (Weaver *et al*., 2007).

The most important atomic constituents of the water molecule are $^{16}0$ and $^{18}0$ ($\delta^{18}0$) and ^1H and ^2H (δ^2H). These have the widest field of application in groundwater studies, including, tracing the origin of the water, the mode of recharge of groundwater and age determination. Oxygen-18 and deuterium analyses refer to the high precision determination of the stable isotope ratio of $^{18}O/^{16}O$ and $^2H/^1H$ respectively in the water molecule. Because of the high precision with which these ratios are measured, it has become customary to express the ratios as relative deviations from an agreed upon standard. The symbol, δ, is used to denote this deviation and is defined as:

$$\delta = \left[\frac{R_{sample} - R_{standard}}{R_{standard}}\right] * 1000\ (‰) \qquad (5)$$

The identical expression is used for δD (or δ^2H). If the value of δ is positive, the sample is enriched with the heavy isotope relative to the standard; a negative sample is isotopically light (Geyh, 2000). The isotopic ratios are compared with the isotopic ratio of Standard Mean Ocean Water (SMOW).

Both these pairs of isotopes are used to describe the processes to which the water has been subjected in the course of the hydrological cycle. The relationship between δ^2H and $\delta^{18}O$ in fresh waters correlate well on a global scale (Craig, 1961). This relationship is described as the Global Meteoric Water Line (GMWL) and is expressed by the equation (Craig, 1961):

$$\delta^2H = 8\delta^{18}O + 10 \quad (6)$$

The GMWL is an average of many regional and local meteoric water lines (LMWL) that differ from the GMWL in slope and/or intercept as a result of different climatic and geographic factors (Clark and Fritz, 1997).

3.12.2. Radio isotopes

Tritium, (^3H), is a radioactive isotope of hydrogen with a half-life of 12.32 years (Fetter, 2001). As such, it has the potential of being used to date groundwater 'ages' in the order of decades. The tritium levels in rainwater are extremely low and the unit used, TU, represents a $^3H/^1H$ ratio of 10^{-18}. Before the advent of nuclear weapon tests, rainfall tritium levels were in the order of 3 to 5 TU. During the period of nuclear weapon tests, rainfall tritium levels reached 5000 TU in the northern hemisphere while its levels never exceeded 100 TU in the southern hemisphere. Present day rainfall tritium levels in the southern hemisphere have returned to pre-bomb values of 3-5 TU, while levels of 80 to 100 TU were measured in the northern hemisphere in 2000 (Clark & Fritz, 1997; Gat and Gonfiantini, 1981). These nuclear events have allowed for the possibility of using tritium as an indicator of recent (post 1955) recharge. The tritium levels in groundwater remain intact underground and are only influenced by mixing with older water and radioactive decay (Weaver *et al*., 2007).

The International Atomic Energy Agency (IAEA) has established the Global Network of Isotopes in Precipitation (GNIP) in order to record changes of ^3H in precipitation. The reference values used during this study was from the Pretoria station (WMO Code 6826200). This database provides sufficiently reliable input curves for extrapolation to nearly area of interest.

CHAPTER FOUR: RESEARCH METHODOLOGY AND APPROACH

4.1. Desktop review

Analysis of all existing hydrometeorological, hydrological, hydrogeological, and hydrochemical data was undertaken as part of the desktop review for the study area. This included delineation of the surface water catchment boundary based on the SRTM DEM (USGS, 2015), collection of relevant meteorological data from the South African Weather Services (SAWS, 2015), groundwater level and flow direction determination based on water level data obtained from the National Groundwater Archive (NGA, 2013) and the Groundwater Resource Information Project (GRIP, 2013) data bases, as well as borehole logs from various sources to determine subsurface hydrogeological conditions. All related reports pertaining to the study area were also reviewed.

4.2. Field measurement, analyses and sampling procedures

A total of 80 water samples were collected from groundwater, surface water, lake, ocean, and rainfall sources during April 2008, September/October 2012 and April/May 2013 (Figure 4.1) sampling regimes. Sampling was conducted in order to ascertain conditions at the onset of the dry season (April/May) and then again when the rainy season commenced (September/October).

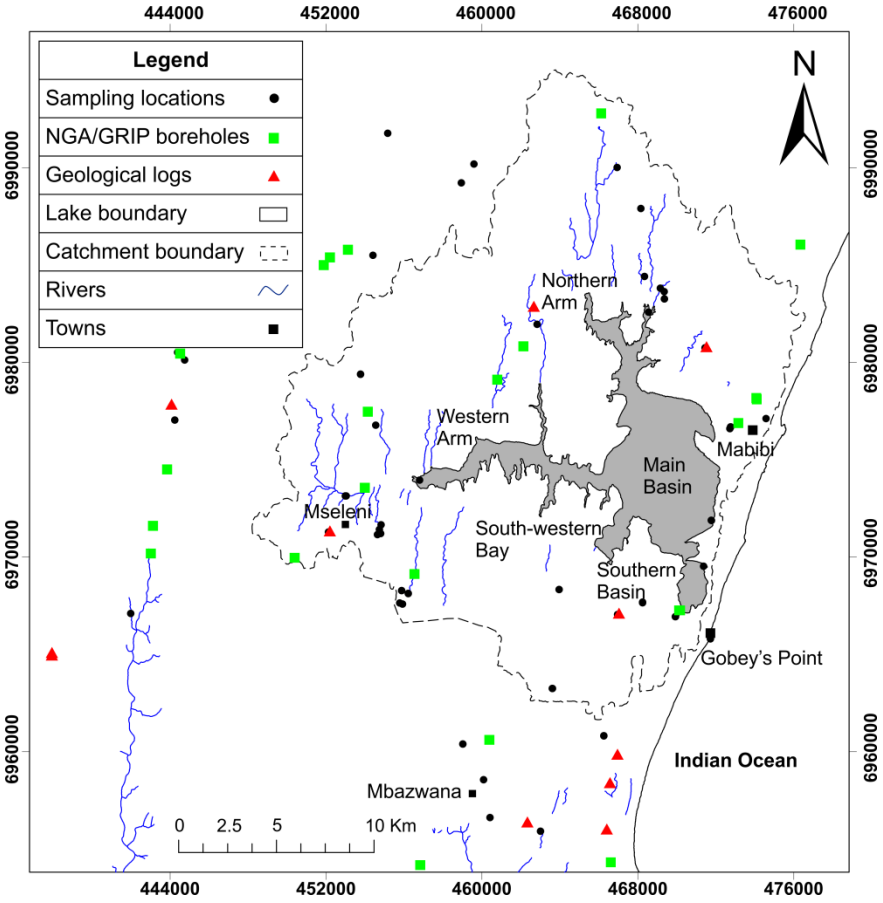

Figure 4.1. Spatial distribution of sampling sites, with proposed surface water catchment boundary in the Lake Sibayi catchment.

Groundwater samples were collected from active boreholes; inactive boreholes were purged of stagnant water to allow for the collection of fresh formation water. Depth to groundwater level data was measured using a Solinst Temperature, Level and Conductivity (TLC) meter. Groundwater samples were collected directly from the pump outlet once measurements of electrical conductivity (EC), temperature, dissolved oxygen (DO) and pH had stabilised. Surface water samples were taken directly from the water bodies (lakes, streams and sea). Samples were collected below the surface (approximately 30 cm) so as to avoid collection of floating debris. Onsite measurement of EC, pH, total dissolved solids (TDS), DO, Eh and temperature were recorded using the Hanna HI 9828 multi-parameter water quality meter. Total alkalinity, bicarbonate and carbonate content were determined through field titrations with hydrochloric acid. Samples undergoing cation and anion analyses were filtered using a 0.45 μm membrane filter while cation samples underwent additional acidification to below pH 2 using ultrapure nitric acid (30% HNO_3).

4.3. Laboratory analysis

Major cation and anion analyses were conducted using Metrohm 882 Compact IC (ion chromatography) while trace elements were analysed using the PerkinElmer NexION 300X Inductively Coupled Plasma Mass Spectroscopy (ICP-MS) both at the School of Geological Sciences, University of KwaZulu-Natal (UKZN).

Stable isotope samples (oxygen-18 and deuterium) were analysed within UKZN's School of Bioresources Engineering and Environmental Hydrology Laboratory using a Los Gatos Research (LGR) DT-100 Liquid Water Isotope Laser Analyser. Samples were reported as $^{2}H/H$ and $^{18}O/^{16}O$ ratios.

Tritium (^{3}H) analyses were conducted at iThemba Environmental Isotope Laboratory, Johannesburg, South Africa following standard procedures.

4.4. Statistical Analyses of hydrochemical data

The chemical composition of groundwater found in coastal regions is generally diverse due to the complex hydrogeological, physical and anthropogenic processes (Kim *et al*., 2005). Due to the complexities involved in these processes, it is often difficult to extract the underlying governing processes (Suk and Lee, 1999). Popular multivariate statistical approaches such as discriminant analyses, factor analysis (with principal components and varimax rotation), and cluster analysis were employed to interpret these governing processes through data reduction and classification (Bonansea *et al*., 2014). The combination of these analytical procedures would allow for the classification of the water samples into distinct groups based on their hydrochemical characteristics (Yang *et al*., 2015).

Factor analyses is a commonly used statistical approach used to explain the relations among multivariate data in terms of smaller, previously unobserved, subsets (factors) that provide insight into the underlying structure of the variables while maintaining minimum loss of information (Hair *et al*., 1992; Suk and Lee, 1999). In this study, the principal component method was employed to transform the various hydrochemical parameters into an orthogonal set of variables called principal components. The rank of the components correlates to the amount of variance they account for, with the first principal component having the highest contribution. To aid in identification of the underlying structure, the factors were linearly transformed into a new set of factors through the use of Kaiser's Varimax factor rotation (Kaiser, 1960).

Cluster analyses applied to the principal components accounting for the greatest variation could then be used to characterise the groundwater hydrochemical system into discrete hydrochemical regimes. The use of the principal components reduces the clustering error caused by data error and multicollinearity (Suk and Lee, 1999). Cluster analyses would classify the variables into homogeneous and distinct groups by linking inter-sample similarities (Hussain *et al*., 2008) based on the components with the greatest influence.

A multifaceted approach involving multivariate statistical techniques such as factor analyses (Principal component) and hierarchical cluster analysis combined with graphical methods (Piper trilinear graphical diagram), and isotopic analyses was applied to identify the distinct hydrochemical regimes. This would assist in the conceptual model design for numerical simulation of the Lake Sibayi catchment.

4.5. Water Balance

The concept of the water balance provides a framework for studying the hydrological behaviour of a catchment and it can be used to identify changes in the water balance components (Zhang *et al*., 1999). To calculate the water balance of the Lake Sibayi, the inflow and outflow components of the hydrological cycle had to be defined. The water balance of the lake can be mathematically represented as:

$$\text{Inflow} - \text{Outflow} = \pm \text{Change in storage} \quad (7)$$

The water balance of Lake Sibayi is given by (Adapted from Pitman and Hutchison, 1975):

$$P_{recip} + S_{runoff} + G_{in} - E_{vapo} - G_{out} - W = \pm \Delta S \quad (8)$$

Where P_{recip} is the precipitation on the surface of the lake, S_{runoff} the surface runoff into the lake including ungauged stream flows, G_{in} the groundwater inflow to the lake, E_{vapo} the open water

evaporation from the surface of the lake, G_{out} is the seepage of water out from the lake into the ocean, W the abstraction from the lake, and $\pm \Delta S$ is the change in storage.

All water balance calculations were determined based on the meteorological data obtained from the Hlabisa Mbazwana Meteorological Station (precipitation), the Mbazwana Airfield Meteorological Station (temperature, humidity and wind-speed readings), and the Makatini Research Centre (sunshine duration) (SAWS, 2015).

4.5.1. Precipitation

Precipitation over the lake was taken from the 46 year (1970 to 2015) mean rainfall data collected from the Hlabisa Mbazwana Meteorological Station (SAWS, 2015).

4.5.2. Runoff

Runoff was measured for gauged catchments and typically estimated for ungauged catchments using the Rational Method which is expressed as follows:

$$q = {}^{CIA}/_{360} \quad (9)$$

Where q is peak runoff rate (m^3/s) for a given frequency of rainfall; C is the runoff coefficient; A is the area of the basin (ha); and I is the intensity of rainfall (mm/h) for design return period equal to the time of concentration.

The runoff coefficient, C, represents the percentage of rainfall that becomes runoff (Tripathi and Singh, 1998). The amount of runoff achieved is dependent on precipitation and land use and is heavily influenced by vegetation, soil type and degree of disturbance, catchment slope and the number and nature of watercourses in the catchment. The land use, vegetation type, and soil type were obtained from the relevant shapefiles for the area.

The contribution of rivers to the water balance is usually achieved through hydrograph analyses. The contribution of Mseleni River to the lake water balance could unfortunately not be achieved due to lack of monitoring systems within the river.

4.5.3. Recharge

The techniques used in this study are the chloride mass balance (CMB), with the results verified against published maps.

Chloride Mass Balance

The application is based on comparison of the chloride concentration in precipitation with the concentration in the soil water or groundwater. The chloride mass balance method can be used to calculate moisture fluxes and recharge rates in the unsaturated zone. These mass balances assume steady-state conditions and conservation of mass between the atmospheric Cl^- input and the Cl^- flux in the subsurface (Selaolo, 1998). For deep infiltration below the root zone, downward moisture flux R (mm/a) is determined by (Edmunds *et al*., 1988; Sharma, 1989):

$$R = \frac{P\ x\ Cl_p}{Cl_{sw}} \tag{10}$$

P is the precipitation (mm/a), Cl_p is the chloride content of in precipitation (mg/l), and Cl_{sw} is the chloride concentration in the soil moisture.

4.5.4. Evaporation and evapotranspiration

Open water evaporation was calculated using the Penman method (Penman, 1948). The basic Penman formula for open water evaporation is:

$$Eo = \frac{\Delta}{\gamma}H + Ea\ /(\frac{\Delta}{\gamma} + 1) \tag{11}$$

Where γ is the psychometric constant and E_a is the aerodynamic coefficient based on air humidity. Δ represents the slope of the curve of saturated vapour pressure plotted against time. *H* is the available heat and is calculated from incoming radiation (R_I) and outgoing radiation (R_O) determined from sunshine records, temperature and humidity.

$$H = R_I(1 - r) - R_O \tag{12}$$

Where *r* is the albedo and equals 0.05 for water. R_I is a function of R_a, the solar radiation modulated by a function of the ratio *n/N,* a measure of the maximum possible sunshine duration. Using $r = 0.05$ gives:

$$R_I(1 - r) = 0.95R_a f_a\left(\frac{n}{N}\right) \tag{13}$$

The function $f_a\left(\frac{n}{N}\right)$ depends on the clarity of the atmosphere and latitude.

$$R_O = \sigma T_a^4\left(0.56 - 0.09\sqrt{e_d}\right)(0.10 + 0.9\ \frac{n}{N}) \tag{14}$$

Where σT_a^4 is the theoretical black body radiation at T_a which is then modified by functions of (e_d) the saturation vapour pressure at dew point temperature and the cloudiness$\left(\frac{n}{N}\right)$.

E_a is found using the coefficients derived by experiment for open water:

$$E_a = 0.35\ (0.5 + u_2/100)(e_a - e_d) \quad (15)$$

The value of Δ is found from the curve of saturated vapour pressure against temperature corresponding to the air temperature, T_a.

The measurements required to calculate open water evaporation are T_a the mean monthly air temperature (C), e_d the mean vapour pressure for the same period (mm of mercury), n is sunshine duration (h day^{-1}) and u_2 mean wind speed at 2 m height above the surface (miles day^{-1}).

Evapotranspiration rates from the plantations and subsequently the catchment were derived from the FAO Penman-Monteith method used to estimate ET_o. The formula is given by (Allen *et al*., 1998):

$$\lambda ET = \frac{\Delta(R_n - G) + p_a c_p \frac{(e_s - e_a)}{r_a}}{\Delta + \gamma(1 + \frac{r_s}{r_a})} \quad (16)$$

where R_n is the net radiation, G is the soil heat flux, (e_s- e_a) represents the vapour pressure deficit of the air, p_a is the mean air density at constant pressure, c_p is the specific heat of the air, Δ represents the slope of the saturation vapour pressure temperature relationship, γ, is the psychrometric constant, and r_s and r_a are the (bulk) surface and aerodynamic resistances.

From the original Penman-Monteith equation (Equation 16), the FAO Penman-Monteith method to estimate ET_o can be derived (Equation 17) (Allen *et al*., 1998):

$$ET_o = \frac{0.408\Delta(R_n - G) + \gamma \frac{900}{T+273} U2(e_s - e_a)}{\Delta + \gamma(1 + 0.34u_2)} \quad (17)$$

Where ET_o is the reference evapotranspiration (mm day^{-1}), R_n the net radiation at the crop surface (MJ m^{-2}day^{-1}), G the soil heat flux density (MJ m^{-2}day^{-1}), T represents the mean daily air temperature at 2 m height (°C), u_2 the wind speed at 2 m height (m s^{-1}), e_s the saturation vapour pressure (kPa), e_a the actual vapour pressure (kPa), $e_s - e_a$ the saturation vapour pressure deficit (kPa), Δ the slope of the vapour pressure curve (kPa °C^{-1}) and γ the psychrometric constant (kPa °C^{-1}).

The reference evapotranspiration, ET_o, provides a standard to which evapotranspiration at different periods of the year or in other regions can be compared and evapotranspiration of other crops can be related. The equation uses standard climatological records of solar radiation (sunshine), air temperature, humidity and wind speed

The FAO Penman-Monteith equation is a close, simple representation of the physical and physiological factors governing the evapotranspiration process. By using the FAO Penman-Monteith

definition for ET_o, one may calculate crop coefficients at research sites by relating the measured crop evapotranspiration (ET_c) with the calculated ET_o:

$$K_c = ET_c / ET_o \quad (18)$$

In the crop coefficient approach, differences in the crop canopy and aerodynamic resistance relative to the hypothetical reference crop are accounted for within the crop coefficient. The K_c factor serves as an aggregation of the physical and physiological differences between crops and the reference definition (Allen *et al*., 1998).

4.5.5. Surface and groundwater abstraction

The lake has been pumped at three different stations for local community water supply. According to the Water use Authorisation Registration Management System (WARMS) (Table 4.1), lake water abstraction for the Manguzi community commenced in June 1975 at a rate of 1.825 x 10^6 m^3/a. This was later increased to 2.128 x 10^6 m^3/a in July 2003. From March 2004, abstraction increased again by an additional 0.496 x 10^6 m^3/a and 0.153 x 10^6 m^3/a for the Mbazwana and Mseleni communities respectively (DWA, 2014). Total abstraction from the lake is therefore 2.8 x 10^6 m^3/a which was substantiated by similar results obtained from intermittent pumping records provided by the uMkhanyakude District Municipality (personal communication with Mr. Petros Zwane).

Table 4.1. WARMS Annual Abstraction from Lake Sibayi for local community water supply.

Water Use No.	**Property**	**Volume (m^3/a)**	**Start Date**
21121910/16	Manguzi town & community	1,825,000	June 1975
21159693/3-5	uMkhanyakude District Municipality	302,585	July 2003
21160084/1	Mabaso tribal authority (Mseleni)	153,300	March 2004
21160066/1	Zikali tribal authority (Mbazwane)	495,950	March 2004
Total Abstraction		2,776,835	

Several small to medium scale groundwater fed schemes are present within the catchment area (Terratest, 2009a, 2009b, 2011, 2014, 2015a, 2015b, 2016a, 2016b; Jeffares and Green, 2012, 2014a, 2014b). These schemes abstract approximately 1.7 x 10^6 m^3/a based on recommended pumping rates and are predominantly used to supplement existing water resources.

Groundwater abstraction from within the catchment for domestic water supply is through numerous hand operated boreholes which intersect the shallow groundwater aquifer. It is difficult to estimate the amount of water abstracted by these boreholes as they are ungauged, a 25 l/person/day human reserve set by the National Water Act (38 of 1998), has therefore been applied to get a rough estimate of groundwater abstraction. This equates to a total abstraction of approximately 4000 m^3/a.

Abstraction from both surface water and groundwater resources within the catchment therefore totals 4.5 x 10^6 m^3/a. Monitoring of water abstraction volumes from the various stakeholders is often difficult as water level and discharge monitoring throughout the coastal plain is limited to non-existent

4.5.6. Groundwater outflow

Groundwater outflow to the sea (seepage) was calculated using Dupuit's equation (Dupuit, 1863):

$$Q = (K(h_0^2 - h_1^2))/2x \quad (19)$$

Where Q is the amount of groundwater outflow to the sea, K is the permeability of the medium, x is the length of the flow path and h_o - h_1 being the head difference above the impermeable floor rocks (datum).

4.6. Numerical Modelling

4.6.1. Modelling Approach

A flowchart detailing the modelling approach, summarised in Figure 4.2, takes cognisance of code selection and verification, model design, calibration, sensitivity analyses, and finally prediction (Anderson and Woessner, 1992). These steps allow for the construction of a site-specific model capable of producing meaningful results. The approach shown in Figure 4.2 provides the ideal process to be followed in modelling studies.

The first step in the modelling protocol is to establish the purpose of the model and thereby the governing equations and code to be used. A conceptual model is then developed where the hydrostratigraphic units and system boundaries are identified. Field data, including information on the water balance, aquifer properties, and hydrologic stresses, are also included. Collection and interpretation of field data is essential in understanding the natural system and identifying the groundwater problem. The quality of the simulations depends largely on the quality of the input data. Selection of the governing equation and computer code is then undertaken. The code is a computer program that contains an algorithm to solve the mathematical model numerically. Verification of both the governing equation and the code respectively would ensure accurate description of the physical processes in the porous media and correct solution of the equations that constitute the mathematical model. During model design, the conceptual model is converted into a suitable model. This would include grid design, time step selection, setting of boundary and initial conditions, and preliminary selection of aquifer parameters and hydrologic stresses. Calibration of the model would establish whether the model can reproduce field-measured heads and flows. This is done through trial-and-error or by automated parameter estimation until the model best approximates field conditions. A sensitivity analyses is included in this step in order to establish the effect of uncertainty on the

calibrated model. Model verification is undertaken to establish greater confidence in the model by using the calibrated model to reproduce a second set of field data. Prediction quantifies the response of the system to future events. An estimation of future change in stresses is necessary to perform the simulation. A sensitivity analyses is also included in this step to quantify the effect of uncertainty in parameter values on the prediction. Clear presentation of model design and results are essential for effective communication of the modelling effort. A post-audit is conducted several years after the modelling study is completed. Should the model prediction be accurate, the model is validated for that particular site. The post-audit would provide new insights into the system's behaviour, which may lead to a redesign of the conceptual model or model parameters.

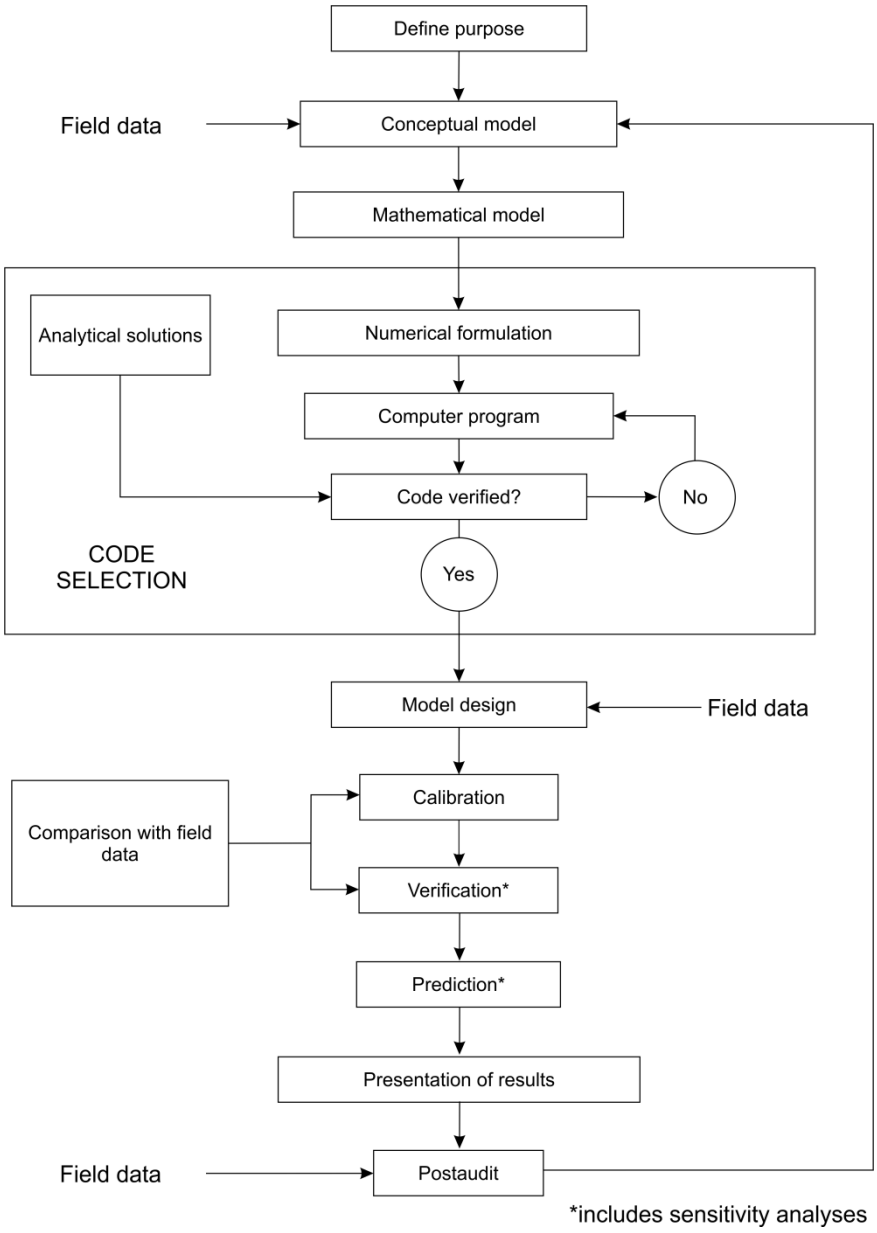

Figure 4.2. Modelling approach for numerical modelling (Adapted from Anderson and Woessner (1992).

4.6.2. Conceptual modelling

The data requirements for successful conceptual model generation based on the various physical and hydrogeologic frameworks are listed in Table 4.2 below (Anderson and Woessner, 1992).

Table 4.2. The physical and hydrological framework requirements for conceptual model formulation and calibration.

Physical framework	
	Geological map and cross sections showing the areal and vertical extent and boundaries of the system.
	Topographic map showing surface water bodies and divides.
	Contour map showing elevation of the base of the aquifers and confining beds.
	Isopach maps showing the thickness of the aquifer and confining beds.
	Maps showing the extent and thickness of stream and lake sediments.
Hydrogeologic framework	
	Water table and potentiometric maps for all the aquifers.
	Hydrographs of groundwater head and surface water levels and discharge rates.
	Maps and cross sections showing the hydraulic conductivity and/or transmissivity distribution.
	Maps and cross sections showing the storage properties of the aquifers and confining beds.
	Hydraulic conductivity values and their distribution for stream and lake sediments.
	Spatial and temporal distribution of rates of evapotranspiration, groundwater recharge, surface water-groundwater interaction, groundwater pumping, and natural groundwater discharge.

From the table above, the physical framework of the model is based on the geometry of the system including the thickness and aerial extent of each hydrostratigraphic unit. The hydrogeological framework includes information on heads and fluxes, which are required for conceptual model formulation and model calibration. Aquifer properties and hydraulic stresses are also needed. The distribution of effective porosity is also required for calculating average linear velocities from head data used for particle tracking. These parameters are generally obtained from on-site field work or existing reports.

The thickness and vertical hydraulic conductivity of stream and lake sediments are required for leakage calculations. These can be estimated from field measurements (Lapham, 1989; Barwell and Lee, 1981). Hydraulic stresses include pumping, recharge, and evapotranspiration.

4.6.3.Definition of model domain

The first, and often the most difficult task in groundwater modelling is the identification of the model area and its boundaries (Dennis, 2014). Defining the model domain distinguishes the area of

investigation from the adjacent groundwater system. The model boundary is therefore the interface between the model area and the surrounding environment. These boundaries, found to border the model domain and, internally, where they represent areas of external influences, such as rivers, wells and lakes, need to be specified. The hydraulic boundary conditions are defined based primarily on conditions such as topography, hydrology and geology. These boundary conditions need to be specified for the entire model domain, and may vary with time.

Model Boundaries

Anderson and Woessner (1992) describe boundary conditions as mathematical statements specifying the dependent variable (head) or the derivative of the dependent variable (flux) at the boundaries of the problem domain. Selecting the correct boundary conditions is a critical component of model design. The boundaries are responsible for the flow pattern in steady-state simulations. Boundary conditions influence transient solutions when the effect of the transient stress reaches the boundary; they therefore require careful consideration so that they provide a realistic simulation.

Physical boundaries of groundwater flow systems are formed by physical features such as an impermeable body of rock or large surface water body. Hydraulic boundaries are formed by hydraulic conditions and include groundwater divides and streamlines. These boundaries are transitory features that may shift location or disappear altogether if hydraulic conditions change.

Three types of model boundary conditions are distinguished by the flux across the boundary (Anderson and Woessner 1992):

- Specified head boundaries (Dirichlet conditions) where the head in the aquifer is set by the boundary condition (Type 1 boundary condition).
- Specified flow boundaries (Neumann conditions) for which flow rate across the boundary is given. A no-flow boundary condition is set by specifying flux to be zero (Type 2 boundary condition).
- Head-dependent flow boundaries (Cauchy or mixed boundary conditions) for which flux across the boundary is determined by the hydraulic gradient between the aquifer and the boundary (Type 3 boundary). This type of boundary condition is sometimes referred to as a mixed boundary condition as it represents a combination of Type 1 and Type 2 boundary conditions.

Specified Head Boundary: According to Anderson and Woessner (1992), a specified head boundary is simulated by setting the head at the relevant boundary nodes equal to known head values. This value is generally constant for lakes and reservoirs, but would vary spatially along a river. Specified head boundaries are used to represent the water table or large surface water bodies, such as the ocean

or harbours, which have a volumetric capacity greater than any groundwater contribution (Kelbe and Germishuyse, 2010). It is important to note that this type of boundary represents an inexhaustible supply of water.

Specified Flow Boundary: Specified flow conditions are used to describe fluxes to surface water bodies, spring discharge, subsurface flux, and seepage to or from bedrock underlying the modelled system (Anderson and Woessner, 1992). These include recharge, evaporation and abstraction/injection wells. The wells are point specific whereas the recharge and evaporation are specified for the entire model area (Kelbe and Germishuyse, 2010).

No-flow boundaries occur when the flux across the boundary is zero. This may represent impermeable bedrock, an impermeable fault zone, a groundwater divide or a streamline. A groundwater divide is generally dynamic and has a direct response to changes within the aquifer (Kelbe and Germishuyse, 2010). A no-flow boundary can also be used to approximate the freshwater/saltwater interface in coastal aquifers (Anderson and Woessner, 1992).

Head-Dependent Flow Boundary: The flux across this type of boundary is dependent on the difference between a user-supplied specified head on one side of the boundary and the model-calculated head on the other side. These generally represent rivers, lakes, estuaries, wetlands and drains (Kelbe *et al*., 2001; Kelbe and Germishuyse, 2010). Evapotranspiration across the water table could also be represented by this type of boundary, where the flux across the boundary is proportional to the depth of the water table below the land surface. It could also be used to represent flow to a drain (Anderson and Woessner, 1992).

4.7. Data interpretation tools

During the data generation stage, primary and secondary data collected from the initial desktop study and field investigation are processed and analysed. Assigning parameters values to the grid is often difficult as the model requires values to be specified at each grid node/cell while field measurements are typically sparse (Anderson and Woessner, 1992). This problem is overcome through the implementation of interpolation techniques. Several different methods are available for interpolating spatial data; however, Kriging was the preferred method during the study.

Statistical interpolation of point measurements of static water levels was undertaken to prepare the initial hydraulic heads for the entire model. As part of the HSU interpolation, digital elevation data (USGS, 2015) was extracted to determine the surface topography of the upper layer of the numerical model, while borehole information from previous sources were used to construct the remaining layer boundaries. These surfaces can then be directly imported into the numerical model.

Golden Software's Surfer was employed for its enhanced interpolation functionality for surface and contour analyses. Various additional utilities of the program were utilised for volume calculations and scatter point coordinate conversion. ESRI ArcGIS was used to manipulate the various vector and raster data from sources. The program was used to digitize several prominent features, determine their areas and delineate the catchment boundaries. Aquachem 4.0 was used for hydrochemical characterisation of the water samples and their visual assessment through Piper, Wilcox and Schoeller diagrams. The statistical software package SPSS version 24 was applied for descriptive statistics, bivariate correlation, factor analysis, and hierarchical cluster analysis of the hydrochemical data collected. Google Earth was used to digitize the latest lake levels used in the study. The advanced editing capability of Corel Draw was used enhance the figures generated from the various programs prior to presentation.

CHAPTER FIVE
HYDROGEOLOGICAL, HYDROCHEMICAL AND ENVIRONMENTAL ISOTOPE CHARACTERISTICS OF THE LAKE SIBAYI SYSTEM

5.1. Hydrogeological units and their hydraulic characteristics

The northern half of the KwaZulu-Natal Coastal Plain in South Africa, in which the Lake Sibayi system is situated, is characterised by sedimentary successions that form a multi-stock-work of aquifer layers and a regional aquiclude as the hydrogeological basement. These formations show varying combinations of sand, silt and clay, which are marine, alluvial and aeolian in origin. They have sufficiently different hydraulic properties to be categorised into distinct hydrogeological units (Kelbe *et al*., 2013). These Mio-Pliocene and Quaternary age sedimentary units constitute primary aquifers in the region (Worthington, 1978 and Meyer and Godfrey, 1995).

The two most productive aquifer systems are the shallow KwaMbonambi Formation and the deep Umkwelane and Uloa Formations (Meyer and Godfrey, 1995; Meyer *et al*., 2001; Jeffares and Green, 2012). The first aquifer unit consists of the unconfined superficial dune sands of the Late Pleistocene KwaMbonambi Formation, which was deposited in response to polyphase dune mobilisation events. This unit extends to variable depths (Botha and Porat, 2007; Porat and Botha, 2008) and is frequently exploited by the local community through hand dug wells (Meyer and Godfrey, 1995). Pumping tests undertaken by Jeffares and Green (2012) revealed sustainable yields of between 190 and 1700 m^3/day while transmissivity averaged 1490 m^2/day. These intergranular units that constitute the upper aquifer have limited variation in grain size and porosity with permeabilities ranging from 0.87 to 15.6 m/d (Meyer and Godfrey, 1995). This permeable and porous upper aquifer unit encounters a seasonally perched high groundwater table above the underlying low yielding silty sands and silts of the Kosi Bay Formation (Porat and Botha, 2008).

Due to its low transmissivity and high adhesive forces, the Kosi Bay Formation (Late Pleistocene) generally results in leaky confined aquifer conditions to the underlying formations (Mkhwanazi, 2010; Jeffares and Green, 2012). The large storage capacity afforded by the Kosi Bay Formation makes it a storage reservoir for the underlying Umkwelane and Uloa Formations. The Kosi Bay Formation could also be exploited if boreholes drilled into it are well designed and developed. Its hydraulic conductivity ranges from 4 to 5 m/d recorded along the eastern shores of Lake St Lucia (Meyer and Godfrey, 1995).

The aquifer that underlies the Kosi Bay Formation is the Mio-Pliocene aged confined/semi confined aquifer unit made up of calcareous sands, and gravels of the Umkwelane and Uloa Formations which constitute the main aquifer in the region (Worthington, 1978; Jeffares and Green, 2012; Kelbe *et al*., 2013). Pumping tests conducted on boreholes tapping this aquifer gave sustainable yields between 40 and 1500 m^3/day, and average permeability, transmissivity and storativity of 4.5 m/day, 116 m^2/day

and 0.019, respectively (Jeffares and Green, 2012; Meyer and Godfrey, 1995). Furthermore, Worthington (1978) reported borehole yields of up to 25 l/s in areas where the aquifer layer is more than 20 m thick. The presence of numerous dissolution channels within the Uloa Formation has increased the porosity significantly, and resulted in it being classified as an intergranular and karstic hydrogeological unit (Meyer and Godfrey, 1995).

The lower most productive aquifer unit is underlain by the Upper Cretaceous siltstone of the St. Lucia Formation. There exists little hydrogeological information regarding this formation, however it is characterised by low yields and low permeability and is therefore considered as the impermeable hydrogeological basement to the overlying aquifers. The main aquifers underlying the Lake Sibayi system are summarised in Table 5.1.

Table 5.1. Hydraulic characteristics of the different aquifer units present in the study area (compiled from various sources).

Aquifer name	Thickness (m)	K (m/d)	T (m^2/day)	Borehole yields (l/s)
Sibayi and KwaMbonambi Formations	20-30*	0.87-15.6 (mean: ~5)	1490	0.5-5
Kosi Bay/Port Durnfort Formation	15-20*	4-5 (mean: 4.3)	-	2-10
Uloa/Umkwelane Formation	5-20	0.5-25 (mean: 4.5)	116	5-25
St Lucia Formation	900	-	-	<1

* The relationship between the KwaMbonambi and Kosi Bay Formations is very complex and therefore the thicknesses of the units in the study area are based on rough approximations.

5.2. Recharge

Groundwater recharge for the study area was calculated using the chloride mass balance (CMB) method which was verified against the published maps or “Qualified Guesses”. Recharge estimated using the CMB method for the saturated zone is presented in Table 5.2 and Figure 5.1. The average chloride concentration in rainfall of 5.5 mg/l, measured by Meyer *et al*. (2001), was used during recharge estimation. The results indicate that the recharge rate for the study area ranges from 32 mm/a to 300 mm/a with an average recharge rate is 126 mm/a (12 % MAP).

Table 5.2. Groundwater recharge estimation from the saturated zone (MAP of 1012 mm/a).

Sample No.	Groundwater Cl (mg/l)	Recharge (mm/a)	Recharge (% MAP)
SIB01	32.8	168.1	16.6
SIB03	18.4	300.2	29.7
SIB04	47.9	115.2	11.4
SIB06	29.9	184.4	18.2
SIB06	41.9	131.6	13.0
SIB09	78.8	70.0	6.9
SIB10	46.0	119.8	11.8
SIB19	126.1	43.7	4.3
SIB20	105.4	52.3	5.2
SIB20	172.6	32.0	3.2
SIB21	65.2	84.6	8.4
SIB22	47.8	115.4	11.4
SIB25	29.2	189.0	18.7
SIB25	39.9	138.3	13.7
SIB26	32.5	169.9	16.8
SIB26	48.9	112.9	11.2
SIB27	46.6	118.2	11.7
SIB27	84.5	65.3	6.4
SIB29	39.6	139.1	13.7
SIB34	72.8	75.7	7.5
SIB38	36.7	150.4	14.9
SIB39	59.7	92.4	9.1
SIB40	32.7	168.6	16.7
SIB40	46.2	119.3	11.8
SIB41	61.8	89.3	8.8
S01	31.7	173.9	17.2
S12	58.3	94.6	9.3
S14	76.5	72.1	7.1
S16	42.5	129.8	12.8
S18	70.6	78.1	7.7
S19	58.9	93.7	9.3
S05	24.5	224.9	22.2
S06	24.5	224.9	22.2
S09	34.4	160.3	15.8
Mean	**54.9**	**126.4**	**12.5**

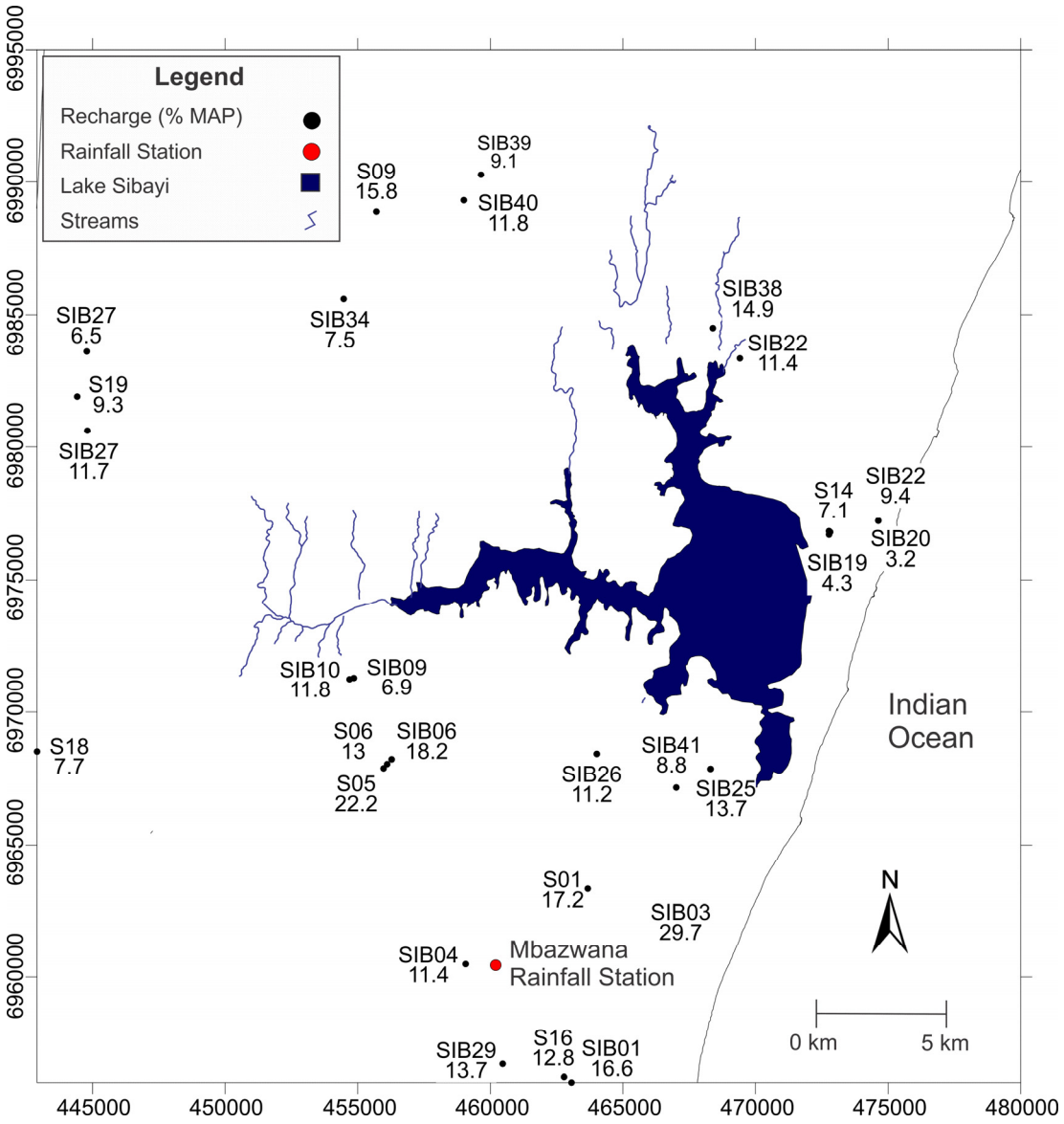

Figure 5.1. Spatial distribution of groundwater recharge within the Lake Sibayi catchment using the CMB method.

Published groundwater recharge maps (Vegter, 1995), ACRU (Schulze, 1989), Groundwater Resources of RSA (WRC, 1995) and Groundwater Harvest Potential (Baron *et al*., 1996) were used to validate the groundwater recharge estimated using the CMB method. These maps were used in conjunction with the physical properties of the catchment, in the form of soil, vegetation, slope and lithology. The "Qualified Guesses" recharge estimate from the soil/vegetation and geology are based on expert options and general equations proposed by Bredenkamp *et al*. (1995) and Kirchner *et al*. (1991). Recharge rates based on the various "Qualified Guesses" are presented in Table 5.3. All of the recharge estimates are in general agreement resulting in an average recharge rate of about 95 mm/a corresponding to a recharge percentage of 10% MAP. These recharge results are comparable with previous groundwater recharge estimated for the Maputaland coastal plain by Worthington (1978), Meyer and Kruger (1987), Bredenkamp (1993), Bredenkamp *et al*. (1995) and Meyer *et al*. (2001).

Table 5.3. Recharge estimation using qualified guesses, after Bredenkamp *et al*., (1995) and Kirchner *et al*., (1991)

Recharge rate source/methods	Recharge rate (mm/a)	% MAP
Vegter	65	6.4
ACRU	90	8.9
Harvest Potential	100	9.9
Soil/vegetation information	97.2	9.6
Geology information	104.6	10.3
GW Resources	110	10.9
Mean	**95**	**10**

5.3. Regional groundwater flow direction

Depth to groundwater measurements obtained from the National Groundwater Archive (NGA, 2013), the Groundwater Resource Information Project (GRIP, 2013), and measurements taken during the course of this research were used to construct a regional groundwater level contour map for the study area. These water level measurements allowed for the determination of groundwater flow direction, location of recharge and discharge areas and the connection between aquifers and surface water systems. The results indicate that the regional groundwater flow direction is eastwards, from the Lebombo Mountains situated in the west (Figure 5.2). The Tshingwe-Sihangwane Sand Megaridge acts as a regional groundwater divide as water is observed to flow away from the ridge to the lower lying areas. Local flow vectors are observed in the vicinity of the major lakes and wetlands which are used to define the extent of the groundwater contributing area to the lake.

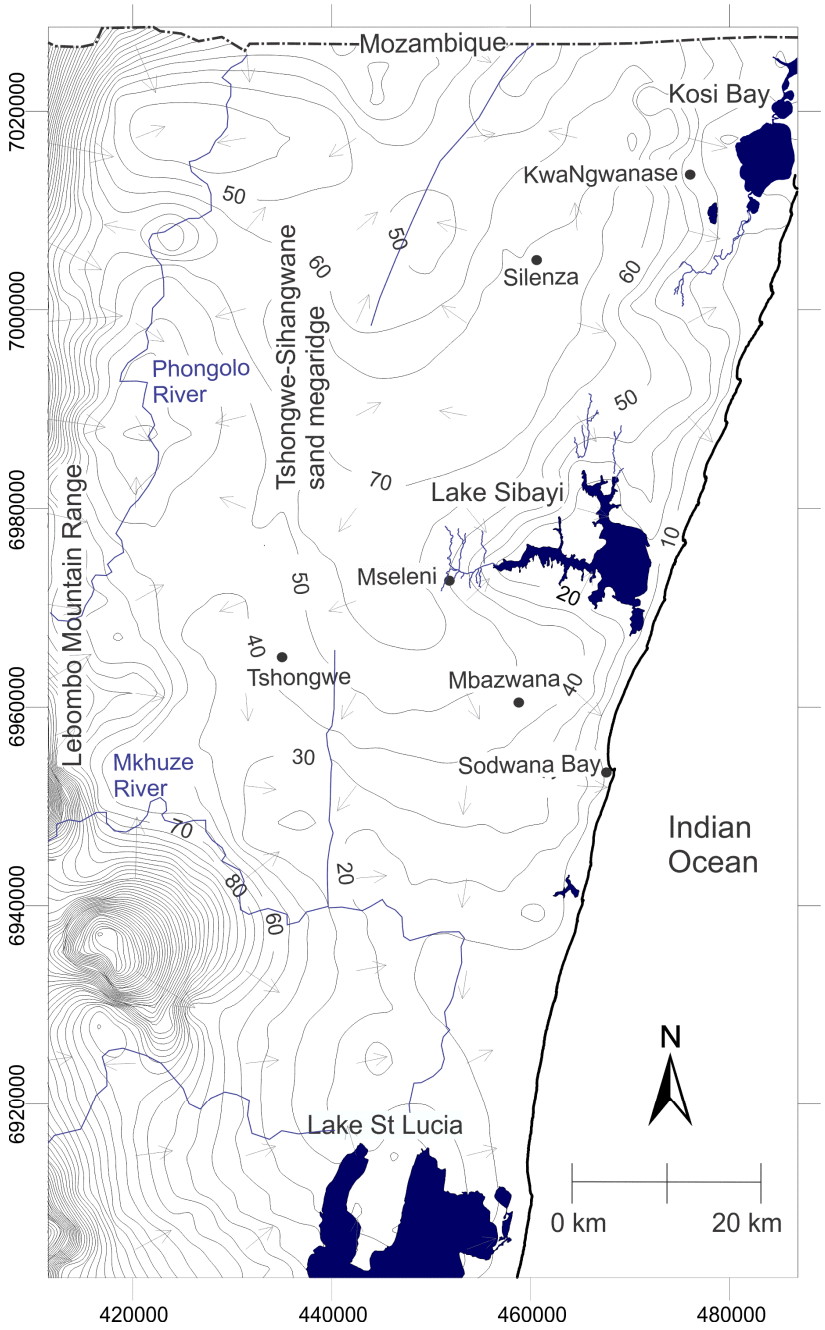

Figure 5.2. Regional groundwater flow distribution map showing local flow vectors (groundwater elevation (m amsl) presented at 10 m contour interval).

5.4. Water balance of Lake Sibayi

Accurate water budgets analysis for the various water resources are prerequisites for sustainable management of the water resource. Water balance provides a framework for studying the hydrological behaviour of a catchment and it can be used to identify changes in the water balance components (Zhang *et al*., 1999). Because of the spatial and temporal variation of the various input and output components, quantification of the water-balance components of large lakes is challenging.

The water balance of Lake Sibayi has been quantified by defining the various inflow and outflow components of the lake. Precipitation over the lake was taken from the forty six year mean rainfall data collected from the Hlabisa Mbazwana Airfield Meteorological Station (SAWS, 2015). Surface runoff from the catchment of the lake was calculated using the runoff coefficients determined using the rational method reported in Tripathi and Singh (1998). The methods takes into account soil type, slope and vegetation cover of the catchment. A very low runoff coefficient of 0.01 or about 1% of MAP was deemed acceptable for a catchment characterised by flat topography, highly permeable sandy soil and a dense vegetation cover. Groundwater inflow was derived from the previously defined recharge rates estimated using the CMB method. This resulted in a recharge rate of 126 mm/a (12% MAP). Open water evaporation was calculated using the Penman method (Shaw, 1994). Lake water outflow in the east through the shallow aquifer to the sea was calculated using Dupuit's equation (Dupuit, 1863). Previous investigations by Miller (2001) indicated the presence of a subsurface paleo-channel, acting as a preferential pathway of lake water to the sea, along the eastern shore of Lake Sibayi. The paleo-channel has subsequently been filled with Holocene age sediments. Geophysical investigations undertaken by Meyer *et al*. (2001) estimated that the paleo-channel has an average depth of 100 m below sea level. This paleo-channel depth, however, could not be verified in this study. For the water balance analysis, the estimation of freshwater outflow to the ocean used an average permeability of 5 m/d , a flow length of 2000 m and a head difference of 19 m, resulting in groundwater outflow of 2.3 x 10^7 m^3/a through 12 km seepage face.

Water users in the area range from agriculture, forestry, town to rural water. Groundwater abstraction from within the lake's catchment and water abstraction from the lake for local community water supply has commenced in the past few years to meet the growing demand. The total amount of water abstracted from both surface and groundwater resources within the catchment is 4.5 x 10^6 m^3/a.

The results of the mean monthly and mean annual long-term (1970 – 2014) water balance for the lake is given in Tables 5.4 and 5.5. The water balance of Lake Sibayi shows that lake levels fluctuate in response to varying amounts of groundwater and surface water inflow to the lake, seepage loss through the coastal dune, abstraction, and evaporation from the lake.

Table 5.4. Estimated long-term (1970 -2014) monthly major water balance components of Lake Sibayi (in 10^6 m^3).

	Jan	Feb	Mar	Apr	May	Jun	Jul	Aug	Sep	Oct	Nov	Dec
P_{recip}	6.08	7.65	7.70	10.59	11.24	8.63	6.01	3.50	2.97	2.53	2.14	4.80
S_{runoff}	0.19	0.24	0.24	0.33	0.35	0.26	0.18	0.11	0.09	0.08	0.07	0.15
G_{in}	4.92	6.19	6.22	8.56	9.09	6.98	4.86	2.83	2.40	2.05	1.73	3.88
G_{out}	1.90	1.90	1.90	1.90	1.90	1.90	1.90	1.90	1.90	1.90	1.90	1.90
E_{vapo}	10.17	11.16	12.21	12.39	11.08	10.36	8.25	6.26	5.15	5.59	7.64	8.84
W	0.37	0.37	0.37	0.37	0.37	0.37	0.37	0.37	0.37	0.37	0.37	0.37
ΔS	-1.25	0.65	-0.32	4.81	7.32	3.24	0.53	-2.09	-1.97	-3.21	-5.97	-2.28

Table 5.5. Long-term (1970 -2014) annual lake water balance of the Lake Sibayi catchment (10^6 m^3).

Lake area (km^2)	Surface water catchment area (km^2)	Groundwater contribution area (km^2)	P_{recip}	S_{runoff}	G_{in}	G_{out}	E_{vapo}	W	ΔS
72.99	521.32	663.23	73.85	2.27	59.72	22.78	109.1	4.49	-0.54

The water balance results of Table 5.4 show strong seasonal variations. Both the mean monthly and annual water balance of the lake indicates that inflows into the lake are less than the outflows from the lake resulting in a negative change in storage (ΔS). Negative change in storage is interpreted as continuous lake level decline which matches observed data of lake level as shown in Figure 5.3. The observed decline is a result of various inflow and outflow factors ranging from increased abstraction rates, the gradual decline in the rate of precipitation, the rapid increase in small scale plantations in the area and ever increasing groundwater pumping from the catchment.

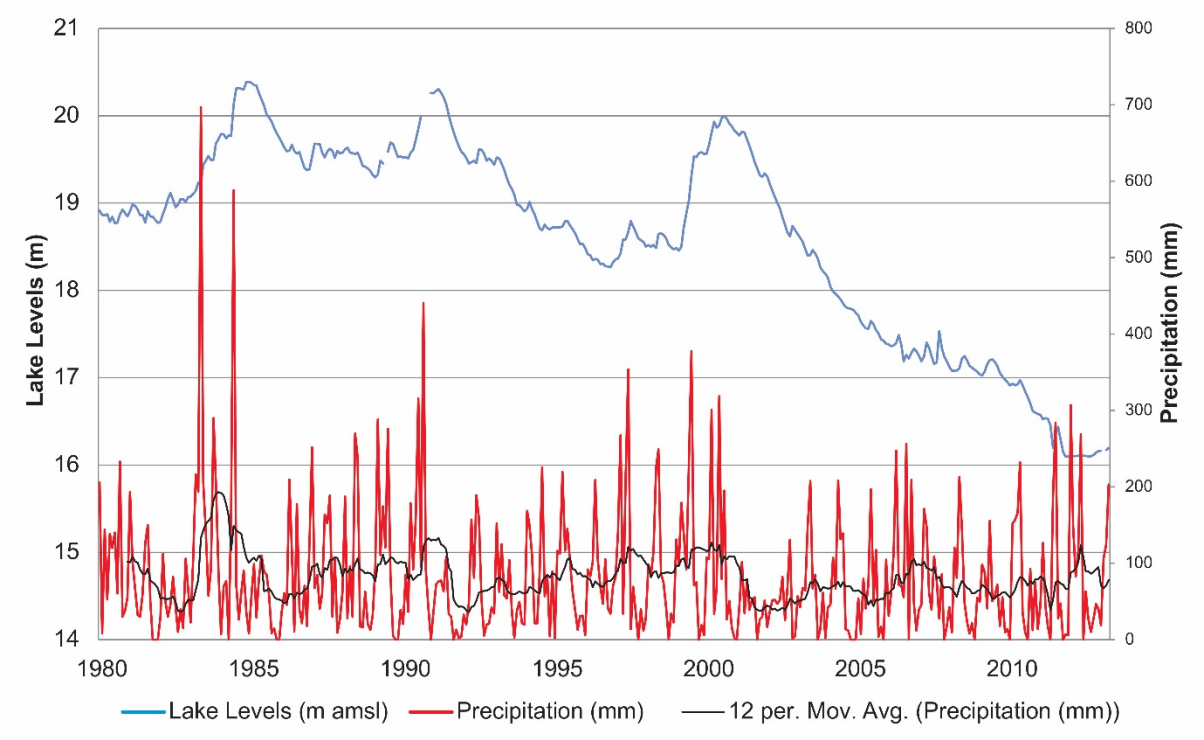

Figure 5.3. Long-term lake-level fluctuations along with monthly precipitation from 1980 to 2012 (DWA, 2013; SAWS, 2015). The 12-month moving average precipitation is shown in black.

The results further show that the major water balance components for Lake Sibayi are evaporation followed by precipitation on the surface of the lake and groundwater inflow. The change in storage was calculated as a residual of the water balance, therefore all errors inherent in each of the water balance components are assumed to be incorporated into the change in storage.

The residence time of water in the lake was estimated to determine the turnover time of water in the lake. Residence time of lake water is calculated using:

$$T_r = s/q \quad (20)$$

where T_r represents the residence time (years), s is the volume of the lake and q the average rate of outflow.

The volume of the lake was calculated from bathymetry data reported by Miller (2001), while the total rate of out flow from the lake was determined by summing all of the outflow components of the water balance in Table 5.3. From a total lake volume measured in 1993 (7.9×10^8 m^3) and out flow volume (1.4×10^8 m^3/a), the residence time of water in the lake is approximately 6 years. The lake volume measured during 1993 by Miller (2001) was used in the calculations as it provided a better estimate of historical conditions than the extremely low volume currently encountered.

5.5. Hydrochemical characteristics of the Lake Sibayi system

Hydrogeochemical processes control the chemistry of water and are commonly used to identify the origin of the groundwater as well as identify problems related to the quality thereof (Kumar *et al*., 2013). Hydrochemical analyses are powerful tools to understand the source of mixing waters in groundwater and surface water systems (Clark and Fritz, 1997; Appelo and Postma, 2005). Hydrochemical parameters for the various water sources within the Lake Sibayi hydrological system were measured to study the relationship between these resources.

A univariate statistical overview of the groundwater hydrochemical data is presented in Table 5.6. The hydrochemical parameters were assessed by determining minimum, maximum, mean, median and standard deviation for each of the 19 variables or parameters.

Table 5.6. Univariate statistical overview of the groundwater results. All values in mg/l unless otherwise stated (SD – Standard Deviation).

Variable	N	Minimum	Maximum	Mean	Median	SD
pH	71	4.7	8.32	6.22	5.95	0.77
Temperature (°C)	49	20.47	26.20	24.59	24.70	0.81
EC (mS/m)	71	17	1244.00	239.37	159.00	258.43
TDS	59	29	634.00	150.58	93.00	135.88
Hardness as $CaCO_3$	46	4.11	160.80	44.79	21.18	46.32
HCO_3^-	38	2	170.11	35.33	12.19	45.43
Alkalinity	37	3	272.00	43.77	11.00	58.06
Na^+	46	12.3	189.00	36.18	27.40	28.80
K^+	46	0	7.26	2.85	2.19	2.02
Mg^{2+}	46	0.8	13.36	4.41	3.48	3.41
Ca^{2+}	46	0.331	46.00	10.68	2.54	14.19
Fe	46	0	30.13	2.20	0.21	5.15
Cl^-	46	18.38	267.57	61.48	46.82	45.85
SO_4^{2-}	46	0.33	155.10	13.76	6.65	27.53
$NO_3^- + NO_2^-$ as N	46	0	109.98	5.08	1.65	16.69
F^-	46	0.018	1.18	0.24	0.13	0.29
δ^2 H (‰)	44	-22.4	19.23	-8.83	-10.74	8.81
δ^{18} O (‰)	44	-4.54	1.51	-2.87	-3.17	1.21
Tritium (T.U.)	37	0	2.20	1.06	1.10	0.58

Based on the TDS concentrations, most of the various water sources can be classified as being fresh water (Appendix E). The pH ranges from 4.7 to 8.3 with a mean of 6.2 indicating that the groundwater is generally slightly acidic. The total hardness of the groundwater ranges from 4.1 to 160 mg/l $CaCO_3$ which based on the criteria of Durfer and Becker (1964) ranges from soft to hard. The hard water types were generally associated with the deep groundwater samples.

The hydrochemical data generated are plotted on a Durov diagram (Durov, 1948), Piper Trilinear diagram (Piper, 1944) and Schoeller diagrams (Schoeller, 1964) (Figure 5.4), illustrating the different water types and dominant chemical species in the waters sampled. The complete analytical results are presented in Table 5.7 with trace elements presented in Appendix F. Additional data for the deep aquifer was obtained from Meyer and Godfrey (2003) and Jeffares and Green (2012) to aid the limited number of samples collected during the field campaigns from the deep aquifer (Table 5.8).

The chemical compositions observed in most of the groundwater samples were similar, dominated by Na^+, Cl^- and HCO_3^-. The samples can generally be divided into distinct groups based on the type of water source. A slight distinction between shallow and deep aquifers appears to be present, where the shallow groundwaters are dominated mainly by a Na-Cl hydrochemical facies, while the deeper boreholes are dominated mainly by a Na-Ca-HCO_3-Cl hydrochemical facies (Figure 5.4). A similar trend was observed during baseline studies of groundwater quality along the Eastern Shores of Lake St Lucia by Bjørkenes *et al*. (2004) and Bjørkenes *et al*. (2006).

Table 5.7. On site and laboratory measured surface water and groundwater physical and chemical parameters generated during this research. All values in mg/l unless otherwise stated

Name	Date	Water point	Water level (m amsl)	pH	Temp. (°C)	EC (mS/m)	TDS	HCO_3^-	Na^+	K^+	Mg^+	Ca^{2+}	Fe	Cl^-	SO_4^{2-}	NO_3^-
SIB01	29/09/12	Groundwater	26.3	5.5	24.0	132	66	10.4	20.1	1.4	0.8	0.7	0.5	32.8	6.9	0.0
SIB03	29/09/12	Groundwater	31.9	6.6	23.8	158	79	67.1	12.3	1.9	1.7	11.2	0.0	18.4	6.8	8.4
SIB04	30/09/12	Groundwater	-	5.6	24.0	198	99	12.2	27.3	1.6	2.5	1.5	0.0	47.9	5.1	11.6
SIB06	07/04/13	Groundwater	50.5	5.7	24.8	118	59	6.1	20.2	0.8	1.0	0.4	0.0	41.9	5.9	2.6
SIB06	30/09/12	Groundwater	50.5	5.5	25.1	124	62	7.9	19.3	1.0	1.0	0.6	0.0	29.9	6.7	4.1
SIB09	09/04/13	Groundwater	-	5.8	24.9	189	94	7.3	31.2	3.5	1.7	0.7	0.0	78.8	6.2	0.8
SIB10	30/09/12	Groundwater	45.2	5.4	25.0	171	85	6.1	25.6	3.0	1.5	0.6	0.0	46.0	5.5	3.4
SIB13	30/09/12	Stream	46.1	7.8	20.8	721	361	257.3	97.4	4.7	10.1	32.0	0.1	110.9	15.2	6.0
SIB16	01/10/12	Lake	16.1	9.0	23.0	648	324	136.6	85.3	8.1	10.6	16.5	0.0	137.8	20.4	5.9
SIB18	08/04/13	Lake	-	8.9	26.6	640	320	150.6	95.4	7.5	10.7	16.7	0.1	219.2	19.7	0.4
SIB19	08/04/13	Groundwater	15.5	6.2	25.5	433	217	13.4	53.0	6.3	5.8	10.7	12.5	126.1	118.7	7.7
SIB20	08/04/13	Groundwater	19.3	7.0	24.7	547	274	170.1	71.2	6.5	8.8	19.6	6.8	172.6	1.8	0.5
SIB20	01/10/12	Groundwater	18.9	7.0	25.0	526	263	129.3	60.0	6.7	7.5	17.5	0.1	105.4	3.6	2.9
SIB21	01/10/12	Groundwater	-	7.2	23.7	392	196	78.7	32.5	2.9	7.5	7.1	6.9	65.2	3.3	2.9
SIB22	01/10/12	Groundwater	28.3	5.8	24.5	174	87	3.7	19.1	2.4	3.9	1.9	0.0	47.8	7.3	3.8
SIB25	08/04/13	Groundwater	25.0	5.7	25.0	133	66	9.8	19.1	1.6	3.4	1.4	1.2	39.9	14.9	0.3
SIB25	01/10/12	Groundwater	24.9	5.8	24.7	146	79	7.3	17.2	1.9	3.6	1.7	1.2	29.2	15.0	2.9
SIB26	08/04/13	Groundwater	-	5.8	24.7	129	64	9.8	20.9	0.7	1.4	1.0	0.1	48.9	3.3	0.4
SIB26	02/10/12	Groundwater	39.6	6.1	24.5	129	65	8.5	20.2	0.7	1.3	1.1	0.5	32.5	5.3	3.0
SIB27	07/04/13	Groundwater	72.3	6.0	24.5	215	148	15.9	35.6	1.9	2.8	0.7	3.6	84.5	8.4	0.4
SIB27	02/10/12	Groundwater	68.6	5.8	26.2	191	95	12.2	30.1	1.9	1.9	0.7	2.3	46.6	8.8	2.8
SIB29	06/04/13	Groundwater	35.5	6.0	24.0	123	61	12.2	18.4	0.0	1.6	1.0	0.0	39.6	6.3	0.5
SIB34	07/04/13	Groundwater	-	6.8	25.0	254	127	86.6	30.3	2.2	4.4	1.5	11.7	72.8	1.2	0.3
SIB38	08/04/13	Groundwater	-	6.5	24.3	108	53	9.8	16.9	1.1	1.2	0.8	0.0	36.7	7.0	0.5
SIB39	09/04/13	Groundwater	75.3	5.9	24.2	157	79	10.4	25.7	0.3	1.7	1.1	0.5	59.7	6.6	0.3
SIB40	09/04/13	Groundwater	75.9	7.2	24.9	322	161	160.4	27.4	4.8	3.6	21.3	6.4	46.2	6.5	0.4

SIB41	26/05/13	Groundwater	33.7	6.3	24.7	192	96	35.4	23.8	1.0	2.1	6.1	0.0	61.8	4.7	0.7
S1	10/04/08	Groundwater	-	5.5	-	130.6	-	22.5	19.5	2.2	2.3	0.9	1.1	31.7	2.5	0.2
S5	11/04/08	Groundwater	-	5.1	-	24.6	-	27.0	19.2	1.6	0.9	0.6	0.0	24.5	3.6	11.8
S6	11/04/08	Groundwater	-	4.9	-	27.9	-	9.5	23.4	1.6	0.8	0.3	0.1	24.5	17.9	4.0
S9	11/04/08	Groundwater	-	4.7	-	443	226	9.0	22.5	0.9	2.0	1.9	2.9	34.4	18.7	2.6
S11	12/04/08	Lake	-	8.5	-	1786	909	128.0	91.7	8.4	10.0	18.1	0.1	138.7	15.5	1.8
S12	12/04/08	Groundwater	-	6.1	-	1058	538	120.0	32.2	3.9	6.0	6.3	30.1	58.3	1.3	2.1
S14	12/04/08	Groundwater	-	5.7	-	915	476	37.0	33.7	4.7	6.1	11.3	2.8	76.5	16.9	1.7
S15	12/04/08	Rain	-	4.5	-	57.4	29	-	0.3	0.2	0.1	0.2	0.0	0.6	3.0	0.6
S16	13/04/08	Groundwater	-	5.6	-	453	231	11.0	26.5	2.2	1.6	0.9	0.1	42.5	4.9	0.3
S17	13/04/08	Groundwater	-	6.9	-	1244	634	102.0	93.9	0.7	1.6	3.0	0.1	75.6	24.7	0.0
S18	13/04/08	Groundwater	-	6.7	-	1010	516	49.5	67.4	3.2	5.6	6.3	2.2	70.6	18.3	6.8
S19	13/04/08	Groundwater	-	5.7	-	1042	532	2.0	46.9	3.4	13.4	2.9	0.1	58.9	12.1	110.0
S20	11/04/08	Stream	-	5.9	-	2120	1083	243.0	108.9	5.2	10.0	34.1	0.2	117.6	14.5	0.4

Table 5.8. Surface water and groundwater physical and chemical parameters sourced from Jeffares and Green (2012, 2014a, 2014b) and Terratest (2009a, 2009b, 2011, 2014, 2015a, 2015b, 2016a, 2016b). All values in mg/l unless otherwise stated

Name	Date	Water point	pH	EC (mS/m)	TDS	HCO_3^-	Na^+	K^+	Mg^+	Ca^{2+}	Fe	Cl^-	SO_4^{2-}	NO_3^-
J&G SIB1	24/11/11	Groundwater	6.0	17		10.0	21.0	1.2	1.6	2.2	0.7	36.0	1.0	0.1
J&G SIB2	25/11/11	Groundwater	7.5	48		136.0	30.0	4.8	10.0	35.0	1.0	46.0	2.6	0.1
Nthongwe	24/11/11	Groundwater	7.4	126		272.0	189.0	5.4	13.0	43.0	0.3	186.0	16.8	0.4
Manaba	25/11/11	Groundwater	7.7	42		112.0	42.0	2.8	6.3	24.0	0.2	47.0	0.3	0.1
Indundubala School	24/05/11	Groundwater	7.2	30.6	174.4	48.0	40.0	3.6	5.4	27.3	0.1	42.4	28.0	2.5
Manzamgwenya	28/07/14	Groundwater	7.1	38.2			43.2	7.3	4.5	38.4	0.0	267.6	155.1	3.5
KwaSonto	02/08/14	Groundwater	6.8	38.1			27.4	6.7	6.3	39.7	0.2	35.2	9.1	0.0
Kwamhlamvu	04/06/15	Groundwater	7.5	23.2	148	26.9	24.1	2.3	7.0	6.1	0.2	48.3	8.3	11.0
Welandlovu	29/01/15	Groundwater	8.3	50.4	323	122.0	42.6	4.2	8.4	43.0	BDL	72.4	7.9	BDL
Coastal Cashews	11/05/16	Groundwater	6.4	24.7		51.0	-	BDL	6.8	8.8	1.0	45.6	5.1	BDL
KwaTembe	11/02/08	Groundwater	7.6	67		60.0	65.0	6.9	11.0	46.0	0.0	53.0	4.0	0.2
Mlamula	02/05/14	Groundwater	7.4	42.2			40.9		9.8	32.5	1.6	39.9	8.4	BDL

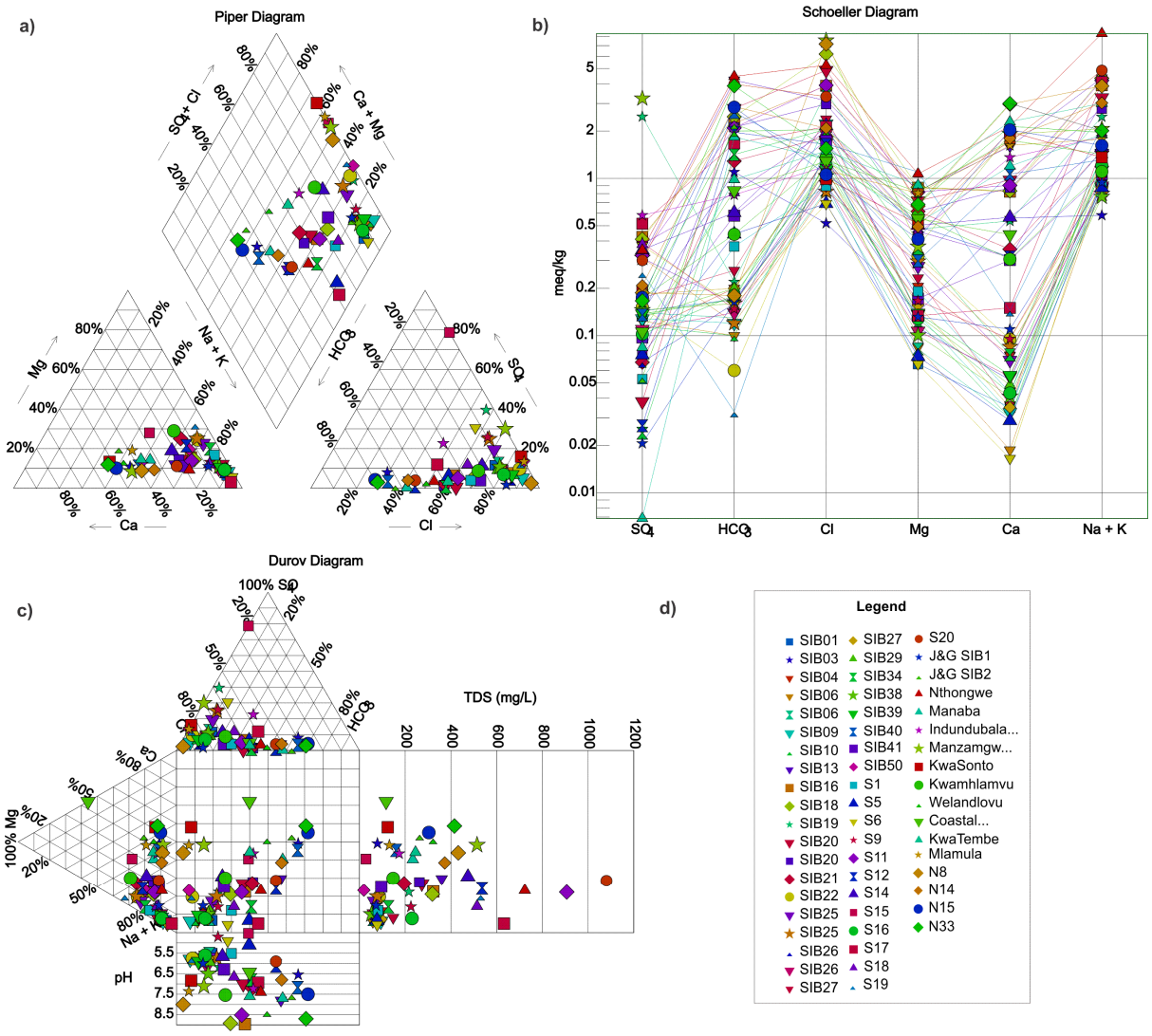

Figure 5.4. Groundwater and surface samples within the Lake Sibayi Catchment plotted on (a) Piper trilinear diagram, (b) Schoeller diagram (c) Durov diagram and (d) indicates the sample labels.

5.6. Statistical analyses of the hydrochemical results

To further illustrate the distinction between the different water types, various statistical analyses were conducted on the hydrochemical results.

5.6.1. Correlation Matrices

To measure the relationship between the various hydrochemical parameters, a bivariate Pearson's correlation matrix of the measured variables was undertaken (Table 5.9). Pearson's product–moment correlation coefficient (R) is a measure of the linear dependence between two variables and is expressed as the covariance of two variables divided by the product of their standard deviation. The resultant dimensionless R value ranges between +1 and -1, where 1 is perfect positive linear

Table 5.9. Pearson's correlation matrices for groundwater hydrochemical data

	EC	pH	Temp	TDS	Na^+	K^+	Ca^{2+}	Mg^{2+}	Cl^-	F^-	HCO_3^-	NO_3^-	SO_4^{2-}	$\delta^{18}O$	δ^2H	Tritium
EC	1															
pH	0.705	1														
Temp	0.178	-0.126	1													
TDS	0.992	0.693	0.169	1												
Na^+	0.923	0.487	0.312	0.930	1											
K^+	0.905	0.543	0.333	0.893	0.849	1										
Ca^{2+}	0.810	0.771	0.058	0.788	0.643	0.795	1									
Mg^{2+}	0.923	0.688	0.071	0.917	0.805	0.794	0.689	1								
Cl^-	0.849	0.449	0.258	0.861	0.954	0.770	0.556	0.764	1							
F^-	0.002	0.016	0.247	0.004	-0.029	-0.139	0.035	-0.133	0.049	1						
HCO_3^-	0.775	0.860	0.002	0.757	0.613	0.680	0.896	0.706	0.534	-0.046	1					
NO_3^-	0.079	-0.148	-0.092	0.061	0.004	0.136	0.070	0.044	-0.079	0.850	-0.136	1				
SO_4^{2-}	0.290	-0.042	0.338	0.286	0.307	0.399	0.156	0.219	0.347	-0.318	-0.161	0.368	1			
$\delta^{18}O$	0.796	0.559	0.004	0.781	0.779	0.664	0.648	0.825	0.731	0.359	0.605	-0.033	0.130	1		
δ^2H	0.749	0.507	-0.010	0.725	0.719	0.623	0.613	0.781	0.639	0.321	0.565	0.023	0.098	0.979	1	
Tritium	0.100	-0.301	0.226	0.075	0.172	0.117	0.053	0.161	0.131	-0.310	-0.201	0.366	0.435	0.405	0.455	1

correlation, 0 is no correlation, and -1 is perfect negative correlation (Borradaile, 2003). This allows for the determination of correlations between several hydrochemical variables.

A strong positive correlation was observed between EC and several major elements, which included Na^+, K^+, Mg^{2+}, Ca^{2+}, Cl^- and HCO_3^-. These elements were also found to be strongly correlated to one another with all correlations found to be significant.

5.6.2. Factor analyses

Factor analyses in the form of Principal components analyses with varimax rotation was performed on the 12 hydrochemical parameters with the main aim of identifying the underlying factors or processes responsible for the groundwater chemistry in the study area.

The results revealed that three principle factors, with eigenvalues greater than 1, explain about 95% of the hydrochemical variation with commonalities generally greater than 0.9 (Table 5.10). These three factors can therefore be used to explain the hydrochemical processes without losing any significant characteristics. Most of the variance is contained within Factor-1 (69.5%), which has a high positive loading factor associated with EC, TDS, Na^+, Mg^+ and Cl^- concentrations. The hydrochemical variables associated with Factor-1 indicates that it could be interpreted as the salinisation factor, which according to Yang *et al*. (2015) refers to an increase in the concentration of total dissolved solids and EC in water often associated with increases in chloride, sodium and magnesium. This could result from the flushing of salt concentrations within the tertiary sands brought about by historical marine transgression events or through rainfall influenced by marine salts and aerosols (Allanson, 1979). These components represent the major processes controlling the salinity of groundwater. Factor-2 represents 17.67% of the total variation in the hydrochemistry and has high positive loadings for pH, HCO_3^-, K^+, Ca^+ and Fe concentrations. The HCO_3^-, K^+ and Ca^+ could be the result of weathering and dissolution of carbonate minerals in calciferous formations and redox processes (Appelo and Postma, 2005). The Fe concentrations would be derived from the leaching of iron rich ferricrete layers associated within the study area (Miller, 2001; Demlie *et al*., 2014). The variables NO_3^- and SO_4^- contribute most strongly to Factor-3, which explains 8.01% of the total variance. The loading for NO_3^- was positive while that of SO_4^- was negative and could result from anthropogenic pollution.

A principal component analyses plot shown in rotated space (Figure 5.5), illustrates the relationship of the various variables relative to the three dominant components as determined in Table 5.10.

Table 5.10. Results of principal component factor analysis of the hydrochemical data with Varimax rotation.

Variable	Communality	Component (Factors)		
		1	2	3
pH	0.932		0.928	
EC	0.998	0.781	0.623	
TDS	0.998	0.780	0.623	
HCO3	0.991		0.867	
Na	0.997	0.922		
K	0.977	0.625	0.746	
Mg	0.987	0.903		
Ca	0.974		0.902	
Fe	0.989		0.822	
Cl	0.995	0.952		
SO4	0.774	-0.415		-0.631
NO3	0.995			0.976
Cumulative % variance		69.5	87.2	95.3

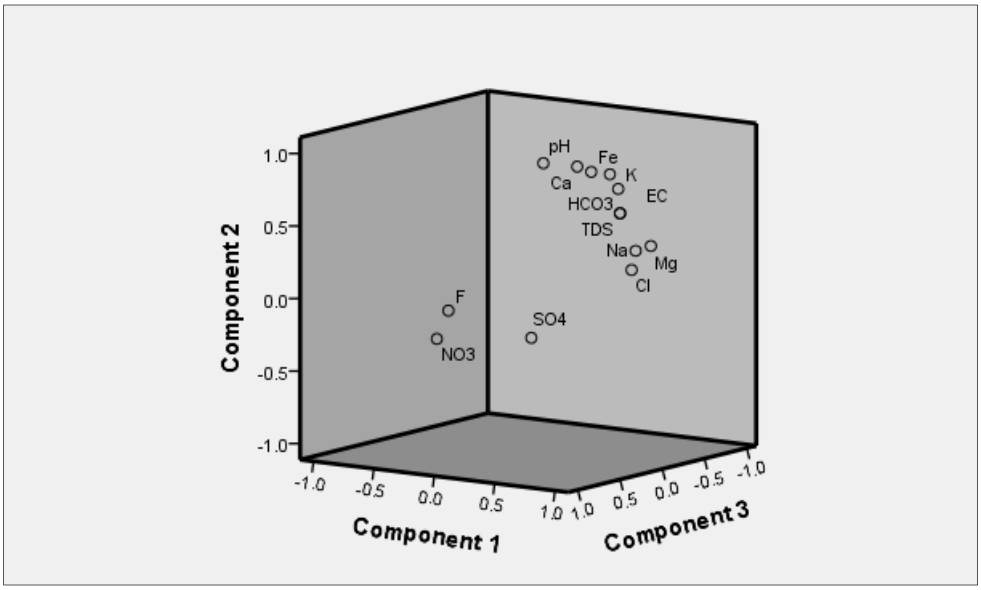

Figure 5.5. Principal component analyses plot of the variables in rotated space.

5.6.3. Cluster Analyses

Cluster analyses allow for the objective analysis of the hydrochemical data to identify areas of similar hydrochemical characteristics (Suk and Lee, 1999). Hierarchical cluster analysis of hydrochemical data was performed using the Ward method with squared Euclidean distance measure. The objective was to group the various water samples into distinct clusters based on their hydrochemistry. The water samples were clustered into two distinct groups representing unique hydrochemical systems (Figure 5.6). The first cluster (C-1) represents the groundwater samples, which is in turn divided into 2 sub-clusters representing the shallow (C-1.1) and deep (C-1.2) aquifers. The deep groundwater cluster

forms an amalgamation between the deep groundwater samples and the shallow groundwater samples collected along the coastal dune cordon east of the lake. The second cluster (C-2) represents the surface water samples with a clear distinction between stream (C-2.1) and lake (C-2.2) samples.

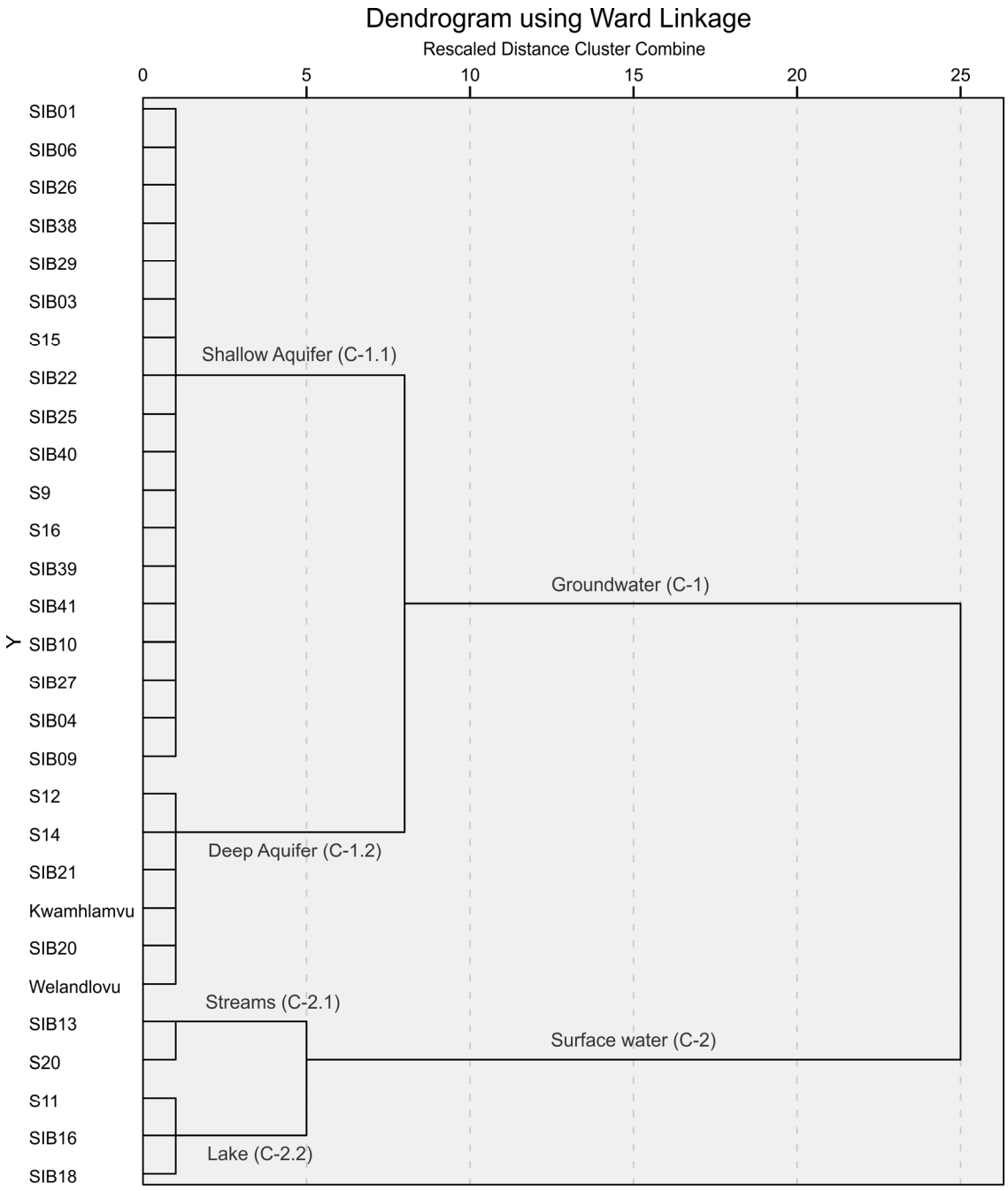

Figure 5.6. Dendrogram of the hierarchical cluster analysis of the water quality parameters of various water sources within the Lake Sibayi catchment using Ward method.

To further illustrate the distinction between the different water types, the samples were grouped according to the shallow and deep groundwater, lake and river statistical clusters in Table 5.11 and Figure 5.7. Based on the univariate statistical analyses of the first principal component, the various

water resources within the catchment have different EC, TDS, Na^+, Mg^+ and Cl^- values. Shallow groundwater samples have relatively low EC values averaging 278 mS/m, while the deeper wells had average EC concentrations of 409 mS/m. The average EC value for the lake is 800 mS/m based on all samples collected from various locations from the lake and at different sampling seasons, which is high compared to the shallow and deep groundwater, indicating the effect of evaporation and long residence time. Similar EC values (1181 mS/m) were observed in the Mseleni River that drains into the lake. The elevated EC could be due to anthropogenic pollution from human waste flowing into the river. The remaining variables displayed a similar trend with the lowest concentrations being observed in the shallow groundwater samples with increased concentrations in the deeper aquifer, while the highest concentrations being observed in the lake and river samples. The concentrations measured for groundwater samples located along the eastern shore of Lake Sibayi, represented an intermediate between groundwater concentrations and those of the lake. The similarity of groundwater hydrochemistry along the eastern dune cordon and lake water chemistry supports the hypothesis that lake water seepage occurs through the coastal dune cordon into the Indian Ocean.

Table 5.11. Univariate statistical analyses of the hydrochemical components with the greatest variation determined from factor analyses.

Samples sources	Variable	EC (mS/m)	TDS (mg/l)	Na (mg/l)	Mg (mg/l)	Cl (mg/l)
Shallow Groundwater	Mean	278.26	147.61	31.61	3.35	56.27
	SD	277.89	143.66	18.63	2.90	32.27
	Min	24.6	29	12.3	0.8	18.38
	Median	172.5	87	25.67	1.962	47.22
	Max	1244	634	93.92	13.36	172.60
Deep Groundwater	Mean	408.69	168.20	47.42	6.84	73.38
	SD	263.24	76.94	44.18	3.34	67.63
	Min	170	93	21	1.6	35.16
	Median	372.5	161	40	6.53	46.62
	Max	1260	323	189	13	267.57
Lake	Mean	800.29	402.43	90.79	10.41	165.22
	SD	434.85	223.47	5.09	0.39	46.71
	Min	615	308	85.3	9.961	137.79
	Median	640	320	91.71	10.6	138.73
	Max	1786	909	95.35	10.67	219.15
River	Mean	1181.33	598.33	103.13	10.06	114.27
	SD	812.96	419.76	8.11	0.06	4.75
	Min	703	351	97.4	10.02	110.91
	Median	721	361	103.13	10.06	114.27
	Max	2120	1083	108.87	10.10	117.63

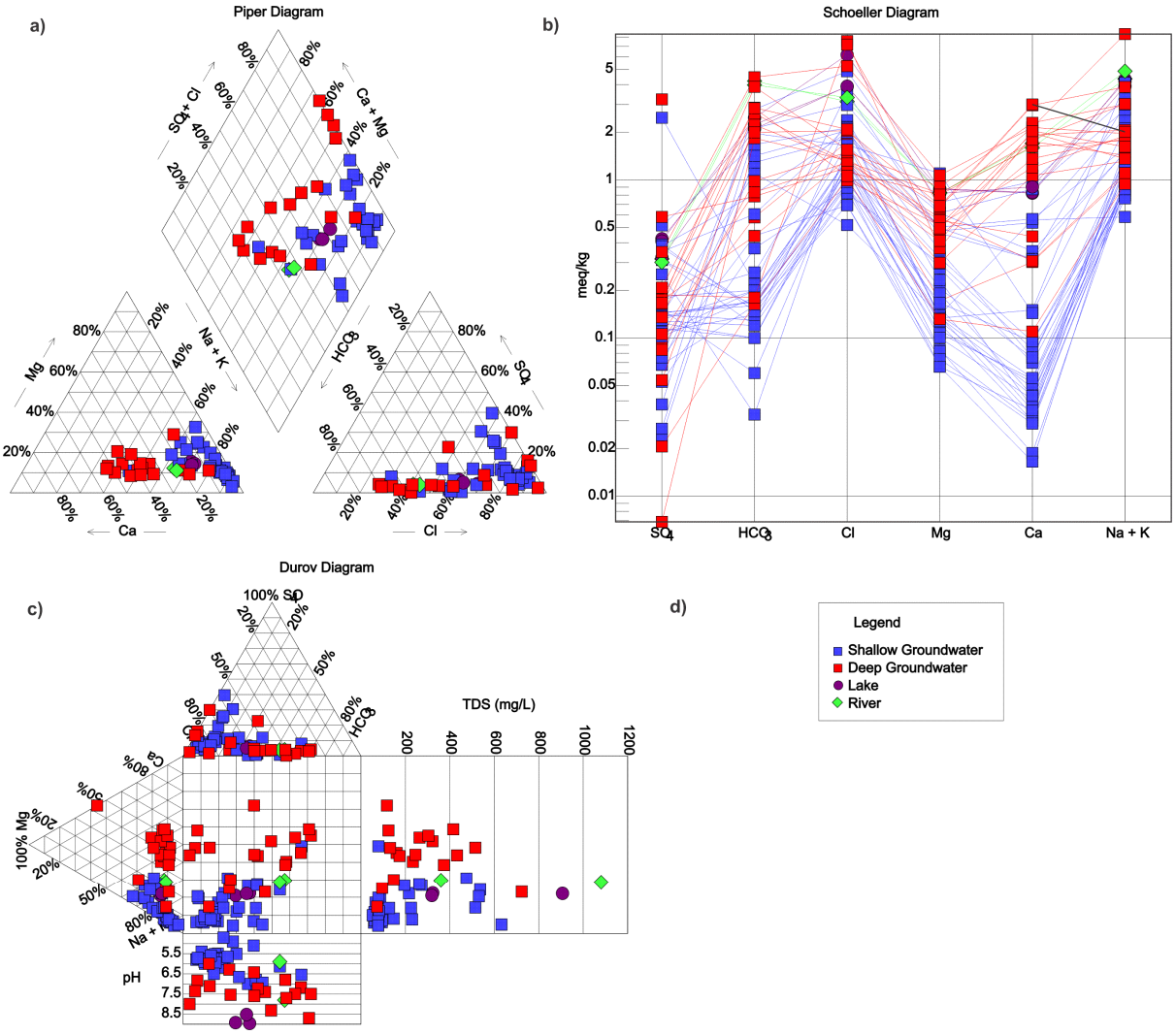

Figure 5.7. Groundwater and surface hydrochemical groups within the Lake Sibayi Catchment plotted on (a) Piper trilinear diagram, (b) Schoeller diagram and (c) Durov diagrams.

According to Maud and Botha (2000), several of the formations were deposited under marine conditions. The dominant Na-Cl character of the groundwater could be attributed to salts being leached from these sediments and dissolved in the groundwater. The saline conditions can also be attributed to sea spray coming from the ocean and carried landward by westerly winds. The hydrochemical distinction between the shallow and deep aquifers could suggest recent recharge from precipitation for shallow aquifer while the deeper water interacts with more carbonaceous units associated with the Uloa and Umkwelane Formations.

5.7. Environmental isotopes characteristics

In order to trace the source and movement of water within the study catchment, various water sources were sampled and analysed for environmental isotopes (^{18}O, Deuterium and tritium) signatures (Table

5.12). The resulting stable isotope plot of δD versus $\delta^{18}O$ (Figure 5.8) along with the Local Meteoric Water Line (LMWL) for Pretoria and global meteoric water line (GMWL).

Table 5.12. Environmental isotope data of the study area.

Sample no.	Date	Water Level (m amsl)	EC (mS/m)	TDS (mg/l)	Temp (°C)	pH	δ D (‰)	$\delta^{18}O$ (‰)	Tritium (T.U.)
S-01	11/04/08	-	131	-	-	5.51	-18.3	-3.94	1.3
S-05	11/04/08	-	25	-	-	5.1	-16.6	-3.95	0.8
S-06	11/04/08	-	28	-	-	4.9	-18.7	-4.09	1.5
S-09	11/04/08	-	443	226	-	4.7	-20	-4.11	2.2
S-10	11/04/08	-	-	-	-	-	22.3	2.38	-
S-11	11/04/08	-	1786	909	-	8.52	20.2	2.11	1.3
S-12	12/04/08	-	1058	538	-	6.13	-4.1	-1.81	0.5
S-13	12/04/08	-	145700	-	-	8.6	5.3	0.43	0.6
S-14	12/04/08	-	915	476	-	5.66	-7.3	-2.68	1.3
S-15	12/04/08	-	57	29	-	4.53	-7.1	-4.06	2.3
S-16	12/04/08	-	453	231	-	5.6	-13.9	-3.82	1.8
S-17	12/04/08	-	1244	634	-	6.94	-22.4	-4.54	0.3
S-18	12/04/08	-	1010	516	-	6.66	-22.3	-4.52	0.1
S-19	13/04/08	-	1042	532	-	5.71	-19.5	-4.19	0.9
S-20	13/04/08	-	2120	1083	-	5.9	-22.4	-4.43	0.7
SIB01	29/09/12	26.28	132	66	23.97	5.5	-10.76	-3.21	1.1
SIB02	29/09/12	35.47	58	29	24.5	7.5	2.13	-1.92	-
SIB03	08/04/13	31.06	158	79	23.77	6.55	-8.07	-2.69	1.1
SIB04	08/04/13	41.79	185	93	23.89	5.95	-8.80	-3.08	1.2
SIB06	07/04/13	45.57	118	59	24.8	5.7	-11.50	-3.22	1.7
SIB07	07/04/13	65	114	57	24.7	5.83	-9.24	-3.28	-
SIB08	07/04/13	47.4	157	79	25.51	5.8	-10.72	-3.10	-
SIB09	09/04/13	52	189	94	24.9	5.8	-13.63	-3.44	-
SIB10	30/09/12	45.78	171	85	24.98	5.4	-13.58	-3.74	0.8
SIB11	30/09/12	-	-	-	-	-	-11.36	-3.45	-
SIB13	07/04/13	-	703	351	19.6	8.1	-13.21	-3.18	-
SIB15	30/09/12	23	652	326	26.87	8.96	21.23	1.92	-
SIB16	30/09/12	22	648	324	22.98	8.96	24.83	2.05	1.1
SIB17	30/09/12	-	58810	25910	23.5	8.36	8.68	0.52	-
SIB18	08/04/13	-	640	320	26.57	8.92	23.49	1.56	1.0
SIB19	26/05/13	13.59	433	217	25.5	6.18	-0.86	-1.49	1.3
SIB20	26/05/13	9.74	547	274	24.7	7	19.23	0.86	1.5
SIB21	07/04/13	33	392	196	23.7	7.2	2.57	-1.18	0.5
SIB22	01/10/12	28	174	87	24.5	5.75	-12.82	-3.24	1.6
SIB23	01/10/12	-	-	-	-	-	-6.71	-2.08	1.0
SIB24	01/10/12	-	-	-	-	-	-1.08	-2.37	-
SIB25	26/05/13	27.89	133	66	25	5.7	-2.24	-1.72	1.5
SIB26	08/04/13	37.01	129	64	24.5	6.12	-3.42	-2.17	1.2
SIB27	07/04/13	66.31	191	148	26.2	5.75	-14.32	-3.51	1.3

SIB28	07/04/13	-	123	-	24	5.95	-11.25	-3.20	-
SIB29	07/04/13	35.2	132	61	24.7	5.7	-9.54	-3.14	-
SIB31	07/04/13	-	175	118	25.18	6.1	-14.33	-3.66	-
SIB34	07/04/13	-	189	127	21.8	6.8	-12.96	-3.31	-
SIB36	07/04/13	-	624	308	24.97	8.96	19.50	1.80	-
SIB37	08/04/13	-	108	312	24.3	6.5	21.62	2.14	-
SIB38	08/04/13	-	157	53	24.2	5.9	-7.88	-2.52	-
SIB39	27/05/13	71.98	322	79	24.9	7.18	-11.79	-2.98	-
SIB40	27/05/13	68.89	192	161	24.73	6.29	-14.05	-3.47	-
SIB50	27/05/13	-	-	-	-	-	12.46	-1.51	-

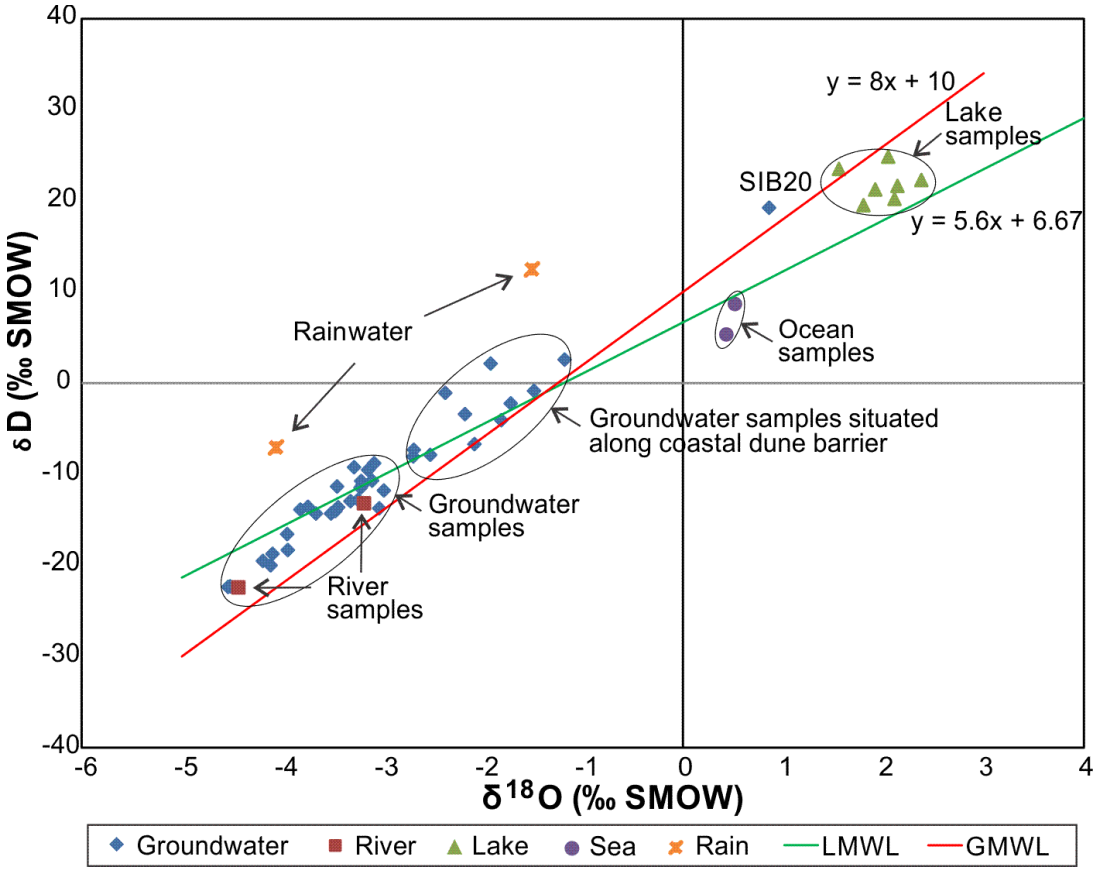

Figure 5.8. Relationship between $\delta^{18}O$ and Deuterium from various water resources within the study area in relation to the LMWL (IAEA, 2012) and GMWL (Craig, 1961).

The river and groundwater samples plot close to the LMWL indicating their meteoric origin, i.e. recharged from local precipitation before evaporation. Samples taken from the Mseleni River (S20 and SIB13) were isotopically depleted and closely related to that of the surrounding groundwater (Figure 5.8), indicating that the river is fed by groundwater flow (a gaining stream). Two rainfall samples collected during two different rainfall events during the course of this study, plot above the LMWL, however, the limited number of samples means that, interpretation of the local rainfall isotopic signatures along with groundwater and surface water isotopic signatures may not yield any relevant conclusion.

Lake water samples show a relative isotopic enrichment with respect to both ^{18}O and deuterium, which is a result of evaporation enrichment (Gat and Gonfiantini, 1981).

However, the unique stable isotope composition of the lake was successfully used as a tracer to determine leakage from the lake to the sea. Groundwater samples collected east of the late along the coastal dune cordon between Lake Sibayi and the Indian Ocean (S12, S14, SIB19, SIB20 and SIB21) display a mixture between lake water and groundwater isotopic signatures. The mixed isotopic signature indicates the movement of lake water through and below the coastal dune cordon to the sea. These results are in accordance with isotope studies conducted by Meyer *et al*. (2001), where it was reported that the water of the lake was found to have a direct hydraulic connection with seepage water occurring along the coast. This was further supported by the fact that groundwater sample SIB20, collected from the dune cordon, has an isotopic signature almost identical to those of the lake samples, revealing the fact that the lake is recharging the aquifer to the east.

The hydrochemical distinction established between the shallow and deep aquifer system could not be confirmed using the isotopic data obtained from the shallow and deep groundwater sample, because of an isotopic data limitation for the deeper aquifer. The single sample (SIB40) taken from the deep aquifer had a similar isotopic signature to that of the shallow groundwater samples, indicating that the deeper aquifer is recharged vertically from meteoric sources through the shallow aquifers.

Low tritium signatures were observed throughout the groundwater of the study area, ranging from 0.1 to 2.3 TU. Given the low background concentrations for South Africa (~2 TU) (IAEA, 2012), combined with a half-life of approximately 12 years, indicate that the groundwater is fed by recent recharge. Unfortunately no tritium samples were collected form the deep aquifer for comparative analyses.

5.8. General water quality of the study area

The groundwater and surface water qualities observed in the study area were evaluated against the South African water quality (SAWQ) guidelines for domestic, agricultural and industrial water use (SAWQ, 1996) as well as the World Health Organization (WHO) guidelines for drinking water (WHO, 2011) (Appendix G). The limits set by the SAWQ (1996) guidelines represent a target range at which no known adverse or anticipated effects would occur through long-term continuous use for the intended purpose. The WHO (2011) guidelines however represent the maximum limit of the element, at which an amount above will result in adverse health effects.

Inorganic groundwater hydrochemistry across the study area is generally of good quality falling within national (SAWQ, 1996) and international (WHO, 2011) water quality standards for different

purposes. Exceedances were primarily experienced in some of the deeper boreholes and in the wells east of the lake along the coastal dune cordon.

Concentrations of chloride, TDS and manganese were in excess of the drinking water guidelines for wells situated along the coastal dune cordon (SIB19, SIB20, SIB21, S12 and S14) while excess sodium and calcium was observed in some of the deep wells. High TDS concentrations in the S20 stream sample could be attributed to anthropogenic sources (from the local communities).

Excessively high iron concentrations, exceeding the domestic and agricultural guidelines, were observed in the deep SIB40 sample and all the wells situated eastward of the lake along the coastal dune cordon. Several of these wells were covered in orangey-red bacteria forming a slimy coating on the borehole water pipes. The only reported health effect of excess iron ingestion is haemochromatosis, a condition that results from prolonged exposure to concentrations in excess of 10 mg/l Fe. Adverse aesthetic effects of excess iron include taste and staining of clothes and pipe work (SAWQ, 1996). The highest iron concentrations were recorded from sample SIB34 (11.7 mg/l), SIB19 (12.5 mg/l) and S12 (30.1 mg/l) associated with known ferricrete exposures. These exposures probably represent ancient deflation surfaces where heavy minerals concentrated (Miller, 2001).

Elevated nitrate concentrations were observed in several of the shallow groundwater samples (S18, SIB19, SIB03, SIB04 and S5) with concentrations ranging from 6.8 to 11.8 mg/l which could result from agricultural or anthropogenic contamination in the area. An excessively high concentration of 110 mg/l was observed in S19 which could also be due to localised contamination. Chromium and arsenic were observed in several of the wells but the concentrations were below guideline values. Few samples show relatively high concentration of zinc (SIB34) and mercury (SIB01 and SIB03).

CHAPTER SIX
HYDROGEOLOGICAL CONCEPTUAL MODELLING OF THE LAKE SIBAYI SYSTEM, NOTHEASTERN SOUTH AFRICA

A conceptual hydrogeological model is one of the most important aspects of groundwater modelling and it forms the basis for developing numerical groundwater flow models. It represents a simplified representation of the hydro-geologic conditions and is used to define the hydrostratigraphic units (HSU) and their hydraulic characteristics, prepare a water budget and define the flow system necessary for the numerical simulation (Anderson and Woessner, 1992). This involves identifying model boundaries, sources/sinks, variation of aquifer properties, hydraulic head distribution and groundwater–surface water interactions. In this regard, the success of any numerical model for the Lake Sibayi catchment depends mainly on the validity of the conceptual model its ability to accurately represent the actual field conditions.

6.1. Groundwater flow around the Lake Sibayi catchment

From measured depth to groundwater and groundwater hydraulic head distribution, the groundwater flow situation around Lake Sibayi has been conceptualised. The hydraulic head measurements were used to construct the groundwater level contour map for the study area, which allowed for the determination of groundwater flow direction, recharge and discharge areas and the interconnection between groundwater and surface water bodies. The results indicate that the overall groundwater flow direction is from west to east, through Lake Sibayi, to the Indian Ocean. However, localised flow conditions are observed, particularly around the lake and wetlands (Figure 6.1), indicating a complex flow pattern, where local flow vectors are observed to feed into the numerous wetland areas found in the coastal plain. The groundwater hydraulic head map further helped to define the extent of the groundwater contributing area to Lake Sibayi, which is substantially different from the surface water catchment area of the lake. A regional groundwater divide was identified west of the surface water catchment of Lake Sibayi, an important boundary condition for the numerical model.

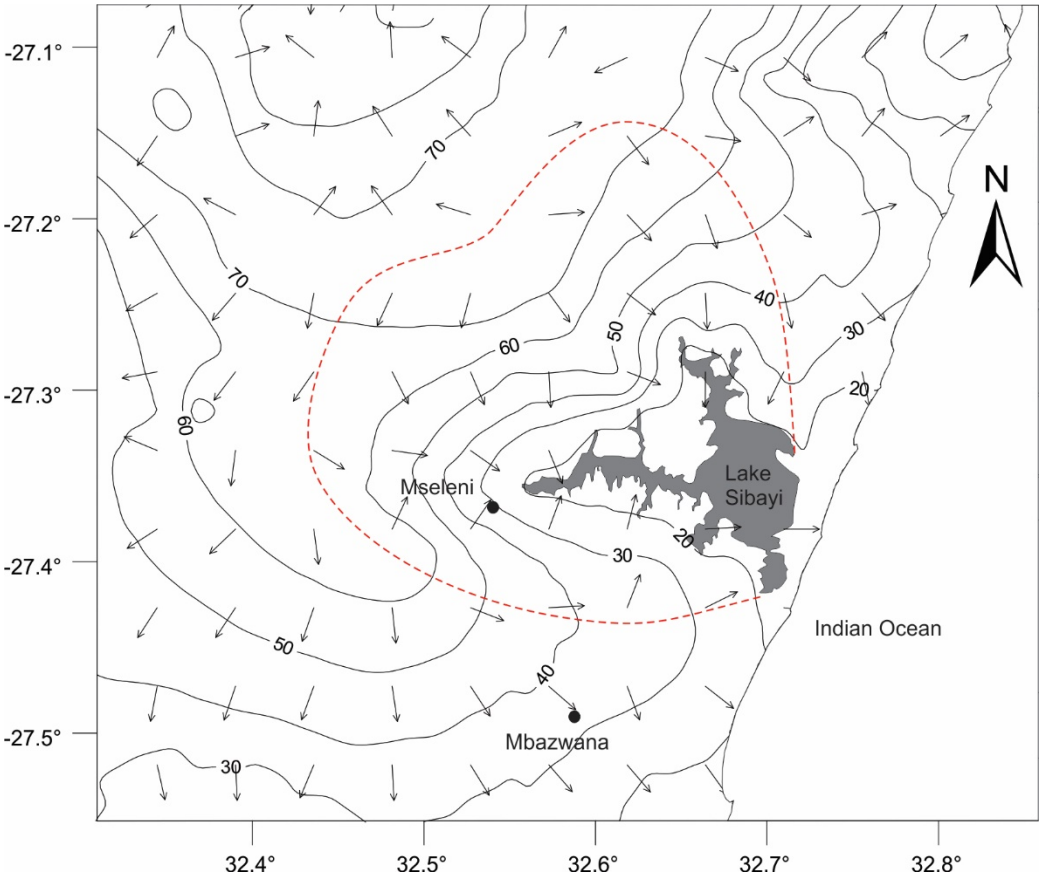

Figure 6.1. Groundwater flow distribution map showing local flow vectors (groundwater elevation (m amsl) presented at 10 m contour interval).

6.2. Geological Conceptual Model for the Lake Sibayi System

In formulating the hydrostratigraphy of an area, several geologic formations may be combined into a single HSU or a geologic formation may be subdivided into aquifers and aquicludes depending on their hydraulic characteristics (Anderson & Woessner, 1992). Understanding the lateral and vertical extent and relationship between the HSUs is essential for accurate conceptual model construction.

During the development of the geological conceptual model for the studied Lake Sibayi catchment, geologic units of similar hydrogeological properties were combined into distinct HSUs. The hydrostratigraphic classification undertaken during the study was similar to that undertaken around the study area by Meyer and Godfrey (1995). The extent and spatial distribution of the various HSUs for the Lake Sibayi system have been sourced from previous geological and hydrogeological investigations. Subsurface conditions in the vicinity of the lake were obtained from seismic investigations by Miller (2001), while borehole information was obtained from Maud and Orr (1975), Hobday (1979), Wolmarans and du Preez (1986). The most comprehensive set of borehole logs were obtained from various drilling reports of Jeffares and Green (Jeffares and Green, 2012, 2014a, 2014b; and Terratest, 2009a, 2009b, 2011, 2014, 2015a, 2015b, 2016a, 2016b). Based on geological and

hydrogeological properties of the various formations, two HSUs and a regional aquiclude or hydrogeological basement have been defined for the study area for modelling purposes. This distinction between the upper/shallow, lower/deep aquifer layers and the bottom aquiclude has been supported by both hydraulic and hydrochemical evidence as well.

Investigations conducted along the eastern shores of St Lucia by Davies, Lynn and Partners (1992), Kelbe and Rawlins (1992) and Meyer *et al*., (1993) revealed that the grain size distribution, as well as the permeability of the different sedimentary units overlying the Uloa Formation do not show significant variation and can therefore be classified as one aquifer unit or HSU. This unit therefore includes the more recent (Holocene) cover sands of the Sibayi Formation, the Pleistocene aeolian sands of the KwaMbonambi Formation, the Kosi Bay and Port Durnford Formations (Figure 6.2). The Kosi Bay Formation represents the dominant member of the upper HSU as its thickness and areal extent constitute the largest proportion of the HSU. The hydraulic characteristics of the unit are therefore skewed towards that of the Kosi Bay Formation.

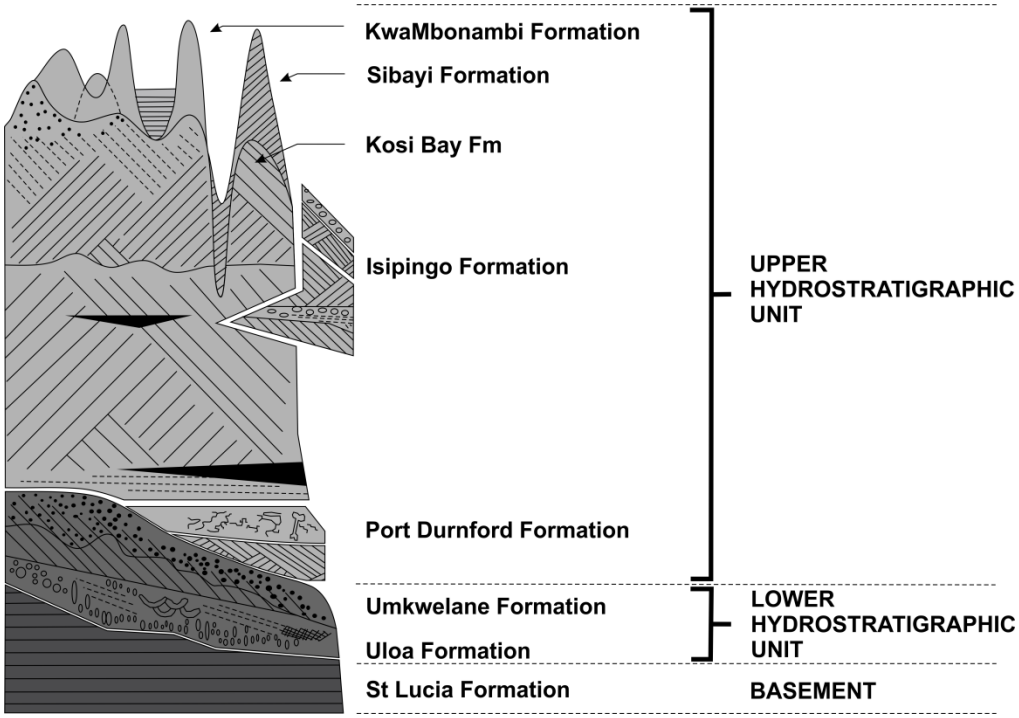

Figure 6.2. Classification of the various geological formations into their respective hydrostratigraphic units (adapted from Porat and Botha, 2008).

The Uloa and Umkwelane Formations are grouped into a lower or deep HSU. This lower HSU comprises both the cross-bedded aeolianites of Umkwelane Formation (Stapleton, 1977) and the stratified shallow-marine calcarenites and interbedded gravel beds of the Uloa Formation (Maud and Orr, 1975; Lui, 1995, Roberts *et al*., 2006). This unit is generally considered to be non-continuous; it was however observed in all of the limited number of deep wells in the study area and was therefore

considered to be continuous throughout the study area. The hydrochemical signature, as well as yield, quality and mode of occurrence is different to that of the overlying sediments and therefore warrants a separate hydrostratigraphic designation (Meyer and Godfrey, 1995). This unit was designated as the high yielding Uloa Formation HSU.

The Cretaceous St Lucia Formation is considered as the regional hydrogeological basement or bottom impermeable boundary. It comprises the Cretaceous age siltstones of the St Lucia Formation. Little hydrogeological information on this formation is available. However, based on the different lithological and depositional characteristics, compared to the overlying units, as well as its low permeability, low yield of boreholes and poor quality water; it has been defined as an aquiclude (Meyer and Godfrey, 1995). In this study, the unit is considered as the hydrogeological basement and hence an impermeable bottom boundary or the impermeable basement layer for numerical modelling.

The average hydraulic characteristics for each of the HSUs are summarised in Table 6.1. The thickness of the upper HSU ranges from 4 m in the vicinity of the lake up to 72 m in the western extremes of the catchment, while the thickness of the lower HSU ranges from 10 m in the north-western parts of the catchment to 25 m in the southern part of the catchment. The hydraulic conductivity of the HSUs was similar with a mean hydraulic conductivity of 5 m/d and 4.5 m/d for the upper and lower HSUs respectively. Storage parameters derived from pumping tests by Kelbe and Rawlins (1992) and Worthington (1975) revealed a specific yield ranging from 0.2 to 0.35 for the unconfined upper HSU and specific storage of 2×10^{-4} for the confined/semi-confined lower HSU.

Table 6.1. Average hydraulic characteristics of the shallow and deep HSUs

	Thickness (m)	Mean K (m/d)	Specific Yield	Specific storage
Upper HSU	4-72	5	0.2-0.35	-
Lower HSU	10-25	4.5	-	2×10^{-4}

6.3. Areal Groundwater Recharge for the Catchment

In the preceding section, published groundwater recharge maps proposed by Vegter (1995), Schulze (1989), WRC (1995) and Baron *et al*. (1996) in conjunction with the physical properties of the catchment, in the form of soil, vegetation, slope and lithology were used to estimate groundwater recharge for the Lake Sibayi catchment. These “Qualified Guesses” methods of groundwater recharge estimates, which are mainly based on the soil/vegetation and geology, expert opinions and general equations proposed by Bredenkamp *et al*. (1995) and Kirchner *et al*. (1991), were compared with groundwater recharge estimated using the chloride mass balance method to validate the recharge values. The various “Qualified Guesses” recharge estimates have largely similar values which averages to 95 mm/a or 10% of the mean annual precipitation (MAP). While the chloride recharge estimate varied from a minimum of 32 mm/a (3.2 % MAP) to a maximum recharge rate of 300 mm/a

(30 % MAP), capturing the spatial variability of groundwater recharge across the studied catchment. The mean of all the chloride mass balance recharge rate estimations is calculated at 126 mm/a (12% MAP) which is slightly higher than that estimated from other various methods. The areal groundwater recharge rate for the studied catchment, therefore, is between 10 and 12% of MAP for the area.

6.4. Water Balance components of the Lake Sibayi system

The development of a successful groundwater–surface water conceptual model requires thorough examination of the various components of the water resources and the main hydrological processes involved in the interaction. All sources of water that flow into the system, as well as the outflows from the system including the flow directions and exit points, should be included in the conceptual model. Inflows may include groundwater recharge from precipitation, adjacent aquifers, overland flow, or recharge from surface water bodies. The outflows are among others, spring discharge, baseflow to streams, evaporation, evapotranspiration and pumping through shallow and deep wells for various purposes, and groundwater outflow into adjacent aquifers.

The main components for the water balance of the Lake Sibayi system include precipitation, surface runoff, groundwater recharge, evaporation, evapotranspiration, groundwater abstraction, lake abstraction, and groundwater outflow to the sea. Consequently, analysing these resources requires a thorough understanding of their interactions. The quantification of these water balance components are crucial to the conceptualization of the system and are used as input parameters to a further numerical groundwater flow modelling exercise.

6.4.1. Precipitation

Rainfall is the main component driving the hydrology of the Lake Sibayi system as it forms the basis of recharge to the groundwater system, runoff into the lake and direct precipitation input on the surface of the lake. The Hlabisa Mbazwana Meteorological Station (Appendix A) was used to determine the amount of precipitation input on the lake surface. The mean annual precipitation for the catchment was therefore 1012 mm/a which equates to a volume of precipitation in the catchment and on the lake surface of 469 x 10^6 m^3/a and 74 x 10^6 m^3/a respectively.

6.4.2. Surface Runoff

The surface runoff component of the water balance of the lake constitutes the portion of precipitation in excess of infiltration that flows into the lake from its surface water catchment. The rate of runoff is controlled by the precipitation and watershed characteristics. Precipitation factors include the characteristics of the rainstorm, its intensity, duration and frequency; while watershed characteristics are based on topography, geology, soil and land use/land cover (Tripathi and Singh, 1998) (Appendix H). Each of the different land uses were assigned a runoff coefficient based on their respective

topography, geology and soil characteristics. A final runoff coefficient of 1% was obtained which translates to a mean annual runoff of 2.3 x 10^6 m^3/a.

6.4.3. Evaporation and evapotranspiration

Evaporation and transpiration are primary mechanisms for the loss of water from a hydrological system and can occur from all water resources in varying amounts and rates. In both cases, water vapour is lost to the atmosphere at a maximum rate determined by the atmospheric demand. This demand is determined by meteorological factors such as radiation, temperature, wind speed, temperature and relative humidity (Jager and van Zyl, 1989).

Evaporation

Evaporation is the primary process of water transfer in the hydrological cycle. It is one of the most difficult to quantify despite it being a large proportion of the water balance (Shaw, 1994). The Penman Combination Method (Penman, 1948) was used to calculate evaporation from Lake Sibayi. The results indicate that the mean annual evaporation rate for the Lake Sibayi is 1495 mm/a (Appendix I) which is equivalent to 109 x10^6 m^3/a.

Evapotranspiration

The rate of evapotranspiration is dependent on many factors; these include the rooting depth and density, the availability of water, the physiology of the plants and the length of the pathway from adsorption in the roots to evaporation in the leaves (Allen *et al*., 1998). The Penman-Monteith combination method has been used to estimate evapotranspiration within the study catchment based on the concept of reference crop evapotranspiration (ET_o) (Allen *et al*., 1998) (Appendix J). The result indicates a mean annual evapotranspiration rate of 1090 mm/a for the lake Sibayi catchment characterised by substantial areas of commercial pine plantation.

6.4.4. Abstraction

Lake Sibayi is used to supply water to several of the neighbouring communities. Lake water abstraction commenced in June 1975 and has progressively increased over the years with total abstraction at 2.8 x$10^6$$m^3$/a presently (DWA, 2014).

Groundwater is pumped from the catchment from several small to medium scale groundwater fed schemes including numerous hand pumps that tap the shallow aquifer for domestic water supply. The estimation of the amount of groundwater abstracted from the schemes approximates 1.7 x 10^6 m^3/a while those for domestic supply, based on a 25 l/person/day water human needs reserve (Nation Water Act), abstract approximately 4000 m^3/a. The total amount of water abstracted from both surface and groundwater resources within the catchment therefore totals 4.5 x 10^6 m^3/a.

6.4.5. Groundwater outflow to the sea

Geological, hydraulic, hydrochemical and environmental isotope data shows that groundwater flows from west to east, through Lake Sibayi to the Indian Ocean. As a result, the lake gets groundwater inflow from the west, where lake stage is lower than groundwater level and it flows out in the east through the aquifer, where lake stage is higher than the groundwater level, eventually discharging freshwater to the sea. Thus, due to the elevated nature of lake levels relative to the sea, groundwater flows through the coastal dune cordon to the Indian Ocean. Similar observation including the presence of fresh-water seepage to the sea opposite the southern end of the lake was reported by Meyer *et al*. (2001). The rate of groundwater outflow to the sea, east of Lake Sibayi, was calculated using Dupuit's equation (Dupuit, 1863). The mean annual groundwater discharge was 23 x 10^6 m^3/a (Appendix K).

6.5. Generalized conceptualization of the hydrological and hydrogeological characteristics of the Lake Sibayi system

All the hydrological information including precipitation, evaporation, surface water runoff, abstraction, as well as geological, hydraulic, hydrogeochemical and environmental isotope information were used to conceptualise the hydrological system of the Lake Sibayi catchment (Figure 6.3). Local geologic, groundwater head distribution, lake level, hydrochemical and environmental isotope data were used to constrain the link between groundwater and the lake. In the western section of the catchment, groundwater flows to the lake where groundwater head is above lake stage, whereas along the eastern section, the presence of mixing between lake and groundwater isotopic compositions indicates that the lake recharges the aquifer. Stable isotope signals further revealed the movement of lake water through and below the coastal dune cordon before eventually discharging into the Indian Ocean. The various conceptual models based estimated inflow and outflow components of the hydrological system is schematically presented in Figure 6.3.

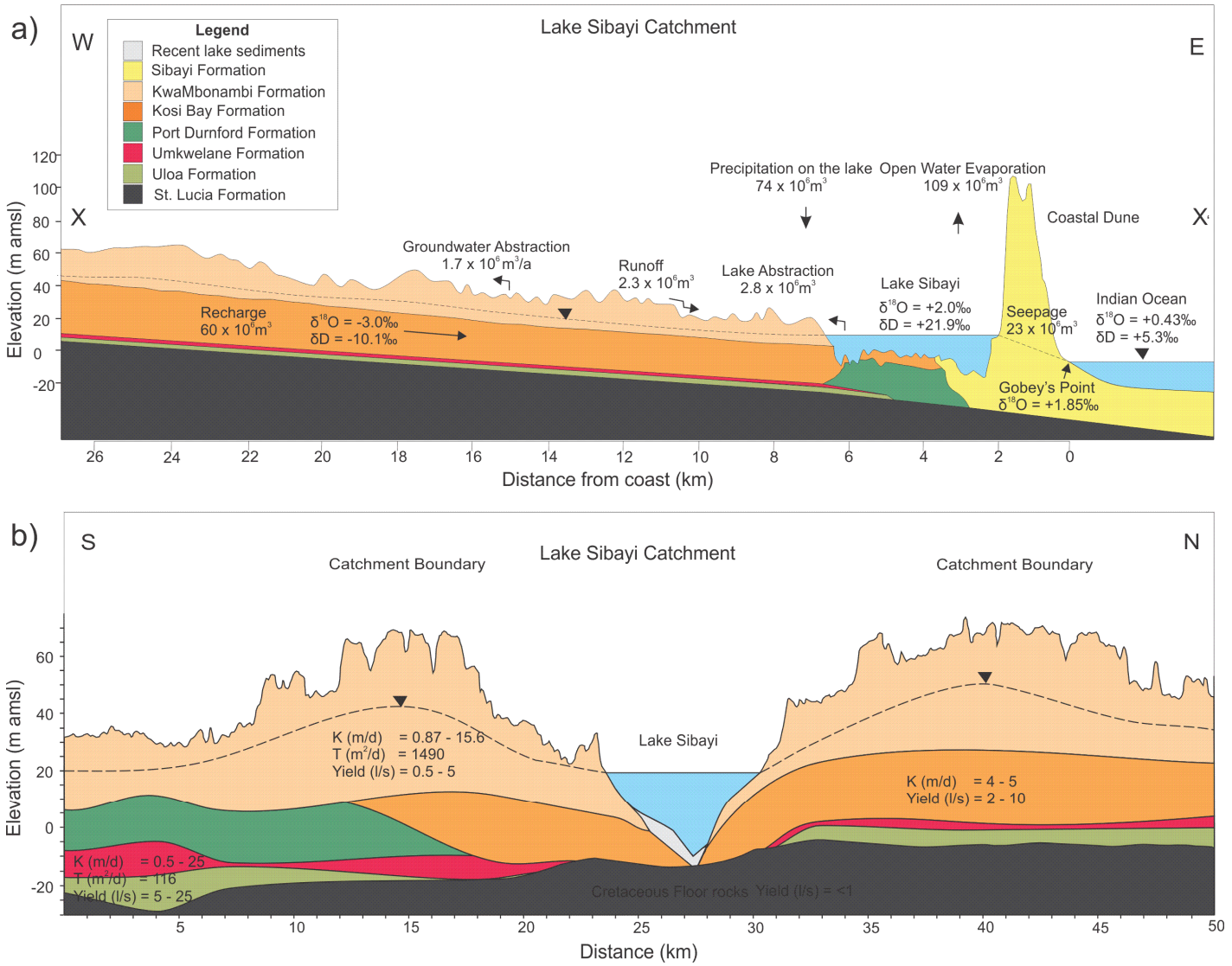

Figure 6.3. Hydrogeological conceptual model of the Lake Sibayi Catchment. a) East-West section b) North-South section.

CHAPTER SEVEN
NUMERICAL GROUNDWATER FLOW MODELLING OF THE LAKE SIBAYI SYSTEM, NORTH-EASTERN SOUTH AFRICA

7.1. Introduction

Lake Sibayi is an important source of water supply to both the neighbouring communities and the environment. It has experienced a significant reduction in lake levels over the past decade, dropping from approximately 20 m amsl in early 2000 to 16 m amsl at present. This decline in lake level could be attributed to the recent increase in water abstraction from the lake and groundwater within the catchment of the lake. The problem is further exacerbated by rapidly increasing pine plantations, which pump a huge amount of groundwater through evapotranspirative processes, and the recent drought. In order to manage this limited freshwater resource effectively, the lake–groundwater interactions within the catchment needs to be fully understood. In recent years, groundwater modelling has become the standard method with which these interactions are studied.

A steady-state and transient numerical groundwater flow model has been calibrated for the Lake Sibayi system using two different approaches, namely, the High-K method and the Lake Package. The numerical model was configured based on the conceptual hydrogeological model described previously. In order to test the validity of the numerical model, the results from the two separate approaches employed to simulate lake-aquifer interactions, i.e. the High-K method (Anderson *et al*., 2002) and the more sophisticated Lake Package (Merritt and Konikow, 2000) would be compared and used to highlight any shortcomings found in each of the two models.

The models were based on the MODFLOW 2005 code (Harbaugh, 2005) with the appropriate packages to simulate the flow dynamics in three dimensions over a period spanning over forty-three years, starting from January 1970 and ending in September 2014. The simulation period was broken down into 536 monthly stress periods with calibrated parameter values for each of the boundary conditions over the simulation period. The initial steady-state model was based on average (equilibrium) conditions of the area to represent the pristine conditions prior to January 1975, before abstraction was introduced. Groundwater Modelling Systems (GMS), which runs on the modular finite difference code, MODFLOW 2005 (Harbaugh, 2005) along with several of its packages were used to characterise the three-dimensional flow conditions around Lake Sibayi.

7.2. Model Design

7.2.1. Model layers

The numerical model was configured as a two layer model based on the HSUs and local physical boundaries described in the preceding chapters. The lower model layer consists of the Miocene-Pliocene Uloa and Umkewalene Formations; while the top model layer consists of all Formations

above the Umkwelane Formation. The upper surface of the bottom layer coinciding with the lower surface of the upper layer which is in-turn bounded by the topographic surface derived from the SRTM based DEM (Figure 7.1). The lower most boundary of the model was derived from the estimated upper surface of the Cretaceous St Lucia Formation, which represents the bottom impermeable layer or no flow boundary condition.

Upper (first) model layer: The upper model layer is made up of the north-south trending coastal dune cordon Sibayi Formation, the unconsolidated redistributed aeolian sands of the KwaMbonambi Formation and the unconsolidated to semi-consolidated Kosi Bay Formation. The surface elevation of these superficial deposits coincides with the surface topography which was derived from the recently gridded 30 m (1 arc second) Shuttle Radar Topography Mission (SRTM) digital elevation data (USGS, 2015) (Figure 7.1).

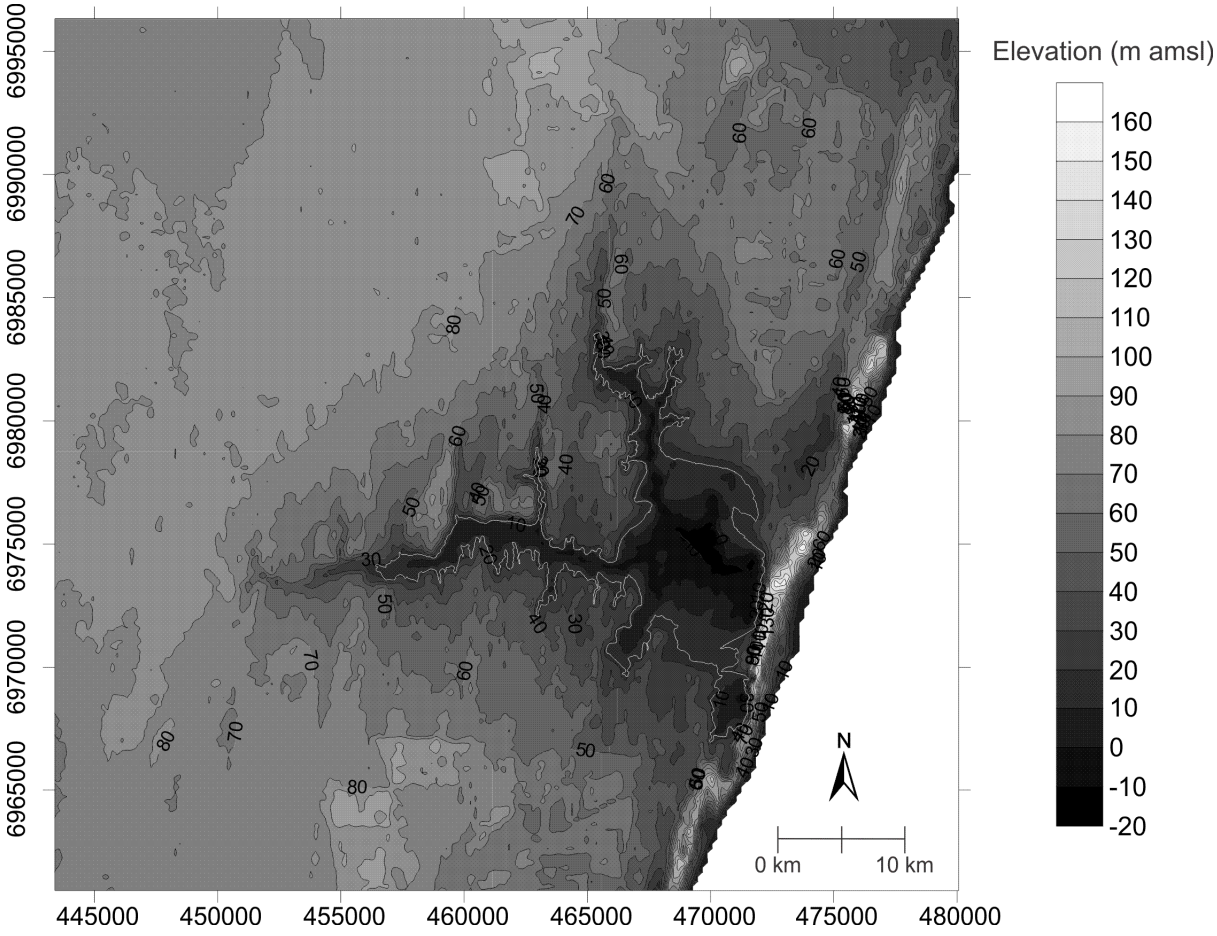

Figure 7.1. Digital elevation model of the topographic surface (USGS, 2015) incorporating the lake bathymetry as measured by Miller (2001).

Lower (second) model layer: The lower model layer consists of the Uloa and Umkwelane Formations which have been observed in all the deep wells in the area and has a maximum thickness of up to 35 m in some areas (Meyer and Godfrey, 2003). The discontinuous and isolated nature of the

Miocene Uloa Formation as proposed by Hobday (1979) has not been observed in the limited number of boreholes analysed in the study area. The estimated upper surface of this model layer is presented in Figure 7.2.

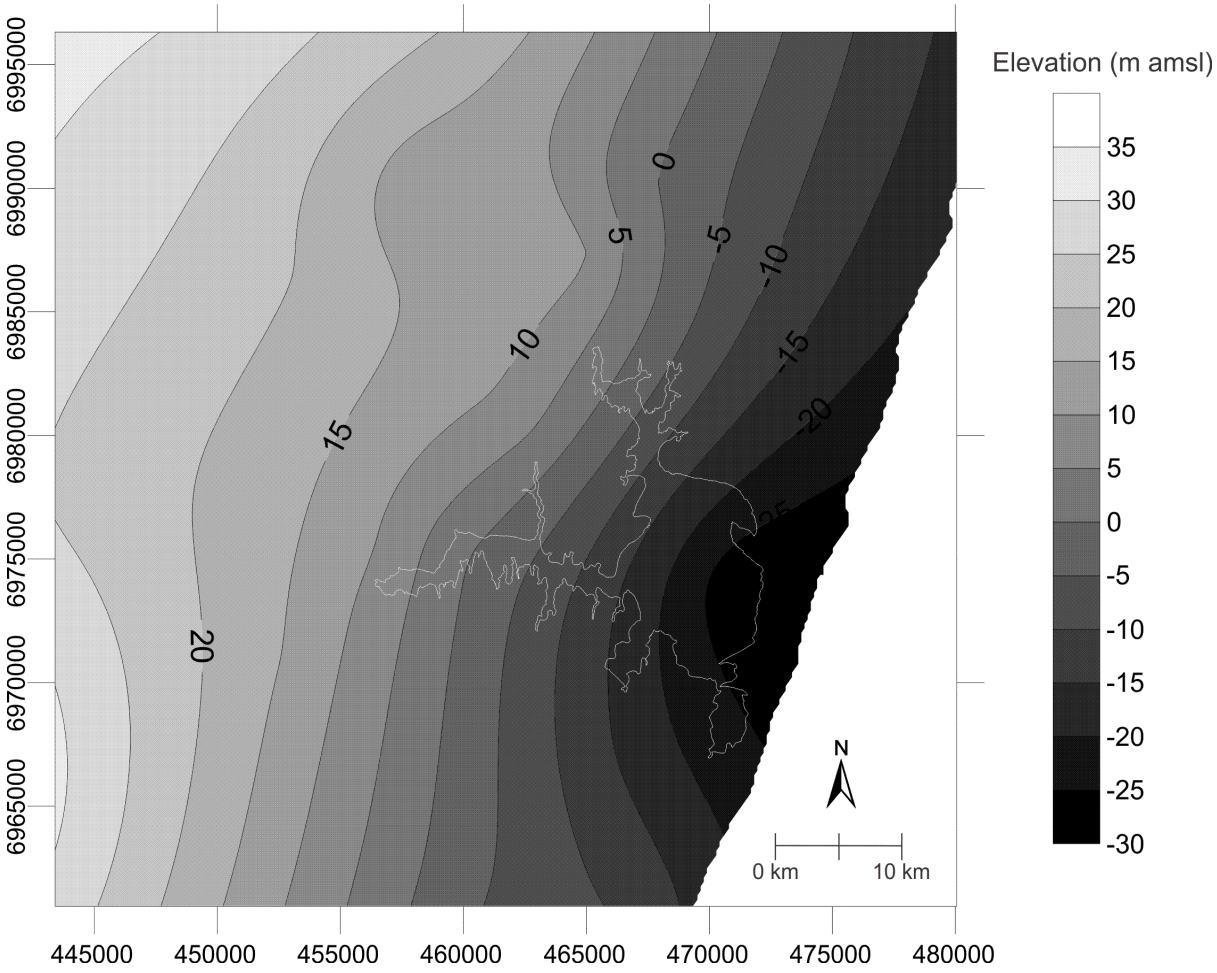

Figure 7.2. Estimated upper surface of the Miocene Uloa Formation (Second model layer)

The bottom model impermeable boundary: The rocks of the Cretaceous age St Lucia Formation underlies the entire Zululand coastal plain with a gently seaward dipping surface of 1 to 3 degrees (Worthington, 1978) which constitutes the base of the model. The surface elevation of this deposit in the Lake Sibayi area was derived by interpolating the deep borehole information obtained from Maud and Orr (1975), Hobday (1979), Wolmarans and du Preez (1986), Jeffares and Green (2012, 2014a, 2014b) and Terratest (2009a, 2009b, 2011, 2014, 2015a, 2015b, 2016a, 2016b) (Figure 7.3). The general dip observed in the catchment based on borehole interpolation is approximately 0.5 degrees with a slightly greater dip observed in the vicinity of the Lake Sibayi.

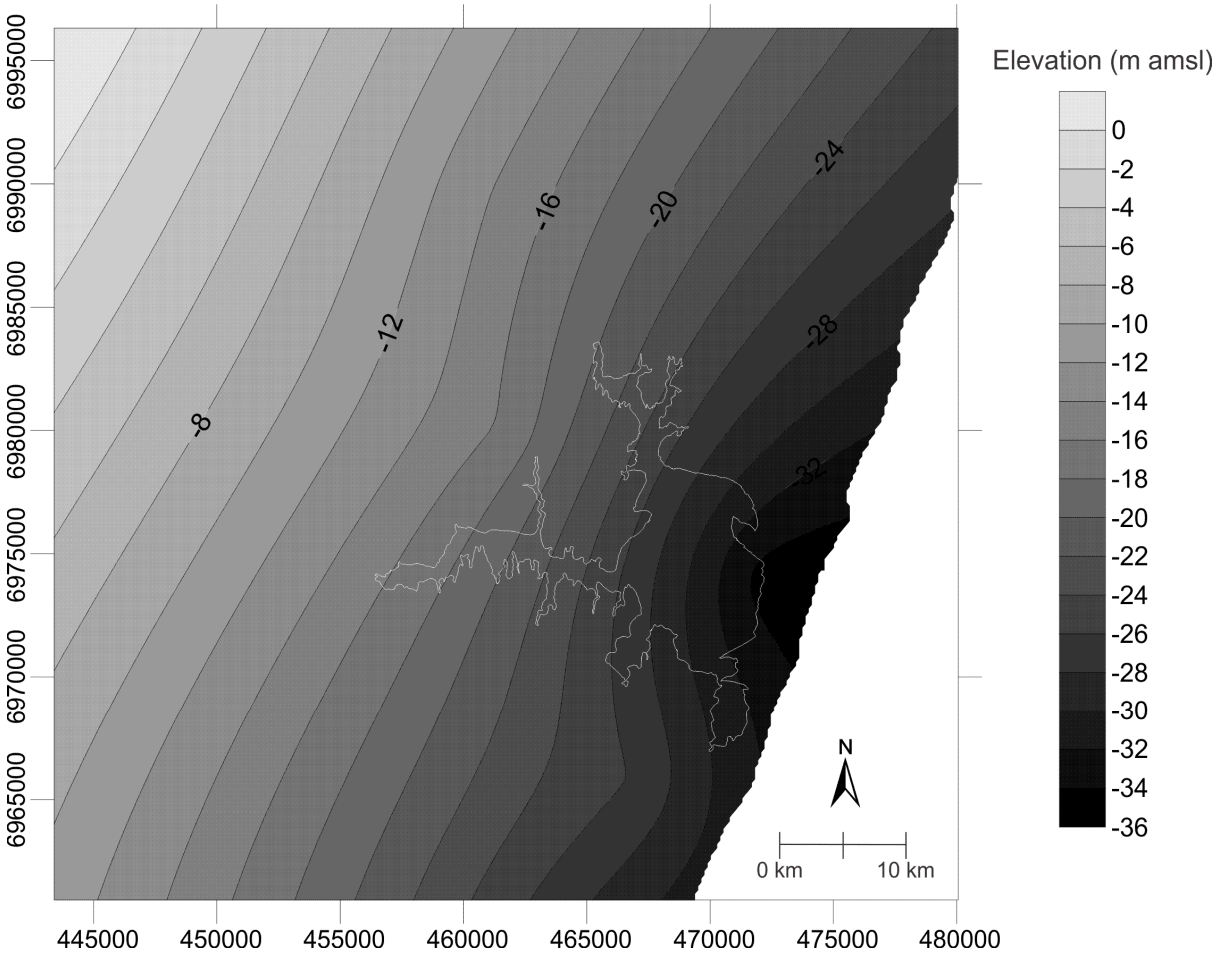

Figure 7.3. Estimated upper surface of the basement St Lucia Formation (Bottom impermeable model layer)

7.2.2. Model domain and model grid design

The horizontal extent of the model domain was initially designed as 36 by 38 km bounded by 442897 m to 480551 m UTM East and 6960245 m to 6997063 m UTM South (Figure 7.4). This area was discretised to a regular model grid of 396 rows and 409 columns corresponding to a cell size of approximately 100 m in both the X and Y directions. The total number of model grid cells is 32392, of which 16477 are active and 15915 are inactive. This grid size was deemed to be suitable for the level of detail required and keeping data handling, computer storage and processing time manageable.

7.2.3. Model boundary conditions

Model boundary conditions represent the interface between the model simulation within the domain and the surrounding environment. Selecting the correct boundary conditions is therefore a critical component of model design and requires careful consideration in order to provide a realistic simulation (Anderson and Woessner, 1992). The various model boundary conditions chosen for the Lake Sibayi model (Figure 7.4) represent the exchange of flow between the lake and the various

components of the system. The boundary for the model area characterises the relationship between the system and the surrounding environment.

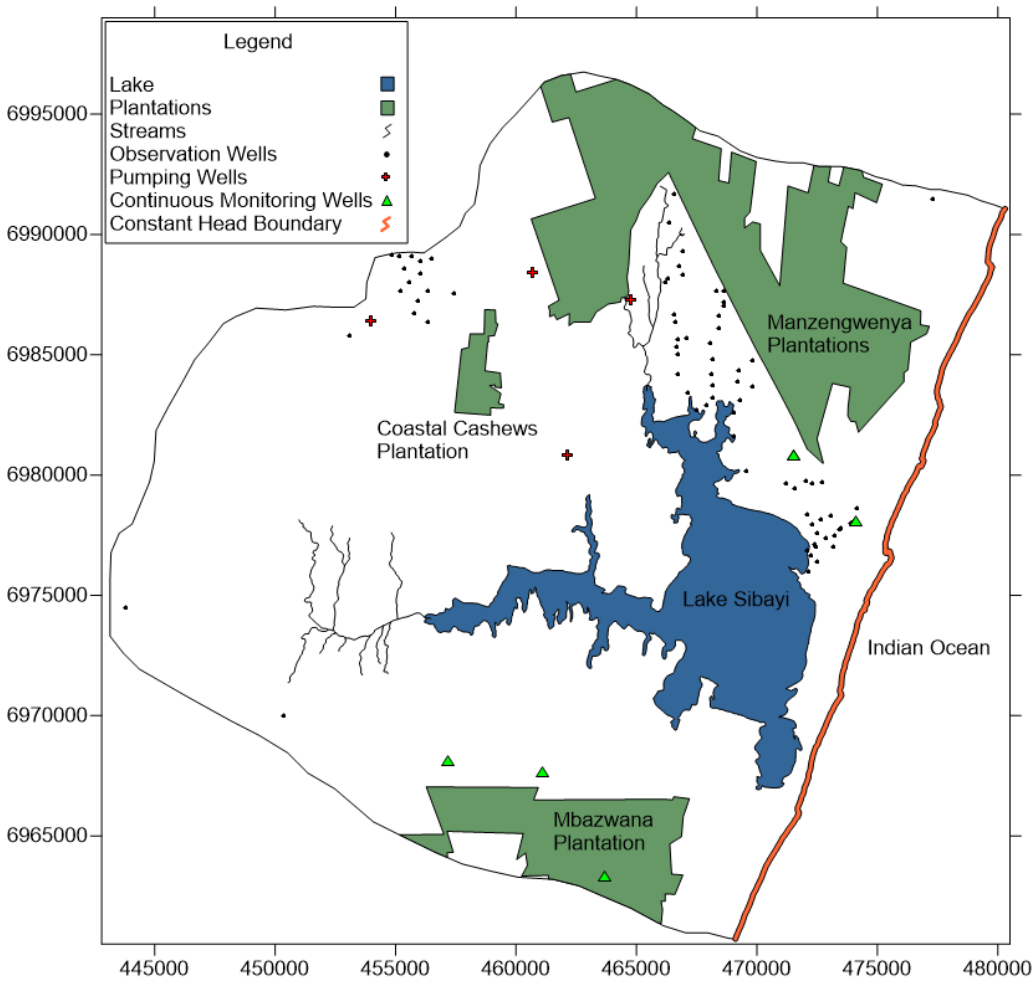

Figure 7.4. Model boundary conditions representing the various inflow and outflow components

Specified Head Boundaries: The eastern boundary along the coastline is set as a Specified-Head package (CHD) (Harbaugh *et al*., 2000) with starting and ending heads of 0 m amsl to represent the constant head Indian Ocean.

Specified Flux Boundaries: The recharge rate for the model domain was derived from monthly rainfall using the "Qualified guesses" and chloride mass balance methods described previously. The recharge rate was applied uniformly to the entire upper surface of the model and applied at a constant rate for the duration of each stress period using the MODLFOW Recharge package (Harbaugh *et al*., 2000). Due to the inability of the High-K method to incorporate the lake water budget, a separate recharge rate was assigned to the lake polygon to represent the resultant lake water budget. A positive change in storage would be represented as positive recharge, while a negative change in storage would be represented as negative recharge.

The groundwater abstraction wells drilled for community water supply are simulated using the Well package (Harbaugh *et al*., 2000). The abstraction rates from these wells ranged from 30 000 to 540 000 m^3/a.

The northern, western and southern boundaries of the model domain were set as no-flow boundaries coinciding with the boundaries of the groundwater contribution area to the lake (groundwater divide) and streamlines defined from groundwater level map. The model domain is much greater than the surface water catchment of the lake, effectively including it.

Head-Dependent Flux Boundary Packages: The recharge rate calculated for the model represents effective recharge that reaches the saturated zone where the interception losses and evapotranspiration has already been accounted for. The Evapotranspiration (ET) package (Harbaugh *et al*., 2000) was therefore only applied to the rapidly transpiring plantations coverage.

A recent study by Brites and Vermeulen (2013) on the water use of *Pinus elliottii* and *Eucalyptus grandis Camaldulensis* located in the Nyalazi plantation, within the St Lucia region was used to establish the evapotranspiration rate for the Mbazwana and Manzengwenya plantations as well as the Mfihlweni/Makhanya Growers (Coastal Cashews). Brites and Vermeulen (2013) estimated a total water usage of 1460 mm/a. Their study takes into consideration the total loss of water in storage as well as the amount of precipitation (water lost through canopy interception, evapotranspiration and the soil moisture zone) over the plantation area. This effective evapotranspiration was used as the evapotranspiration rate for the current study and scenario analyses. A rooting depth of 12 m (Kelbe and Rawlins, 1992) was assigned to the plantations and was maintained for the duration of the model simulations.

The perennial Mseleni and Velindlovu Rivers flowing into Lake Sibayi were incorporated into the model using the Stream (STR) package (Prudic, 1989). The streams were created using a series of Stream Arcs digitised in accordance with the river shapefile with the stream top and bottom elevations defined for each of the stream junctions (nodes). These elevations allowed for the slope of the stream segments (sections between junction) to be calculated. The streams were given a constant width of 5 m, while based on stream shape and flow characteristics, the streams were given a sinuosity ranging from 1 to 1.5 and a roughness coefficient of 0.03. Due to the limited hydraulic information available for the streams in the area, the stream beds were assumed to have a hydraulic conductivity of 10 m/day as proposed by Kelbe (2009) for similar streams feeding into Lake Nhlabane south of St Lucia.

The Lake (LAK3) Package (Merritt and Konikow, 2000) was employed in order to simulate lake conditions. The Lake Package allows for automatic stage computation by MODFLOW based on the lake water budget. Precipitation over the lake was established from rainfall data collected form the Mbazwana Airfield Meteorological Station (SAWS, 2015). Surface runoff into the lake was

calculated using the runoff coefficient determined using the rational formula reported in Tripathi and Singh (1998). A runoff coefficient of 1% was deemed acceptable given the flat topography and sandy soils within the catchment. Open water evaporation was calculated using the Penman method (Penman, 1948), and supplemented with pan evaporation data for periods when meteorological information was not available. The lake water abstraction volumes were derived from registered usage from DWS (2015). The storage capacity of the lake was determined automatically based on the lake bathymetry which was obtained from the study conducted by Miller (2001).

The Lake Package also allows for the inclusion of lakebed sediments which affect the flow between the aquifer and the lake. The effect of the lakebed sediments is represented by the leakance term which is a function of lakebed thickness and hydraulic conductivity. The lakebed sediments consist primarily of very fine-grained to medium-grained quartz sand (Figure 7.5), while Gyttja, a dark grey to black organic-rich mud is found in the deeper and more sheltered areas of Lake Sibayi (Miller, 2001). Additionally, the GAGE package (Merritt and Konikow, 2000) was used in conjunction with the Lake Package to allow gaging stations to be added to lake to provide detailed time series lake level data.

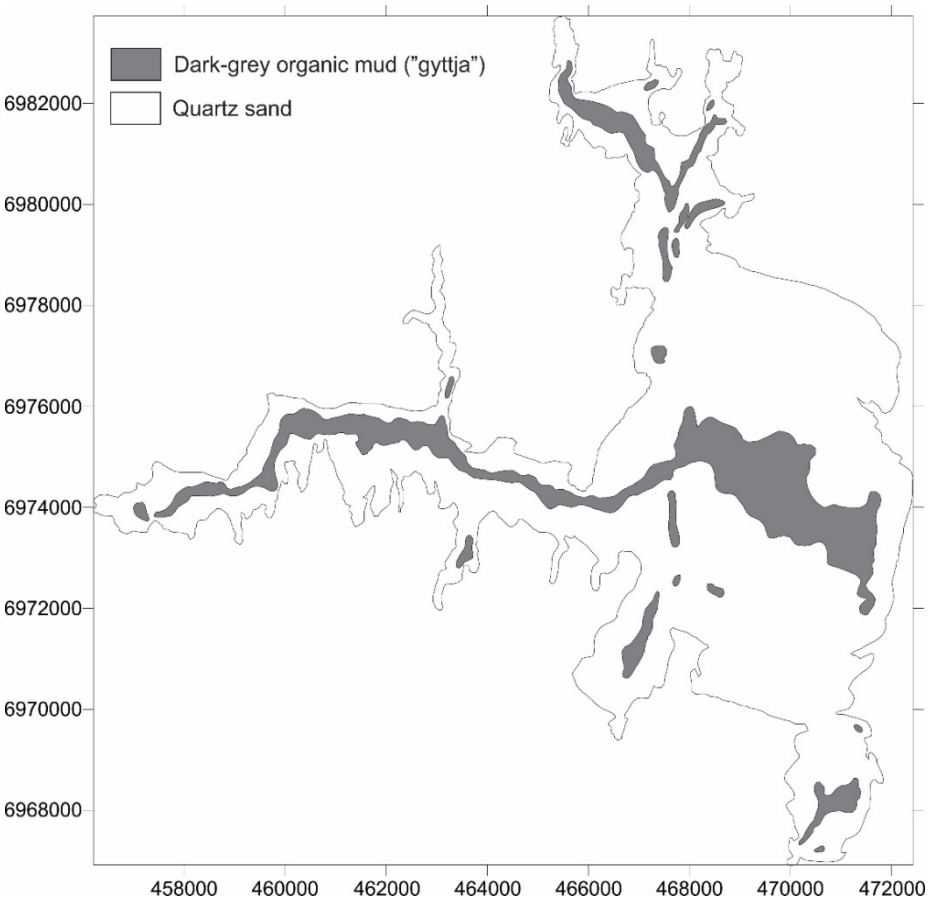

Figure 7.5. Sediment type distribution in Lake Sibayi (Adapted after Miller, 2001).

7.2.4. Initial conditions

The initial conditions describe the hydraulic head distribution throughout the model domain at the start of the simulation (Anderson & Woessner, 1992). Good initial conditions are imperative for convergence and allows for confidence in model simulation results. The groundwater head distribution shown in Figure 6.1 was used as initial conditions for the model. The water level distribution map was used as the initial conditions for the steady-state model; the simulated head distribution was subsequently used as the initial conditions for the transient model.

7.2.5. Solvers used

The GMG (Geometric Multigrid) Solver (Wilson and Naff, 2004) and SIP (Strongly Implicit Procedure) Package (Harbaugh *et al*., 2000) were used for the High-K and Lake Package simulations, respectively. Both solvers were used to solve the finite difference equations in each step of the MODFLOW stress period.

7.2.6. Representation of the lake

The current lake area covers approximately 58 km^2 (Google Earth, 2014) which is significantly lower than historical coverages. The lake coverage was therefore set at 73 km^2 measured in August 1993 as part of the bathymetric survey of the lake (Miller, 2001). The 1993 lake stage of 19.49 m amsl and its corresponding surface area approximates the conditions that existed in 1970 (predevelopment), where the surface of the lake was 19.5 m amsl (Pitman and Hutchinson, 1975) and used as initial lake polygon for modelling. The bathymetry of the lake was added to the surface topography of the lake polygon. In the steady-state simulation, the lake was given an initial stage of 19.5 m amsl measured at the end the 1970 hydrological year.

7.2.7. Sensitivity Analysis

Sensitivity analysis is an essential component of the modelling process as it allows for the determination of the certainty (uncertainty) of aquifer parameters, stress and boundary conditions in the calibrated model (Anderson and Woessner, 1992). It also provides information on which model parameters are most important to the simulated system. Sensitivity analyses inherently forms part of the calibration process with the most sensitive parameters having the greatest effect on the model. Sensitivity analysis can be conducted either manually or automatically. Manual analyses require variables to be multiplied by certain factors with the resultant hydraulic head compared to measured head and the deviation noted. The greater the change in heads and change in the residual error, the greater the sensitivity. The automatic approach was preferred as it computes parameter sensitivity directly. GMS has built in functionality which allows for automatic sensitivity analyses on a set of selected parameters. PEST computes the sensitivities of each parameter and plots which parameters

have the greatest influence on the model. The parameters with the greatest sensitivity will be the principal parameters for matching computed and observed heads.

7.2.8. Calibration techniques

The purpose of model calibration is to demonstrate that the model is capable of producing field-measured heads and flows. This can be accomplished by adjusting certain parameters and boundary conditions within a pre-determined range of error criterion, until the best fit between simulated and observed heads and flows within the catchment is achieved.

Model calibration can be achieved either through trial-and-error or through automated calibration. During trial-and-error calibration, model parameters are iteratively adjusted until there is an acceptable level of agreement between the simulated and the observed values. These parameters are adjusted in sequential modelling runs until the computed heads match the calibration target (Anderson and Woessner, 1992). Inverse modelling, providing automated parameter estimation, provides better calibration results by systematically adjusting the input parameters until the difference between the computed and observed values are minimized.

Steady-state model calibration

Steady-state calibration errors: Commonly applied error quantification methods, i.e. mean error, mean absolute error and root mean squared error as well as the standard regression coefficient, R^2 were analysed as part of the quantitative model evaluation.

The mean error (ME) is the mean difference between measured head (h_m) and simulated heads (h_s):

$$ME = \frac{1}{n}\sum_{i=1}^{n}(h_m - h_s)i \quad (21)$$

The mean absolute error (MAE) is the mean of the absolute value of the difference in measured head (h_m) and simulated head (h_s):

$$MAE = \frac{1}{n}\sum_{i=1}^{n}|(h_m - h_s)i| \quad (22)$$

The root mean square error (RMS) or the standard deviation is the average of the square difference in the measured (h_m) and simulated (h_s) heads:

$$RMS = \left[\frac{1}{n}\sum_{i=1}^{n}(h_m - h_s)i^2\right]^{0.5} \quad (23)$$

The coefficient of determination (R^2) is a statistical measure of how closely a certain function fits a particular set of experimental data. The R^2 value represents how closely the data fits to the regression

line. The closer the value approximates 1, the better the correlation between the observed and simulated heads.

$$R^2 = \frac{\sum(\bar{m}-m)^2 - \sum(s-m)^2}{\sum(\bar{m}-m)^2} \quad (24)$$

Where $\bar{m}$ is the mean of observed lake level, m, the observed lake level and s, the simulated lake level.

Trial-and-error calibration: The trial-and-error calibration method is through manual adjustment of aquifer hydraulic parameters until the simulated heads best approximated field conditions. During steady-state calibration, hydraulic conductivity, recharge and lake parameters were varied until the output simulation best corresponded to the observed conditions.

Steady-state automated calibration: The most commonly used non-linear inverse modelling parameter estimation code, PEST (Doherty *et al*., 2010), was used to perform automated parameter estimation for the Lake Sibayi system. Hydrological parameters such as hydraulic conductivity for the two model layers and recharge were automatically calibrated for the steady-state model. The parameters were given a realistic range within which they could be varied. PEST varied the parameters with their associated calibration error until the best solution was achieved with the lowest statistical uncertainty.

Initial model execution: The initial hydraulic stresses (lake levels, groundwater levels, evaporation, and precipitation) used for steady-state calibration generally represent long term average measurements. Unfortunately, due to the limited number of investigations in the study area, such information was not available for some of the stresses. The initial piezometric surface therefore represents an average groundwater level obtained from groundwater level monitoring of three field investigations on April 2008, September/October 2012 and April/May 2013. This was supplemented by data from Jeffares and Green (2012, 2014a, 2014b) and Terratest (2009a, 2009b, 2011, 2014, 2015a, 2015b, 2016a, 2016b) where possible. It should be noted that these readings were taken when the system was already under stress and are therefore lower than historical measurements. The initial model water balance input parameters were derived from the four year measurements (1970 to 1974) representing pristine conditions prior to the commencement of lake abstraction.

The steady-state calibration was accomplished using lake stage measurements and 47 observation wells scattered throughout the catchment. Steady-state calibration was accomplished by minimising the difference between the simulated water levels and measured lake stage and groundwater levels.

Transient model calibration

A transient model represents a time variant simulation. The transient models are run using the calibrated simulation results of the steady-state aquifer heads as the starting heads. Continuous groundwater and lake level measurements are essential in this regards as they provide the calibration target for the transient model. The transient model was run on monthly time steps spanning from January 1970 till September 2014.

Storage parameters: The transient simulation requires the storage coefficients of the various aquifers. During the transient calibration, all steady-state model parameters were kept constant and only the parameters relating to storage were varied. The storage parameters, specific storage and specific yield for each layer were initially adjusted using trial-and-error and later using PEST to determine the most statistically correct values.

Initial conditions: The initial conditions for the transient model refer to the head distribution throughout the system at the beginning of the simulation and are therefore considered boundary conditions in time. The initial conditions specified for the transient simulation were the resultant head distribution generated from the preceding steady-state simulation. These model generated head values ensure that the initial head data and the model hydrologic inputs and parameters are consistent (Franke, 1987).

Stress periods and time steps: Selection of an appropriate time step is a critical component of transient model design as it can strongly influence the numerical results (Anderson & Woessner, 1992). As mentioned previously, the simulation time period spans from 1970 to 2014, on a monthly time step. The transient models was therefore designed with a total of 536 stress periods, each representing one month and a single time step was used for each stress period. This time step was deemed suitable and represented a good compromise between model variability and computation time.

Transient observation data: Monthly lake level measurements (1975 to 2014) were used as the main calibration target for the transient simulations. These transient lake levels were supplemented with time series groundwater level measurements within the model domain (Table 7.1) (DWA, 2016).

The measured groundwater level data has low confidence due to a significant number of recording errors; as such the data required extensive screening for quality before being deemed suitable for calibration purposes.

Table 7.1. Groundwater monitoring boreholes with time series water level measurements.

Monitoring well	Measurement duration	Elevation (m amsl)	Mean groundwater level (m amsl)
Mbazwana	01/03/2004 - present	60	48.7
Mabaso	01/03/2004 - present	71	49.8
Sibaya 02	16/02/2012 - present	43	35.9
Sibaya 1B	16/02/2012 - present	41	20.4
Sibaya 1A	16/02/2012 - present	41	27.3
Mabibi	16/09/1999 - present	21	13.7

7.3. Modelling the Lake Sibayi System using the High-K Method

The lake cells in the High-K method are represented by a hypothetical porous medium with a very high hydraulic conductivity, generally three orders of magnitude greater than that of the surrounding aquifer. This configuration would allow the Lake to be fully connected to the aquifer with little resistance to flow between the lake water body and the groundwater flow regime. The resulting groundwater level generated for the lake polygon cells using this method is considered as the lake stage. For the lake polygon, a partial mass balance is necessary to determine the inflows and outflows to the lake. The mass balance components included precipitation on the lake, evaporation from the surface of the lake, runoff into and abstraction from the lake, where the resultant net mass balance value is set as recharge for the lake polygon as this functionality was absent in the High-K method. This lake "recharge" value can be either positive indicating inflows to the lake are higher or negative when the outflows are higher. This mass balance for Lake Sibayi presented in Figure 7.6.

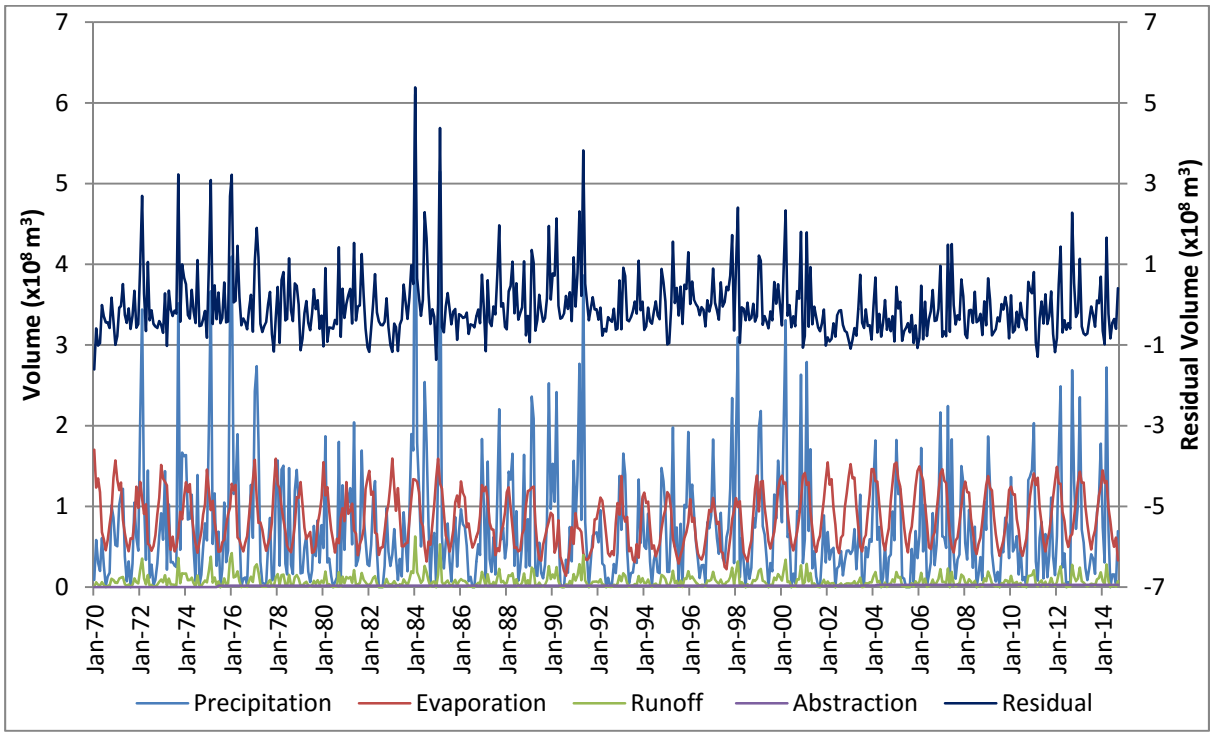

Figure 7.6. Transient lake mass balance components for lake Sibayi with the resultant residual volume used to represent the recharge to lake cells in the High-K method

7.3.1. Sensitivity analyses

The sensitivity analyses was calculated for both, the steady-state and transient High-K models. The High-K steady-state model was found to be the most sensitive to recharge and the hydraulic conductivity of Layer 1 (the upper HSU). The calibration of these parameters was used to minimise the difference between the measured and simulated values of the piezometric heads and lake levels. The calibration of the model focused primarily on the fit to lake levels and, to a lesser extent, groundwater levels. The sensitivity of the parameters evaluated during the steady-state and transient model calibrations are listed in Figure 7.7. Transient sensitivity analyses focused only on storage parameters and were found to be predominantly dependent on the specific storage of the second layer.

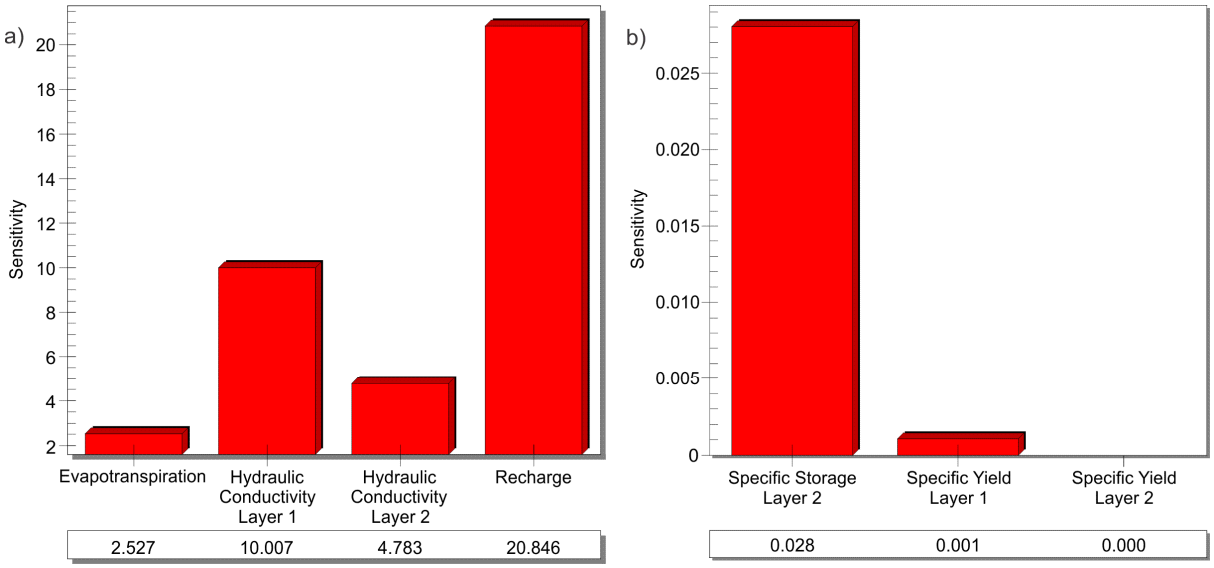

Figure 7.7. The relative sensitivities of the various model parameters for steady-state simulation (a) and transient simulation (b).

7.3.2. Steady-state trial-and-error calibration

The High-K model run was calibrated using the trial and error calibration method through manual adjustment of aquifer hydraulic parameters until the simulated heads best approximated field conditions. During steady-state calibration, hydraulic conductivity, recharge and lake parameters were varied until the output simulation best corresponded to the observed conditions.

The initial values for the storage coefficients of each layer were estimated from values of specific storage from various sources including Worthington (1975) and Kelbe and Rawlins (1992). These authors reported a specific yield of 35% for the unconsolidated Holocene sands and 20% for the Port Durnford Formation. Given the leaky confined aquifer conditions of the Kosi Bay Formation, which constitute the majority of the upper hydrostratigraphic unit, a specific yield of 20% was chosen, coinciding with that of the Port Durnford Formation. A storage coefficient of 2×10^{-4} was chosen for

the semi-confined lower model layer. The open water surface of Lake Sibayi in the High-K method was assigned a storage coefficient of 99% representing infinite storage.

The hydraulic conductivity was increased for the upper and lower model layer to 5 m/d and 7 m/d respectively. The vertical hydraulic conductivity was assumed to be same as the horizontal hydraulic conductivity as its variance had no effect on the model. The overall recharge rate was subsequently adjusted to 7% of the MAP over the entire model domain. These recharge values are lower than that documented by Kelbe and Germishuyse (2010), however it accounts for the decreasing recharge gradient from the coast inland. Parameters relating to the lake mass balance were also varied. Measured parameters such as precipitation, evaporation and abstraction were not altered, while the estimated runoff was varied until the calibration was successful.

7.3.3. Steady-state automated calibration

Automated calibration through the use of PEST was undertaken to determine the optimal values for hydraulic conductivity and recharge values for the High-K method (Table 7.2). The calibrated hydraulic conductivity for the upper model layer was 4.4 m/d which is slightly lower than a measured value of 5 m/d. However, it corresponds well with the average hydraulic conductivity of the Kosi Bay and Port Durnford Formations proposed by Meyer and Godfrey (1995). The calibrated hydraulic conductivity for the lower model layer is 6.1 m/d which is within the range of values (from 0.5 to 25 m/d) reported by Meyer and Godfrey (1995). The lower than expected calibrated hydraulic conductivity could be correlated to the discontinuous nature of the highly permeable unit as it was mapped as a continuous layer. The calibrated recharge rate of 9.5% MAP is within the estimated range using the “Qualified Guesses” and chloride mass balance methods described in previous chapters.

Table 7.2. Calibrated parameter values for the High-K method

Parameter	Calibrated value
Hydraulic Conductivity for the upper model layer	4.4 m/d
Hydraulic Conductivity for the lower model layer	6.1 m/d
Recharge	9.5% MAP

7.3.4. Evaluation of steady-state calibration

The calibration results were evaluated both qualitatively and quantitatively. The calibrated results were assessed based on error associated with the calibration target and assessment of the water balance. The calibration targets were hydraulic head, hydraulic head gradient, and fluxes.

The plots of the measured water level against simulated water levels for the steady-state High-K method (Figure 7.8) gives an R^2 of 0.98 indicating a good fit. The comprehensive list of residuals provided in Appendix M.

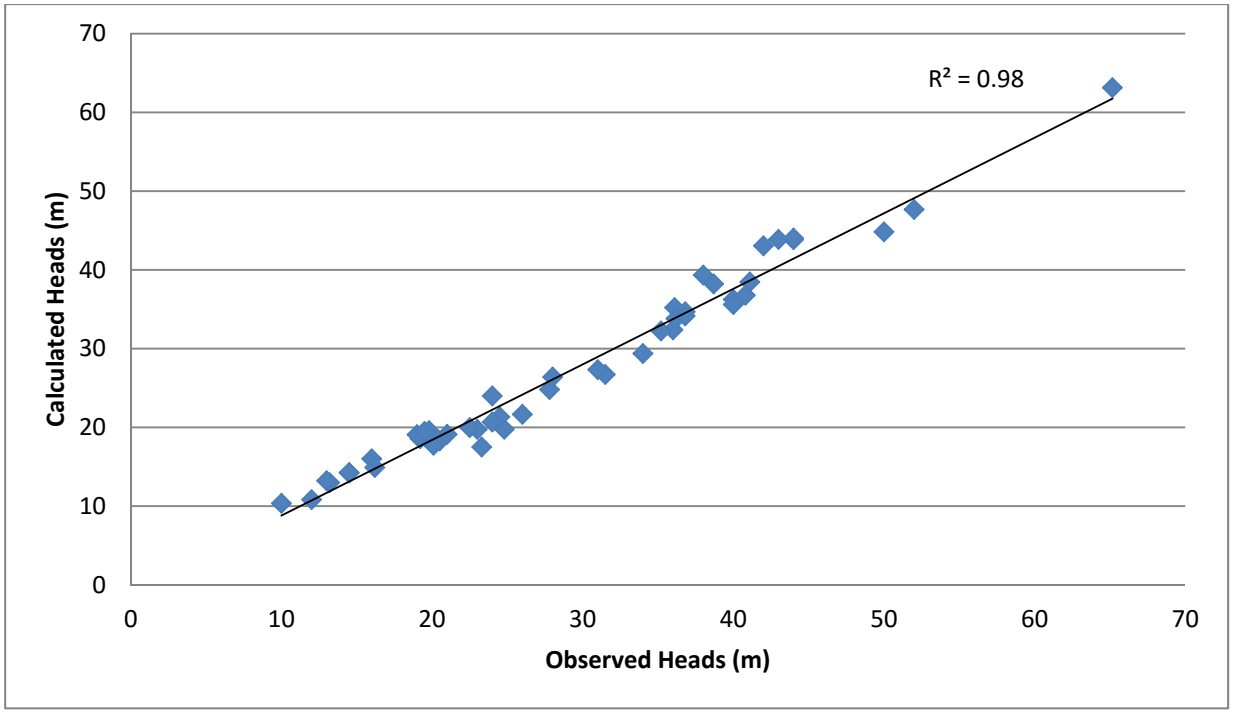

Figure 7.8. Scatter plot of computed vs. observed heads for the steady-state High-K simulation

The model was deemed suitably calibrated as there is an acceptable correlation between the observed and simulated piezometric heads (Figure 7.8) which is in agreement with the conceptual model. The calibrated model outputs were further evaluated by assessing the mean error, mean absolute error and root mean squared error. The steady-state calibration errors for the High-K method (Table 7.3) were deemed to be within acceptable ranges.

Table 7.3. High-K steady-state model calibration error criterion.

Evaluation Criteria	Error value
Mean error (m)	-1.98
Mean absolute error (m)	2.15
Root mean square error (m)	2.74
Coefficient of determination (R^2)	0.98

Comparative analyses between the contour maps of measured and simulated hydraulic head distribution allowed for a visual qualitative assessment of the spatial distribution of errors in the calibration. Simulated groundwater flow direction was also analysed and compared to flow direction observed in the conceptual model. The simulated hydraulic head distribution and groundwater flow direction for the High-K method (Figures 7.9) compared favourably to those derived from the conceptual model. GMS allows for the residual of the computed and observed values for each observation well to be displayed as “calibration targets”. These provide feedback on the magnitude and spatial distribution of the observation errors. The calibration targets computed by GMS represent the observed value with an interval added or subtracted to give the top and bottom of the target

respectively. If the computed value lies within the target, the bar is green. When it's within 200% of the target, it is yellow and if it's outside of 200% of the target, the bar is red. Several of the error bars in the vicinity of the lake were green indicating that they fall within the specified 1 m interval. The interval was set at 1 m with a 95% confidence interval.

The model was able to best simulate the areas immediately to the north and east of the lake as they approximate the observed heads. The model struggles to simulate the heads towards the western extremes of the catchment as indicated by the high residuals observed in the area. The flow directions are similar to those observed in Figure 6.1 which indicated a general flow towards the Indian Ocean with local flow towards the lake.

Additionally, a valid solution for the High-K method would be that the model produces a constant water level across the surface of the lake. The best simulation was achieved when the hydraulic conductivity of the lake cells were set at 10 000 times that of the surrounding aquifer, this resulted in a head drop across the 5 km wide main basin of the lake of 0.02 m resulting in a hydraulic gradient across the lake of 4 x 10^{-6} m/m.

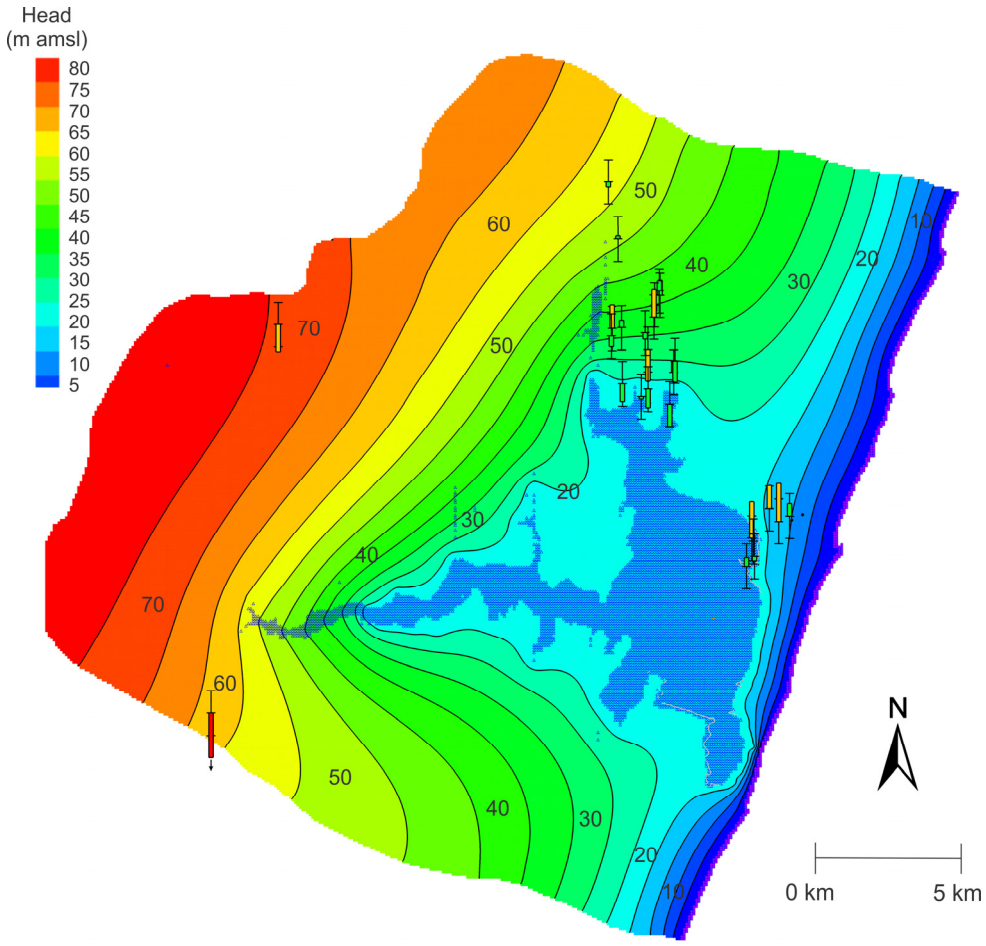

Figure 7.9. Contour map of simulated groundwater head distribution with associated error bars for the High-K method

The water budget allows for the quantification of the various inflow and outflow components for the model domain. A smaller difference between the inflow and outflow components indicates a good water balance estimation by the model and can be considered as one measure of the validity of the model. The steady-state groundwater budget for the High-K method is shown in Tables 7.4. The difference between the inflow and outflow for the steady-state water balance had minimal error and was essentially zero.

Table 7.4. Average steady-state water budget for the model domain using the High-K method

Sources/Sinks	**Inflow (m^3/a)**	**Outflow (m^3/a)**
Constant head	0.0	-36489186
Wells	0.0	-21026976
Et	0.0	-7136043
Recharge	64652205	0.0
Lake seepage	-	-
Total Source/Sink	64652205	-64652205
Summary	**In – Out (m^3/a)**	**% difference**
Sources/Sinks	**0.068**	**1.06 x10^{-7}**

7.3.5. Evaluation of transient model calibration for the High-K method

Transient calibration focused on the storage parameters related to specific yield and specific storage. Continuous monthly lake level readings at W7R001 station for Lake Sibayi were used to calibrate the transient model. Sensitivity analyses of the High-K method showed that it was almost entirely dependent on the specific storage of the second layer. Specific yield for the second layer was also specified in case the water table dropped below the confining layer resulting in the second layer becoming unconfined.

The transient calibration was assessed in the same way as the steady-state calibration and employed several of the same techniques. The transient model was calibrated based on continuous monthly lake level readings supported by some groundwater readings from the catchment. The transient model was based on the previously calibrated steady-state model and therefore only required calibration of the storage parameters. Trial-and-error calibration of the transient model required varying the storage parameters for the two model layers. The calibrated storage parameters used for the High-K method were a specific yield of 0.25 for the upper layer and a specific storage of 0.05 for the second layer.

The modelled transient lake levels were compared to measured lake level time series. The results were evaluated against calibration errors in the same way as the steady-state model and the various calibration errors are reported in Table 7.5. The R^2 value of 0.64 and 0.32 for the lake level and aquifer heads respectively, indicates a relatively poor fit between measured and simulated lake stages and aquifer heads.

Table 7.5. Transient High-K model calibration errors for lake level and aquifer calibration

Evaluation Criteria	Lake level	Aquifer heads
Mean error (m)	-1.05	-11.34
Mean absolute error (m)	1.47	11.34
Root mean square error (m)	1.63	13.99
Coefficient of determination (R^2)	0.64	0.32

Like the steady-state calibration, a transient scatter plot of the measured and calculated heads for the aquifer and lake stage was used to evaluate the results of the High-K model. The scatter plot of the transient model simulation indicates significant variation of the results when measured against time series lake levels (Figure 7.10).

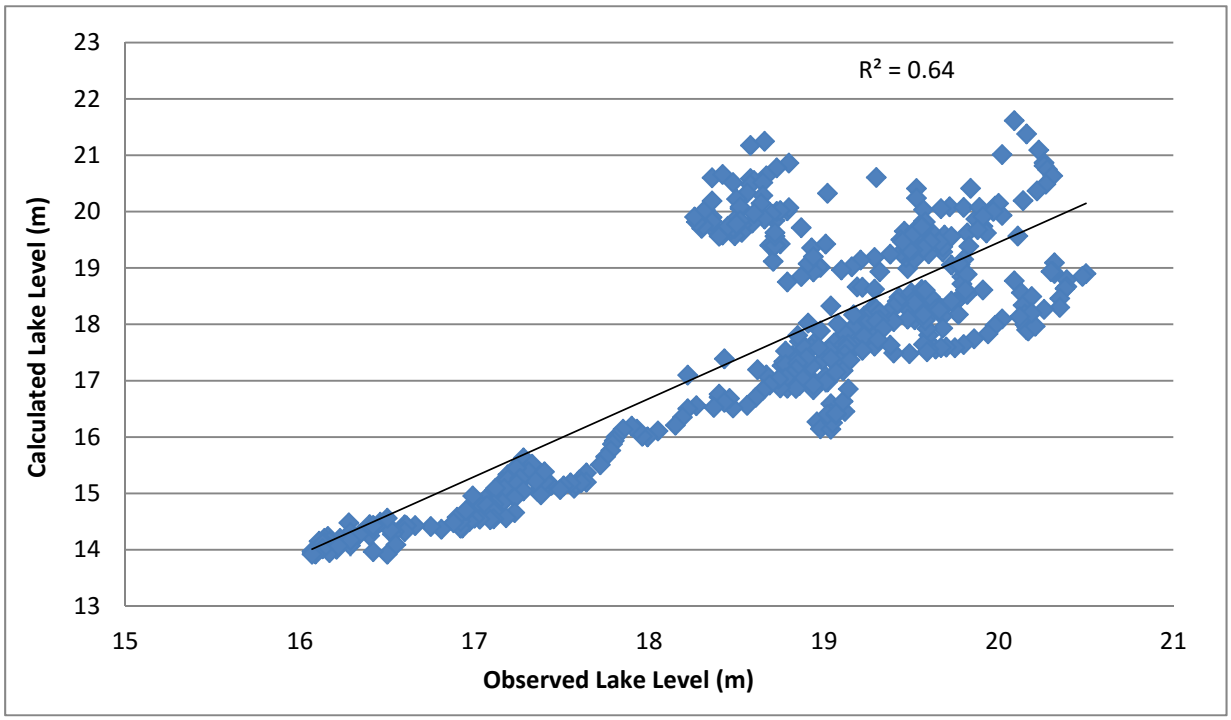

Figure 7.10. Transient scatter plot data of observed and simulated heads for the High-K method (1975 to 2014).

Generally, the transient model lake level simulation results for Lake Sibayi using the High-K method are in agreement with the measured values, but struggles to accurately simulate the observed lake stage (Figure 7.11). The model appears to have significant variability in the results where high lake levels are over-estimated and low lake levels underestimated as indicated by the large residual error. The large error could result from the lack of adequate time varying data.

Suspicious readings obtained from the DWA (2016) groundwater readings resulted in the complete removal of some of the wells. The erroneous readings combined with high errors observed for the

aquifer heads (Table 7.5) resulted in less importance being given to the groundwater levels with calibration predominantly focussing on lake levels.

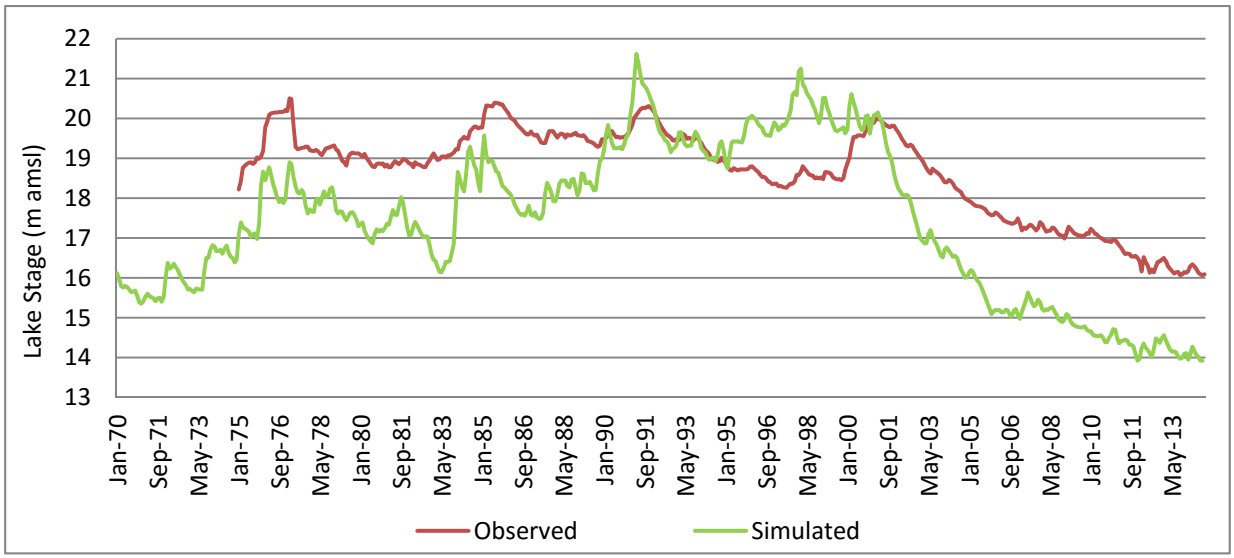

Figure 7.11. Time series plot of observed and High-K method simulated lake levels from January 1970 to September 2014.

The steady-state calibration results for the High-K method proves that the model is able to accurately simulate the observed conditions. However, the results of the transient calibration indicate that the model struggles to simulate the more complex transient conditions (Figure 7.11). The model results tend to be highly variable by over- and underestimating the observed transient lake stages and aquifer heads. This fluctuation is due to the highly conductive nature of the method which is very sensitive to changes in recharge. The lack of adequate simulation is verified by the high residual between the observed and simulated results combined with a low R^2 value of 0.64 (Table 7.5).

The inability of the High-K method to accurately simulate observed conditions for the modelled system prompted the need for a more complex modelling approach to be adopted. As a result, the more sophisticated Lake Package was employed to better simulate the field conditions.

7.4. Modelling the Lake Sibayi system using the Lake Package

The Lake Package (Merritt and Konikow, 2000) was subsequently employed in order to simulate the lake levels within Lake Sibayi. The Lake Package allows for automatic stage computation by MODFLOW based on the lake water budget. Most of the input parameters to the Lake Package including precipitation over the lake surface, surface runoff into the lake from the catchment, open water evaporation, and abstraction from the lake were pre-processed, quantified and conceptualized in the preceding chapters. The storage capacity of the lake was determined automatically by the model using the lake bathymetry input based on measurement conducted by Miller (2001).

The GAGE package (Merritt and Konikow, 2000) was used in conjunction with the Lake Package to allow gaging stations to be added to the lake to provide detailed time series lake stage. The lake package also allows for the inclusion of lakebed sediments which affect the flow between the aquifer and the lake. The effect of the lakebed sediments is represented by the leakance term which is a function of the lakebed thickness and the hydraulic conductivity.

7.4.1. Sensitivity Analyses

The sensitivity analyses approach followed in the Lake Package application was identical to that of the High-K method. The sensitivity of the parameters evaluated during the steady-state and transient model calibrations are listed in Figure 7.12. The steady-state model of the Lake Package was found to be most sensitive to recharge followed by hydraulic conductivity of both model layers (Figure 7.12a). Transient sensitivity analyses focused only on storage parameters with the transient Lake Package model being most sensitive to changes in specific yield of the first layer followed by specific storage of the second layer (Figure 7.12b).

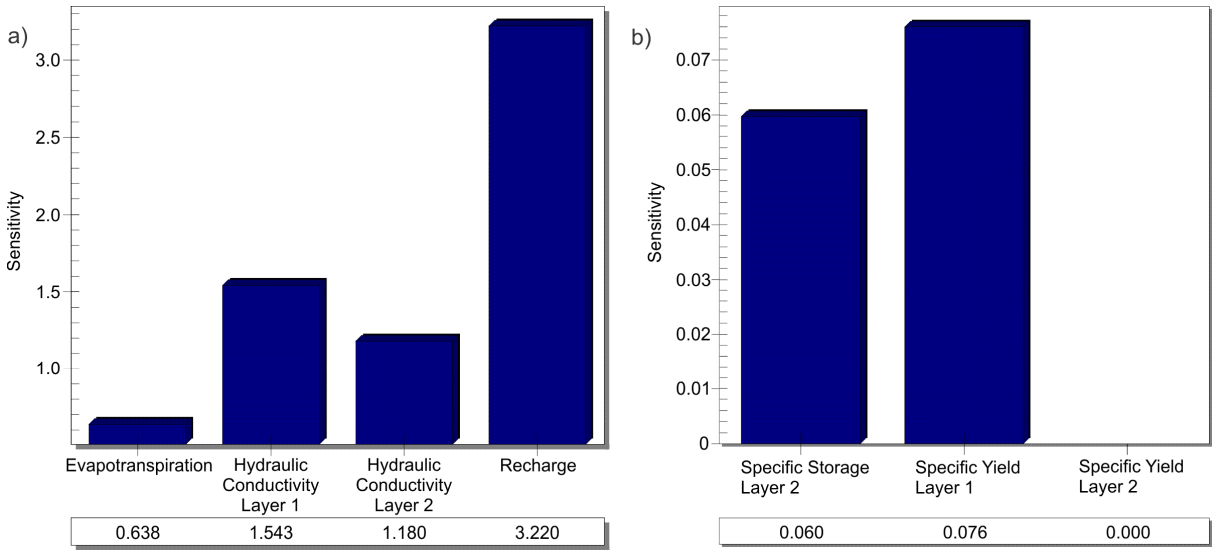

Figure 7.12. The relative sensitivity of the various water balance components for the Lake Package simulation steady-state simulation (a) and the relative sensitivity of the storage parameters for the transient simulation (b).

7.4.2. Steady-state calibration

The steady-state Lake Package was based on the initial piezometric surface computed using the previously defined High-K method. The package didn't require further calibration and therefore has the same calibration values as the High-K method.

7.4.3. Steady-state calibration errors

The model results show low residuals in the majority of the observation wells (Appendix N) and a good correlation between measured and simulated lake levels (Figure 7.13). The calibrated model outputs were further evaluated by assessing the mean error, mean absolute error and root mean squared error. The model attained a mean error of – 1.98 m while the mean absolute error and root mean square error were 2.15 and 2.74 m, respectively (Table 7.6). The regression coefficient (R^2) between simulated and observed data is 0.98, which is more than satisfactory.

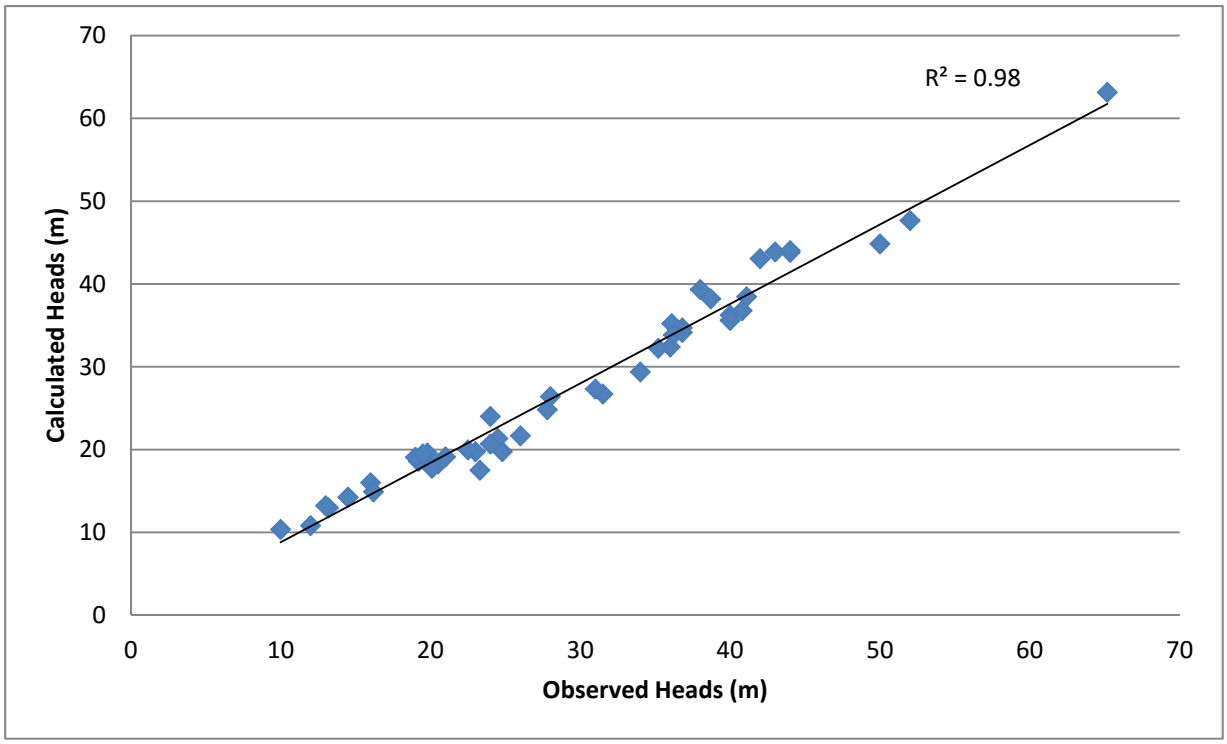

Figure 7.13. Scatter plot of computed vs. observed heads for the Lake Package

Table 7.6. Lake Package steady-state model calibration error

Evaluation Criteria	Error value
Mean error (m)	-1.98
Mean absolute error (m)	2.15
Root mean square error (m)	2.74
Coefficient of determination (R^2)	0.98

7.4.4. Evaluation of steady-state calibration

A qualitative evaluation of the steady-state calibration for the Lake Package was undertaken to provide a visual assessment of the simulated hydraulic head distribution. Simulated groundwater flow direction was also analysed and compared to flow direction observed in the conceptual model. Like the High-K method, the simulated hydraulic head distribution and groundwater flow direction for the

Lake Package model (Figures 7.14) compares favourably to the flow direction contours derived from the conceptual model. Similarly, the model was able to best simulate the hydraulic heads in the areas immediately to the north and east of the lake as they have the lowest residuals between simulated and observed. High residuals were observed towards the west where the model struggled to simulate the observed hydraulic head distribution.

The model was deemed suitably calibrated as an acceptable correlation between the observed and simulated piezometric heads are within the pre-established calibration target and in agreement with the conceptual model.

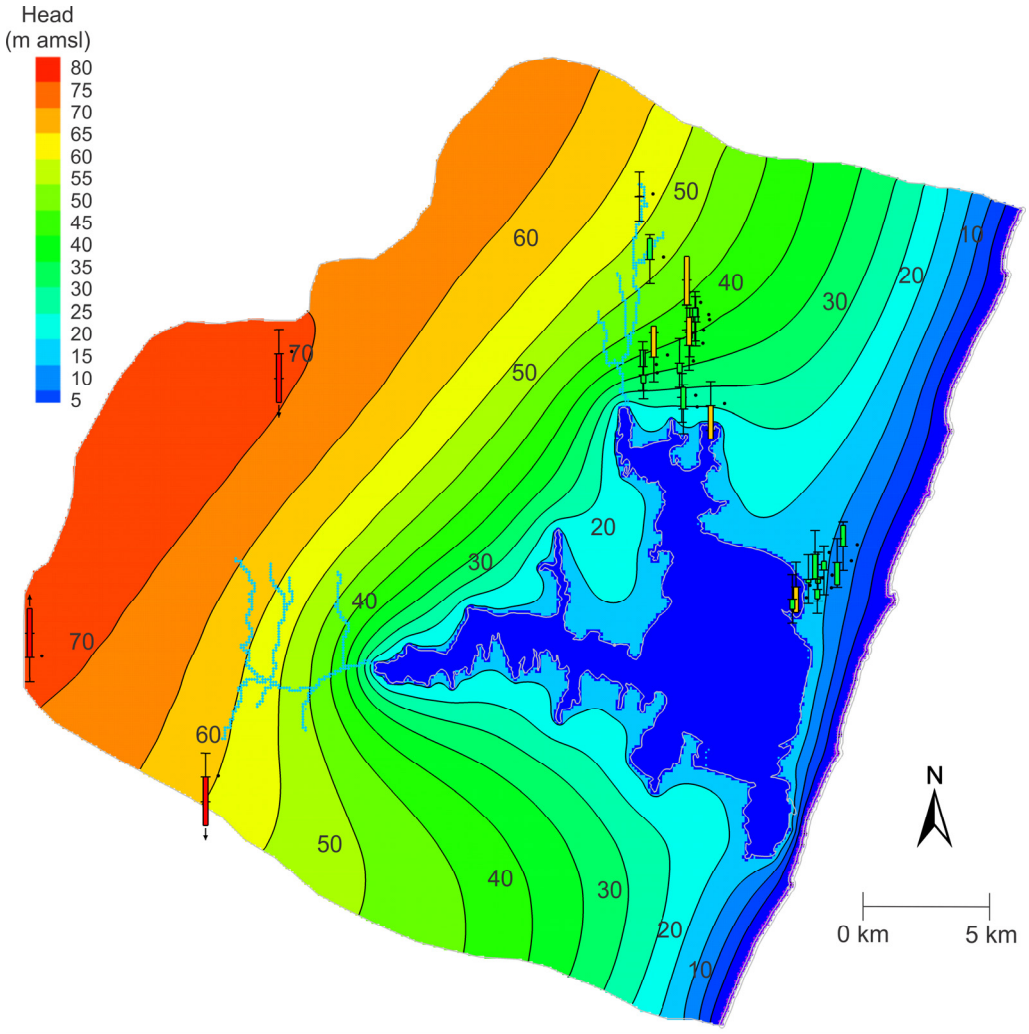

Figure 7.14. Contour map of simulated groundwater head distribution with associated error bars for the Lake Package

The steady-state modelled water budget for the Lake Package shown in Tables 7.7 allow for the quantification and assessment of the various inflow and outflow components of the modelled system. The small difference between the inflow and outflow components observed indicates satisfactory

model output. The difference between the inflow and outflow for the water budget was -1.4 x 10^5 m^3/a which amounts to a 0.2% difference.

Table 7.7. Lake Package steady-state modelled water budget for the model domain.

Sources/Sinks	**Inflow (m^3/a)**	**Outflow (m^3/a)**
Constant head	0.0	-35446268
Wells	0.0	0.0
Et	0.0	-7136043
Recharge	58462873	0.0
Lake seepage	20288983	-36306067
Total Source/Sink	78751856	-78888378
Summary	**In – Out (m^3/a)**	**% difference**
Sources/Sinks	**-136521**	**-0.17**

7.4.5. Evaluation of transient calibration for the Lake Package model

Trial-and-error calibration of the transient model required varying the storage parameters. The calibrated storage parameters used for the Lake Package were a specific yield of 0.25 for the upper layer and a specific storage of 0.05 for the second layer. Based on these calibrated storage parameters, the maximum residual was found to be 1.44 m.

The Lake Package transient model results were evaluated against calibration errors in the same way as the steady-state model with the various error criterions. The transient model calibration errors are reported in table 7.8. Evaluation of the various error, i.e. mean error, mean absolute error and root mean squared error, indicate that the model was able to satisfactorily simulate the observed conditions. The residuals of the transient model are relatively low. This was further substantiated by a good regression coefficient of 0.90 between the observed and simulated hydraulic heads (Figure 7.15).

Table 7.8. Lake Package transient model calibration error

Evaluation Criteria	Lake stage	Aquifer heads
Mean error (m)	-0.15	-5.83
Mean absolute error (m)	0.45	6.34
Root mean square error (m)	0.55	7.89
Coefficient of determination (R^2)	0.90	0.36

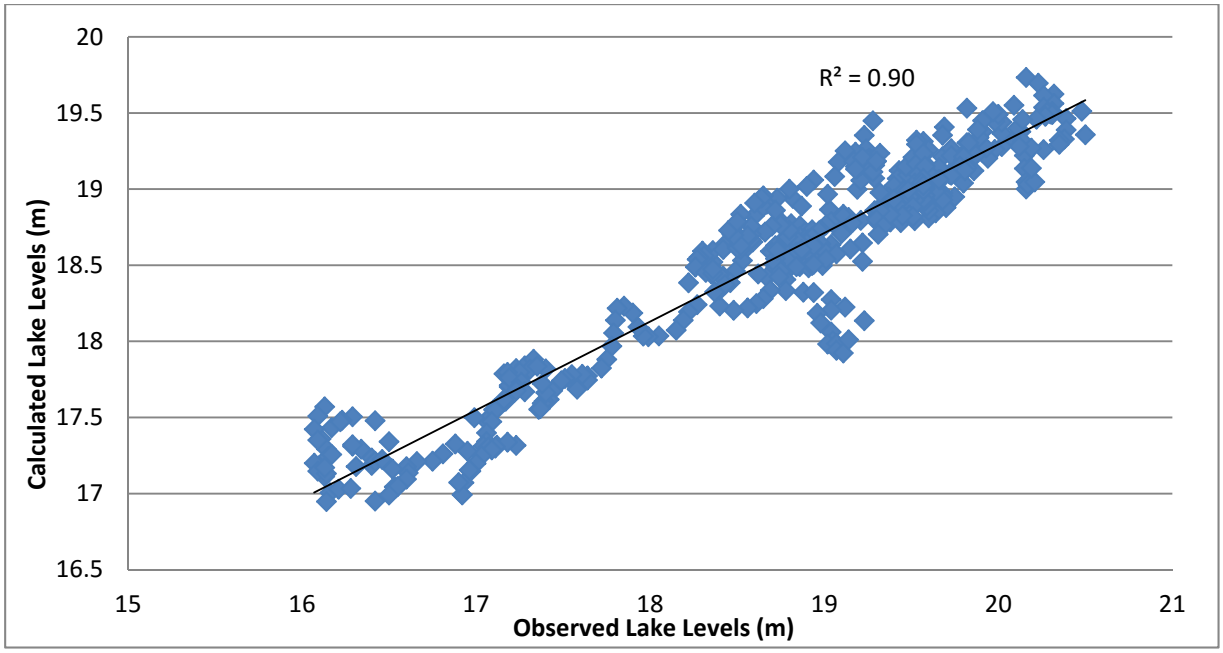

Figure 7.15. Lake Package Transient scatter plot observed versus simulated lake stage for the period between 1975 and 2014.

The Lake Package transient model simulations results along with time series lake level are presented in Figure 7.16. The transient Lake Package model results are, generally, in agreement with the measured values. This implies that the lake package model has satisfactorily simulated the fluctuations of the observed lake stage. The model struggled to simulate periods of rapid lake level rise (mostly driven by cyclone events) and lake level declines related to prolonged drought events.

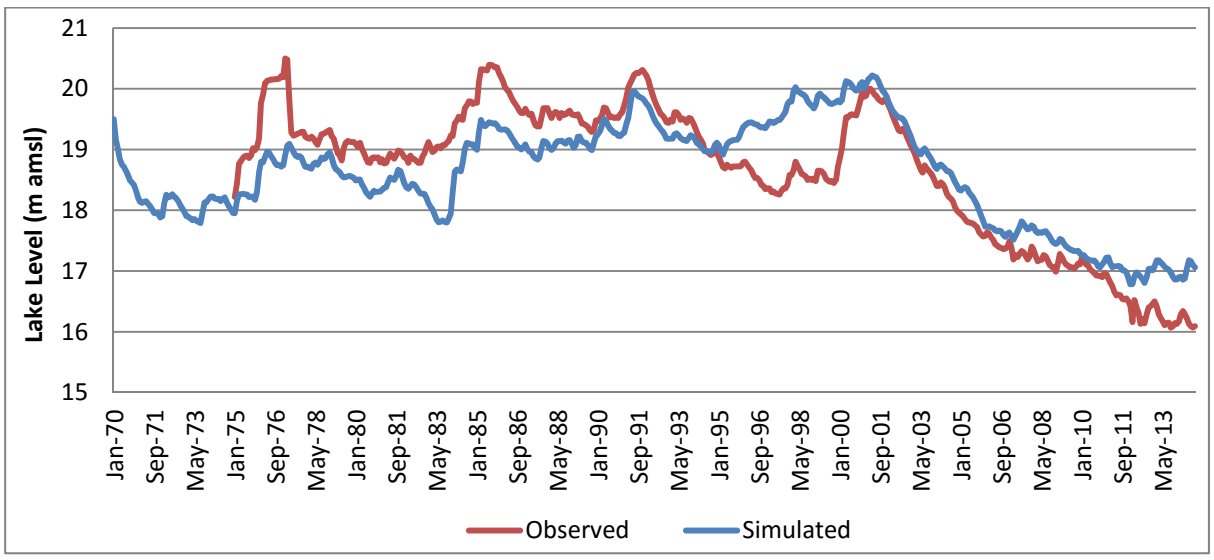

Figure 7.16. Time series plot of observed and Lake Package simulated lake levels from January 1970 to September 2014.

Given the high correlation between the steady-state and transient calibration results, combined with qualitative and quantitative analyses of the model errors, the Lake Package modelling has simulated measured conditions within acceptable error margins.

7.5. Long-term (Transient/Time series) water balance analyses

The computed long-term (1970 to 2014) catchment water balance that includes all water inflow and outflow components for the transient Lake Package and High-K models are shown in Figures 7.17 and 7.18, respectively. The results for both methods show that recharge is the primary inflow parameter followed by water from storage and then lake inflow when using the Lake Package. Throughout the simulation period, lake outflow has generally exceeded lake inflow except after intensive storm events which are reflected by a lake level rise. The contribution from recharge is significantly more pronounced when using the High-K method as it was shown that the model is very sensitive to changes in recharge. As the High-K method lacks lake water balance functionality found in the Lake Package, the resultant change in storage was incorporated as either positive or negative recharge which either increased or decreased the contribution from recharge. The discharge, through the coastal dune cordon, across the constant head boundary to the Indian Ocean, varies throughout the simulation period and is dependent on the lake and groundwater levels for each time step. The amount of storage available for a particular time varies depending on the computed amount of storage available from the previous time step. Evapotranspiration from the plantations has remained constant indicating that the water table never dropped below the rooting depth of 12 m. Should water levels decrease significantly, the water table depth would decrease below the rooting depth providing less water to the plantations. The effects of groundwater pumping are minor and are only visible during the part of the simulation once pumping commenced. The amount of inflow and outflow generated by the stream package was in equilibrium and depended on the fluctuating water level above the base of the stream. The Stream Package was incompatible with the High-K simulation, and because of its minor contribution, it was subsequently removed from the model.

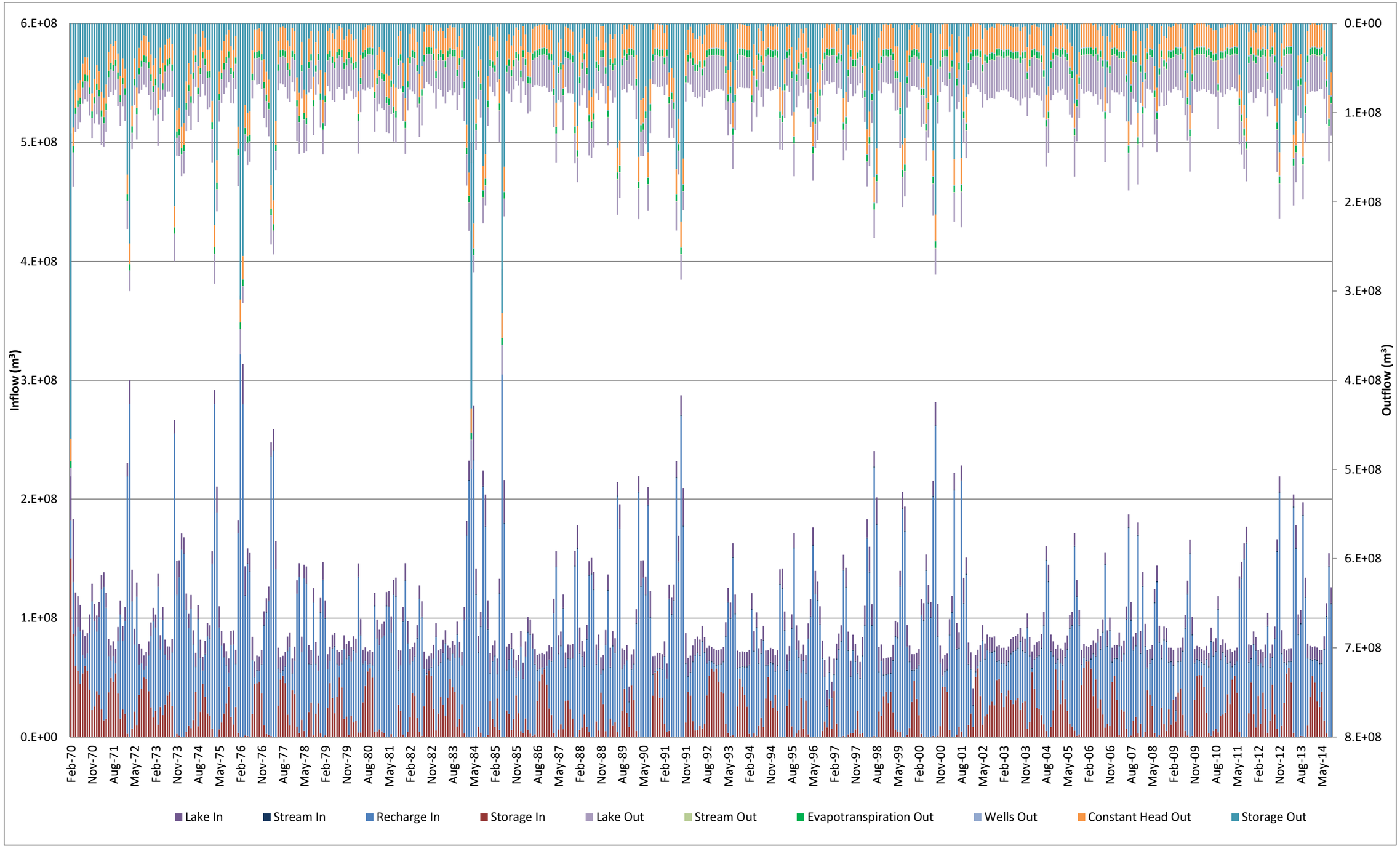

Figure 7.17. Long-term (1970 -2014) model domain water balance components for the Lake Package showing the various inflows and outflows.

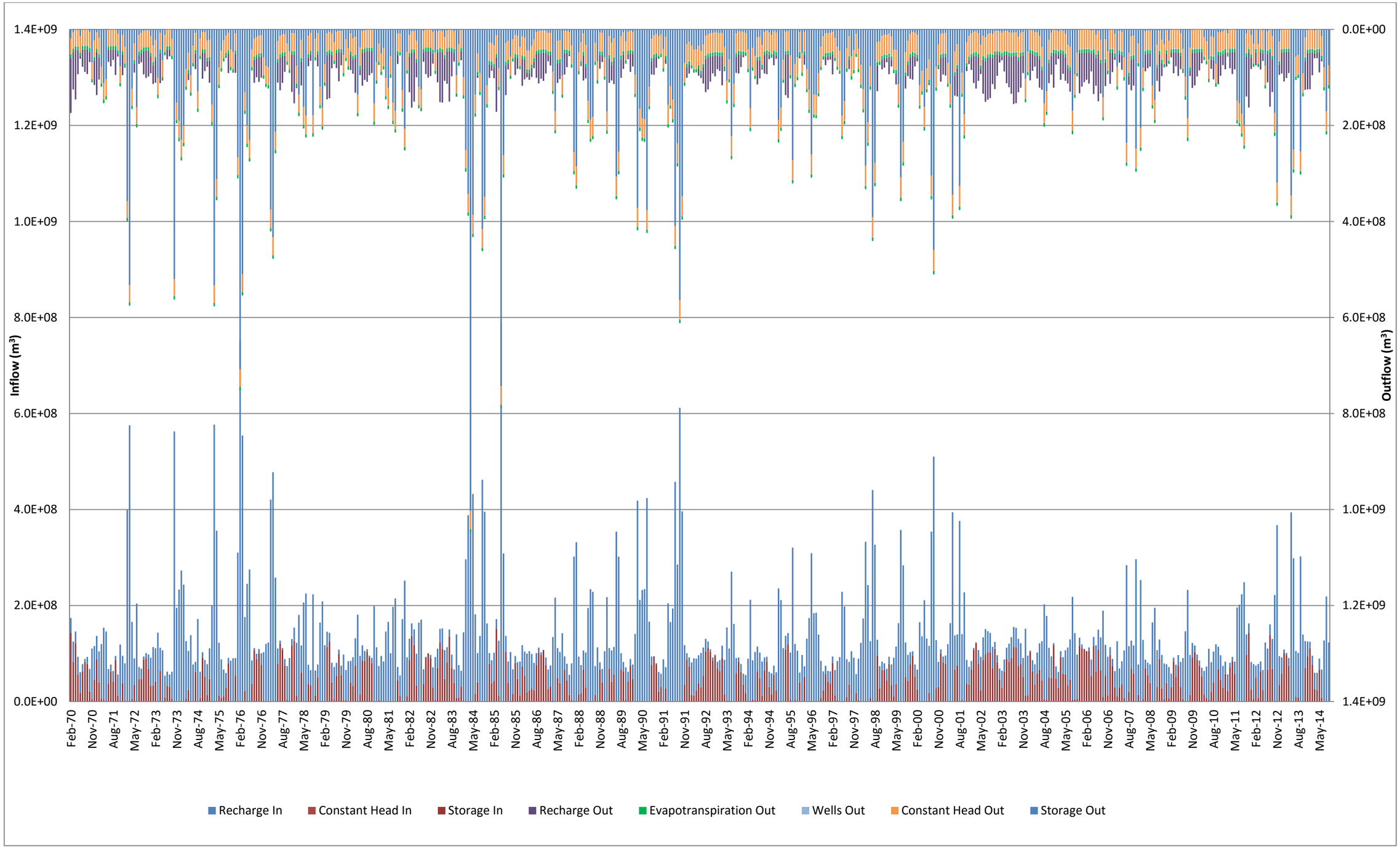

Figure 7.18. Long-term (1970 -2014) model domain water balance for the High-K method showing the various components of inflows and outflows.

7.6. Scenario analyses

One of the main purposes of the modelling exercise is to establish the impact various stress scenarios would have on the hydrological conditions in the study area. The calibrated groundwater model can be used to evaluate the hydrological response of the lake and the groundwater to either anthropogenic or natural stresses. This was done by modifying the appropriate parameters to represent the proposed scenario. The effect of the changes is dependent on the sensitivity of the model to the particular parameter and the scale as to which it is altered. The scenarios chosen for the model would aid in management strategies as it aims to address future land use and climate change and provide useful information for future planning and decision making. Based on the calibration results, the High-K method and Lake Package model were both deemed suitable for scenario analyses.

Været *et al*. (2008) reports predictions of a warmer and wetter climate for the South African east coast by the year 2100. Based on nearly 80 years of data (1928-2005), the climate change prediction for the St Lucia area, located south of the current model area, would be a 2-3°C increase in temperature and a 5 to 10% increase in precipitation. The increased evaporation caused by the temperature rise would be counteracted by the higher rainfall. These meteorological predictions were accompanied by a 0.4 m increase in sea level. The impact of each of the scenarios was simulated using the Lake Package and High-K method, and the results compared.

7.6.1. Evaluation of the various scenario results

The climate change predictions reported in Været *et al*. (2008, 2009) indicates a wetter and warmer climate. However, due to the uncertainty of these predictions, various scenarios were included to encompass the most possible conditions as well as a worst case scenario (Table 7.9). The changes in evaporation, precipitation and land use affect the mass balance of the model and thereby changing the flow across the recharge and discharge boundaries. The impacts of the scenarios are presented as a series of steady-state model simulations (Figures 7.19 through 7.23), while the effect on lake levels and catchment water balance is presented in Tables 7.10 and 7.11, respectively.

Table 7.9. Description of proposed scenarios for model simulation

<table>
<tr><td>Scenario</td><td colspan="5">Description</td></tr>
<tr><td>Scenario 1</td><td colspan="5">Addition of three proposed forestry applications within the Lake Sibayi model domain reported by Dennis (2014).</td></tr>
<tr><td></td><td>Plantation</td><td>X</td><td>Y</td><td>Area (m^2)</td><td>Estimated water use (m^3/a) *</td></tr>
<tr><td></td><td>Ngutshana</td><td>457292</td><td>6987720</td><td>950 000</td><td>1146100</td></tr>
<tr><td></td><td>Sonto 1</td><td>457469</td><td>6982578</td><td>8 000 000</td><td>9652790</td></tr>
<tr><td></td><td>Kwanhlamnu</td><td>457410</td><td>6979801</td><td>2 900 000</td><td>3499255</td></tr>
<tr><td>Scenario 2</td><td colspan="5">5% increase in open water evaporation and evapotranspiration and a 10% decrease in precipitation.</td></tr>
<tr><td>Scenario 3</td><td colspan="5">5% decrease in open water evaporation and evapotranspiration and a 10% increase in precipitation.</td></tr>
<tr><td>Scenario 4</td><td colspan="5">Worst case scenario which combines the proposed plantation applications with the decreased precipitation and increased evapotranspiration.</td></tr>
</table>

For all of the scenarios, the model input parameters other than those used in the formulation of the scenarios remained unchanged from those used in the calibrated model.

Scenario 1

Land use change in the form of increased plantation sizes has a significant impact on the groundwater and surface water regimes within the study area. This increased plantation coverage has the ability to pump huge amount of groundwater thereby decreasing groundwater levels, and consequent drying up of streams. On the other hand, their removal results in a rise in the water table (Været *et al*., 2009). The exact shapes of the proposed plantations are not known and therefore, they are incorporated as squares around their locations. The evapotranspiration rate for the plantations were set at 1460 mm/a (Brites and Vermeulen, 2013), which equates to a water use of 16 l/d per tree with a tree planted every 2 m. The High-K modelled scenario shows that the increase in the plantation size has had a marked impact on lake levels (Figure 7.19b), while the Lake Package model response is less apparent (Figure 7.19a). The Lake Package model results in no change in lake levels while the High-K model resulted in a 40 cm lake level reduction. A groundwater level reduction was also observed within the vicinity of the proposed plantations due to the 6 x 10^5 m^3/a increase in groundwater withdrawal by the plantations, with the groundwater level decline more apparent in the High-K model output.

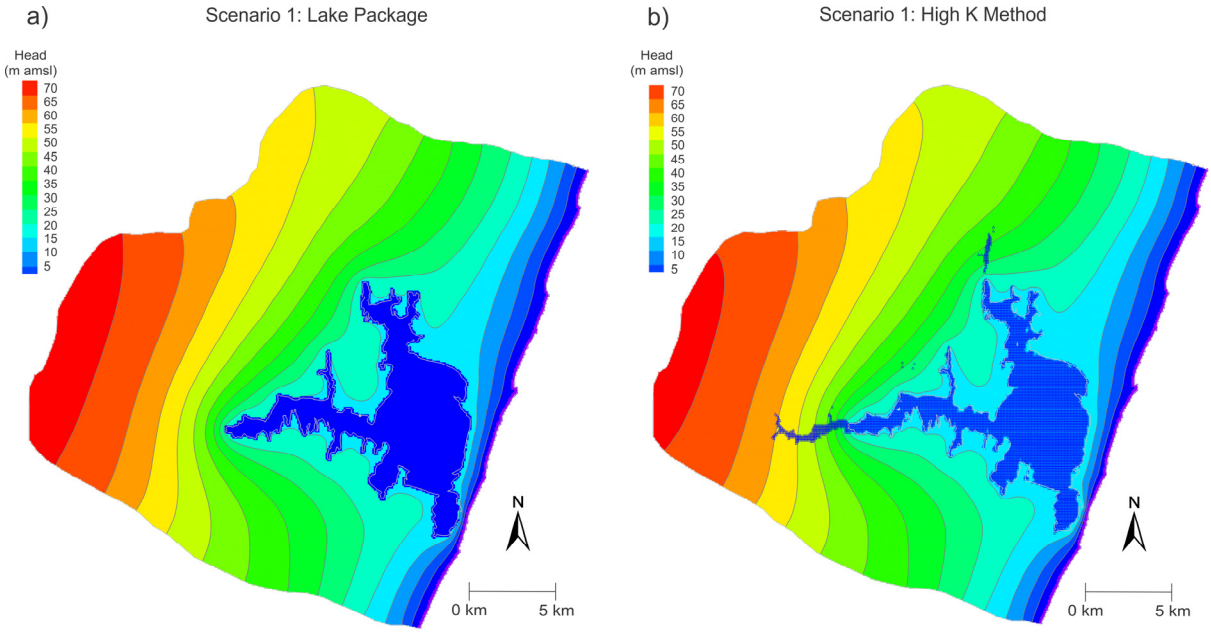

Figure 7.19. Contour plot of Scenario 1 including the proposed forestry applications

Scenario 2

When the climate change predictions of Været *et al*. (2008) were applied to the Penman open water evaporation calculation, a 2°C increase in temperature resulted in an approximate 5% increase in open water evaporation. When the temperature increase was applied to the FAO Penman-Monteith evapotranspiration equation (Allen *et al*., 1998), it resulted in approximately 5% increase in the

evapotranspiration rate. The effect of increased temperature on other factors such as sunshine duration and humidity were however ignored for these calculations. In this scenario precipitation was decreased by 10% which was accompanied by a decrease in the recharge rate. The lake was found to be extremely sensitive to the increased evaporation as the lake level for the High-K method dropped over 14 m to 5.04 m amsl. The level drop resulted in water only being present in the deeper areas of the lake as well as drying out of western arm as indicated by the red dry cells (Figure 7.20b). The effect was less pronounced when using the Lake Package with a relatively smaller lake level reduction of 10 cm (Figure 7.20a). The reduction in water levels throughout the rest of the catchment was less pronounced and did not drop below the plantation rooting depth as there was no reduction in evapotranspiration.

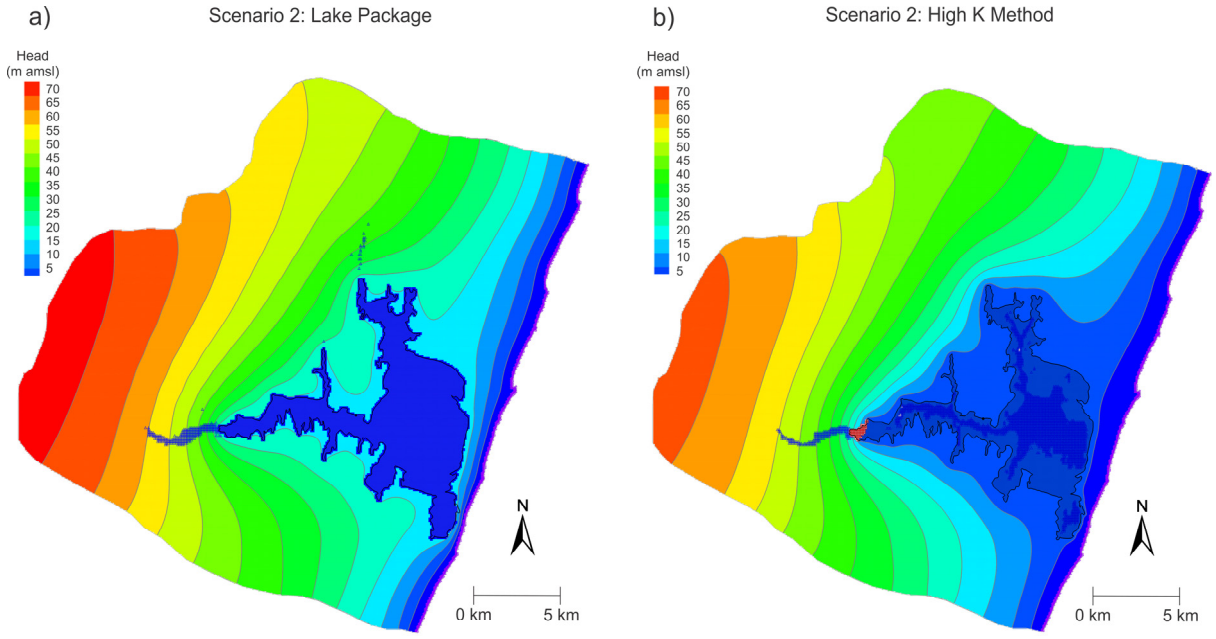

Figure 7.20. Contour plot of Scenario 2 where precipitation has been decreased by 10% and evaporation increased by 5%.

Scenario 3

The 3rd model scenario was run with a 10% increase in precipitation, and an accompanying increase in recharge, while decreasing evaporation and evapotranspiration by 5%. Running this scenario using the High-K method showed a significant increase in lake level (by about 12 m), flooding the low lying areas around the lake (Figure 22b). The model run using the Lake Package produced a less pronounced lake level rise with only the northern and western arms of the lake around Velindlovu and Mseleni streams flooded (Figure 21a).

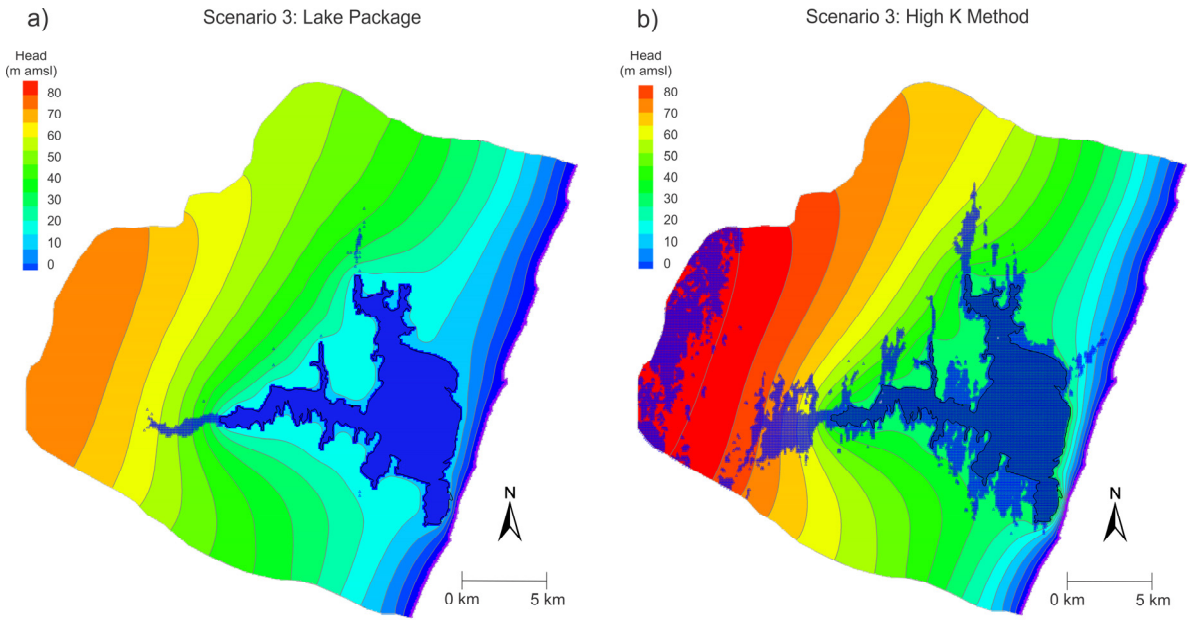

Figure 7.21. Contour plot of Scenario 3 where precipitation has been increased by 10% and evaporation decreased by 5%.

Scenario 4

Scenario 4 represents the worst case scenario and incorporates the compounded effects of scenarios 1 and 2. The outcome does not represent a significant change from scenario 3 as they are both extreme conditions of a highly stressed environment where not much further change will occur. The extremely low water levels highly reduce the hydraulic gradient towards the ocean and with the significantly reduced pressure head allowing for the possibility of salt water intrusion in the eastern region of the lake (Figure 7.22). The threat of salt water intrusion would be assessed through particle tracking in future simulations.

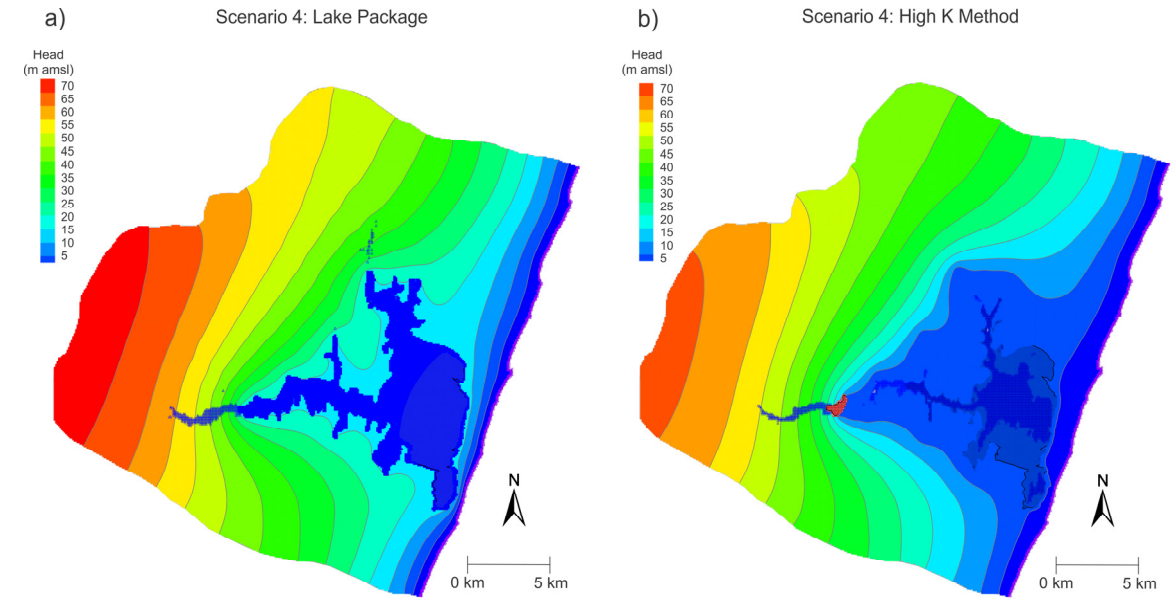

Figure 7.22. Modelled groundwater and lake level map for Scenario 4 representing the worst case scenario.

For most of the scenarios, the regional groundwater flow pattern has remained the same with the major variation limited to the vicinity of the lake. The use of the High-K method results in a much larger variance in the computed water level. This is due to the representation of the lake with highly conductive cells which is more responsive to the various changes. The fact that lake water balance components are input as net flux represented as positive or negative recharge for the High-K lake cells, it resulted in significant fluctuations of the water levels in the vicinity of the lake.

Table 7.10. Simulated lake levels for the various scenarios obtained using the Lake Package and High-K method.

	Computed lake stage (m amsl)	
	Lake Package	High-K Method
Scenario 1	19.54	19.10
Scenario 2	19.42	5.04
Scenario 3	22.70	31.12
Scenario 4	19.34	4.47

Table 7.11. Computed water balance components for the various model scenario.

		High-K method		Lake Package	
	Sources/Sinks	Inflow (m^3/a)	Outflow (m^3/a)	Inflow (m^3/a)	Outflow (m^3/a)
Scenario 1: Proposed Forestry Applications					
	Constant heads	0	-3.14E+07	0	-3.10E+07
	Streams	4.94E+05	-4.94E+05	6.13E+05	-6.18E+05
	Recharge	5.31E+07	-1.40E+07	5.66E+07	0
	Evapotranspiration	0	-7.77E+06	0	-7.77E+06
	Lake	-	-	1.70E+07	-3.21E+07
Scenario 2: Decrease precipitation and increase evaporation	Constant heads	0	-1.25E+07	0	-2.81E+07
	Streams	1.85E+05	-1.85E+05	6.26E+05	-6.32E+05
	Recharge	4.79E+07	-2.82E+07	5.10E+07	0
	Evapotranspiration	0	-7.14E+06	0	-7.14E+06
	Lake			1.44E+07	-2.92E+07
Scenario 3: Increase precipitation and decrease evaporation	Constant heads	0	-5.18E+07	0	-3.56E+07
	Streams	1.74E+06	-1.75E+06	1.27E+06	-1.27E+06
	Recharge	5.89E+07	0	6.23E+07	0
	Evapotranspiration	0	-7.14E+06	0	-7.14E+06
	Lake			1.99E+07	-3.41E+07
Scenario 4: Decrease precipitation and increased evaporation combined with proposed forestry applications	Constant heads	0	-1.19E+07	0	-2.68E+07
	Streams	1.91E+05	-1.91E+05	6.14E+05	-6.14E+05
	Recharge	4.79E+07	-2.82E+07	5.10E+07	0
	Evapotranspiration	0	-7.77E+06	0	-7.77E+06
	Lake			1.32E+07	-2.78E+07

7.7. Model Limitations

Numerical models represent simplified versions of the physical system and therefore inherently contain some degree of uncertainty. Uncertainty is introduced to the system through uncertainties in many of the input parameters and boundary conditions or through the representation of real world conditions in the conceptual model.

The main challenges developing the numerical groundwater models for the Lake Sibayi system has been limitation in reliable and extensive data for the study area. The poorly measured water level data quality means that the calibration process was very difficult. Several lake-related inflow and outflow parameters had to be assumed for the model as well. The runoff from the studied catchment was estimated using the best information available as no stream flow data was available. The open water evaporation data was obtained from pan evaporation data which was multiplied with the pan coefficients proposed by Pitman and Hutchinson (1975) based on only 6 years of data. Lake abstraction rates were based on data provided by DWS with minimum validation. Therefore, the model's inability to accurately simulate the significant lake level reduction over the last decade could in-part be due to unaccounted water losses or withdrawals. However, it could also be due to an inherent limitation of the Lake Package as it does not respond well to rapid changes of various input parameters (Merritt and Konikow, 2000).

7.8. Evaluation of the Lake Package and High-K method

Both the Lake Package and High-K simulations generally match well with the observed values. The High-K method, though not as accurate as the Lake Package, was able to effectively simulate the lake/aquifer interactions within the study area. Anderson *et al*. (2002) noted several advantages and disadvantages of using the High-K method. The advantages include its simplicity and ease of use while also being stable over a wide range of conditions. Disadvantages include that the method is limited to simple application problems such as seepage lakes, not being able to accommodate changes in lake surface areas without additional programming, and large number of iterations and smaller convergence criteria are required. Merritt and Konikow (2000) describe several advantages of the Lake Package. The Lake Package is more sophisticated as it allows for the development of more realistic simulations of lake/aquifer interactions, particularly lake water balances. The lake water budget accounts for atmospheric fluxes including recharge and evaporation, overland runoff, withdrawal from, or inflow to the lake, and any subsurface fluxes into and out of the lake which could vary based on lake surface area. The package further allows the lake to expand and contract based on the lake geometry and computed lake stage and lake volume consistent with the water budget. Depending on these factors, the lake level might decrease forming separate lakes each with its own water balance, or allow for separate lakes to coalesce forming larger lakes as water levels rise.

Another advantage of the lake package is that it allows for the integration of the Stream Package (Prudic, 1989) so that these complex stream-lake interactions could be modelled, which is impossible with the High-K method. The Lake Package represents lakebed leakance according to mapped lakebed sediment characteristics unlike the High-K method where the lake is seamlessly connected to the aquifer but in reality may not be always.

The High-K method was found to be highly sensitive to changes in the recharge regime and displayed substantial fluctuations in simulated lake levels in response to varying inflow and outflow components. These simulated lake level fluctuations were less apparent when the Lake Package was used. The High-K method also gave a low R^2 value of 0.64 and 0.32, for the lake and aquifer respectively, which indicates a relatively poor fit between measured and simulated lake stages and aquifer heads. The High-K technique is therefore most suitable for simple applications; however, complex lake-aquifer interactions are better simulated using the Lake Package along with the stream package.

7.9. Summary

The sustainable development of the water resource of Lake Sibayi and its catchment is essential. To effectively manage this water resource, a three-dimensional numerical steady-state and transient model has been developed following two independent approaches. The modular finite difference modelling code, MODFLOW with its several packages and Groundwater Modelling Systems (GMS) were used to simulate lake-aquifer interactions through appropriate boundary conditions in the Lake Sibayi catchment. The model consisted of 2 layers, these representing the upper and lower HSU resting on the impermeable Cretaceous basement. The investigation compared and contrasted the two approaches, i.e. the High-K and the more sophisticated Lake Package to simulate lake-aquifer interactions. The suitably calibrated steady-state models provided the initial conditions to simulate long-term lake level fluctuations on a monthly time step from January 1970 to September 2014. The Lake Package simulated the long-term fluctuations in lake level and aquifer heads as it took cognisance of various lake water balance components compared to the High-K method. The response of Lake Sibayi under different climate and land use change scenarios was simulated using both methods. The High-K method is highly sensitive to changes in the recharge regime. It displayed substantial fluctuations in simulated lake levels in response to varying inflow and outflow components. These simulated lake level fluctuations were less apparent when the Lake Package was used. Therefore, the High-K technique is most suitable for simple applications; however, complex lake-aquifer interactions are better simulated using the Lake Package along with the stream package.

CHAPTER EIGHT: CONCLUSIONS AND RECOMMENDATIONS

Geological, hydrological, hydrogeological, hydrochemical and environmental isotope data were integrated and interpreted to conceptualise the hydrogeology of the Lake Sibayi Catchment to provide a better understanding of the groundwater-surface water interactions within the area. The conceptual model developed reveals that Lake Sibayi is connected hydraulically to the groundwater and gets subsurface recharge through the sandy substrate, as it forms an extension of the shallow groundwater regime. Based on the conceptual model developed, groundwater and surface water in the study area are highly interconnected. Therefore, developing one resource should consider the impacts on the other.

Various data sources ranging from rainfall, evaporation and lake-level records, in combination with the bathymetric profile of the lake have been used to establish the principal components of the water balance for Lake Sibayi. The groundwater recharge estimated using the CMB method and from published maps resulted in recharge rates of 126 mm/a (12% MAP) and 95 mm/a (10% MAP), respectively. The total evaporation and evapotranspiration from the lake and its catchment is estimated at 1 495 mm/a and 1 090 mm/a respectively. Estimated surface water runoff from the catchment to the lake is about 1% of MAP. Calculated lake water outflow to the sea through the dune cordon opposite the lake, along a 12 km seepage face, is 2.3 x 10^7 m^3/a. The total amount of water abstracted from both surface and groundwater resources within the catchment is about 4.5 x 10^6 m^3/a.

Lake water balance and observed lake levels show a continuous lake level decline. This decline in lake level is attributed to the recent increase in water abstraction from the lake and groundwater within the catchment. Following a sharp reduction in rainfall after 2000, which was observed in the lake following a short lag period, the commencement of increased lake abstraction was implemented. Precipitation started increasing again around 2003; however, a rebound of lake levels was not observed due to the increased abstraction. During late 2004, lake levels declined below the drought lake level of 18 m as proposed by Meyer and Godfrey (2003) during their reserve determination for Lake Sibayi. The problem is further exacerbated by rapidly increasing pine plantations which pump a huge amount of groundwater through evapotranspirative processes. Thus, the water levels of Lake Sibayi fluctuate constantly in response to varying amounts of groundwater and surface water discharge into the lake, seepage loss through the coastal dunes, abstraction, and evaporation from the lake surface. Should the declining lake level trend continue unabated, the lake would undergo lake segmentation, as has already been observed in the Southern Basin which has nearly completely separated from the Main Basin. Additionally, extremely low water levels would highly reduce the hydraulic gradient from the lake towards the ocean, allowing for the possibility of salt water intrusion in the eastern region of the lake.

Hydrochemical signatures show slight variation in chemical characteristics between the shallow and deep groundwater systems. The shallow groundwater and deep groundwater systems are characterised by Na-Cl and Na-Ca-HCO_3-Cl water facies, respectively. Shallow groundwater samples have relatively low EC values averaging 278 mS/m, while the deeper wells had average EC concentrations of 409 mS/m. Groundwater samples collected along the dune cordon, show a similar hydrochemical and environmental isotope composition as that of the lake. Groundwater hydraulic head data, hydrochemical and environmental isotope signatures determined along the coastal dune cordon, between the lake and Ocean, give conclusive evidences for seepage from the lake through the coastal dune cordon to the Indian Ocean. Results of principal component factor analysis were used to perform hierarchical cluster analysis of hydrochemical data. The first cluster represents the groundwater samples, which is in turn divided into 2 sub-clusters representing the shallow and deep aquifers, while the second cluster represents the surface water samples with a clear distinction between stream and lake samples.

To ensure sustainable development and effective management of the water resources within the Lake Sibayi catchment, a three-dimensional numerical model of the lake was created. The two layer steady-state and transient models were constructed to compare and contrast two independent modelling approaches, which consisted of the High-K method and more sophisticated Lake Package to simulate lake-aquifer interactions. The transient model calibration results show that the Lake Package was more suitable in simulating lake level fluctuations with low calibration errors. The calibrated groundwater flow models were further used to evaluate the hydrological response of the lake and the groundwater system to various climate and land use stress scenarios. Once again, the Lake Package was the preferred method as the High-K method proved to be very sensitive to changes in model input, simulating rapid changes to the system. The High-K technique is therefore most suitable for simple applications, while complex lake-aquifer interactions are better simulated using the Lake Package.

The following are recommendations emanated from the present study:

- Determination of baseline stream flow measurements on the main streams in the area, especially the Mseleni River, would allow for accurate computation of stream flow contribution to the lake;
- The lake level gauging station (W7R001) needs to be lowered as lake levels are currently below the gauging station. The new gauge elevation needs to be surveyed to allow for accurate lake level measurements;
- Collection of continuous groundwater level measurements by DWA needs to be improved as some of the data had to be disregarded due to incorrect field measurements from the continuous data loggers;

- Further research is recommended to better understand the water use of different plant types in various hydrogeological settings and at various stages of growth;
- Based on current lake levels, it is recommended that the proposed forestry applications be halted until lake levels have recovered;
- An assessment needs to be undertaken to get a better estimate of lake and groundwater abstraction within the catchment. Should the demand for water increase further, it is recommended not to increase abstraction, but rather focus on improving management strategies related to the currently available resource such as leak detection, water conservation and water reuse.

REFERENCES

Albaugh, J. M., Dye, P. J., and King, J. S., 2013. Eucalyptus and Water Use in South Africa. International Journal of Forestry Research. 2013, 1-11.

Allanson, B. R., 1979. Lake Sibayi. Monographiae Biologicae, In: Illies, J. (Ed.), Dr. Junk Publications, Hague, Boston, London, 353 pp.

Allen, R. G., Pereira, L. S., Raes, D., and Smith, M., 1998. Crop Evapotranspiration: Guidelines for Computing Crop Water Requirements. Food and Agriculture Organization of the United Nations. Rome, Italy.

Allison, G. B., Gee, G. W., and Tyler, S. W., 1994. Vadose zone techniques for estimating groundwater recharge in arid and semi-regional. Soil Science Society of America Journal 58, 6-14.

Allison, G. B., Hughes, M. W., and Leaney, F. W. J., 1984. Effect of climate and vegetation on oxygen-18 and deuterium profiles in soil. Isotope Hydrology. Proceedings Symposium Vienna, IAEA, 105-123.

Anderson, M. P., and Woessner, W. W., 1992. Applied Groundwater Modelling; Simulation of Flow and Advective Transport. Academic Press, London, 381 pp.

Anderson, M. P., Hunt, R. J., Krohelski, J., and Chung, K., 2002. Using High Hydraulic Conductivity Nodes to Simulate Seepage Lakes. Ground Water 40, 117-122.

Appelo, C. A. J., and Postma, D., 2005. Geochemistry, Groundwater and Pollution, 2nd Edition. Balkema, Amsterdam, 649 pp.

Australian Groundwater Consultants. 1975. Richards Bay Groundwater Investigations – Richards Bay Heavy Minerals Project. Confidential Report.

Baron, J., Seward, P. and Seymour, A., 1996. The Groundwater Harvest Potential Map of the Republic of South Africa. DWAF Report No. Gh3917. Department of Water Affairs and Forestry, Pretoria, South Africa.

Barwell, V. K. and Lee, D. R., 1981. Determination of horizontal –to-vertical hydraulic conductivity ratios from seepage measurements on lake beds. Water Resources Research 17, 565-570.

Basson, M. S., Van Niekerk, P. H., and Van Rooyen, J. A., 1997. Overview of Water Resources Availability and Utilisation in South Africa. Department of Water Affairs and Forestry, Pretoria, South Africa 72 pp.

Bazuhair, S.A., and Wood, W. W., 1996. Chloride mass balance method for estimating groundwater recharge in arid areas: Examples from western Saudi Arabia. Journal of Hydrology 186, 153-159.

Beekman, H. E., and Xu, Y., 2003. Review of groundwater recharge estimation in arid and semi-arid Southern Africa. In: Xu, Y., and Beekman, H. E. (Eds.) Groundwater Recharge Estimation in South Africa. UNESCO IHP Series No. 64, 3-18.

Bjørkenes, M., Haldorsen, S., Mulder, J., Kelbe, B., and Ellery, F., 2006. Baseline groundwater quality in the coastal aquifer of St. Lucia, South Africa. Urban Groundwater Management and Sustainability, 233-240.

Bjørkenes, M., Wejden, B., and Kelbe, B., 2004. Hydrogeology in the Coastal Aquifer of St Lucia, South Africa: Groundwater Chemistry. Paper for Urban Groundwater Workshop, Baku, Azerbaijan.

Bonansea M., Ledesma C., Rodriguea C., and Pinotti L., 2014. Water quality assessment using multivariate statistical techniques in Rio Tercero Reservoir, Argentina. Hydrology Research, in press.

Borradaile, G. J., 2003. Statistics of earth science data; their distribution in time, space, and orientation. Springer, New York, 351 pp.

Botha, G. A. and Singh R., 2012. Geological, geohydrological and development potential zonation influences; environmental management framework for uMkhanyakude District, KwaZulu-Natal. Council for Geoscience, Pretoria, South Africa.

Botha, G. A., 1997. The Maputaland Group: A Provisional Lithostratigraphy for Coastal KwaZulu-Natal. Maputaland focus on the Quaternary evolution of the south-east African coastal plain. International Union for Quaternary Research Workshop Abstracts, Council for Geoscience, Pretoria, 21-26 pp.

Botha, G. A., and Porat, N., 2007. Soil chronosequence development on the southeast African coastal plain, Maputaland, South Africa. Quaternary International 162-163, 111-132.

Botha, G. A., Bristow, C. S., Porat, N., Duller, G. A. T., Armitage, S. J., Roberts, H. M., Clarke, B. M., Kota, M. W., and Schoeman, P., 2003. Evidence for dune reactivation from ground

penetrating radar (GPR) profiles on the Maputaland coastal plain, South Africa. In: Bristow, C.S. and Jol, H.M. (Eds.), Ground Penetrating Radar: Applications in Sedimentology. Geological Society, London, Special Publications 211, 26-46.

Boucher, K., 1975. Global Climate. The English Universities Press Ltd., London, 323 pp.

Bredehoeft, J. D., Neuzil, C. E., and Milly, P. C. D., 1983. Regional flow in the Dakota Aquifer: a study of 11the role of confining layers. USGS, Water Supply Paper 2237, 45 pp.

Bredenkamp, D. B., 1993. Recharge estimation based on chloride profiles. Dept. of Water Affairs and Forestry, Pretoria, Report GH 3804, 22 pp.

Bredenkamp, D. B., 2008. Short Course on Estimation of Groundwater Recharge: Summary of a presentation at Western Cape University.

Bredenkamp, D. B., Botha, L. J., Van Tonder, G. J., and Van Rensburg, H. J., 1995. Manual on Quantitative Estimation of Groundwater Recharge and Aquifer Storativity. Water Research Commision Report No. TT 73, Pretoria, South Africa.

Brites, C. M., and Vermeulen, D., 2013. The Environmental Impacts of Groundwater on the St Lucia Wetland. National Groundwater Conference, Durban, 22 pp.

Bruton, M. N., Smith, M., and Taylor, R. H., 1980. A brief history of human involvement in Maputaland. In: Bruton, M. N., Cooper, K. H. (Eds.), Studies on the Ecology of Maputaland. Rhodes University, Grahamstown, pp. 382-407.

Cattell, R. B., 1966. The scree test for the number of factors. Multivariate Behavioral Research 1, 245-276.

Clark, I. D., Fritz, P., 1997. Environmental Isotopes in Hydrogeology. Lewis Publishers, New York, 328 pp.

Combrink, X., Korrûbel, J. L., Kyle, R., Taylor, R., and Ross, P., 2011. Evidence of a declining Nile crocodile (Crocodylus niloticus) population at Lake Sibaya, South Africa. South African Journal of Wildlife Research 41, 145-157.

Cooper, M. R, and McCarthy, M. I., 1988. The stratigraphy of the Uloa Formation. Extended Abstract 22nd Earth Science Congress Geological Society, 121-124 pp.

Council, G. W., 1998. A lake package for MODFLOW: Proceedings of MODFLOW 98 Conference, Golden, Colorado 2, 675-682.

Council, G. W., 1997 .Simulating Lake-Groundwater Interaction with MODFLOW. Proceedings of the 1997 Georgia Water Resources Conference, The University of Georgia.

Craig, H., 1961. Isotopic variations in meteoric waters. Science 133, 1702–1703.

Davies, Lynn and Partners, 1992. Landform geomorphology and geology. In: Coastal and Environmental Services. Environmental Impact Assessment. Eastern Shores of Lake St Lucia (Kingsa/Tojan Lease Area). Specialist Reports Volume 1: Biophysical environment (Chapter 2), Grahamstown, South Africa, 22-56 pp.

Demlie, M., Hingston, E., and Mnisi, Z., 2014. A study of the sources, human health implications and low cost treatment options of iron rich groundwater in the northern coastal areas of KwaZulu-Natal, South Africa. Journal of Geochemical Exploration 144, 504-510.

Dennis, I. 2014. Determining the impact of proposed SRFA development in the W70 and W32 catchments on the water resources supporting sensitive habitats (e.g. lakes). Domestic water supply and the iSimangaliso World Heritage Site and RAMSAR. Interim Report. Centre for Water Sciences and Management, North-West University.

Diab, R. D., and Sokolic, F., 1996. Report on Wind and Wind Turbine Monitoring at Mabibi – Period: September 1994 to February 1996. Department of Mineral & Energy Affairs, Report, 8 pp.

Dingle, R. V., Siesser, W. G., and Newton, A. R., 1983. Mesozoic and tertiary geology of Southern Africa. Balkema, Rotterdam, 375 pp.

Doherty, J. E., Hunt, R. J., and Tonkin, M. J., 2010. Approaches to highly parameterized inversion: A guide to using PEST for model-parameter and predictive-uncertainty analysis. U.S. Geological Survey Scientific Investigations Report No. 5211, 71 pp.

Dupuit, J., 1863. Étudesthéoriquesetpractiquessur le mouvement des eauxdans les canauxdécouvertset á travers les terrains perméables, 2nd Ed. Dunod, Paris. In: Fetter, C. W. (Ed.), Applied Hydrogeology. Prentice-Hall International Limited, London.

Durfer, C. N, and Becker, E., 1964. Public water supplies of the 100 largest cities in the United States. U.S. Geological Survey Water Supply 1812, 372 pp.

Durov, S. A., 1948. Natural waters and graphic representation of their compositions. Dokl Akad Nauk SSSR 59, 87-90.

DWA, 2013. Lake water levels. Directorate: Hydrological Services, Department of Water Affairs, Pretoria, South Africa.

DWA, 2014. Usutu-Mhlatuze WMA water usage. Department of Water Affairs, Pretoria, South Africa.

DWA, 2016. Usuthu-Mhlathuzi WMA Continuous Groundwater Level Readings. Department of Water Affairs, Pretoria, South Africa.

Edmunds, W. M., Darling, W. G., and Kinniburgh, D. G., 1988. Solute profile techniques for recharge estimation in semi-arid and arid terrain. In: Simmers, I. (Ed.). Estimation of Natural Groundwater Recharge, Reidel Publishing, Massachusetts, 139–157.

Eriksson, E., and Khunakasem, V., 1969. Chloride concentration in groundwater, recharge rate and rate of deposition of chloride in the Israel coastal plain. Journal of Hydrology 7, 178–197.

Ezemvelo KZN Wildlife, 2011. KwaZulu-Natal Land Cover 2008 V1.1. Unpublished GIS Coverage (Clp_KZN_2008_LC_V1_1_grid_w31.zip), Biodiversity Conservation Planning Division, Ezemvelo KZN Wildlife, P. O. Box 13053, Cascades, Pietermaritzburg, 3202.

Fetter, C. W., 2001. Applied Hydrogeology, 4th Ed. Prentice Hall, New Jersey, p. 598.

Fockema, P. D., 1986. The heavy mineral deposits of Richards Bay, 2301-2307. In: Anhauesser, C. R., Maske, S. (Eds.), Mineral Deposits of Southern Africa, Vol. 2, 2335 pp.

Franke, O. L., Reilly, T. E., and Bennet, G. D., 1987. Definition of boundary and initial conditions in the analyses of saturated ground water flow systems – An Introduction. Techniques of Water-Resources Investigations of the United States Geological Survey, 22 pp.

Frankel, J. J., 1966. The basal rocks of the Tertiary at Uloa, Zululand, South Africa. Geological Magazine 103, 214-230.

Garstang, M., Kelbe, B. E., Emmitt, G. D. and London, W. B., 1987. Generation of convective storms over the escarpment of north-eastern South Africa. Monthly Weather Review, Vol 115, No. 2, 429-443.

Gat, J. R., Gonfiantini, R., 1981. Stable Isotope Hydrology. Tech. Report 210. IAEA, Vienna, 337 pp.

Geological Survey, 1985a. 1:250,000 geological series map, 2632 Kosibaai.

Geological Survey, 1985b. 1:250,000 geological series map, 27 ½ 32 St Lucia.

Geyh, M., 2000. Environmental isotopes in the hydrological cycle. Principles and applications. Groundwater – saturated and unsaturated zone. Technical documents in hydrology. UNESCO, Vol. 6, 36 pp.

Gianniou, S. K., and Antonopoulos, V. Z., 2007. Evaporation and energy budget in Lake Vegoritis, Greece. Journal of Hydrology 345, 212-223.

Goodman, P. S., 1990. Soil, vegetation and large herbivores relations in Mkhuzi Game Reserve, Natal. PhD Thesis, University of Witwaterand, Johannesburg.

Google Earth 7.1.2., 2014. Lake Sibayi, -27.340754°, 32.671193°, eye elevation 25 km. Digital Globe 2014. URL: http://www.earth.google.com (accessed 26 January 2014).

Green, A. N., and Uken, R., 2005. First observations of sea-level indicators related to glacial maxima at Sodwana Bay, northern KwaZulu-Natal. South African Journal of Science, 101, 236-238.

GRIP, 2013. Groundwater Resource Information Project. Digital Information as Supplied by the Department of Water Affairs.

Hair, J. T, Anderson, R. E., Tatham, R. L., and Black, W. C., 1992. Multivariate data analysis with readings 3rd Ed. Macmillan, New York, 426-496.

Harbaugh, A. W., 2005, MODFLOW-2005, The U.S. Geological Survey modular ground-water model - the Ground-Water Flow Process: U.S. Geological Survey Techniques and Methods, 253 pp.

Harbaugh, A. W., Banta, E. R., Hill, M. C., and McDonald, M. G., 2000. MODFLOW-2000, The U.S. Geological Survey Modular Ground-Water Model - User guide to modularization concepts and the ground-water flow process. U.S. Geological Survey Open-File Report No. 92, 121 pp.

Hill, R. I., 1979. Bathymetry, morphometry and hydrology of Lake Sibaya. In: Allanson, R. R. (Eds.). Lake Sibaya, Monographiae Biologicae. 36, Dr. W Junk, The Hague, 34-41.

Hobday, D. K., 1979. Geological evolution and geomorphology of the Zululand coastal plain. In: Allanson, B. R. (Ed.), Lake Sibaya. Monographiae Biologicae. Dr. Junk Publications, Hague, Boston, London, 20 pp.

Hobday, D.K., and Orme, A.R., 1974. The Port Durnford Formation: A major Pleistocene Barrier Lagoon complex along the Zululand coast. Transactions of the Geological Society of South Africa 77, 141 - 149.

Hunt, R. J., and Krohelski, J. T., 1996. The application of analytic element model to investigate groundwater–lake interactions at Pretty Lake, Wisconsin. Journal of Lake Reservoir Management 12, 487-495.

Hunt, R. J., Haitjema, H. M., Krohelski, J. T., and Feinstein, D. T., 2003. Simulating Ground Water-Lake Interactions: Approaches and Insights. Ground Water 41, 227-237.

Hunt, R. J., Lin, Y., Krohelski, J. T., and Juckem, P. F., 2000. Simulation of the shallow hydrologic system in the vicinity of Middle Genesee Lake, Wisconsin, using analytic elements and parameter estimation. U.S. Geological Survey Water Resources Investigations Report No. 4136, 21 pp.

Hunter, I. T., 1988. Climate and weather off Natal. In: Schumann, E. H. (Ed.), Coastal Ocean Studies Off Natal, South Africa. Lecture Notes on Coastal and Estuarine Studies 26, 81–100.

Hussain M., Ahmed S. M., and Abderrahman W., 2008. Cluster analysis and quality assessment of logged water at an irrigation project, eastern Saudi Arabia. Journal of Environmental Management 86, 297-307.

Hutchinson, I. P. G., and Pitman, W. V., 1973. Climatology and Hydrology of the St Lucia Lake System. Hydrological Research Unit, Report 1/73, University of the Witwatersrand, Johannesburg.

IAEA, 2012. Global Network of Isotopes in Precipitation. The GNIP Database. (http://www-naweb.iaea.org/napc/ih/GNIP/userupdate/description/1stpage.html) (accessed 12.10.12).

iSimangaliso. 2015. (http://isimangaliso.com/newsflash/isimangalisos-december-drought-watch/.) Last Accessed on 06/12/2015.

Jager, J. M., and van Zyl, W. H., 1989. Atmospheric evaporative demand and evaporation coefficient concepts. Water SA 15, 103-110.

Jeffares and Green, 2012. uMkhanyakude District Municipality Groundwater Monitoring Network. Implementation Report. Jeffares and Green (Pty) Ltd., Project Number 2911.

Jeffares and Green, 2014a. Report to Jeffares & Green (Pty) Ltd on Groundwater Implementation at Manzamgwenya. Jeffares & Green (Pty) Ltd., Reference 03708R01.

Jeffares and Green, 2014b. Report to Jeffares & Green (Pty) Ltd on Groundwater Implementation at Kwasonto. Jeffares & Green (Pty) Ltd., Reference 03709R01.

Joubert, P., and Johnson, M. R., 1998. Abridged Lexicon of South Africa Stratigraphy. South African Committee for Stratigraphy, Council for Geoscience, 160 pp.

Kaiser, H. F., 1960. The application of electronic computers to factor analysis. Educational and Psychological Measurement 20, 141-151.

Kelbe, B. E., 2009. Nlabane and Zulti North Groundwater Model for Water Resources Analyses. Hydrological Research and Training Specialists.

Kelbe, B. E., Germishuyse, T., 2010. Groundwater/Surface Water Relationships with Specific Reference to Maputaland. WRC Report No. 1168/1/10. Water Research Commission, Pretoria, South Africa, 243 pp.

Kelbe, B. E., Germishuyse, T., Snyman, N., Fourie, I., 2001. Geohydrological Studies of the Primary Coastal Aquifer in Zululand. Water Research Commision Report No. 720/1. Water Research Commission, Pretoria, South Africa.

Kelbe, B. E., and Rawlins, B. K., 1992. Hydrology: Environmental Impact Assessment for Eastern Shores of Lake St. Lucia. In: Coastal and Environmental Services. Environmental Impact Assessment – Eastern Shores of Lake St. Lucia (Kingsa/Tojan Lease Area). Rhodes University, Grahamstown, South Africa.

Kelbe, B. E., Taylor, R. H., and Haldorsen, S., 2013. Groundwater hydrology. In: Perissinotto, R., Stretch, D. D., Taylor, R. H. (Eds.), Ecology and Conservation of Estuarine Ecosystems: Lake St Lucia as a Global Model. Cambridge University Press, 486 pp.

Kennedy, W. J. and Klinger, H. C., 1975. Cretaceous faunas from Zululand and Natal, South Africa. Introduction, Stratigraphy. Bulletin British Museum of Natural History, Geology, 25, 265-315.

Kienzle, S. W., and Schulze, R. E., 1992. A simulation model to assess the effect of afforestation on ground-water resources in deep sandy soils. Water SA 18, 265-272.

Kim J. H., Kim R. H., Lee J., Cheong T. J., Yum B. W., and Chang N. W., 2005. Multivariate statistical analysis to identify the major factors governing ground water quality in the coastal area of Kimje, South Korea. Hydrological Processes 19, 1261-1276.

Kirchner, R., Van Tonder, G. J. and Lukas, E., 1991. Exploitation potential of Karoo aquifers. WRC Report No. 170/1/91, Water Research Commission, Pretoria, South Africa, 283 pp.

Knott, J. T., and Olimpio, J. C., 1986. Estimation of recharge rates to the sand and gravel aquifer using environmental tritium. USGS Water Supply Paper 2297, 26 pp.

Krabbenhoft, D. P., Anderson, M. P., and Bowser, C. J., 1990. Estimating groundwater exchange with lakes. 2. Calibration of a three-dimensional, solute transport model to a stable isotope plume. Water Resource Research 26, 2455-2462.

Kruger, G. P., 1986. An investigation into the feasibility of rice cultivation on the Ngwavuma Coastal Plain, northern Natal. A report on the results of a hydrogeological and geomorphological survey. IDC Confidential Internal Report, 42 pp.

Kruger, G. P., and Meyer, R., 1988. A sedimentological model for the northern Zululand coastal plain. Geological Society of South Africa Geocongress '88, Extended Abstracts, Durban, 423-425.

Kumar, S. P. J., Elango, L., James, E. J., 2013. Assessment of hydrochemistry and groundwater quality in the coastal area of South Chennai, India. Arabian Journal of Geosciences 7, 2641-2653.

Lapham, W. W., 1989. Use of temperature profiles beneath streams to determine rates of vertical ground water flow and vertical hydraulic conductivity. U.S. Geological Survey Water Supply Paper 2337 pp.

Lee, R. W., and Strickland, D. J., 1988. Geochemistry of groundwater in Tertiary and Cretaceous sediments of the South Eastern Coastal Plain in eastern Georgia, South Carolina and south eastern Norht Carolina. Water Resource Research 24, 291-304.

Lee, T. M., 1996. Hydrogeologic controls on the groundwater interactions with an acidic lake in karst terrain, Lake Barco, Florida. Water Resource Research 32, 831-844.

Lui, K. W., 1995. Diagenesis of the Neogene Uloa Formation of Zululand, South Africa. South African Journal of Geology 98, 25-34.

Martin, A. K., and Flemming, B. W., 1988. Physiography, structure and geological evolution of the Natal continental shelf. In, Schumann, E. H. (Ed.), Coastal Ocean Studies off Natal, South Africa. Lecture Notes on Coastal and Estuarine Studies, 26, 11-46.

Maud, R. R., 1980. The climate and geology of Maputaland. In: Bruton, M. N., Cooper, K. H. (Eds.) Studies on the ecology of Maputaland. Rhodes University and the Natal branch of the Wildlife Society of Southern Africa, 1-7.

Maud, R. R., 1993. Port Durnford Formation. In: Quaternary Geology of the Natal and Zululand coast South Africa. IUGS/CLIP/GSO Fieldguide. 32 pp.

Maud, R. R., and Orr, W. N., 1975. Aspects of post-Karroo geology in the Richards Bay area. Transactions of the Geological Society South Africa 78, 101-109.

Maud, R. R, and Botha, G. A., 2000. Deposits of the south eastern and southern coasts. In: T.C. Partridge, and R.R. Maud (Ed.), The Cenozoic evolution of Southern Africa, Vol. 10. Oxford Monographs on Geology and Geophysics, 19-32.

Maxey, G. B., 1964. Hydrostratigraphic units. Journal of Hydrology 2, 124-129.

McDonald, M. G., and Harbaugh, A. W., 1988. A modular three-dimensional finite-difference ground-water flow model: Techniques of Water-Resources Investigations of the United States Geological Survey, 586 pp.

Merritt, M. L., and Konikow, L. F., 2000. Documentation of a Computer Program to Simulate Lake-Aquifer Interaction Using the MODFLOW Ground-Water Flow Model and the MOC3D Solute-Transport Model. U.S. Geological Survey Water-Resources Investigations Report No. 4167, 146 pp.

Meyer, R. and Kruger, G. P., 1987. Geophysical and geohydrological investigations along the Zululand coastal plain. Abstracts, Hydrological Sciences Symposium Proceedings: Volume 1, Rhodes University, Grahamstown, South Africa, 299-311.

Meyer, R., and Godfrey, L., 1995. KwaZulu-Natal Geohydrological Mapping Project: Mapping Unit 7. Report No. EMAP-C-95024, CSIR, Pretoria, South Africa, 38 pp.

Meyer, R., De Beer, J. H. and Blume, J., 1982. A geophysical-geohydrological study of an area around Lake Sibaya, northern Zululand, Report No. KOM/Gf/81/1, Geophysics Division, National Physical Research Laboratory, CSIR, Pretoria, 32 pp.

Meyer, R., and Godfrey, L., 2003. Report on the Geohydrology Around Lake Sibaya, Northern Zululand Coastal Plain, KwaZulu-Natal. Division of Water Environment and Forestry Technology. Report No. ENV-PC 2003-003, CSIR, Pretoria, South Africa.

Meyer, R., McCarthy, M. J., and Eglington, B. M., 1993. Further investigation of the geology and geohydrology of the dune cordon on the eastern shores of Lake St. Lucia. Division of Earth, Marine and Atmospheric Science and Technology, Report No. EMAP-C-93032 CSIR, Pretoria, South Africa.

Meyer, R., Talma, A. S., Duvenhage, A. W. A., Eglington, B. M., Taljaard, J., Botha, J. P., Verwey, J., and van der Voort, I., 2001. Geohydrological Investigation and Evaluation of the Zululand Coastal Aquifer. Water Research Commission, Report No. 221/1/ 1, 51 pp.

Middleton, B.J., and Bailey, A.K., 2009. Water Resources of South Africa, 2005 Study (WR2005) Book of Maps Version 1. Report No. TT382. Water Research Commission, Pretoria, South Africa, 188 pp.

Midgley, D. C., Pitman, W. V., and Middleton, B. J., 1994. Surface Water Resources of South Africa 1990: User's Manual. WRC Report No. 298/1/94. Water Resource Commission, Pretoria, South Africa.

Miller, W. R., 1994. Morphology and bathymetry of Lake Sibaya. South African Geological Survey Report 1994-0162, 30 pp.

Miller, W. R., 1996. Sequence stratigraphy of the latest Mesozoic and Cenozoic sediments below Lake Sibaya, Northern KwaZulu-Natal. South African Geological Survey Report 1996-0318, 38 pp.

Miller, W. R., 1998. The Sedimentology of Lake Sibaya Northern KwaZulu-Natal. South African Geological Survey Report 1998-0139, 26 pp.

Miller, W. R., 2001. The Bathymetry, Sedimentology and Seismic Stratigraphy of Lake Sibaya, Northern KwaZulu-Natal. Bulletin 131. Council for Geoscience, Pretoria, 94 pp.

Mkhwanazi, M. N., 2010. Establishment of the Relationship between the Sediments Mineral Composition and Groundwater Quality of the Primary Aquifers in the Maputaland Coastal Plain. MSc thesis, University of Zululand, 183 pp.

Money, D. C. 1988. Climate and Environmental Systems. Unwin Hyman, London, 186 pp.

Mountain, A., 1990. Paradise Under Pressure. Southern Book Publishers, Johannesburg, 149 pp.

NASA. 2006. NASA's Earth Science Enterprise Scientific Data Purchase Program. https://zulu.ssc.nasa.gov/mrsid/. Accessed on 07-08-06.

Nel, J. L., Driver, A., Strydom, W. F., Maherry, A., Petersen, C., Hill, L., Roux, D. J., Nieneber, S., van Deventer, H., Swartz, E., and Smith-Adao, L. B., 2011. Atlas of Freshwater Ecosystem Priority Areas in South Africa: Maps to Support Sustainable Development of Water Resources. Report to the Water Research Commission. WRC Report No. TT 500/11, 70 pp.

NGA, 2013. National Groundwater Archive. Digital Information as Supplied by the Department of Water Affairs.

Obura, D. O., Church, J. E., and Gabrié, C., 2012. Assessing Marine World Heritage from an Ecosystem Perspective: The Western Indian Ocean. World Heritage Centre, United Nations Education, Science and Cultural Organization (UNESCO), 124 pp.

Penman, H. L., 1948. Natural evaporation from open water, bare soil and grass. Proceedings of the Royal Society of London. Series A, Mathematical and Physical Sciences 193, 120-143.

Peters, J. G., 1987. Field heterogeneity: some basic issues, Water Resources Research 16, 443-448.

Piper, A. M., 1944. A graphic procedure in the geochemical interpretation of water analyses: American Geophysical Union Transactions 25, 914-923.

Pitman, W. V., and Hutchison, I. P. G., 1975. A preliminary Hydrological Study of Lake Sibaya. Report 4/75. Hydrology Research Unit, University of the Witwatersrand. Johannesburg, 35 pp.

Poehls, D. J., and Smith, G. J., 2009. Encyclopedic dictionary of hydrogeology. Elsevier, Amsterdam, p. 224.

Porat, N., and Botha, G. A., 2008. The chronology of dune development on the Maputaland coastal plain, southeast Africa. Quaternary Science Reviews 27, 1024-1046.

Prickett, T. A., 1975. Modelling Techniques for Groundwater Evaluation. Advances in Hydroscience. Academic Press, New York, 143 pp.

Prudic, D. E., 1989. Documentation of a computer program to simulate stream-aquifer relations using a modular, finite-difference, ground-water flow model. U.S. Geological Survey Open-File Report No. 729, 113 pp.

Prudic, D. E., Konikow, L. F., and Banta, E. R., 2004. A New Streamflow Routing (SFR1) Package to Simulate Stream-Aquifer Interaction with MODFLOW- 2000. USGS Open-File Report No. 1042, 104 pp.

Ramsay, P. J., 1991. Sedimentology, Coral Reef Zonation, and Late Pleistocene Coastline Models of the Sodwana Bay Continental Shelf, Northern Zululand. Unpublished PhD Thesis. University of Natal, 202 pp.

Ramsay, P. J., 1995. 9000 years of sea-level change along the southern African coastline. Quaternary International, 31, 71-75.

Ramsay, P. J., Cooper, J. A. G., 2002. Late Quaternary sea-level change in South Africa. Quaternary Research, 57, 82-90.

Roberts, D. L., Botha, G. A., Maud, R. R. and Pether, J., 2006. Coastal Cenozoic Deposits. In: Johnson, M. R., Anhaeusser, C. R., Thomas, R. J. (Eds.), The Geology of South Africa. The Geological Society of South Africa, Johannesburg, 691 pp.

SAWQ, 1996. South African Water Quality Guidelines. Department of Water Affairs, Domestic Water Use (2nd Ed).

SAWS, 2015. South African Weather Service. Durban Weather Office-Meteorological Data.

Scanlon, B. R., Healy, R. W. and Cook, P. G., 2002. Choosing appropriate techniques for quantifying groundwater recharge; Hydrogeology Journal 10, 18-39.

Schoeller, H., 1964. La classification geochimique des eaux. I.A.S.H. Publication No. 64, General Assembly of Berkeley 4, 16-24.

Schulze, R. E., Maharaj, J., Lynch, S. D., Howe, B. J., and Melvil-Tomson, B., 1997. South African Atlas of Agrohydrology and Climatology. Report No. TT 82. Water Research Commission, Pretoria, South Africa.

Schulze, R., 1989. ACRU: Background, concepts and theory. Agricultural Catchments Research Unit, Department of Agricultural Engineering, University of Natal, Pietermaritzburg, South Africa. ACRU Report 35. Water Research Commission No. 154/189. Pretoria, South Africa.

Scott, D. F., 1993. Rooting strategies by plantation trees on deep sands. In: Proceedings of the 6th South African National Hydrological Symposium, University of Natal, Pietermaritzburg, Volume 1, 155-162.

Seaber, P. R., 1988. Hydrostratigraphic units, In: Back, W., Rosenshein, J. S., and Seaber, P. R. (Eds.), Hydrology. The Geology of North America. Geological Society America 2, 9-14.

Selaolo, E. T., 1998. Tracer studies and groundwater recharge assessment in the Eastern fringe of the Botswana Kalahari. Published Ph.D. thesis, Free University of Amsterdam. GRES project publication.

Sharma, M. L., 1989. Groundwater Recharge. Balkema, Rotterdam, 323 pp.

Shaw, E. M., 1994. Hydrology in Practice. Chapman & Hall, London, 569 pp.

Shone, R. W., 2006. Onshore post-Karoo Mesozoic Deposits. In: Johnson, M. R., Anhaeusser, C. R., Thomas, R. J., (Eds.). The Geology of South Africa. Geological Society of South Africa and Council for Geoscience, 541-552.

Simmers, I., 1988. Estimation of natural groundwater recharge. In: Simmers, I. (Ed.), Proceedings NATO Advanced Research Workshop on Estimation of Natural Recharge of Groundwater, Antalya, Turkey, March 1987. NATO ASI Series C222, Reidel Publishing Company, Dordrecht, 510 pp.

SACS (South African Committee for Stratigraphy). 1980. Stratigraphy of South Africa. Part 1 (Comp. L. E. Kent). Lithostratigraphy of the Republic of South Africa, South-West Africa/Namibia, and the Republics of Bophuthatswana, Transkei and Venda. Handbook of the Geology Survey South Africa 8, 569-573.

Stapleton, R, P., 1977. Planktonic Foraminifera and the age of the Uloa Pecten bed. Papers on Biostratigraphic Research Bulletin Geological Society of South Africa 60, 11-17.

Statistics South Africa, 2012. Census 2011 Municipal report, KwaZulu-Natal. Report No. 03-01-53, 195 pp.

Suk, H., and Lee, K. K., 1999. Characterisation of a groundwater hydrochemical system through multivariate analysis: Clustering into ground water zones. Groundwater 37, 358–366.

Sunder, S. S. 1993. The Ecological, Economic and Social Effects of Eucalyptus. Proceedings. Regional expert consultation on eucalyptus. Forestry Group, Food and Agriculture Organization of the United Nations.

Swenson, F. A., 1968. New theory of recharge to the Artesian Basin of the Dakotas. Geological Society of America Bulletin 79, 163-182.

Taylor, R. H., 2013. St Lucia 2001 to 2012: A Decade of Drought. Management interventions and what have learnt about the ecosystem. Water Research Commission, Report No. TT 576/13, 168 pp.

Terratest, 2009a. KwaTembe Groundwater Feasibility Study. Terratest (Pty) Ltd., Project Number 161791.

Terratest, 2009b. KwaTembe Implementation Results DWAF BH No: KZN090011. Terratest (Pty) Ltd., Project Number 161785.

Terratest, 2011. Agri-Business Development Agency Mbazwane Goat Farm Groundwater Implementation Report DWA BH No: KZN 110119. Terratest (Pty) Ltd., Project Number 41097.

Terratest, 2014. Mlamula Stock Watering Groundwater Implementation Report DWAF BH No: KZN140021 Order Number: OR-061640. Terratest (Pty) Ltd., Project Number 41407.

Terratest, 2015a. Department Of Agriculture and Environmental Affairs, Umkhanyakude District Municipality: Kwanhlamvu Dip Groundwater Implementation Report. Terratest (Pty) Ltd., Reference 41491R03.

Terratest, 2015b. Department Of Agriculture and Environmental Affairs, Umkhanyakude District Municipality: Welandlovu Groundwater Implementation Report. Terratest (Pty) Ltd., Reference 41491R06.

Terratest, 2016a. Coastal Cashews Agri Project Groundwater Implementation Report. Terratest (Pty) Ltd., Order Number: C0280125.

Terratest, 2016b. Department Of Agriculture and Rural Development: Mnseleni Nursery Groundwater Implementation Report. Terratest (Pty) Ltd., Reference 41630.

Tripathi, R. P., and Singh, H. P., 1998. Soil Erosion and Conservation. Wiley Eastern Limited, New Delhi, p. 305.

USGS. 2015. Earth Explorer. https://earthexplorer.usgs.gov/. Accessed 05/11/15.

Været, L., Haldorsen, H., Kelbe, B. E., and Botha, G. A., 2008. Changes in climate and sea level in Maputaland, south-eastern Africa: from palaeodata to near future model scenarios. In: Været, L. 2008. Responses to global change and management actions in coastal groundwater resources, Maputaland, southeast Africa. PhD thesis, Norwegian University of Life Sciences, Norway.

Været, L., Kelbe, B., and Haldorsen, S., 2009. A modelling study on the effects of land management and climatic variation on groundwater inflow to Lake St Lucia, South Africa. Hydrogeology Journal 17, 1949-1967.

Van Heerden, I. L. and Swart, D. H., 1986. St Lucia Research. Volume 1: An assessment of past and present geomorphological and sedimentary processes operative in the St Lucia estuary and environments. CSIR Report 569. CSIR, Stellenbosch, South Africa. 60 pp.

Van Tonder, G. and Xu, Y., 2001. Recharge – Programme to estimate recharge and the groundwater reserve. http://www.unesco.org/water. Accessed May 2015.

Van Wyk, W. L., 1963. Groundwater studies in northern Natal, Zululand and surrounding areas. South African Geological Survey Memoirs 52, 127 pp.

Vegter, J. R., 1995. An explanation of a set of national groundwater maps. WRC Report No. TT 74/95, Water Research Commission, Pretoria, South Africa, 67 pp.

Wang, H. F., and Anderson, M. P., 1995. Introduction to Groundwater Modeling: Finite Difference and Finite Element Methods. Academic Press. San Diego, 237 pp.

Waterloo Hydrogeologic, 2015. Conceptual Modeling Tutorial.

Watkeys, M. K., Mason, T. R., and Goodman, P. S., 1993. The role of geology in the development of Maputaland, South Africa. 1. African Earth Sciences, 16, 205-221.

Weaver, J. M. C., Cave, L., Talma, S., 2007. Groundwater Sampling a Comprehensive Guide for Sampling Methods. Water Research Commission. Report No TT 303/07, 183 pp.

Wilson, J. D. and Naff, R. L., 2004. The U.S. Geological Survey modular ground-water model -- GMG linear equation solver package documentation. U.S. Geological Survey Open-File Report 1261, 47 pp.

Wolmarans, L G., and du Preez, J. W., 1986. South African Geological Survey. Map Explanation Sheet 271/232 (St. Lucia). Council for Geoscience, Pretoria.

Worthington, P. F., 1978. Groundwater conditions in the Zululand coastal plain around Richards Bay. Report, FIS 182, CSIR, Pretoria, South Africa, 209 pp.

WRC, 1995. Groundwater resources of the Republic of South Africa – Sheet 2: Saturated interstices, mean annual recharge, base flow, depth to groundwater, groundwater quality, hydrochemical types. Water Research Commission, Pretoria, South Africa.

WRC. (http://www.droughtsa.org.za/images/Background_to_current_drought_situation_in_South_Africa). Last Accessed on 03/06/2016.

Wright, C. I., 1995. The sedimentary dynamics of the St Lucia and Mfolozi estuary mouths, Zululand, South Africa. Bulletin, Geological Survey of South Africa, 109, 61 pp.

Wright, C. I., 1999. The Cenozoic evolution of the northern KwaZulu-Natal coastal plain. Ph.D. thesis, Department of Geology and Computer Sciences, University of Natal, Durban, 253 pp.

Wright, C. I., 2002. Aspects of the Cenozoic Evolution of the Northern KwaZulu-Natal Coastal Plain, South Africa. Bulletin 132, Council for Geoscience, 120 pp.

Wright, C. I., Mason, T. R., 1993. Management and sediment dynamics of St Lucia Estuary Mouth, Zululand, South Africa. Environmental Geology, 22, 227-241.

Wright, C. I., Mason, T. R., 1990. The sedimentation of Lake Sibaya, Northern KwaZulu-Natal. South African Geological Survey Report 1990-0147, 12 pp.

Wright, C. I., Miller, W. R., Cooper, J. A. G., 2000. The late Cenozoic evolution of coastal water bodies in Northern KwaZulu-Natal, South Africa. Marine Geology 167, 207– 229.

Yang, Q, Zhang, J, Wang, Y, Fang, Y, and Martín, J. D., 2015. Multivariate Statistical Analysis of Hydrochemical Data for Shallow Ground Water Quality Factor Identification in a Coastal Aquifer. Polish Journal of Environmental Studies 24, 769-776.

Zhang, L., Dawes, W. R., and Walker, G. R., 1999. Predicting the Effect of Vegetation Changes on Catchment Average Water Balance. Cooperative Research Centre for Catchment Hydrology, CSIRO Land and Water, Technical Report 12, 42 pp.

APPENDICES

Appendix A. Monthly precipitation (mm) for the Hlabisa Mbazwana meteorological station (1970 – 2014)

	October	November	December	January	February	March	April	May	June	July	August	September	Annual
1970/71	116	98	60	58	116	131	139	43	9	36	0	33	839
1971/72	120	70	52	236	393	121	39	165	13	32	3	11	1253
1972/73	33	72	104	67	164	25	117	35	36	30	28	401	1114
1973/74	53	190	185	187	96	97	131	53	8	159	3	18	1179
1974/75	55	90	66	223	418	61	133	30	78	0	26	120	1301
1975/76	35	52	382	468	132	143	216	82	1	12	14	4	1540
1976/77	82	145	70	277	313	205	36	6	5	4	59	98	1299
1977/78	10	12	134	179	30	167	172	33	18	168	32	19	974
1978/79	136	166	116	20	21	56	73	22	7	24	87	44	771
1979/80	94	35	88	55	213	35	40	16	0	7	14	206	803
1980/81	8	144	53	139	120	140	61	233	30	38	55	193	1213
1981/82	101	66	32	30	60	126	150	50	0	0	0	30	645
1982/83	112	50	30	46	82	42	10	40	15	106	64	23	620
1983/84	107	217	194	697	205	140	58	93	290	205	90	7	2301
1984/85	70	77	0	170	588	72	27	64	90	36	8	58	1257
1985/86	99	29	80	110	89	85	59	9	15	0	0	36	610
1986/87	61	46	210	114	11	178	40	22	71	18	129	252	1147
1987/88	68	85	41	60	163	152	189	30	107	9	27	62	993
1988/89	187	28	96	30	270	238	17	16	63	21	13	32	1010
1989/90	94	288	111	174	121	276	85	5	0	0	39	20	1213
1990/91	85	36	179	92	158	316	95	441	92	41	0	38	1572
1991/92	72	76	78	64	109	33	30	0	13	2	4	33	514
1992/93	20	49	157	81	189	159	53	5	20	21	42	34	829
1993/94	152	63	125	58	54	104	36	2	38	50	21	20	723
1994/95	169	150	110	22	22	92	226	57	84	4	89	2	1026
1995/96	116	113	219	117	145	103	63	39	13	31	31	6	997
1996/97	92	83	101	209	104	69	47	105	41	34	71	82	1038
1997/98	140	268	34	212	354	14	69	35	0	40	12	28	1204
1998/99	98	84	115	225	249	87	74	42	0	34	23	131	1161
1999/00	97	179	139	92	229	378	71	75	0	19	6	108	1391
2001/02	45	102	35	78	39	53	56	0	27	30	51	17	530

	October	November	December	January	February	March	April	May	June	July	August	September	Annual
2002/03	37	52	52	47	52	82	26	68	131	1	5	57	608
2003/04	42	68	64	150	208	67	85	0	14	62	2	42	803
2004/05	46	107	67	208	132	139	14	12	0	0	0	54	778
2005/06	8	79	41	73	197	51	117	4	17	35	105	31	756
2006/07	60	114	247	72	71	56	256	0	209	46	12	39	1180
2007/08	46	171	148	62	39	109	77	28	86	0	18	43	826
2008/09	10	120	81	213	143	48	23	8	22	0	55	50	772
2009/10	98	89	41	156	51	57	72	18	56	10	14	0	660
2010/11	152	157	166	232	36	9	81	92	13	75	14	45	1072
2011/12	127	43	17	142	188	284	28	48	0	7	6	307	1196
2012/13	148	82	117	269	152	63	27	10	27	47	41	19	1000
2013/14	106	124	203	85	35	311	81	0	18	18	5	79	1064
Average	**83**	**105**	**105**	**145**	**154**	**118**	**82**	**48**	**41**	**35**	**29**	**66**	**1012**

Appendix B. Monthly open water evaporation (mm) from the Class A pan (W7E001) evaporation data from 1970 to 1997 supplemented with monthly open water evaporation estimation using the Penman method (Penman, 1948) from 1997 to 2014.

	October	November	December	January	February	March	April	May	June	July	August	September	Annual
1970/71	179	223	216	198	174	174	119	85	84	101	142	130	1823
1971/72	166	152	174	166	151	131	147	78	77	97	87	137	1565
1972/73	159	167	223	172	166	148	97	79	93	82	105	119	1609
1973/74	157	180	208	184	166	161	146	95	77	87	154	170	1784
1974/75	191	176	215	195	177	130	106	102	64	85	118	152	1709
1975/76	142	142	135	191	171	159	98	71	82	98	122	133	1544
1976/77	161	185	183	218	146	114	110	85	92	98	124	146	1662
1977/78	141	147	232	177	148	135	120	92	71	83	79	116	1541
1978/79	130	159	160	193	159	126	110	102	70	89	116	109	1522
1979/80	144	108	132	162	162	151	120	100	95	71	118	134	1496
1980/81	128	161	121	142	129	125	100	90	80	84	153	98	1410
1981/82	119	186	195	150	145	153	107	71	52	100	107	133	1517
1982/83	147	134	166	153	162	117	151	121	76	117	143	119	1605
1983/84	169	165	190	168	165	146	124	105	58	80	108	94	1571
1984/85	113	121	143	163	144	147	108	78	58	56	58	132	1321
1985/86	135	158	150	142	120	111	108	95	86	94	116	158	1471
1986/87	122	140	155	154	182	163	132	108	111	84	105	91	1545
1987/88	118	143	133	176	177	152	104	91	90	68	111	146	1508
1988/89	147	160	170	167	131	164	133	94	70	86	133	164	1618
1989/90	160	117	153	145	124	112	101	85	96	67	133	119	1410
1990/91	122	189	134	149	134	136	107	82	59	73	105	113	1403
1991/92	126	152	147	164	161	164	131	103	85	96	107	137	1574
1992/93	152	179	141	189	159	112	116	65	81	77	105	110	1484
1993/94	91	127	184	155	149	141	103	74	92	66	88	96	1366
1994/95	128	142	124	161	139	139	88	68	47	59	82	100	1276
1995/96	117	121	122	137	123	107	72	58	59	64	85	117	1180
1996/97	127	134	165	137	126	98	101	65	65	47	53	82	1200
1997/98	106	101	142	149	140	133	108	61	48	57	89	128	1261
1998/99	139	163	175	114	154	150	113	91	65	73	96	120	1453

	October	November	December	January	February	March	April	May	June	July	August	September	Annual
1999/00	136	162	169	168	151	148	107	82	62	69	94	121	1468
2000/01	130	145	175	172	149	148	107	83	59	66	93	112	1439
2001/02	133	146	169	188	149	153	112	88	57	64	100	113	1473
2002/03	151	156	174	185	159	155	114	85	58	67	98	113	1514
2003/04	139	153	186	178	154	149	117	87	63	69	100	128	1524
2004/05	163	173	193	187	157	142	114	85	63	65	107	132	1583
2005/06	152	168	183	182	165	151	118	89	57	72	101	119	1556
2006/07	142	157	177	177	155	147	110	74	56	65	94	108	1463
2007/08	121	135	151	159	139	134	97	79	55	62	87	108	1326
2008/09	124	141	160	167	145	137	101	75	57	59	80	101	1347
2009/10	111	122	153	151	135	131	97	81	53	59	80	105	1278
2010/11	133	152	164	171	149	155	112	90	64	68	96	119	1471
2011/12	132	150	166	181	152	146	106	94	68	76	102	116	1488
2012/13	131	144	165	174	152	148	113	90	70	71	100	123	1481
2013/14	136	152	158	176	152	150	112	92	68	76	100	58	1430
Average	**139**	**153**	**167**	**170**	**152**	**142**	**113**	**86**	**71**	**77**	**105**	**121**	**1495**

Appendix C. Monthly Temperature (°C) for the Mbazwana Airfield meteorological station (1997 – 2014)

Year	**January**	**February**	**March**	**April**	**May**	**June**	**July**	**August**	**September**	**October**	**November**	**December**
1997								19.9	21.4	22.0	23.7	24.5
1998	24.9	26.6	27.0	25.1	21.9	20.1	20.1	21.0	22.5	23.0	25.3	25.8
1999		27.0	26.7	24.3	22.2	20.3	20.2	21.0	21.6	22.2	26.0	27.0
2000	25.7	27.3	26.7	23.4	20.6	20.5	19.6	21.1	21.6	22.0	23.5	25.7
2001	25.2	25.9	26.1	22.9	20.3	19.1	17.7	19.8	20.2	22.3	24.2	24.7
2002	26.5	25.0	25.3	23.6	21.0	17.9	17.5	21.6	21.2	23.2	22.4	25.4
2003	26.8	27.3	26.3	24.4	21.1	18.4	18.5	19.2	21.3	23.0	24.0	25.7
2004	26.3	26.0	24.8	23.6	20.8	18.6	17.5	20.6	20.4	22.8	25.2	26.5
2005	26.7	26.3	24.3	23.2	21.0	19.3	18.4	21.4	22.3	22.6	24.2	24.4
2006	26.2	27.5	24.9	24.1	20.5	18.4	19.8	19.6	20.5	22.9	23.6	25.4
2007	25.6	25.9			16.8	18.0	17.6	19.4	21.3	21.0	22.4	23.2
2008	24.5	24.6	23.6	20.7	20.1	17.8	17.8	19.0	19.4	20.8	23.7	24.7
2009	25.8	25.5	24.1	21.3	19.1	18.0	16.1	17.2	19.0	19.3	19.7	23.6
2010	23.1	23.9	23.1	20.8	20.4	16.9	16.7	17.2	19.8	22.8	24.8	25.5
2011	26.0	26.0	27.6	23.7	22.2	19.5	18.2	19.9	23.5	22.7	25.0	25.2
2012	27.2	27.1	25.9	22.5	22.8	20.2	19.8	21.1	21.5	23.0	23.8	25.6
2013	26.5	26.7	25.6	23.3	21.9	20.8	19.8	20.7	22.7	22.3	24.7	24.6
2014	26.9	27.2	26.5	23.7	22.4	20.6	20.0	21.7				
Average	**25.9**	**26.2**	**25.5**	**23.1**	**20.9**	**19.1**	**18.5**	**20.1**	**21.2**	**22.2**	**23.9**	**25.1**

Appendix D. Monthly average Wind Speed (m/s) for the Mbazwana Airfield meteorological station (1997 – 2014)

Year	**January**	**February**	**March**	**April**	**May**	**June**	**July**	**August**	**September**	**October**	**November**	**December**
1997								2.4	2.6	3.7	3.3	4
1998	4	2.4	2.6	2	1.7	1.7	2.6	2.5	3.8	3.3	4	3.5
1999	2.8	2.5	1.5	1.7	2.5	2	2.3	2.3	3.7	3.7	3.7	2.6
2000	2.7	2.1	1.4	1.7	1.5	1.5	1.3	1.8	3.5	3.1	3.6	3.6
2001	2.9	2.2	1.7	1.6	1.7	1.2	2	2.1	3.1	3.3	3.2	3.8
2002	4.3	2.7	3.1	2.2	2	1.7	1.7	2.2	2.5	4.5	4.4	3.7
2003	3.2	2.7	2.3	1.9	1.4	1.6	2.1	3.5	3.3	3.9	4	4.4
2004	3.3	2.6	2.3	2	1.7	1.7	2	2.1	3.5	4.1	3.8	3.6
2005	2.8	2.4	1.8	2.3	1.7	1.8	1.8	2.8	3.3	3.7	4.2	3.7
2006	3.2	2.8	2.6	2.4	2.1	1.3	2.2	2.8	3.1	3.4	3.6	3.3
2007	2.6	2.6			1.3	1.5	1.5	1.8	1.3	1.5	1.6	1.3
2008	1	0.8	1	1.3	1.2	1.2	1	1.7	2	1.8	1.7	1.6
2009	1.5	1.4	1.1	1.5	1	1.4	1.6	1.6	1.9	2.1	1.9	1.7
2010	1.3	1.2	1.2	1.4	1.4	1.6	1.4	1.5	1.8	1.7	2.1	1.9
2011	2	1.3	0.9	1.2	1	1.3	1.6	1.8	1.3	1.6	1.6	1.5
2012	1.6	1	1	1.1	1.2	1.4	1.6	1.6	2	1.6	1.7	1.4
2013	1.6	1.2	1.2	1.4	1.3	1.5	1.3	1.7	1.8	1.8	1.9	1.4
2014	1.3	0.9	1.2	1.2	1.5	1.4	1.6	1.2	2.3			
Average	**2.5**	**1.9**	**1.7**	**1.7**	**1.5**	**1.5**	**1.7**	**2.1**	**2.6**	**2.9**	**3.0**	**2.8**

Appendix E. Onsite measured groundwater and surface water hydrochemical parameters in the study area

Sample ID	Date Measured	Water Point	Elevation (m amsl)	Water Level (m amsl)	pH	DO (mg/l)	Eh (mVolt)	ORP (mVolt)	Temp (°C)	EC mS/m	TDS (mg/l)	TAL (mg/l)	Hardness (mg $CaCO_3$/l)
SIB01	29/09/2012	Groundwater	34.0	26.3	5.5	0.6	80.6	51.0	24.0	132	66	8.5	5.0
SIB02	08/04/2013	Shallow	60.0	47.5	7.5	2.4	-44.0	-85.0	24.5	58	29	20.0	
SIB02	29/09/2012	Shallow	60.0	47.0	7.0				24.0	79	39		
SIB03	29/09/2012	Shallow	46.9	31.9	6.6	0.3	32.0	14.9	23.8	158	79	55.0	35.0
SIB04	08/04/2013	Shallow	64.7		6.1	3.0	36.0	48.0	24.0	180	90	10.5	
SIB04	27/05/2013	Shallow	64.7	45.5	6.0	3.5	7.0	-18.9	23.9	185	93		
SIB04	30/09/2012	Shallow	64.7		5.6	1.5	89.0	174.0	24.0	198	99	10.0	14.0
SIB06	07/04/2013	Shallow	66.9	50.5	5.7	3.2	87.0	134.0	24.8	118	59	5.0	5.1
SIB06	30/09/2012	Shallow	66.9	50.5	5.5	1.2	82.4	91.7	25.1	124	62	6.5	5.6
SIB07	30/09/2012	Shallow	70.2	50.3	5.7	1.8	80.0	128.0	24.9	115	57		
SIB07	07/04/2013	Shallow	70.2		5.8	3.2	73.6	135.1	24.7	114	57		
SIB08	30/09/2012	Shallow	69.1	51.6	5.6	2.3	88.0	148.0	24.6	159	80		
SIB08	07/04/2013	Shallow	69.0	51.4	5.8	3.9	26.1	63.1	25.5	157	79		
SIB09	30/09/2012	Shallow	63.8		5.6	2.3	84.0	118.0	25.0	193	97		
SIB09	09/04/2013	Shallow	63.8		5.8	3.5	69.0	142.0	24.9	189	94	6.0	8.4
SIB10	30/09/2012	Shallow	59.4	45.2	5.4	1.5	99.0	154.0	25.0	171	85	5.0	7.7
SIB11	30/09/2012	Shallow	64.1		7.1	1.0	-4.0	-78.0	24.6	438	219		
SIB13	07/04/2013	River	45.9	45.9	8.1	2.9	-47.0	-27.0	19.6	703	351	240.0	
SIB13	30/09/2012	River	46.1	46.1	7.8	1.5	-33.6	-30.0	20.8	721	361	211.0	121.4
SIB15	30/09/2012	Lake	16.1	16.1	8.3	1.0	-55.0	62.0	22.1	637	318		
SIB15	07/04/2013	Lake	16.1	16.1	9.0	5.2	-89.6	-7.6	26.9	652	326		
SIB16	01/10/2012	Lake	16.1	16.1	9.0	2.0	-90.3	28.0	23.0	648	324	112.0	84.7
SIB17	01/10/2012	Ocean	0.0	0.0	8.4	1.9	-60.0	76.0	23.5	58810		119.5	6104.1
SIB18	08/04/2013	Lake	16.1		8.9	4.6	-87.9	46.5	26.6	640	320	123.5	85.4
SIB19	01/10/2012	Shallow	29.8	14.8	6.0	0.9	68.0	32.3	24.6	355	178		
SIB19	08/04/2013	Shallow	29.9	15.5	6.2	1.9	51.0	-7.0	25.5	433	217	11.0	50.5
SIB20	08/04/2013	Shallow	28.6	19.3	7.0	1.6	-17.0	-65.0	24.7	547	274	139.5	84.8
SIB20	01/10/2012	Shallow	28.6	18.9	7.0	1.5	1.9	-85.5	25.0	526	263	106.0	74.5
SIB21	01/10/2012	Shallow	41.8		7.2	2.3	-9.5	-98.0	23.7	392	196	64.5	48.5
SIB22	01/10/2012	Shallow	35.5	28.3	5.8	2.3	46.0	79.0	24.5	174	87	3.0	20.7

SIB23	01/10/2012	Shallow	38.2	30.8	5.6	1.8	83.9	135.0	24.3	141	71		
SIB24	01/10/2012	Stream	31.5	31.5	5.3	0.8	92.0	91.0	20.5	357	179		
SIB25	08/04/2013	Shallow	36.0	25.0	5.7	1.6	84.0	-12.0	25.0	133	66	8.0	17.2
SIB25	01/10/2012	Shallow	36.0	24.9	5.8	2.2	90.8	-44.7	24.7	146	79	6.0	19.0
SIB26	08/04/2013	Shallow	50.6		5.8	3.1	61.0	33.0	24.7	129	64	8.0	8.2
SIB26	02/10/2012	Shallow	50.6	39.6	6.1	2.3	65.0	95.0	24.5	129	65	7.0	8.1
SIB27	07/04/2013	Shallow	84.0	72.3	6.0	1.5	56.0	19.0	24.5	215	148	13.0	13.4
SIB27	02/10/2012	Shallow	80.1	68.6	5.8	1.2	79.0	53.0	26.2	191	95	10.0	9.5
SIB28	02/10/2012	Shallow	78.8	55.5	5.2	0.5	51.0	127.0	25.5	183	91		
SIB29	06/04/2013	Shallow	46.3	35.5	6.0	1.7	51.0	23.0	24.0	123	61	10.0	9.1
SIB30	07/04/2013	Shallow	72.6		5.7	2.8	79.0	50.0	24.7	132	56	15.0	
SIB31	07/04/2013	Shallow	67.3		5.7	2.5	82.0	136.0	25.0	236	118	6.0	
SIB32	07/04/2013	Shallow	59.1	42.1	6.1	3.8	52.7	112.3	25.2	175	87		
SIB33	07/04/2013	Shallow	58.3		5.9	2.4	59.0	95.0	24.8	231	115		
SIB34	07/04/2013	Shallow	81.6		6.8	0.8	11.0	-65.0	25.0	254	127	71.0	21.6
SIB35	07/04/2013	River	54.8		6.8	1.6	4.0	-8.0	21.8	189	94		
SIB36	07/04/2013	Lake	16.1		9.9	5.2	-134.8	-15.7	25.9	615	308		
SIB37	08/04/2013	Lake	16.1		9.0	5.4	-88.4	33.2	25.0	624	312		
SIB38	08/04/2013	Shallow	41.6		6.5	2.3	52.0	112.0	24.3	108	53	8.0	7.1
SIB39	09/04/2013	Shallow	86.3	75.3	5.9	1.3	56.0	107.0	24.2	157	79	8.5	9.7
SIB40	09/04/2013	Deep	89.0	75.9	7.2	3.8	-4.5	-84.8	24.9	322	161	131.5	68.2
SIB41	26/05/2013	Deep	40.4	33.7	6.3	2.4	25.4	10.0	24.7	192	96	29.0	23.7
SIB42	26/05/2013	Deep	45.5	25.6	6.2	5.0	27.9	39.0	25.5	187	93		
SIB43	26/05/2013	Shallow	45.5	32.4	5.6	4.0	55.0	63.0	25.0	121	61		
SIB44	26/05/2013	Shallow	56.4	46.7	5.8	2.7	55.7	74.5	24.8	145	73		
SIB45	26/05/2013	Shallow	63.8	55.1	5.7	2.7	65.0	43.5	24.7	168	84		
SIB47	27/05/2013	Shallow	82.5	64.2	6.3	1.5	23.7	-17.3	24.8	206	103		
SIB48	27/05/2013	Deep	82.0		7.4	1.7	-18.6	-18.2	23.3	364	182		
SIB49	27/05/2013	Shallow	86.8	79.3	5.9	1.6	36.1	-63.0	25.1	160	80		
SIB50	08/04/2013	Rain	50.1							88			5.4

Appendix F. Trace element concentration of groundwater and surface water in the study area (ppm).

	Li	Al	Si	Cr	Mn	Co	Ni	Cu	Zn	As	Cd	Cs	Ba	Hg	Pb	U
SIB01	0.0021	0.0231	3.1318	0.0024	0.0122	0.0007	BDL	0.0008	0.0416	0.0010	BDL	BDL	0.0804	0.0102	BDL	
SIB03	0.0022	0.0043	3.7237	BDL	0.0146	BDL	BDL	0.0010	0.3836	0.0007	BDL	BDL	0.0967	0.0026	0.0009	
SIB04	0.0014	0.0039	4.3470	BDL	0.0219	0.0006	BDL	0.0013	0.2633	0.0007	BDL	BDL	0.1480	0.0013	0.0048	
SIB06	BDL	BDL	6.1380	BDL	0.0022	BDL	BDL	0.0012	0.0272	0.0034	0.0004	0.0002	0.0824	BDL	BDL	0.0006
SIB06	0.0008	0.0016	6.1930	BDL	0.0030	BDL	BDL	0.0010	0.0621	0.0005	BDL	BDL	0.1153	BDL	BDL	
SIB09	0.0029	BDL	6.8860	BDL	0.0040	BDL	BDL	0.0017	0.0234	0.0035	BDL	0.0001	0.0905	BDL	0.0011	0.0005
SIB10	0.0029	0.0027	6.6422	BDL	0.0039	BDL	BDL	0.0014	0.0569	0.0007	BDL	BDL	0.1173	BDL	BDL	
SIB13	0.0104	0.0014	11.0466	BDL	0.0476	BDL	BDL	0.0029	0.0189	0.0056	BDL	BDL	0.1786	BDL	BDL	
SIB16	0.0056	0.0017	8.0789	BDL	BDL	BDL	BDL	0.0046	0.0162	0.0045	BDL	BDL	0.1939	BDL	BDL	
SIB17	0.9258	BDL	BDL	BDL	BDL	BDL	BDL	BDL	BDL	0.3096	BDL	BDL	BDL	BDL	BDL	
SIB18	0.0010	BDL	8.8880	BDL	0.0008	BDL	BDL	0.0037	0.0171	0.0100	BDL	BDL	0.1496	BDL	BDL	0.0010
SIB19	0.0007	0.0085	11.2200	0.0014	0.0825	0.0152	0.0164	0.0058	0.7315	0.0047	0.0005	BDL	0.1364	BDL	0.0011	0.0005
SIB20	BDL	BDL	6.0940	BDL	0.0686	BDL	BDL	0.0039	0.0220	0.0107	BDL	BDL	0.1115	BDL	BDL	0.0009
SIB20	0.0038	0.0004	4.5882	BDL	0.0582	BDL	BDL	0.0018	0.0161	0.0025	BDL	BDL	0.1112	BDL	BDL	
SIB21	BDL	0.0038	3.4944	BDL	0.2832	BDL	BDL	0.0019	0.0198	0.0029	BDL	BDL	0.1466	BDL	BDL	
SIB22	0.0006	0.0568	2.3362	0.0006	0.0245	BDL	BDL	0.0015	1.5405	0.0008	BDL	BDL	0.0912	BDL	0.0006	
SIB25	BDL	0.0564	2.8930	0.0015	0.0232	BDL	BDL	0.0018	0.0857	0.0045	BDL	BDL	0.1914	BDL	BDL	0.0005
SIB25	BDL	0.1214	2.8357	0.0014	0.0266	0.0005	BDL	0.0013	0.1428	0.0016	BDL	BDL	0.2009	BDL	BDL	
SIB26	BDL	0.0264	3.7620	0.0009	0.0156	BDL	BDL	0.0013	0.1309	0.0036	BDL	BDL	0.1617	BDL	BDL	0.0005
SIB26	BDL	0.0033	3.6940	0.0007	0.0156	BDL	BDL	0.0007	0.1133	0.0010	BDL	BDL	0.0687	BDL	BDL	
SIB27	BDL	0.0032	5.9950	0.0012	0.0110	0.0038	0.0020	0.0024	0.2101	0.0089	BDL	BDL	0.3179	BDL	BDL	0.0005
SIB27	BDL	0.0062	6.0095	0.0012	0.0092	0.0020	BDL	0.0018	0.3602	0.0049	BDL	BDL	0.4010	BDL	BDL	
SIB29	BDL	0.0117	2.7830	0.0011	0.0244	BDL	BDL	0.0016	0.1562	0.0035	BDL	BDL	0.2618	BDL	BDL	0.0005
SIB34	0.0021	BDL	9.8120	BDL	0.0586	0.0029	0.0023	0.0014	9.3280	0.0052	BDL	0.0001	0.1551	BDL	BDL	BDL
SIB38	0.0005	0.0062	4.1800	0.0009	0.0103	BDL	BDL	0.0012	0.0729	0.0034	BDL	0.0000	0.0793	BDL	0.0013	0.0006
SIB39	BDL	0.0079	7.2380	0.0010	0.0143	BDL	BDL	0.0038	0.0267	0.0040	BDL	BDL	0.0680	BDL	BDL	0.0005
SIB40	0.0018	0.0021	11.3300	BDL	0.0653	BDL	BDL	0.0012	0.0200	0.0042	BDL	BDL	0.1419	BDL	BDL	BDL
SIB41	0.0028	0.0004	3.2780	BDL	0.0185	BDL	BDL	0.0014	0.0871	0.0036	BDL	BDL	0.1793	BDL	BDL	0.0005
SIB50	BDL	0.0011	BDL	BDL	0.0077	BDL	BDL	0.0016	0.0251	0.0033	BDL	BDL	0.0275	BDL	BDL	BDL

Appendix G. South African Water Quality guidelines for domestic, industry and agricultural use (SAWQ, 1996) and WHO (drinking water) Guidelines (WHO, 2011) (concentrations in mg/l unless otherwise stated)

	SAWQ (1996)			
	Domestic	Industry	Agriculture	WHO (2011)
Alkalinity (as CaCO3)		0-1200		
Aluminium	0 - 0.15		0 - 5	0.9
Arsenic	0 - 0.01		0 - 0.1	0.01
Cadmium	0 - 5		0 - 10	0.003
Calcium	0 - 32			
Chloride	0 - 100	0 - 500	0 - 100	
Chromium(VI)	0 - 0.05		0 - 0.1	0.05
Cobalt			0 - 0.05	
Copper	0 - 1		0 - 0.2	2
Fluoride	0 - 1		0 - 2	1.5
Iron	0 - 0.1	0 - 10.0	0 - 5	
Lead	0 - 0.01		0 - 0.2	0.01
Magnesium	0 - 30			
Manganese	0 - 0.05	0 - 10.0	0 -10	
Mercury	0 - 0.001			0.006
Molybdenum			0 - 0.01	
Nickel			0 - 0.20	0.07
Nitrate+Nitrite	0 - 6		0 - 5	53
Potassium	0 - 50			
Silica			0 - 150	
Sodium	0 - 100		~70	
Sulphate	0 - 200	0 - 500		
Zinc	0 - 3		0 - 1	
pH	6 – 9	5 – 10	6.5 - 8.4	
TDS (mg/l)	0 - 450	0 - 1 600	~40	
Barium				0.7
Selenium				0.04

Appendix H. Estimated monthly runoff volume into the lake (10^6 m^3).

Year	Oct	Nov	Dec	Jan	Feb	Mar	Apr	May	Jun	Jul	Aug	Sep	Total
1969/70				0.02	0.15	0.08	0.05	0.16	0.07	0.00	0.03	0.05	
1970/71	0.26	0.22	0.13	0.13	0.26	0.29	0.31	0.10	0.02	0.08	0.00	0.07	1.88
1971/72	0.27	0.16	0.12	0.53	0.88	0.27	0.09	0.37	0.03	0.07	0.01	0.02	2.81
1972/73	0.07	0.16	0.23	0.15	0.37	0.06	0.26	0.08	0.08	0.07	0.06	0.90	2.50
1973/74	0.12	0.43	0.42	0.42	0.21	0.22	0.29	0.12	0.02	0.36	0.01	0.04	2.64
1974/75	0.12	0.20	0.15	0.50	0.94	0.14	0.30	0.07	0.18	0.00	0.06	0.27	2.92
1975/76	0.08	0.12	0.86	1.05	0.30	0.32	0.48	0.18	0.00	0.03	0.03	0.01	3.45
1976/77	0.18	0.32	0.16	0.62	0.70	0.46	0.08	0.01	0.01	0.01	0.13	0.22	2.91
1977/78	0.02	0.03	0.30	0.40	0.07	0.37	0.38	0.07	0.04	0.38	0.07	0.04	2.18
1978/79	0.31	0.37	0.26	0.04	0.05	0.13	0.16	0.05	0.02	0.05	0.19	0.10	1.73
1979/80	0.21	0.08	0.20	0.12	0.48	0.08	0.09	0.04	0.00	0.02	0.03	0.46	1.80
1980/81	0.02	0.32	0.12	0.31	0.27	0.31	0.14	0.52	0.07	0.09	0.12	0.43	2.72
1981/82	0.23	0.15	0.07	0.07	0.13	0.28	0.34	0.11	0.00	0.00	0.00	0.07	1.45
1982/83	0.25	0.11	0.07	0.10	0.18	0.09	0.02	0.09	0.03	0.24	0.14	0.05	1.39
1983/84	0.24	0.49	0.43	1.56	0.46	0.31	0.13	0.21	0.65	0.46	0.20	0.02	5.16
1984/85	0.16	0.17	0.00	0.38	1.32	0.16	0.06	0.14	0.20	0.08	0.02	0.13	2.82
1985/86	0.22	0.07	0.18	0.25	0.20	0.19	0.13	0.02	0.03	0.00	0.00	0.08	1.37
1986/87	0.14	0.10	0.47	0.25	0.02	0.40	0.09	0.05	0.16	0.04	0.29	0.56	2.57
1987/88	0.15	0.19	0.09	0.13	0.37	0.34	0.42	0.07	0.24	0.02	0.06	0.14	2.23
1988/89	0.42	0.06	0.22	0.07	0.60	0.53	0.04	0.04	0.14	0.05	0.03	0.07	2.26
1989/90	0.21	0.65	0.25	0.39	0.27	0.62	0.19	0.01	0.00	0.00	0.09	0.05	2.72
1990/91	0.19	0.08	0.40	0.21	0.36	0.71	0.21	0.99	0.21	0.09	0.00	0.08	3.52
1991/92	0.16	0.17	0.17	0.14	0.24	0.07	0.07	0.00	0.03	0.00	0.01	0.07	1.15
1992/93	0.04	0.11	0.35	0.18	0.42	0.36	0.12	0.01	0.04	0.05	0.09	0.08	1.86
1993/94	0.34	0.14	0.28	0.13	0.12	0.23	0.08	0.01	0.08	0.11	0.05	0.04	1.62
1994/95	0.38	0.34	0.25	0.05	0.05	0.21	0.51	0.13	0.19	0.01	0.20	0.00	2.30
1995/96	0.26	0.25	0.49	0.26	0.33	0.23	0.14	0.09	0.03	0.07	0.07	0.01	2.23
1996/97	0.21	0.19	0.23	0.47	0.23	0.15	0.11	0.24	0.09	0.08	0.16	0.18	2.33
1997/98	0.31	0.60	0.08	0.47	0.79	0.03	0.15	0.08	0.00	0.09	0.03	0.06	2.70
1998/99	0.22	0.19	0.26	0.50	0.56	0.19	0.17	0.09	0.00	0.08	0.05	0.29	2.60
1999/00	0.22	0.40	0.31	0.21	0.51	0.85	0.16	0.17	0.00	0.04	0.01	0.24	3.12

2000/01	0.24	0.67	0.08	0.15	0.71	0.18	0.44	0.06	0.11	0.03	0.00	0.00	2.68
2001/02	0.10	0.23	0.08	0.17	0.09	0.12	0.12	0.00	0.06	0.07	0.11	0.04	1.19
2002/03	0.08	0.12	0.12	0.11	0.12	0.18	0.06	0.15	0.29	0.00	0.01	0.13	1.36
2003/04	0.10	0.15	0.14	0.34	0.47	0.15	0.19	0.00	0.03	0.14	0.00	0.09	1.80
2004/05	0.10	0.24	0.15	0.47	0.29	0.31	0.03	0.03	0.00	0.00	0.00	0.12	1.74
2005/06	0.02	0.18	0.09	0.16	0.44	0.11	0.26	0.01	0.04	0.08	0.23	0.07	1.70
2006/07	0.13	0.25	0.55	0.16	0.16	0.12	0.57	0.00	0.47	0.10	0.03	0.09	2.65
2007/08	0.10	0.38	0.33	0.14	0.09	0.24	0.17	0.06	0.19	0.00	0.04	0.10	1.85
2008/09	0.02	0.27	0.18	0.48	0.32	0.11	0.05	0.02	0.05	0.00	0.12	0.11	1.73
2009/10	0.22	0.20	0.09	0.35	0.11	0.13	0.16	0.04	0.12	0.02	0.03	0.00	1.48
2010/11	0.34	0.35	0.37	0.52	0.08	0.02	0.18	0.21	0.03	0.17	0.03	0.10	2.40
2011/12	0.28	0.10	0.04	0.32	0.42	0.64	0.06	0.11	0.00	0.02	0.01	0.69	2.68
2012/13	0.33	0.18	0.26	0.60	0.34	0.14	0.06	0.02	0.06	0.10	0.09	0.04	2.24
2013/14	0.24	0.28	0.46	0.19	0.08	0.70	0.18	0.00	0.04	0.04	0.01	0.18	2.38

Appendix I. Open water evaporation rates estimated using the Penman method (Penman, 1948).

	JAN	FEB	MAR	APR	MAY	JUN	JUL	AUG	SEP	OCT	NOV	DEC	Annual
Ra (mm H2O/day)	17.08	15.86	13.80	11.38	9.23	8.16	8.56	10.27	12.69	14.95	16.61	17.32	155.91
Temp (°C)	26.50	26.70	25.60	23.30	21.90	20.75	19.75	20.70	22.70	23.00	23.75	25.60	280.25
Ta (°F)	79.70	80.06	78.08	73.94	71.42	69.35	67.55	69.26	72.86	73.40	74.75	78.08	888.45
Relative humidity (%)	0.80	0.75	0.77	0.77	0.86	0.81	0.80	0.73	0.73	0.81	0.77	0.76	9.36
es (mb)	34.74	35.15	32.93	28.69	26.35	24.56	23.08	24.48	27.67	28.18	29.48	32.93	348.26
ea (mb)	34.74	35.15	32.93	28.69	26.35	24.56	23.08	24.48	27.67	28.18	29.48	32.93	348.26
ed (mb)	27.79	26.36	25.36	22.09	22.66	19.89	18.37	17.97	20.17	22.82	22.70	25.03	271.24
u10 (m/s)	1.60	1.20	1.20	1.40	1.30	1.50	1.43	1.97	2.02	1.60	1.70	1.40	
u2 (m/s)	1.20	0.90	0.90	1.05	0.97	1.12	1.07	1.47	1.51	1.20	1.27	1.05	13.70
miles/s	0.00	0.00	0.00	0.00	0.00	0.00	0.00	0.00	0.00	0.00	0.00	0.00	0.01
u2 (miles/day)	64.25	48.19	48.19	56.22	52.20	60.23	57.23	79.07	81.15	64.25	68.26	56.22	735.44
n (h/day)	6.63	6.96	7.17	7.19	7.61	6.71	7.26	7.63	6.65	5.66	5.68	6.14	81.29
N (h/day)	13.66	13.08	12.34	11.56	10.78	10.44	10.58	11.22	12.00	12.78	13.42	13.82	145.68
n/N	0.49	0.53	0.58	0.62	0.71	0.64	0.69	0.68	0.55	0.44	0.42	0.44	6.80
RI (1-r) (mm/day)	7.25	7.12	6.55	5.64	4.98	4.13	4.53	5.41	5.84	6.01	6.51	6.98	70.98
Ta (kelvin)	300	300	299	296	295	294	293	294	296	296	297	299	749
σTa4 (mm/day)	15.72	15.76	15.53	15.06	14.78	14.55	14.35	14.54	14.94	15.00	15.15	15.53	180.90
Ro (mm/day)	0.72	0.89	1.03	1.36	1.43	1.56	1.79	1.85	1.39	0.97	0.96	0.85	14.82
H (mm/day)	6.53	6.23	5.52	4.28	3.55	2.57	2.74	3.56	4.45	5.04	5.56	6.13	56.16
Ea (mm/day)	2.78	3.02	2.60	2.45	1.32	1.80	1.77	2.94	3.44	2.14	2.81	2.94	30.01
Δ (mb/°C)	0.20	0.21	0.20	0.17	0.16	0.15	0.14	0.15	0.17	0.17	0.18	0.20	2.10
γ	0.07	0.07	0.07	0.07	0.07	0.07	0.07	0.07	0.07	0.07	0.07	0.07	0.80
Δ/γ	3.05	3.08	2.91	2.58	2.40	2.25	2.14	2.25	2.50	2.54	2.65	2.91	31.28
Eo (mm/day)	5.60	5.44	4.77	3.77	2.90	2.33	2.43	3.37	4.16	4.22	4.80	5.32	49.12
Eo (mm/month)	174	152	148	113	90	70	75	104	125	131	144	165	**1491.46**

Appendix J. Reference crop evapotranspiration calculated using the FAO Penman – Monteith method (Allen at al., 1998) (a) corrected for land use based on Kc values (b)

a)

	January	**February**	**March**	**April**	**May**	**June**	**July**	**August**	**September**	**October**	**November**	**December**
T min	21.20	21.38	20.49	17.85	14.60	12.59	12.18	13.84	15.52	17.46	19.28	20.47
T max	30.36	30.90	30.39	28.37	26.94	25.33	24.66	26.07	26.79	26.96	28.45	29.78
T mean	25.78	26.14	25.44	23.11	20.77	18.96	18.42	19.96	21.16	22.21	23.86	25.13
Humidity	82.80	84.63	87.27	88.80	89.13	90.50	91.20	87.27	83.00	81.67	80.53	80.40
U2 m/s 10m	2.55	1.99	1.71	1.71	1.54	1.53	1.78	2.14	2.67	2.89	3.01	2.77
U2 m/s 2m	1.91	1.49	1.28	1.28	1.15	1.14	1.33	1.60	2.00	2.16	2.25	2.07
P @ 77m	100.33	100.33	100.33	100.33	100.33	100.33	100.33	100.33	100.33	100.33	100.33	100.33
days	31.00	28.00	31.00	30.00	31.00	30.00	31.00	31.00	30.00	31.00	30.00	31.00
γ	0.07	0.07	0.07	0.07	0.07	0.07	0.07	0.07	0.07	0.07	0.07	0.07
e^o (T min)	2.52	2.54	2.41	2.05	1.66	1.46	1.42	1.58	1.76	2.00	2.24	2.41
eo (T max)	4.33	4.47	4.34	3.86	3.55	3.23	3.10	3.38	3.52	3.56	3.88	4.19
eo (T mean)	3.32	3.39	3.25	2.83	2.45	2.19	2.12	2.33	2.51	2.68	2.96	3.19
es	3.42	3.51	3.38	2.95	2.61	2.34	2.26	2.48	2.64	2.78	3.06	3.30
Δ	0.20	0.20	0.19	0.17	0.15	0.14	0.13	0.14	0.15	0.16	0.18	0.19
ea eo T min	0.73	0.73	0.73	0.71	0.69	0.68	0.68	0.69	0.69	0.71	0.72	0.73
ea T min	2.52	2.54	2.41	2.05	1.66	1.46	1.42	1.58	1.76	2.00	2.24	2.41
ea RH mean	2.84	2.97	2.95	2.62	2.32	2.12	2.06	2.16	2.19	2.27	2.46	2.65
es -ea	0.91	0.96	0.96	0.91	0.95	0.89	0.84	0.90	0.88	0.78	0.82	0.89
J	16.00	47.00	75.00	106.00	136.00	167.00	197.00	228.00	259.00	289.00	320.00	350.00
ϕ	-0.48	-0.48	-0.48	-0.48	-0.48	-0.48	-0.48	-0.48	-0.48	-0.48	-0.48	-0.48
dr	1.03	1.02	1.01	0.99	0.98	0.97	0.97	0.98	0.99	1.01	1.02	1.03
δ	-0.37	-0.22	-0.04	0.17	0.33	0.41	0.37	0.23	0.03	-0.18	-0.34	-0.41
ωs	1.83	1.69	1.59	1.48	1.39	1.34	1.36	1.45	1.56	1.66	1.76	1.80
$\sin(\phi)\sin(\delta)$	0.17	0.10	0.02	-0.08	-0.15	-0.18	-0.17	-0.11	-0.01	0.08	0.15	0.18
$\cos(\phi)\cos(\delta)$	0.83	0.86	0.88	0.87	0.84	0.81	0.82	0.86	0.88	0.87	0.83	0.81
Ra	42.83	39.66	34.66	27.95	22.43	19.77	20.95	25.63	32.15	38.01	42.02	43.58
N (hours)	13.96	12.92	12.16	11.30	10.60	10.25	10.42	11.04	11.88	12.71	13.43	13.75
n (hours)	6.63	6.96	7.17	7.19	7.61	6.71	7.26	7.63	6.65	5.66	5.68	6.14

Rs	20.88	20.60	18.88	15.88	13.66	11.41	12.54	15.27	17.03	17.96	19.39	20.63
	January	**February**	**March**	**April**	**May**	**June**	**July**	**August**	**September**	**October**	**November**	**December**
Rso	32.19	29.81	26.05	21.00	16.86	14.86	15.75	19.26	24.16	28.57	31.58	32.75
Rns	16.08	15.86	14.54	12.23	10.52	8.78	9.66	11.76	13.12	13.83	14.93	15.88
Rs/Rso	0.65	0.69	0.72	0.76	0.81	0.77	0.80	0.79	0.70	0.63	0.61	0.63
T mink4	36.81	36.90	36.46	35.17	33.62	32.69	32.50	33.27	34.05	34.98	35.86	36.45
T maxk4	41.61	41.91	41.63	40.53	39.77	38.92	38.57	39.31	39.69	39.78	40.57	41.30
Rnl	2.43	2.68	3.01	3.55	4.35	4.20	4.46	4.28	3.42	2.65	2.39	2.39
Rn	13.65	13.18	11.53	8.68	6.16	4.58	5.19	7.47	9.70	11.18	12.54	13.50
G month	0.07	-0.02	-0.21	-0.33	-0.29	-0.16	0.07	0.19	0.16	0.19	0.20	0.13
Eto day	4.70	4.54	4.01	3.16	2.47	2.02	2.23	2.97	3.64	3.90	4.34	4.67
Eto month	**145.81**	**127.04**	**124.19**	**94.71**	**76.68**	**60.66**	**69.14**	**91.98**	**109.14**	**120.77**	**130.25**	**144.73**
Eto year												**1295.08**

b)

Kc	**Monthly Eto based on Kc Values**												**Total**	**% of Catchment**
Plantation	145.81	127.04	124.19	94.71	76.68	60.66	69.14	91.98	109.14	120.77	130.25	144.73	1295	**233**
Bushland	109.36	95.28	93.14	71.03	57.51	45.49	51.85	68.98	81.85	90.58	97.69	108.55	971	**369**
Grassland	123.94	107.98	105.56	80.50	65.18	51.56	58.77	78.18	92.77	102.66	110.71	123.02	1101	**462**
Wetland	145.81	127.04	124.19	94.71	76.68	60.66	69.14	91.98	109.14	120.77	130.25	144.73	1295	**26**
Total														**1090**

Appendix K. Estimated monthly groundwater seepage (10^6 m^3) from the lake to the ocean using Dupuit's equation (Dupuit, 1863).

	Oct	Nov	Dec	Jan	Feb	Mar	Apr	May	Jun	Jul	Aug	Sep
1980/1981	1.92	1.92	1.92	1.91	1.92	1.91	1.91	1.92	1.93	1.92	1.92	1.92
1981/1982	1.93	1.93	1.93	1.92	1.92	1.91	1.92	1.92	1.92	1.91	1.91	1.91
1982/1983	1.92	1.93	1.94	1.95	1.94	1.93	1.93	1.94	1.94	1.94	1.94	1.94
1983/1984	1.95	1.95	1.96	1.96	1.98	1.99	1.99	1.99	1.99	2.01	2.02	2.02
1984/1985	2.02	2.02	2.02	2.02	2.06	2.08	2.08	2.08	2.08	2.09	2.09	2.09
1985/1986	2.09	2.08	2.08	2.07	2.06	2.05	2.04	2.04	2.03	2.02	2.02	2.01
1986/1987	2.01	2.00	2.00	2.01	2.00	2.00	2.00	1.99	1.98	1.98	1.98	1.99
1987/1988	2.01	2.01	2.01	2.00	1.99	2.00	2.00	2.00	1.99	2.00	2.00	2.00
1988/1989	2.00	2.01	2.00	2.00	2.00	2.00	1.99	1.98	1.98	1.98	1.98	1.97
1989/1990	1.97	1.97	1.99	1.99	1.99	2.00	2.01	2.01	2.00	1.99	1.99	1.99
1990/1991	1.99	1.99	2.00	2.00	2.02	2.03	2.04	2.06	2.06	2.07	2.07	2.07
1991/1992	2.08	2.08	2.08	2.07	2.06	2.05	2.04	2.03	2.02	2.01	2.00	2.00
1992/1993	1.99	1.99	1.99	1.99	1.99	2.00	2.00	2.00	1.99	1.99	1.99	1.98
1993/1994	1.99	1.99	1.98	1.98	1.97	1.96	1.95	1.95	1.93	1.93	1.93	1.92
1994/1995	1.93	1.94	1.93	1.92	1.91	1.90	1.90	1.91	1.90	1.90	1.90	1.90
1995/1996	1.90	1.90	1.91	1.91	1.91	1.91	1.90	1.90	1.89	1.88	1.88	1.88
1996/1997	1.87	1.87	1.86	1.86	1.86	1.86	1.86	1.86	1.85	1.85	1.86	1.86
1997/1998	1.86	1.87	1.89	1.89	1.90	1.91	1.91	1.90	1.89	1.89	1.89	1.88
1998/1999	1.88	1.88	1.88	1.88	1.90	1.90	1.89	1.89	1.88	1.88	1.88	1.88
1999/2000	1.87	1.88	1.90	1.92	1.94	1.97	1.99	1.99	2.00	2.00	2.00	2.00
2000/2001	2.01	2.02	2.04	2.03	2.03	2.04	2.05	2.04	2.04	2.03	2.03	2.02
2001/2002	2.02	2.03	2.02	2.02	2.01	2.00	1.99	1.98	1.97	1.97	1.97	1.97
2002/2003	1.96	1.95	1.94	1.94	1.93	1.92	1.91	1.90	1.89	1.91	1.90	1.90
2003/2004	1.89	1.89	1.88	1.87	1.87	1.88	1.87	1.86	1.85	1.85	1.85	1.84
2004/2005	1.83	1.82	1.82	1.82	1.81	1.81	1.80	1.80	1.80	1.80	1.80	1.79
2005/2006	1.79	1.78	1.78	1.78	1.79	1.78	1.77	1.77	1.76	1.76	1.76	1.76
2006/2007	1.75	1.76	1.76	1.77	1.76	1.74	1.74	1.74	1.75	1.75	1.75	1.74
2007/2008	1.74	1.74	1.76	1.75	1.74	1.73	1.73	1.77	1.75	1.74	1.74	1.73
2008/2009	1.72	1.72	1.72	1.73	1.74	1.74	1.74	1.73	1.73	1.73	1.72	1.72
2009/2010	1.72	1.72	1.73	1.74	1.74	1.74	1.73	1.72	1.72	1.71	1.71	1.71
2010/2011	1.71	1.71	1.71	1.71	1.71	1.70	1.69	1.68	1.67	1.67	1.67	1.67
2011/2012	1.66	1.66	1.66	1.66	1.63	1.64	1.65	1.64	1.62	1.62	1.62	1.62
2012/2013	1.62	1.62	1.62	1.62	1.62	1.62	1.62	1.62	1.62	1.62	1.62	1.62
2013/2014	1.96	1.63	1.59	1.60	1.82	1.83	1.69	1.63	1.60	1.53	1.61	1.62

Appendix L. Estimated monthly groundwater inflow into Lake Sibayi (10^6 m^3)

Year	October	November	December	January	February	March	April	May	June	July	August	September	Total
1969/70				0.68	4.42	2.29	1.53	4.60	2.00	0.11	1.00	1.35	
1970/71	7.67	6.53	3.95	3.83	7.71	8.67	9.22	2.87	0.56	2.41	0.00	2.21	55.61
1971/72	7.93	4.62	3.42	15.66	26.04	8.04	2.56	10.93	0.88	2.11	0.21	0.70	83.11
1972/73	2.22	4.79	6.92	4.45	10.87	1.64	7.75	2.33	2.37	2.01	1.88	26.62	73.85
1973/74	3.51	12.61	12.28	12.39	6.33	6.41	8.68	3.54	0.54	10.51	0.19	1.17	78.17
1974/75	3.65	5.98	4.38	14.81	27.75	4.06	8.79	2.00	5.20	0.00	1.72	7.93	86.26
1975/76	2.34	3.42	25.34	31.01	8.74	9.48	14.35	5.46	0.07	0.80	0.91	0.25	102.16
1976/77	5.42	9.59	4.64	18.38	20.73	13.60	2.40	0.37	0.33	0.27	3.91	6.49	86.12
1977/78	0.64	0.80	8.91	11.88	2.01	11.04	11.38	2.19	1.19	11.16	2.14	1.23	64.57
1978/79	9.05	11.00	7.72	1.30	1.36	3.71	4.83	1.45	0.46	1.58	5.74	2.91	51.12
1979/80	6.26	2.30	5.82	3.66	14.15	2.31	2.68	1.07	0.00	0.46	0.94	13.63	53.28
1980/81	0.54	9.55	3.50	9.19	7.96	9.29	4.01	15.45	1.99	2.52	3.65	12.81	80.46
1981/82	6.71	4.38	2.13	1.99	3.98	8.36	9.95	3.32	0.00	0.00	0.00	1.99	42.80
1982/83	7.43	3.32	1.99	3.05	5.44	2.79	0.66	2.65	1.01	7.02	4.26	1.49	41.11
1983/84	7.07	14.36	12.83	46.22	13.60	9.30	3.81	6.17	19.23	13.60	5.97	0.46	152.62
1984/85	4.62	5.07	0.00	11.27	39.00	4.74	1.76	4.21	5.97	2.39	0.53	3.81	83.38
1985/86	6.57	1.92	5.31	7.30	5.90	5.64	3.88	0.56	0.96	0.00	0.00	2.39	40.42
1986/87	4.01	3.02	13.89	7.53	0.73	11.77	2.62	1.43	4.68	1.19	8.52	16.68	76.07
1987/88	4.48	5.60	2.69	3.99	10.84	10.09	12.52	2.00	7.12	0.61	1.79	4.13	65.85
1988/89	12.41	1.86	6.37	1.98	17.88	15.78	1.15	1.06	4.16	1.36	0.84	2.12	66.97
1989/90	6.20	19.11	7.34	11.57	8.01	18.29	5.63	0.33	0.00	0.01	2.57	1.35	80.42
1990/91	5.64	2.41	11.85	6.09	10.51	20.94	6.31	29.24	6.08	2.72	0.00	2.49	104.29
1991/92	4.80	5.05	5.14	4.21	7.22	2.21	2.01	0.00	0.87	0.14	0.26	2.16	34.07
1992/93	1.33	3.22	10.43	5.38	12.53	10.53	3.48	0.34	1.31	1.37	2.79	2.27	54.97
1993/94	10.09	4.15	8.28	3.85	3.59	6.90	2.37	0.15	2.51	3.28	1.42	1.31	47.92
1994/95	11.18	9.94	7.29	1.43	1.43	6.07	14.97	3.78	5.58	0.29	5.93	0.13	68.02
1995/96	7.71	7.49	14.55	7.73	9.62	6.84	4.20	2.58	0.86	2.05	2.08	0.40	66.10
1996/97	6.09	5.52	6.71	13.85	6.90	4.58	3.13	6.96	2.73	2.25	4.68	5.42	68.81
1997/98	9.25	17.74	2.25	14.03	23.45	0.93	4.58	2.35	0.00	2.65	0.78	1.82	79.84
1998/99	6.51	5.58	7.63	14.92	16.51	5.74	4.93	2.75	0.00	2.25	1.49	8.69	77.02
1999/00	6.43	11.87	9.22	6.08	15.15	25.04	4.71	4.97	0.00	1.26	0.40	7.13	92.27

2000/01	7.00	19.93	2.25	4.51	21.12	5.27	12.93	1.76	3.35	0.99	0.13	0.00	79.26
2001/02	2.97	6.73	2.32	5.17	2.59	3.48	3.68	0.00	1.76	1.98	3.38	1.09	35.16
2002/03	2.45	3.42	3.45	3.12	3.45	5.44	1.69	4.48	8.68	0.08	0.30	3.75	40.30
2003/04	2.81	4.48	4.26	9.95	13.76	4.44	5.64	0.00	0.93	4.08	0.13	2.79	53.27
2004/05	3.05	7.10	4.41	13.80	8.72	9.22	0.91	0.80	0.00	0.00	0.00	3.58	51.59
2005/06	0.50	5.27	2.72	4.82	13.05	3.35	7.77	0.23	1.13	2.32	6.94	2.06	50.15
2006/07	3.95	7.53	16.39	4.75	4.68	3.68	16.99	0.00	13.86	3.05	0.80	2.59	78.26
2007/08	3.06	11.35	9.80	4.11	2.59	7.24	5.13	1.82	5.67	0.00	1.16	2.82	54.76
2008/09	0.64	7.99	5.37	14.13	9.49	3.19	1.53	0.53	1.43	0.00	3.65	3.28	51.23
2009/10	6.50	5.87	2.72	10.32	3.36	3.75	4.78	1.19	3.68	0.66	0.93	0.00	43.75
2010/11	10.05	10.40	11.01	15.39	2.40	0.62	5.37	6.12	0.83	4.97	0.94	2.96	71.07
2011/12	8.40	2.85	1.13	9.43	12.45	18.84	1.86	3.15	0.00	0.46	0.40	20.35	79.32
2012/13	9.81	5.47	7.73	17.81	10.09	4.18	1.79	0.66	1.79	3.08	2.69	1.25	66.34
2013/14	7.02	8.22	13.46	5.64	2.32	20.60	5.37	0.00	1.19	1.19	0.30	5.24	70.56

Appendix M. Observed and steady-state computed aquifer heads for the High-K simulation

Observation Well	Observed groundwater head (m)	Computed groundwater head (m)	Residual (m)
2732ADR0003	65.17	63.30	-1.87
2732BCV1172	19.2	18.59	-0.61
2732BCV1180	27.8	24.72	-3.08
2732BCV1181	26	21.39	-4.61
2732BCV1182	31.5	26.65	-4.85
2732BCV1165	13.2	12.99	-0.21
2732BCV1169	20.5	18.29	-2.21
2732BCV1171	23.3	17.53	-5.77
2732BCV1166	14.5	14.26	-0.24
2732BCV1167	14.5	14.26	-0.24
2732BCV1174	19	19.10	0.10
2732BCV1176	21	19.13	-1.87
2732BCV1168	20.1	17.76	-2.34
2732BCV1175	24.8	19.81	-4.99
2732BCV1179	23	19.67	-3.33
2732BCV1183	24.5	21.43	-3.07
2732BCV1185	28	26.39	-1.61
2732BCV1186	24	24.00	0.00
2732BCV1187	36.8	34.68	-2.12
2732BCV1188	34	29.37	-4.63
2732BCV1189	36	32.36	-3.64
2732BAV0139	44	43.82	-0.18
2732BAV0140	43	43.86	0.86
2732BCV1190	24	20.75	-3.25
2732BCV1191	19.8	19.59	-0.21
2732BCV1193	22.5	20.06	-2.44
2732BAV0141	38	39.33	1.33
2732BAV0142	44	44.04	0.04
2732BAV0143	50	44.86	-5.14
2732BCV1192	36.1	35.20	-0.90
2732BCV1194	36.2	33.82	-2.38
2732BCV1195	35.2	32.20	-3.00
2732BAV0145	38.7	38.20	-0.50
2732BAV0146	52	47.70	-4.30
2732BAV0148	42	43.06	1.06
2732BCV1196	31	27.29	-3.71
2732BCV1197	16	16.02	0.02
2732BCV1198	10	10.37	0.37
2732BCV1203	16.2	14.92	-1.28
2732BCV1204	12	10.85	-1.15
2732BAV0147	41.1	38.48	-2.62
2732BAV0149	40	36.26	-3.74
2732BCV1205	13	13.24	0.24
2732BAV0151	40.8	36.79	-4.01
2732BAV0152	40	35.59	-4.41
2732BAV0153	36.8	34.13	-2.67
2732BCV1202	19.5	19.50	0.00

Appendix N. Observed and steady-state computed aquifer heads for the Lake Package simulation

Observation Well	Observed groundwater head (m)	Computed groundwater head (m)	Residual (m)
2732ADR0003	65.17	63.15	-2.02
2732BCV1172	19.2	18.57	-0.63
2732BCV1180	27.8	24.82	-2.98
2732BCV1181	26	21.66	-4.34
2732BCV1182	31.5	26.72	-4.78
2732BCV1165	13.2	12.97	-0.23
2732BCV1169	20.5	18.28	-2.22
2732BCV1171	23.3	17.51	-5.79
2732BCV1166	14.5	14.24	-0.26
2732BCV1167	14.5	14.24	-0.26
2732BCV1174	19	19.08	0.08
2732BCV1176	21	19.11	-1.89
2732BCV1168	20.1	17.74	-2.36
2732BCV1175	24.8	19.76	-5.04
2732BCV1179	23	19.75	-3.25
2732BCV1183	24.5	21.33	-3.17
2732BCV1185	28	26.40	-1.60
2732BCV1186	24	24.00	0.00
2732BCV1187	36.8	34.69	-2.11
2732BCV1188	34	29.39	-4.61
2732BCV1189	36	32.39	-3.61
2732BAV0139	44	43.83	-0.17
2732BAV0140	43	43.87	0.87
2732BCV1190	24	20.68	-3.32
2732BCV1191	19.8	19.58	-0.22
2732BCV1193	22.5	19.97	-2.53
2732BAV0141	38	39.34	1.34
2732BAV0142	44	44.03	0.03
2732BAV0143	50	44.84	-5.16
2732BCV1192	36.1	35.22	-0.88
2732BCV1194	36.2	33.84	-2.36
2732BCV1195	35.2	32.24	-2.96
2732BAV0145	38.7	38.21	-0.49
2732BAV0146	52	47.67	-4.33
2732BAV0148	42	43.06	1.06
2732BCV1196	31	27.32	-3.68
2732BCV1197	16	16.00	0.00
2732BCV1198	10	10.35	0.35
2732BCV1203	16.2	14.91	-1.29
2732BCV1204	12	10.83	-1.17
2732BAV0147	41.1	38.47	-2.63
2732BAV0149	40	36.25	-3.75
2732BCV1205	13	13.22	0.22
2732BAV0151	40.8	36.78	-4.02
2732BAV0152	40	35.60	-4.40
2732BAV0153	36.8	34.15	-2.65
2732BCV1202	19.5	19.48	-0.02